# Metabolic Adaptations to Micro-Environmental Stress in Tumour Spheroids

Hannah Beth Smith




Nuffield Department of Clinical Laboratory Sciences

University of Oxford

Thesis submitted for the degree of Doctor of Philosophy

Green Templeton College

2014

## Acknowledgments

Firstly thank you to my supervisor, Richard Callaghan, without whom this project would not have been possible, his guidance and support were invaluable. Also, many thanks to the Callaghan family for their hospitality during my trip to the ANU in Canberra.

I would like to thank my co-supervisors; Mary Board, for her excellent advice and encouragement throughout this project and Jacqueline Boultwood, for welcoming me into her group.

Thank you to Helen Turley for teaching me the basics of immunohistochemistry, Andrea Pellagatti for his help with the gene expression analysis and Lucy Ambrose, whose instruction was essential for the glycolytic flux assays.

I would also like to acknowledge Kristy, Eva and Richard whose company made the lab a brighter place.

I would like to acknowledge the Medical Research Council for funding this project.

Also, thank you to my family whose love and understanding have seen me through all the ups and downs of this project. Finally thanks to my partner, Matt, who helped me so much, especially enduring all the early morning starts getting me to the train on time to get back to Oxford!

## Abstract

Alterations in energy metabolism due to factors including cellular stress from the hostile tumour micro-environment are a emerging cancer hallmark. Distinct hypoxic and quiescent cell populations develop, which are resistant to chemotherapy due to lack of proliferation, drug inactivity in the altered redox status of the cell and enhanced drug biotransformation. The present study characterises the metabolic strategies employed by these distinct populations of cancer cells. The *in vitro* 3-dimensional tumour spheroid model, which reflects tumour architecture and behaviour, cultured under different micro-environmental conditions was utilized in this study. Metabolic enzyme activity and expression, overall metabolic flux rates for nutrients, metabolomics profiles of specific pathways and tissue status were assessed. Metabolic adaptations consistent with the Warburg effect were observed in fully oxygenated, proliferative tumour spheroids, with glucose being metabolised to produce lactate. Additionally, metabolomics investigations determined glucose was metabolised by the pentose phosphate pathway, demonstrated by high enrichment of glucose-derived carbon in 6-phophogluconate. The extraction of 39.7 ± 7.6 μ moles (mg protein) $^{-1}$ glutamine from the medium over 24 hours was observed in these spheroids, consistent with glutaminolysis pathway activity. A 2-fold higher rate of glycolytic flux (measured by production of 3h2O from 5-$^{3}$H-glucose) was measured in hypoxic tumour spheroids, despite reduced levels of glycolytic enzymes being determined. Surprisingly, although lower rates of glycolysis (2.6-fold) were measured in quiescent spheroids, increased glycolytic enzyme activities (HK 1.9 fold, PK 2 fold and LDH 1.8 fold), glucose (1.9 fold over 24 hours) and glutamine uptake (5.5 fold over 12 hours) as well as lactate production (1.8 fold) were measured, relative to their proliferating counterparts. This study demonstrates that metabolic strategies employed by tumour spheroids differ upon exposure to distinct micro-environmental stresses, additionally identifying hexokinase as a potential therapeutic target for the inhibition of glycolysis under all micro-environmental stress conditions analysed.

## Table of Abbreviations

| Abbreviation | Description |
|---|---|
| 2D | Two-dimensional |
| 3D | Three-dimensional |
| 6PG | 6-phosphogluconate |
| ACL | ATP-citrate lyase |
| ADP | Adenosine diphosphate |
| AMP | Adenosine monophosphate |
| ATP | Adenosine triphosphate |
| CA | Carbonic anhydrases |
| CHC | a-cyano-4-hydroxycinnamate |
| DHEA | Dehydropiandrosterone |
| DNA | Deoxyribonucleic acid |
| EMT | Epithelial-mesenchymal transition |
| EPO | Erythropoietin |
| F1,6BP | Fructoe-1,6-bisphosphate |
| F2,6BP | Fructose-2,6-bisphosphate |
| FDG | [$^{18}$F]-flurodeoxyglucose |
| FNFTG | [$^{18}$F]-N-(methyl-(2-fluoroethyl)-1H-[1,2,3]triazole-4-yl) glucosamine |
| G6PDH | Glucose-6-phosphate dehydrogenase |
| GLDH | Glutamate dehydrogenase |
| GLS | Glutaminase |
| GLUT | Glucose transporter family |
| GSH | Glutathione |
| GTP | Guanosine-5'-triphosphate |
| HIF1 | Hypoxia inducible factor-1 |
| HK | Hexokinase |
| hnRNP | Heterogeneous nuclear ribonucleoprotein |
| HRP | Horseradish peroxidase |
| LDH | Lactate dehydrogenase |
| MCT | Monocarboxylate transporter |
| MCTS | Multicellular tumour spheroid |
| mTORC1 | Mammalian target of rapamycin complex 1 |

| | |
|---|---|
| NAD(P) | Nicotinamide adenine dinucleotide (phosphate) |
| NHE1 | Sodium/proton exchanger |
| PEP | Phosphoenolpyruvate |
| PET | Positron emission tomography |
| PFK1 | Phosphofructokinase 1 |
| PFK2/FBPase or PFKFB | 6-phosphofructo-2-kinase/fructose-2,6-bisphosphatase |
| $pH_{ex}$ | Extracellular pH |
| $pH_{in}$ | Intracellular pH |
| PI3K | Phophoinositide 3 kinase |
| PK | Pyruvate kinase |
| PPP | Pentose phosphate pathway |
| R5P | Ribose 5 phosphate |
| ROS | Reactive oxygen species |
| RT PCR | Reverse transcription polymerase chain reaction |
| SCO2 | Synthesis of Cytochrome c Oxidase 2 |
| SGLT | Sodium dependent glucose transporters |
| shRNA | Short hairpin RNA |
| TCA cycle | Tricarboxylic acid cycle |
| TIGAR | TP53-induced-glycolysis-and apoptosis regulator |
| TS | Tumour spheroid |
| $TS^H$ | Hypoxic tumour spheroids |
| $TS^N$ | Normoxic Proliferating TS |
| $TS^Q$ | Quiescent Tumour spheroids |
| uPAR | Plasminogen activator receptor |
| V-ATPase | Vaculolar proton pump |
| VDAC | Voltage dependent anion channel |
| VEGF | Vascular endothelial growth factor |
| VHL | Von Hippel-Lindau protein |
| $V_{max}$ | Maximum measured enzyme activity or capacity |

# Table of Contents

**Acknowledgments** ..... **ii**

**Abstract** ..... **iii**

**Table of Abbreviations** ..... **iv**

**1. Introduction - Metabolic adaptations to micro-environmental stress in cancer** ..... **1**

**1.1 The reprogrammed metabolism of cancer cells** ..... **3**

1.1.1 Alterations in the glycolytic pathway in cancer ..... 3

1.1.2 The pentose phosphate pathway ..... 21

1.1.3 Glutamine metabolism in cancer cells ..... 24

1.1.4 Lactate metabolism in cancer cells ..... 28

**1.2 Cell Signalling and metabolic adaptations in cancer** ..... **33**

1.2.1 Dysregulation of the Akt pathway ..... 33

1.2.2 p53 and cancer metabolism ..... 34

1.2.3 cMyc ..... 37

1.2.4 HIF-1 ..... 39

**1.3 The tumour micro-environment and metabolic adaptations in cancer** ..... **42**

1.3.1 Tumour hypoxia ..... 44

1.3.2 Acidosis ..... 48

1.3.3 Quiescence ..... 50

**1.4 Summary and project aims** ..... **54**

**2. Materials and Methods** ..... **61**

**2.1 Materials** ..... **61**

**2.2 Methods** ..... **62**

2.2.1 Generation and analysis of the tumour spheroid model ..... 62

2.2.2 TS metabolic adaptations ..... 66
2.2.3 Metabolite concentrations ..... 68
2.2.3 Intracellular metabolite analysis ..... 69
2.2.4 Data Analysis ..... 69
**3.1 Establishing Micro-environmental Stress in Tumour Spheroids ..... 74**
**3.1.1 Tumour spheroid growth ..... 75**
**3.1.2 Generation of quiescent TS ..... 77**
**3.1.3 Generation of hypoxic TS ..... 80**
**3.1.4 Metabolic regulators ..... 83**
**3.1.5 Summary and conclusions ..... 85**
**3.2 Nutrient utilization ..... 88**
**3.2.1 Glucose ..... 88**
**3.2.2 Glutamine ..... 95**
**3.2.3 Lactate ..... 98**
**3.2.4 Summary and conclusions ..... 102**
**3.3 Intracellular metabolic adaptations ..... 104**
**3.3.1 Glycolytic pathway enzymes ..... 105**
**3.3.2 Glutaminolytic pathway enzymes ..... 110**
**3.3.3 Shunt Enzymes ..... 112**
**3.3.4 Summary of intracellular adaptations ..... 116**
**4. Discussion ..... 120**
**4.1 Proliferating tumour spheroids ($TS^N$) ..... 122**
**4.3 Hypoxic tumour spheroids ($TS^H$) ..... 129**
**4.4 Quiescent tumour spheroids ($TS^Q$) ..... 140**
**4.5 Conclusions ..... 152**

**5. Appendix ..... 159**

**5.1 Isoprotomer Distribution ..... 159**

**5.2 Gene expression profiling ..... 161**

5.2.1 Gene expression profiling methods ..... 161

5.2.2 Gene Expression profiling of key metabolic enzymes ..... 161

**6. References ..... 162**

# 1. Introduction - Metabolic adaptations to micro-environmental stress in cancer

Cancer is the third leading cause of death worldwide (Thun et al., 2010) and approximately 331,000 people in the UK were diagnosed with cancer in 2011 (Cancer Research UK, 2014). It clearly represents a major burden to global health. Cancer is a series of diseases characterised by uncontrolled cell proliferation and its development is a multistep process during which tumour cells obtain several genetic mutations. The mutations allow: self-sufficiency in growth signalling, insensitivity to antigrowth signals, evasion of apoptosis, limitless replicative potential, promotion of angiogenesis and invasion of host tissues. These key changes in tumour physiology are known as the hallmarks of cancer and were first described by Hanahan and Weinberg (Hanahan and Weinberg, 2000).

The physiology of tumours differs from that of normal tissues, characterized by hypoxia, nutrient deprivation, hydrostatic pressure and a build up of toxic metabolites (Sutherland, 1986; Vaupel, 2004). This hostile environment is principally due to the insufficient vasculature and lack of lymphatic drainage in the tumour (Brown and Giaccia, 1998; Leu et al., 2000). These adverse features of the micro-environment effect the proliferative capacity and viability of cells in the tumour, leading to the development of distinct proliferating, quiescent and

necrotic regions, which are illustrated in *Figure 1* (Brown and Giaccia, 1998; Sutherland, 1986). Moreover, the tumour micro-environment is known to contribute to the failure of many cancer therapies (Jackson, 1989; Rofstad et al., 2000).

Alterations in cancer energy metabolism were first observed by Otto Warburg, who noticed that cancer cells, even in the presence of oxygen, ferment glucose to form lactic acid a process called aerobic glycolysis (Warburg, 1956b). Alterations in energy metabolism have consistently been observed to be a common feature of cancers and are recognised as an emerging cancer hallmark (Hanahan and Weinberg, 2011).

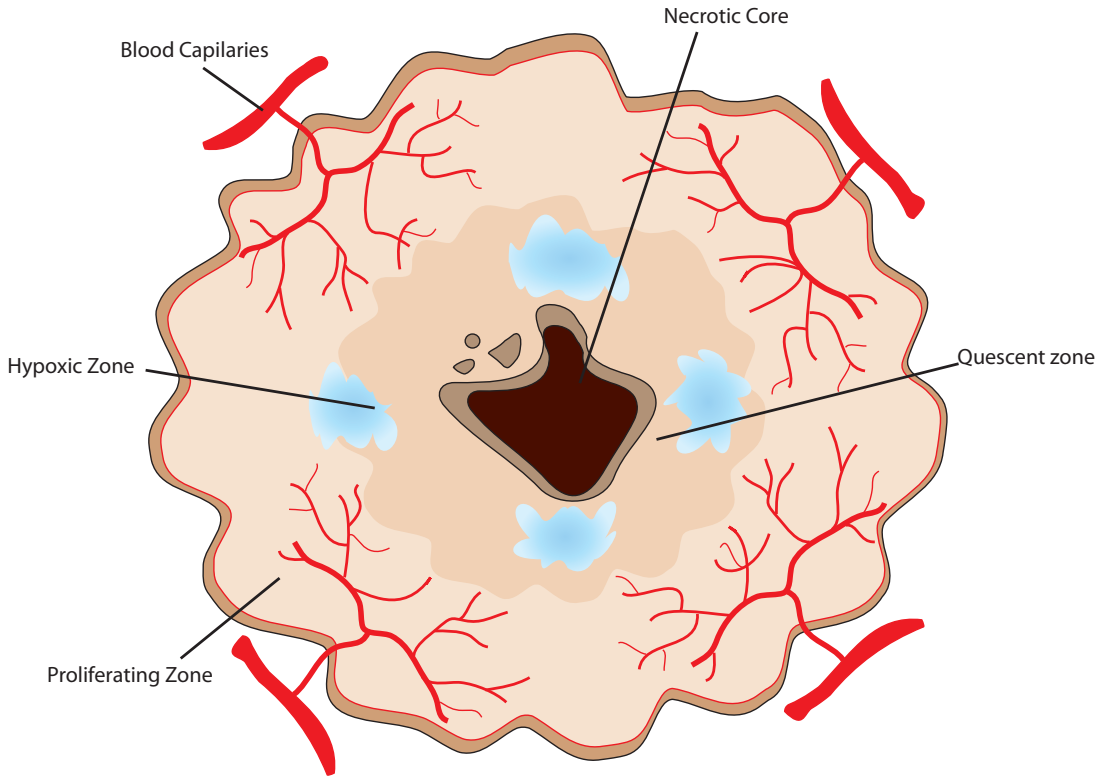



***Figure 1. The tumour micro-environment****. Schematic illustrating some of the different micro-environments and the populations of cells present within tumours.*

## 1.1 The reprogrammed metabolism of cancer cells

The metabolic requirements of rapidly proliferating cancer cells differ drastically from those of normal cells in the body. Numerous studies have shown that cancerous cells reorganise their metabolism utilizing glucose and glutamine to supply sufficient nutrients to support the synthesis of proteins, lipids and nucleic acids required for rapid proliferation. The mechanisms by which these metabolic alterations occur are not yet completely understood and are most likely due to multiple factors. These include activation of oncogenes such as HIF-1 and cMyc which regulate glycolytic gene expression (Cairns et al., 2011). DNA mutations may affect metabolic enzymes directly or via regulators such as p53 that alter expression levels (reviewed in (Chen et al., 2007b)). Finally, changes in the tumour micro-environment, such as the development of hypoxic regions, may also contribute to these metabolic alterations (Cairns et al., 2011). These factors will be further discussed in sections 1.2 and 1.3. This section will summarise the overall adaptations in metabolic pathways observed in solid tumours to date.

### 1.1.1 Alterations in the glycolytic pathway in cancer

Glucose metabolism was demonstrated to differ in cancer cells following the observation of high rates of lactate production from glucose fermentation in the presence of oxygen in ascites cancer cells (Warburg, 1956b). Furthermore, it was

determined that these cells derived 50% of their energy from glycolysis (Warburg, 1956b; Warburg et al., 1927). This was supported by Nakashima et al, who also showed that AS-30D hepatoma cells produced over 50% of their ATP from glycolysis (Nakashima et al., 1984). Additionally experiments looking at glycolysis in cancer cells have revealed that the glycolytic rate, measured by lactate production, is to 9-13 times higher in AS-30D and HeLa cells than in normal hepatocytes (Marin-Hernandez et al., 2006). This increased reliance on glycolysis, which is maintained in the presence of normal oxygen tensions, is referred to as the Warburg effect or aerobic glycolysis. This effect and how it differs to metabolism in normal differentiated cells is illustrated in *Figure 2*. Warburg postulated that this phenomenon was due to dysfunctional mitochondria (Warburg, 1956a, b). However subsequent investigations proved this hypothesis to be incorrect with studies showing purified mitochondria from slow growing hepatomas had little difference in their capacity to respire relative to normal liver mitochondria (Moreno-Sanchez et al., 2007; Pedersen, 2007; Pedersen et al., 1970; Ward and Thompson, 2012). Further experiments have revealed that aerobic glycolysis is not uniquely a feature of cancer cells, it is used in proliferating lymphocytes for example. Wang and colleagues illustrated this, by measuring the rate of DNA synthesis and lactate production in lymphocytes stimulated by concanavalin A to undergo a discrete proliferation of one to two cell divisions. They found that the rate of lactate production closely correlated with DNA synthesis suggesting utilization aerobic glycolysis during cellular division (*Figure 2*)(Wang et al., 1976).

Increased glucose consumption has been determined to be a prevalent feature of cancer metabolism, which may be exploited clinically for cancer detection using the imaging technique positron emission tomography (PET) with the glucose analogue [$^{18}$F]-flurodeoxyglucose (FDG) (reviewed in (Mankoff et al., 2007)). Studies using this technique have correlated increased glucose uptake to tumour aggressiveness and poor prognosis (Gatenby and Gillies, 2004; Kunkel et al., 2003; Mochiki et al., 2004). Finally, analysis of microarray data has determined that the genes encoding the enzymes of glycolysis are over expressed in the majority of cancers (Altenberg and Greulich, 2004).

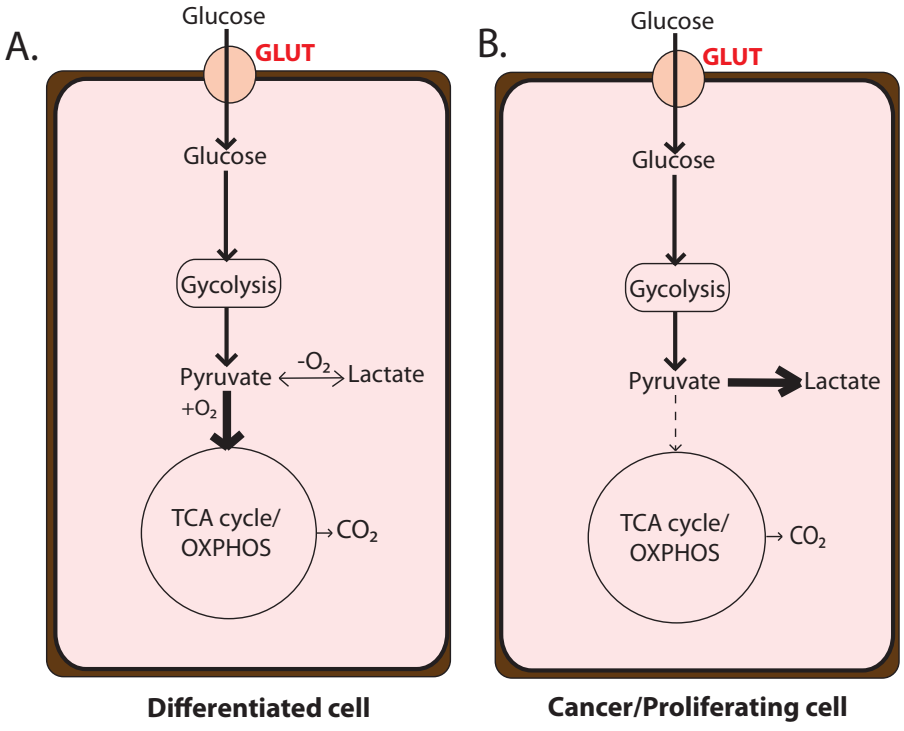



***Figure 2 The Warburg effect vs normal cellular metabolism.*** *Normal differentiated cells generate the majority of their ATP via oxidative phosphorylation (A), which yields 36 ATP per glucose molecule metabolised. These cells only produce lactate in the absence of oxygen via anaerobic glycolysis. Cancer or proliferating cells however employ the Warburg effect (aerobic glycolysis) (B) metabolising glucose to produce lactate even in the presence of sufficient oxygen, this type of metabolism yields 2 ATP per glucose molecule metabolised but has a number of other advantages for the cell.*

The prevalence of the Warburg effect and its correlation with tumour aggressiveness suggests that it confers an important proliferative advantage to cancer cells (Gatenby and Gillies, 2004). These include biosynthetic advantages, since actively proliferating cells require glucose to produce biomass as well as ATP and therefore it is counter productive for cells to completely oxidise glucose to carbon dioxide (Vander Heiden et al., 2009). Consequently, the glycolytic intermediumtes can be used for biosynthesis, for example glucose-6-phosphate can be siphoned off to the pentose phosphate pathway to produce ribose-5-phosphate for synthesis of nucleic acids. The Warburg effect is additionally advantageous to cancer cell survival; the glycolytic metabolism allows the cells to survive fluctuating oxygen conditions resulting from transient variations in tumour perfusion (Dewhirst, 2009) (Gatenby and Gillies, 2004; Kroemer and Pouyssegur, 2008). Furthermore, cells using aerobic glycolysis have been shown to exhibit high ATP/ADP ratios, which have been linked to evasion of cell death and chemoresistance (Vander Heiden et al., 2009; Zhou et al., 2011). For example, investigations of drug resistance in human LoVo colon carcinoma cells, used a drug sensitive parental line and two variably resistant sub-lines, to demonstrate that resistance increased with the rate of aerobic glycolysis and ATP content (Fanciulli et al., 2000). Finally, lactic acid produced from aerobic glycolysis contributes to extracellular acidosis, favouring tumour invasion (reviewed in (Swietach et al., 2007)) and has been demonstrated to suppress infiltrating T cell function (Fischer et al., 2007).

The flux through metabolic pathways such as glycolysis can be regulated by a number of different mechanisms. These include long-term mechanisms such as up or down regulation of enzyme expression, or the expression of alternate isoenzymes. Studies by Alternberg and Greulich have shown that most glycolytic enzymes are over-expressed in 70% of human cancers (Altenberg and Greulich, 2004). Shorter-term mechanisms include enzyme activation or inhibition e.g. by allosteric effectors or by covalent modification. For example, phosphofructokinase-1 (PFK-1) is allosterically inhibited by lactate, which favours dissociation of the active PFK-1 tetramer into dimers (Costa Leite et al., 2007). Finally, flux can be regulated by the accessibility of substrates either via compartmentalization or by the use of metabolites in branching pathways. This was demonstrated by Boada and colleagues, who showed flux through the oxidative pentose phosphate pathway was increased in cells with reduced phosphofructokinase activator fructose-2,6-bisphosphate concentration (Boada et al., 2000). This was hypothesised to be due to accumulation of glucose-6-phophate. In addition, pyruvate dehydrogenase is inhibited by phosphorylation in many cancers due to the activity of pyruvate dehydrogenase kinase 1, thereby reducing flux of pyruvate into the TCA cycle (McFate et al., 2008).

A simplified version of the glycolytic pathway is illustrated in *Figure 3*. Analysis of metabolic control in HeLa cervical cancer cells and AS-30D rodent hepatoma cells has indicated that control of glycolytic flux lies predominantly at the beginning of the pathway. The majority of flux control being attributed to the glucose transport (GLUT) and hexokinase steps, with phosphofructokinase 1

exerting less control (Marin-Hernandez et al., 2010; Marin-Hernandez et al., 2006). These reactions, in addition to the reaction catalysed by pyruvate kinase, are the sites at which the glycolytic pathway is subject to the greatest regulation, and shall be further investigated in the subsequent sections of this report.

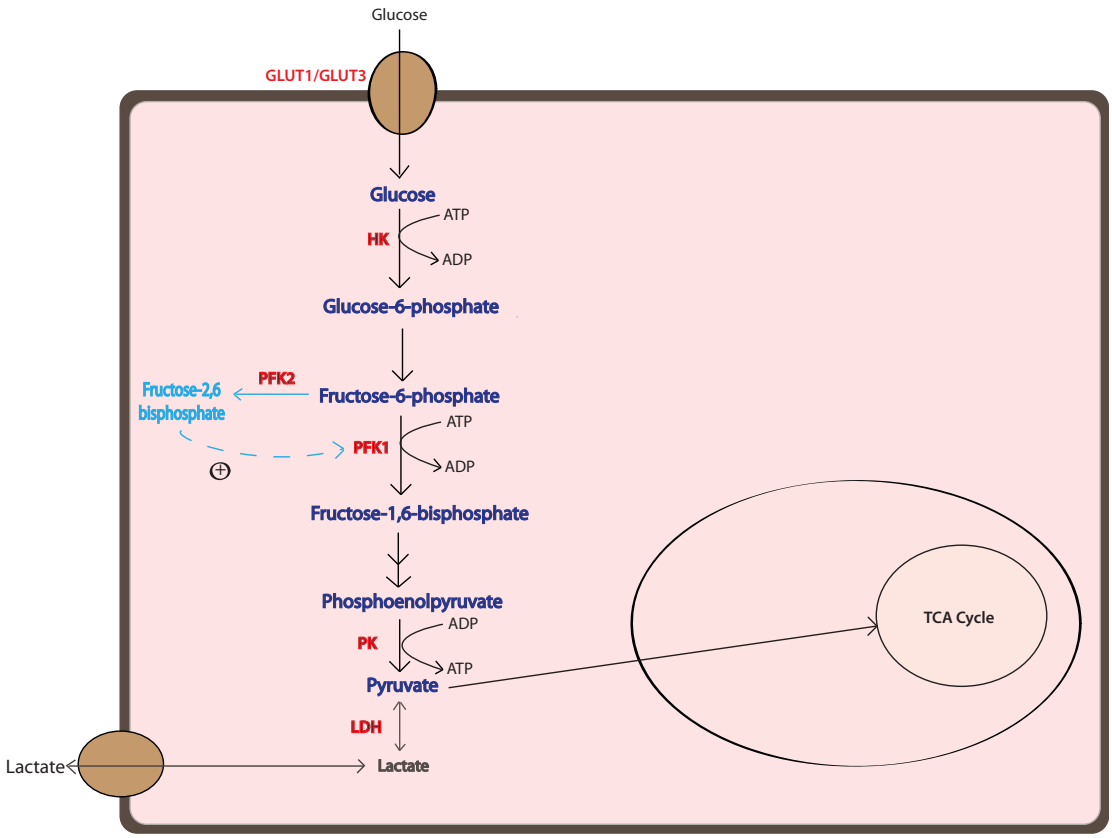



***Figure 3. The Glycolytic pathway.*** *A schematic illustrating the glycolytic pathway. Glycolytic metabolites are highlighted in blue and enzymes in red. Abbreviations Glucose transporter (GLUT), Hexokinase (HK), Phosphofructokinase (PFK), Pyruvate Kinase (PK) and Lactate dehydrogenase (LDH).*

#### *1.1.1.1 Glucose transport*

Glucose transport across mammalian cell membranes is mediumted by two transporter families; the sodium dependent glucose transporters (SGLT) and the glucose transporter family (GLUTs) that mediumte facilitated diffusion (Wood and Trayhurn, 2003). The SGLT family actively transport glucose across the cell membrane utilizing the sodium electrochemical gradient. Although SGLT1

expression has been demonstrated in several cancers including those of the ovary, pancreas and colon (Casneuf et al., 2008; Guo et al., 2011; Lai et al., 2012), the majority of studies to date have focused on the role of the GLUT transporters in cancer. Fourteen distinct members of the GLUT family have been identified which are grouped into three classes based on their structure and sequence. Class 1 contains the well-characterised transporters GLUT1-4, and GLUT14 which is thought to be a duplication of GLUT3 (Augustin, 2010; Calvo et al., 2010). GLUT1 was the first member of this family to be discovered; it is thought to be responsible for basal glucose uptake in most tissues of the body. GLUT1 has a high affinity for glucose, $K_m \sim 3$ mM and its expression level usually correlates with the rate of glucose metabolism (Calvo et al., 2010; Uldry and Thorens, 2004). GLUT2 has a much lower affinity for glucose than GLUT1 ($K_m$~17 mM), allowing it to function in glucose sensing in pancreatic β cells, the liver and kidneys (Uldry and Thorens, 2004; Wood and Trayhurn, 2003). The highest affinity transporter GLUT3 ($K_m$ (2-deoxy-D-glucose)~1.4 mM) is expressed in tissues such as the brain and testes, which have substantial glucose demands, the former is almost reliant on this fuel (Airley and Mobasheri, 2007; Haber et al., 1993; Uldry and Thorens, 2004; Wood and Trayhurn, 2003). Finally, GLUT4 ($K_m$ ~5 mM) is termed the "insulin-responsive" isoform, it is expressed in skeletal muscle, heart and adipose tissue and is translocated to the cell membrane from intracellular vesicles in response to insulin signalling (Uldry and Thorens, 2004; Wood and Trayhurn, 2003).

Numerous studies have revealed that tumours frequently over-express members of the GLUT family (Calvo et al., 2010; Macheda et al., 2005; Medina and Owen, 2002). Increased expression of GLUT1 has been observed in almost all human cancers including, breast, endometrial, renal, hepatic, pancreatic, colorectal, brain, bladder, lung, cervical and ovarian (Brown and Wahl, 1993; Cantuaria et al., 2001; Chang et al., 2000; Krzeslak et al., 2012; Nagase et al., 1995; Nishioka et al., 1992; Rudlowski et al., 2003; Yamamoto et al., 1990). GLUT1 expression has been observed to positively correlate with tumour characteristics such as higher histological grade (Amann and Hellerbrand, 2009; Kang et al., 2002) as well as poorer survival rates (Cooper et al., 2003; Jun et al., 2011; Kang et al., 2002; Younes et al., 1997a). Conversely, although GLUT1 expression was shown to be significantly associated with a better response to chemotherapy, patients with tumours over-expressing GLUT1 had significantly worse disease free survival rates (Cantuaria et al., 2001). This could possibly be due to tumour recurrence from cancer cells surviving chemotherapy, where over-expression of GLUT1 would provide an advantage leading to re-growth of more aggressive tumours (Cantuaria et al., 2001).

There are a number of factors responsible for the up-regulation of GLUT1 in cancer including micro environmental and oncogenic factors. For example, a hypoxic micro-environment has been demonstrated to stimulate GLUT1 expression via several distinct mechanisms. Firstly activated HIF-1 binding to a hypoxia response element within the GLUT1 promoter leads to increased GLUT1 expression (Chen et al., 2001). In addition, studies in a rat liver cell line

determined that GLUT1 mRNA half life was increased to more than 8 hours, relative to 1.5 hours in control cells in response to treatment with the oxidative phosphorylation inhibitor azide (Behrooz and Ismail-Beigi, 1997). This suggests reductions in oxidative phosphorylation results in the stabilisation of GLUT1 mRNA. Over expression of the oncogenic transcription factor cMyc had also been shown to increase GLUT1 mRNA expression and stimulate glucose uptake in Rat1a fibroblasts (Osthus et al., 2000). Finally, investigations have demonstrated that the tumour suppressor p53 plays a role in the regulation of GLUT1. Luciferase reporter assays were used to show that wild type p53 decreases GLUT1 promoter activity to approximately 50% of basal levels (Schwartzenberg-Bar-Yoseph et al., 2004).

The GLUT3 transporter has also been demonstrated to be over-expressed in a number of different types of cancer including; brain, head and neck, pancreas, colon, breast, lung and ovary (Nishioka et al., 1992; Yamamoto et al., 1990; Younes et al., 1997a) (Boado et al., 1994; Medina and Owen, 2002; Younes et al., 1997b). In addition, high GLUT3 expression has been shown to negatively correlate with survival in a broad range of tumour types including brain, breast, colon, ovary and lung (Flavahan et al., 2013). Like GLUT1, GLUT 3 expression has been demonstrated using differential PCR to be induced by hypoxia (1% oxygen), in HeLa cells (O'Rourke et al., 1996). Investigations using mouse hepatoma cells containing a mutation in HIF-1β showed that this induction is dependent on HIF-1 activity (O'Rourke et al., 1996).

Over expression of GLUT4 has been demonstrated in breast and gastric cancers and the transporter has been demonstrated to be important in myeloma (McBrayer et al., 2012; Medina and Owen, 2002). Expression of the GLUT4 transporter is down regulated by mutations in the p53 protein (Schwartzenberg-Bar-Yoseph et al., 2004). Additionally, activation of the Akt oncogene has been shown to promote translocation of GLUT4 to the cell membrane from endosomal vesicles (Kohn et al., 1996). Studies on myocardial ischemia have also suggested that GLUT4 translocation to the membrane occurs in response to acute hypoxia in non-cancerous tissue (Young et al., 1997).

Glucose transporters are therefore over-expressed in numerous cancers and are thought to represent a key control point in the regulation of glycolytic flux (Marin-Hernandez et al., 2006). Moreover, their level of expression reflects tumour status and treatment outcome (Flavahan et al., 2013; Kang et al., 2002). The high affinity of GLUT1, 3 and 4 for glucose means that these transporters would be expected to be saturated at normal blood glucose concentrations of 5.5 mM, indicating that glucose uptake into the cell is dependent on the level of expression of these transporters at the cell membrane. Therefore the entry point of glucose to the cell is a key factor in cancer cell survival.

#### *1.1.1.2 Hexokinase*

The first reaction in the glycolytic pathway is the phosphorylation of glucose to form glucose-6-phosphate, and is catalysed by hexokinase. This reaction essentially traps glucose in the cell since GLUT is a passive transporter (*Figure*

*3*). There are four isozymes of mammalian hexokinase with primarily the hexokinase II (HKII) isoform being over-expressed in cancer cells (Mathupala et al., 2009; Ros and Schulze, 2013; Wilson, 2003). Studies in glioblastoma, lung and breast cancer showed that HKII expression was elevated in tumour samples relative to corresponding normal tissue (Palmieri et al., 2009; Patra et al., 2013; Wolf et al., 2011). Its expression was correlated with tumour pathological grade and with poor patient prognosis. (Palmieri et al., 2009; Patra et al., 2013; Wolf et al., 2011).

A number of features of the HKII isozyme explain its preferential over-expression in cancer. HKII is a 100KDa protein thought to have arisen from gene duplication and fusion of an ancestral 50KDa hexokinase. In contrast to the other hexokinase isoforms, HKII has retained catalytic activity in both N and C terminal halves (Tsai and Wilson, 1996). Characterisation of the enzyme has determined that it has a high affinity for glucose ($K_m$= 0.3 mM)(Wilson, 2003), its activity is regulated via product inhibition by glucose-6-phosphate ($K_i$= 0.02 mM) (Sui and Wilson, 1997; Wilson, 2003). It is associated with the mitochondrial outer membrane via interaction with its N terminal hydrophobic sequence (Wilson, 2003). Pederson and colleagues demonstrated that when HKII is associated with the voltage dependent anion channel (VDAC) in the outer mitochondrial membrane, it is less sensitive to inhibition by glucose-6-phosphate, has an enhanced affinity for ATP and has preferential access to mitochondrial generated ATP (Arora and Pedersen, 1988; Bustamante and Pedersen, 1977, 1980; Nakashima et al., 1986; Nakashima et al., 1988).

In addition to its catalytic role in phosphorylating glucose, HKII has been linked to a number of other important functions in cancer cells. Several studies have demonstrated that association of HKII with the VDAC affects cell survival and inhibition of apoptosis (Mathupala et al., 2006; Robey and Hay, 2006). Additionally, the over-expression of HKII in human lung epithelial-like A549 cells resulted in a two-fold decrease in cell death on exposure to oxidative stress such as hyperoxia or 1 mM hydrogen peroxide relative to control cells (Ahmad et al., 2002). Finally, studies in mouse models of lung and breast cancer showed that HKII was required for tumour initiation and maintenance. For example, HKII knockout in k-ras induced mouse models of non small cell lung carcinoma had reduced tumour burden, reduced proliferation and delayed mortality (Patra et al., 2013).

Studies in rat AS-30D hepatoma cells have shown that the gene for HKII is amplified five fold relative to normal hepatocytes (Rempel et al., 1996). There are a number of mechanisms responsible for the over expression of HKII in tumour cells. For example, HKII is regulated at the transcriptional level by HIF-1, cMyc, glucose, and p53 (Kim et al., 2007b; Mathupala et al., 1997; Mathupala et al., 2001; Rempel et al., 1996; Riddle et al., 2000). Furthermore, recent studies have demonstrated that HKII expression is also down regulated by the microRNA, miR-143 (Fang et al., 2012; Peschiaroli et al., 2013).

HK is therefore a highly regulated enzyme with a number of different roles in the cell, hence it is potentially a key site of flux control in the glycolytic pathway (Marin-Hernandez et al., 2006).

#### *1.1.1.3 Phosphofructokinase 1*

Phosphofructokinase 1 (PFK1) is a tightly regulated enzyme in the glycolytic pathway that catalyses the ATP dependent phosphorylation of fructose-6-phosphate to form fructose-1,6-bisphosphate and ADP, illustrated in *Figure 3*. Active PFK1 is a tetramer, the composition of which depends on tissue specific expression of the isoforms of its monomers; PFK-M the muscle isoform, PFK-L in liver and PFK-P in platelets (Mor et al., 2011). The enzyme is highly regulated at the transcriptional, post-transcriptional and allosteric levels and is therefore thought to be a key point of control of flux through glycolysis in normal non-tumorigenic tissues. Regulation of PFK1 allows it to respond to the bioenergetic status of the cell and its regulatory mechanisms are often exploited in tumour cells. Studies have demonstrated that overexpression and increased activity of PFK1 in tumour cells results in the enzyme having reduced control over glycolytic flux (Marin-Hernandez et al., 2010; Marin-Hernandez et al., 2006).

Investigations in both cancer cell lines and cancer tissue samples have indicated that PFK1 isozyme expression patterns are altered upon malignant transformation. Zancan and colleagues used RT-PCR to show the expression of PFK-L mRNA strongly correlated with aggressiveness and glycolytic efficiency, the ratio of lactate produced to glucose consumed, in breast cancer cell lines (Zancan et al., 2010). More recently, Wang and colleagues used western

immunobloting to reveal a change in the predominant PFK-1 isoform expressed in human breast cancer and paracancer tissue samples (Wang et al., 2013). They determined that PFK-P was the prevalent isoform in cancer tissues switching from PFK-L in paracancer tissues, they also showed a significant positive correlation between PFK-1 activity and PFK-P expression (Wang et al., 2013). These differences could be due to different experimental conditions, for example the use of cell lines versus tissue samples, or, to complexities in PFK1 regulation. For example, the PFK-L gene has been shown to contain a HIF-1 response element and undergoes hypoxia inducible transcription (Semenza et al., 1994).

In addition to regulation at the transcriptional level, PFK-1 is subject to complex post translational and allosteric regulation. Studies by Yi et al, demonstrated glycosylation of PFK-1 by O-linked β-N-acetylglucosamine in multiple cell lines from human solid tumours including breast, liver, colon and cervical cells. Experiments using 293T cells determined that glycosylation occurred at serine 529 in response to hypoxia resulting in inhibition of PFK1 activity, consequently decreasing glycolytic flux, which caused increased pentose phosphate pathway flux (Yi et al., 2012). PFK-1 is allosterically inhibited by lactate, which has been shown to favour dissociation of the active PFK-1 tetramer to less active dimers (Costa Leite et al., 2007). ATP, citrate and long chain fatty acids also allosterically inhibit PFK-1 (Jenkins et al., 2011; Mor et al.; Sola-Penna et al., 2010). On the other hand AMP, ADP and $NH_4^+$ allosterically activate PFK-1, implying that PFK-1 is sensitive to the bioenergetic status of the cell (Mor et al.; Sola-Penna et al., 2010).

The most important regulator of PFK-1 is the modulator fructose-2,6-bisphosphate (F2,6BP), formed under conditions of high fructose-6-phosphate availability. F2,6BP is synthesised and degraded by the bifunctional enzyme 6-phosphofructo-2-kinase/fructose-2,6-bisphosphatase (PFK2/FBPase or PFKFB) (*Figure 3*)(Chesney, 2006; Hue and Rousseau, 1993), of which there are four isoforms. Cancer cells express increased levels of the PFKFB3 isoform (referred to as ubiquitous PFK2, placental PFK-2 or PRG1 (Atsumi et al., 2002)) which has the highest ratio of kinase to phosphatase activity, essentially functioning only as a kinase (Atsumi et al., 2002; Sakakibara et al., 1997). Investigations on PFKFB3 have determined it is induced by hypoxia. Analysis of the PFKFB3 promoter revealed a hypoxia response element and studies demonstrating HIF1 binding and transactivation of the gene confirmed that PFKFB3 is a HIF-1 target gene (Minchenko et al., 2002; Obach et al., 2004). Finally F2,6BP levels are also regulated by p53 via TIGAR (TP53-induced-glycolysis-and apoptosis regulator), which functions as a bisphosphatase reducing F2,6BP levels in the cell (Bensaad et al., 2006).

Hence PFK is highly regulated transcriptionally, post-transcriptionally and allosterically, resulting in its activity being highly responsive to the bioenergetic status of the cell. This is exploited in cancer cells, perhaps explaining the low flux control exerted by this enzyme in previous studies (Marin-Hernandez et al., 2006).

#### *1.1.1.4 Pyruvate Kinase*

Pyruvate kinase (PK) catalyses the final step in the glycolytic pathway, transfer of a phosphate group from phosphoenolpyruvate (PEP) to ADP producing pyruvate and ATP (*Figure 3*) (Mazurek, 2011). There are four isoforms of PK encoded by two genes PK-L and PK-M. Alternative splicing of PK-L produces PK-L and PK-R and the PK-M gene produces PKM1 and PKM2 due to the inclusion of exon 9 or 10 respectively (Noguchi et al., 1986; Tsutsumi et al., 1988). PKM1 is expressed in tissues with high-energy demands, for example the brain or muscle, whereas PKM2 is expressed in tissues such as adipose and lung in addition to proliferating cells such as embryonic cells and adult stem cells (Israelsen et al., 2013; Mazurek, 2011; Mukherjee et al., 2013).

PKM was identified as being a potential HIF-1 inducible gene in a screen of HIF-1 responsive genes (Semenza et al., 1994). The mRNA of PKM was induced in Hep3B and HeLa cells in response to the known HIF-1 inducers, hypoxia, cobalt chloride and desferrioxamine (Semenza et al., 1994). Analysis of the PKM2 gene sequence identified a HIF-1 binding site within the first intron of the gene and luciferase reporter assays indicated that HIF-1 binding increased transcription (Luo et al., 2011). Alternative splicing of the PKM gene is also regulated indirectly by cMyc through its up-regulation of the heterogeneous nuclear ribonucleoproteins (hnRNPs), hnRNPI, hnRNPA1 and hnRNPA2. These hnRNPs bind repressively to the sequences flanking exon 9, causing the inclusion of exon 10 and hence PKM2 expression (David et al., 2010).

Many studies have determined that the PKM2 isoform is predominantly expressed in cancer cells (Christofk et al., 2008a; Wong et al., 2013). Investigations including those by Mukherjee and colleagues, show that the expression and levels of PKM2 protein are significantly up-regulated in aggressive glioblastoma multiforme compared to normal brain tissue (Mukherjee et al., 2013). From their studies in a mouse model of breast cancer, Christofk and colleagues hypothesized that cancer cells switch expression during tumorigenesis to the PKM2 isoform (Christofk et al., 2008a). However, this has been contested. For example, Bluemlein et al used mass spectrometry to demonstrate that although PKM was expressed at higher levels in a number of different types of human cancer tissue samples compared to control tissues, there was no difference in proportion of PKM isoforms, PKM2 being predominant in both (Bluemlein et al., 2011).

The PKM2 isoform is distinct from the other PK isoforms in that it occurs in both a highly active tetrameric form and an almost inactive dimeric form (Mazurek et al., 2005; Zwerschke et al., 1999). The quaternary structure of PKM2 is regulated by a number of different factors, illustrated in *Figure 4*, that reflect the metabolic status of the cell. This includes feed-forward regulation by the glycolytic intermediate fructose-1,6-bisphosphate (F16BP), which promotes formation of the active tetramer (Ashizawa et al., 1991). Additionally, the amino acid serine, which can be synthesised from the glycolytic intermediate glycerate-3-phosphate, allosterically activates PKM2, increasing its affinity for PEP by 2.3 fold (Chaneton et al., 2012; Mazurek et al., 2005). Conversely, phosphorylation of

PKM2 at tyrosine residue $Y^{105}$, or PKM2 binding of tyrosine phosphorylated peptides, disrupts F16BP binding and inhibits the tetramer formation and hence enzyme activity (Christofk et al., 2008b; Hitosugi et al., 2009). Phosphorylation of $Y^{105}$ was demonstrated in various human tumour cell lines, including those from lung, breast and prostate cancers (Hitosugi et al., 2009). PKM2 is additionally inhibited by amino acids such as alanine, saturated and monounsaturated fatty acids and by increases in intracellular reactive oxygen species (ROS), through oxidation of cysteine residue, $C^{358}$ (Anastasiou et al., 2011; Mazurek et al., 2005; Wu and Le, 2012). The proportion of PKM2 in the active tetramer vs the inactive dimer therefore varies depending on the current metabolic status of the cell.

This variation between active and inactive forms has a number of advantages for proliferating cells. When PKM2 is an inactive dimer, upstream phosphometabolites in the glycolytic pathway accumulate. The metabolites may thereby be siphoned off for biosynthetic pathways (Mazurek, 2011; Mazurek et al., 1997). For example glucose-6-phosphate can enter the pentose phosphate pathway to produce ribose sugars, or dihydroxyacetone-phosphate used for phospholipid synthesis. In addition, low PKM2 activity results in low ATP:ADP ratios thus ensuring PFK1 activation (Wu and Le, 2012).

Numerous investigations have also revealed further roles for PKM2. Recent studies have shown that PKM2 can localise to the nucleus in response to signals such as interleukin-3 stimulation (Hoshino et al., 2007) or epidermal growth factor receptor activation (Yang et al.) where it can participate in the regulation

of gene transcription (Gao et al., 2012; Yang et al., 2011). Interestingly PKM2 can also bind to HIF-1α promoting HIF-1 transactivation of its target genes (Luo et al., 2011), thus participating in a positive feedback loop.

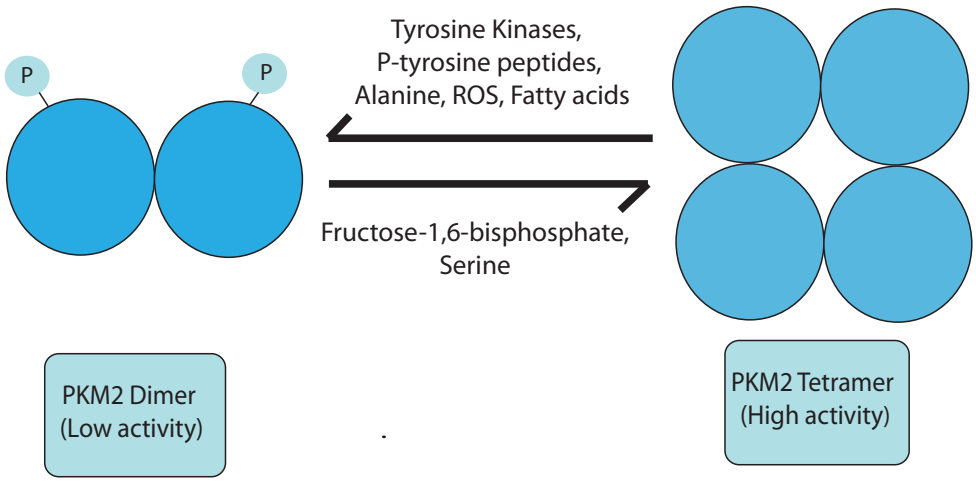



***Figure 4. Regulation of PKM2 quaternary structure.*** *PKM2 switches between a highly active tetramer and an inactive dimer. This transition is influenced by a number of different factors that indicate the bioenergetic status of the cell. Fructose-1,6-phosphate and serine promote the active tetramer, while phosphorylation at tyrosine 105, tyrosine phosphorylated peptides, saturated and monounsaturated fatty acids, reactive oxygen species and alanine promote the formation of the inactive dimer.*

PKM2 is therefore a significant enzyme in cancer metabolism. It is highly regulated at multiple levels responding to nutritional and stress signals (reviewed (Wu and Le, 2012) and it also exerts regulation upon gene expression per se (Luo et al., 2011). PK would therefore be thought to be a prime point for flux regulation.

### 1.1.2 The pentose phosphate pathway

The pentose phosphate pathway (PPP), illustrated in *Figure 5*, is a branch or shunt pathway from glycolysis, whose major function is the production of NADPH, glutathione (GSH), and ribose-5-phosphate (R5P) (Wood, 1986).

NADPH is essential in cellular metabolism, functioning as a cofactor in the biosynthesis of many macromolecles. It also provides reducing power to regenerate gluthathione, which is important in scavenging and detoxifying ROS (Cairns et al., 2011). R5P is produced in the oxidative phase of the PPP and is used for nucleotide synthesis. In rapidly dividing cancer cells the PPP has been shown to contribute to a significant proportion of the ribose incorporated into nucleic acids. For example Boros et al determined that the pathway contributed 85% of the ribose incorporated into RNA in cultured pancreatic cancer cells (Boros et al., 1997).

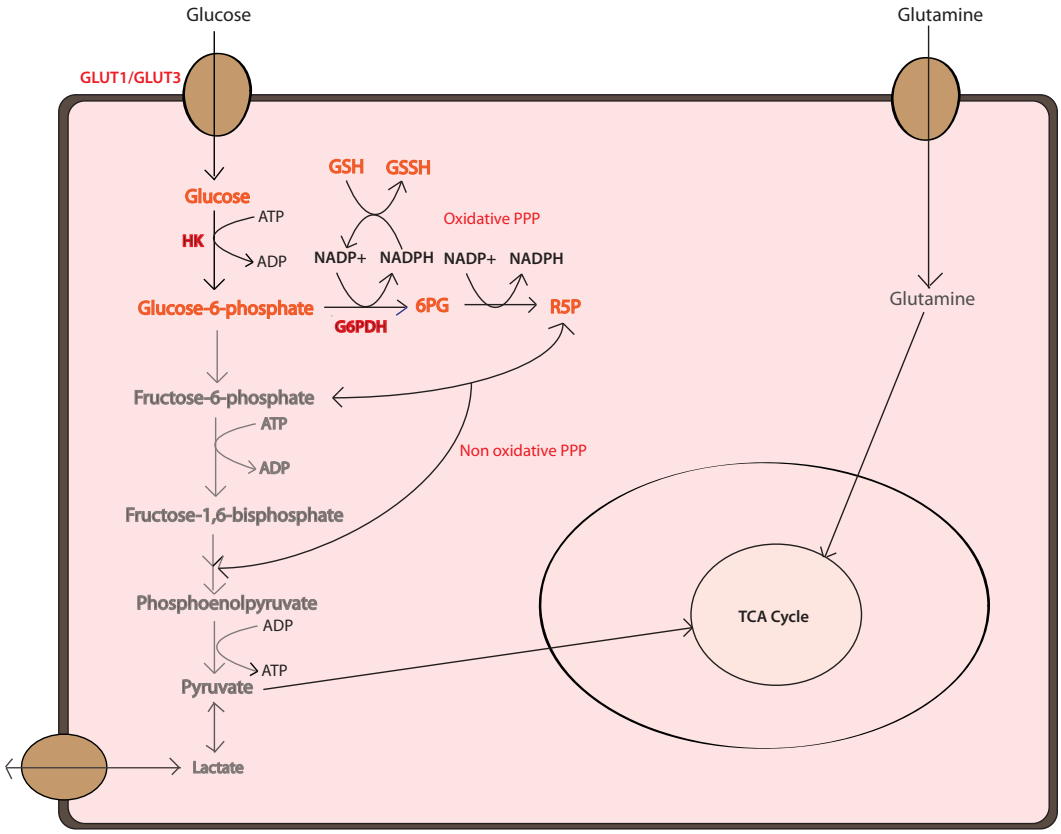



***Figure 5. The Pentose Phosphate Pathway.*** *A simplified schematic of the pentose phosphate pathway which branches from the glycolytic pathway. Metabolites are indicated in orange and are abbreviated 6 phosphogluconate (6PG), ribose-5-phosphate (R5P), reduced glutathione (GSH) and oxidised glutathione (GSSH). The enzyme glucose-6-phosphate dehydrogenase (G6PDH, red) catalyses the initial step in the oxidative branch of this pathway.*

The PPP consists of two distinct branches (*Figure 5*); the non-reversible oxidative branch that produces NADPH and R5P and the non oxidative branch which catalyses the conversion of sugars to produce R5P or glycolytic intermediumtes (reviewed in (Riganti et al., 2012)). Glucose-6-phosphate dehydrogenase (G6PDH) is a tightly regulated enzyme that catalyses the initial step in the oxidative branch and is often referred to as the rate limiting enzyme in this branch (Stanton, 2012). Both the activity and expression of G6PDH has been shown to be elevated in many different cancers compared to normal tissue (Board et al., 1990; Chen et al., 2007a; Wang et al., 2012). Moreover, Tian et al correlated G6PDH activity with cell growth (Tian et al., 1998). In addition, over-expression of G6PDH in NIH-3T3 cells resulted in tumorigenic transformation, with rapid proliferation, loss of contact inhibition and anchorage independent growth (Kuo et al., 2000).

G6PDH is regulated at both the transcriptional and post transcriptionl level. One of the major determinants of G6PDH activity is the ratio of [$NADP^+$]/[NADPH] in the cell, with $NADP^+$ allosterically activating the enzyme (Holten et al., 1976; Luzzatto, 1967). Determination of the structure of G6PDH revealed that in addition to the substrate binding stite, there is an additional $NADP^+$ binding site (Au et al., 2000). Binding of $NADP^+$ to this site stablised the enzyme in the active dimeric conformation (Au et al., 2000). Investigations also found that G6PDH activity is inhibited by p53 binding directly to the enzyme (Jiang et al., 2011). G6PDH expression is positively regulated by a number of factors that indicate

cellular redox and proliferation status including vitamin C, vitamin D, insulin and mTOR (Bao et al., 2008; Duvel et al., 2010; Puskas et al., 2000; Stanton, 2012; Wagle et al., 1998).

The PPP plays an essential role in cancer metabolism, providing intermediumtes necessary for nucteotide synthesis (hence proliferation), in addition to protecting the cells against oxidative damage therefore reducing the efficacy of many chemo and radiotherapy (Riganti et al., 2012). G6PDH is a highly regulated component of this pathway whose activity is frequently increased in cancer to generate biomass to sustain high rates of proliferation.

### 1.1.3 Glutamine metabolism in cancer cells

Glutamine is the most abundant amino acid in plasma and is a key nutrient for cancer cells (Bergstrom et al., 1974). The importance of glutamine was initially demonstrated in studies showing the requirement of glutamine for optimum growth of HeLa cells (Eagle, 1955; Eagle et al., 1956). This has been corroborated by further research in different cell lines and culture models, determining that glutamine deprivation inhibits cancer cell growth (Tannock et al., 1986). *In vitro* experiments have also demonstrated increased glutamine consumption in human hepatoma cell lines compared to normal hepatocytes (Bode et al., 1995).

Glutamine is metabolised by the glutaminolysis pathway, illustrated in *Figure 6*, and performs several important roles within cells. These include: the use of the carbon skeleton for anaplerosis and its oxidation for energy production. (Daye

and Wellen, 2012; DeBerardinis et al., 2007) The amino and amine groups of glutamine provide nitrogen donation for the synthesis of nucleotides. Finally glutamine is a precursor of glutathione, which is a major cellular antioxidant (Daye and Wellen, 2012).

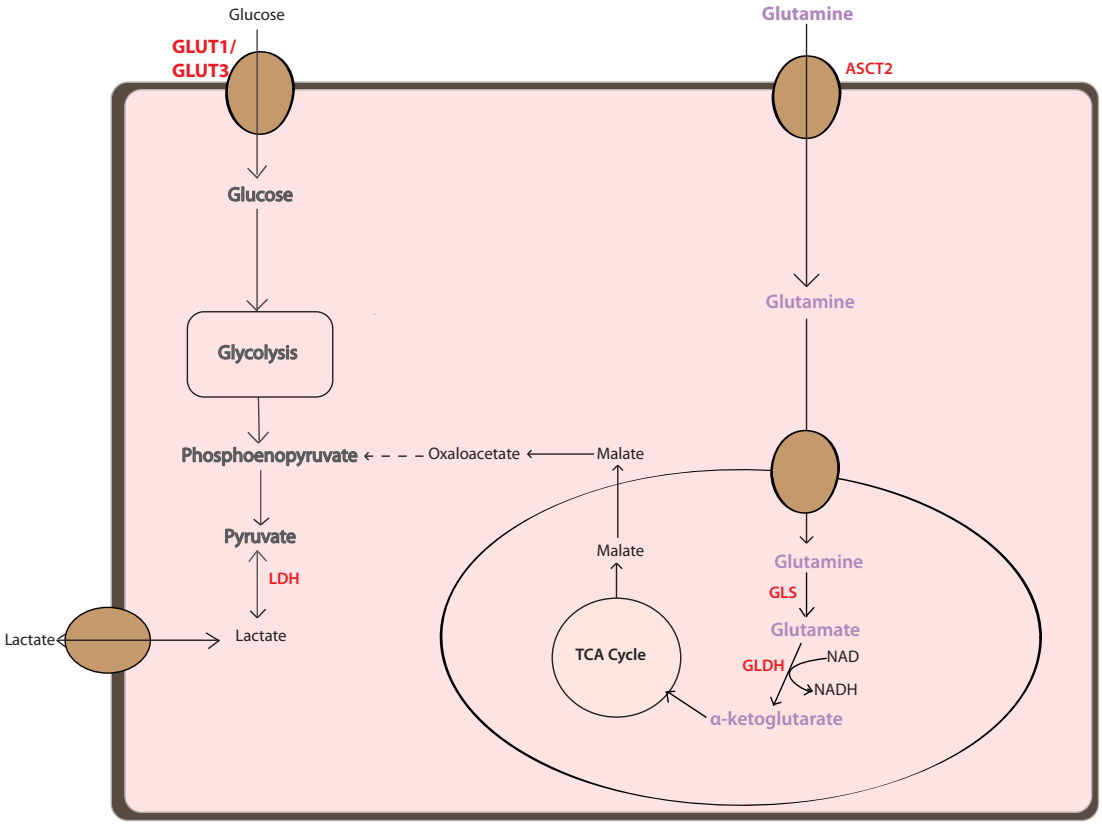



***Figure 6. The Glutaminolysis pathway.*** *A schematic of the glutaminolysis pathway, a highly utilized pathway in cancer cells by which glutamine is metabolised to the TCA cycle intermediate α-ketoglutarate. Key metabolites are indicated in purple. Glutamine is transported into the cell by the amino acid exchanger ASCT2 (Red) prior to being hydrolysed by glutaminase (GLS, Red) and finally oxidatively deaminated by glutamate dehydrogenase (GLDH). Glutamine derived carbon can be metabolised to lactate via the malate reaction as shown.*

Whilst there are several different families of transporters that can mediumte cellular glutamine uptake, there are no transporters that are specific for glutamine (Bode, 2001). The $Na^+$ coupled amino acid exchanger ASCT2 (gene name SLC1A5) is up-regulated in an array of different cancerous tissues and is

thought to be a key mediumtor of tumour glutamine uptake (Fuchs and Bode, 2005). The expression of ASCT2 is regulated both by the availability of glutamine and by the oncogenic transcription factor cMyc (Bungard and McGivan, 2004; Wise et al., 2008). The importance of ASCT2 in cancer cell growth and viability has been highlighted in several studies. For example, Fuchs and colleagues showed that ASCT2 knockdown in SK-hepatoma cells using antisense RNA resulted in cellular apoptosis (Fuchs et al., 2004). More recently, studies in melanoma cell lines have show that the knockdown of ASCT2 using shRNA, or its inhibition using Benzylserine resulted inhibited mTORC1 signalling and cell proliferation (Wang et al., 2014).

Once imported into the cell by ASCTS glutamine is hydrolysed to produce glutamate in the mitochondrial matrix by the enzyme glutaminase (GLS) (*Figure 6*). There are two isoforms of glutaminase, GLS1 (kidney type) which is up regulated with increased rates of proliferation and GLS2 (liver type) that is present in cells that are in a quiescent or resting state (Perez-Gomez et al., 2005). The importance of GLS in cancer cells was demonstrated in antisense mRNA silencing studies. Silencing resulted in decreased cell growth rates in Ehrlich ascites carcinoma cells and loss of tumorigenic potential in *in vivo* mouse experiments (Lobo et al., 2000). Expression of GLS1 is indirectly activated by the oncogenic transcription factor cMyc through its repression of the microRNA's miR-23a and miR23b (Gao et al., 2009). In contrast, studies have determined that expression of GLS2 is induced by the tumour suppressor p53 (Suzuki et al., 2010).

There are a number of possible metabolic fates for the glutamate produced by glutaminase. It can be converted to the antioxidant glutathione by glutamate cysteine ligase (Lu, 2013). Alternatively Glutamate dehydrogenase (GLDH) catalyses the reversible oxidative deamination of glutamate to form the TCA cycle intermediate α-ketoglutarate, using $NAD(P)^+$ as a coenzyme (*Figure 6*) (Li et al., 2010; Plaitakis and Zaganas, 2001). The α ketoglutarate supplied by this reaction can be oxidised completely via the TCA cycle, used as an anaplerotic precursor for biosynthesis, or it can be converted to lactate via the malic enzyme (Hensley et al., 2013). Metabolic profiling in glioblastoma cells revealed that the majority of glutamine derived carbon was secreted as lactate allowing robust generation of NADPH, which is required for anabolic processes including fatty acid and nuclotide synthesis (DeBerardinis et al., 2007). The importance of glutaminolysis and GLDH has further been demonstrated in glioblastoma cells, where GLDH activity is increased in response to glucose deprivation and is essential for the survival of cells with impaired glycolysis (Yang et al., 2009).

The GLDH enzyme is a key point of regulation in the glutaminolysis pathway being subject to a complex web of allosteric regulation and post-translational modification. GLDH is subject to ADP-ribosylation by SIRT 4 which inhibits GLDH activity, for example in response to DNA damage (Haigis et al., 2006; Herrero-Yraola et al., 2001; Jeong et al., 2013). Jeong and colleagues demonstrated that SIRT4 mediumted inhibition of GLDH in response to DNA damage resulted in decreased proliferation and promoted cell cycle arrest,

thereby illustrating the importance of glutamine metabolism for proliferation (Jeong et al., 2013). In addition, recent studies have shown that transcription of SIRT4 is repressed by the mammalian target of rapamycin complex 1 (mTORC1), a key regulator of cell growth that is often deregulated in cancers, resulting in increased GLDH activity (Csibi et al., 2013). GLDH is allosterically inhibited by cellular markers of high-energy metabolic status including, GTP, ATP and NADPH. The enzyme is also activated by ADP and leucine hence its activation status reflects the metabolic status of the cell (reviewed extensively in (Li et al., 2010; Smith and Stanley, 2008)).

### 1.1.4 Lactate metabolism in cancer cells

Increased lactate production in cancer cells under aerobic conditions was an important observation of the Warburg effect (Warburg et al., 1927). Lactate is produced in cancer cells from the metabolism of both glucose and glutamine (DeBerardinis et al., 2007), as shown in *Figure 3* and *Figure 6*. High lactate levels have been found to correlate with metastasis, tumour recurrence and poor clinical outcome in several types of human cancers, including head and neck, cervical and non-small cell lung cancer (Walenta et al., 2000).

Lactate is generated from pyruvate by the bidirectional enzyme lactate dehydrogenase (LDH) with the simultaneous conversion of NADH to $NAD^+$. This regeneration of $NAD^+$ is vital to enble continued glycolysis. There are five different isoforms of the active LDH tetrameric enzyme dependent on its composition of LDH-A (LDH-M) and LDH-B (LDH-H). LDH-A is predominantly

found in highly glycolytic tissues such as skeletal muscle and kinetically favours the converison of pyruvate to lactate. LDH-B (LDH-H) is found in aerobic tissues such as the heart and favours the reverse reaction (Adeva et al., 2013)).

Elevated expression of LDH-A has been observed in numerous human cancers (Goldman et al., 1964) and it is a known target of the oncogenic transcription factors HIF-1 and cMyc (Firth et al., 1995). Mass spectrometry studies determined that the oncogenic receptor tyrosine kinase FGFR1 phosphorylates LDH-A at residues Y10 and Y83. Further phosphoproteomic experiments revealed that LDH-A is commonly phosphorylated at Y10 in both human cancer tissue samples and cell lines. Tyrosine phosphorylation of LDH-A was shown to enhance ennzyme activity by promoting both the formation of the active tetramer and the binding of NADH (Fan et al., 2011). The importance of LDH-A activity in the Warburg effect has been demonstrated in several studies. For example, knock-down of LDH-A by short hairpin RNAs in the breast cancer cell line, 4T1, resulted in reduced glucose consumption, lower glycolysis, increased oxygen consumption and elevated rates of oxidative phosphoryation. These metabolic alterations were also associated with delayed metastasis and reduced tumour growth relative to control cells (Fantin et al., 2006). However the causal nature of this associatiation is not known.

The role of LDH-B in cancer metabolism is less understood than that of LDH-A at the present time. Investigations have shown silencing of LDH-B expression by promoter methylation in different types of cancer including, colon rectal,

prostate, breast and gastric (Brown et al., 2013; Leiblich et al., 2006; Maekawa et al., 2003; Thangaraju et al., 2009). Conversely, LDH-B over-expression has been reported in KRAS mutant lung tumours, testicular germ cell tumours and in triple-negative breast cancers relative to other breast cancer subtypes (McCleland et al., 2013; McCleland et al., 2012; Rodriguez et al., 2003). Additionally, high tumour expression of LDH-B in breast cancer and lung adenocarcinoma patients correlated to a poorer clinical outcome (McCleland et al., 2013; McCleland et al., 2012). These contradictory findings suggest that the role of LDH-B in cancer metabolism may be specific to the tissue or tumour in context. Further work is therefore required to fully elucidate the pathways regulating LDH-B in cancer.

Tumour cells utilize a number of mechanisms to prevent cytoplasmic acidification including the up-regulation of monocarboxylate transporters (MCTs) to avoid lactate accumulation in the cell. MCT isoforms 1-4 facilitate the bidirectional symport of monocarboxylates, including lactate and pyruvate and protons across the cell membrane (Halestrap and Price, 1999). The MCT1 and MCT4 isoforms are thought to play a key role in cancer cell metabolism. Increases in the levels of MCT1 and MCT4 has been observed in many tumour tissue samples relative to normal control tissues including glioblastoma, prostate cancer, colon cancer, and breast cancer (Miranda-Goncalves et al., 2013; Pertega-Gomes et al., 2011; Pinheiro et al., 2010; Pinheiro et al., 2008a).

MCT1 is expressed in the majority of tissues in the body, it mediumtes the import or export of lactate from cells depending upon their metabolic status (Halestrap and Wilson, 2012). Whilst MCT4 is predominantly expressed in glycolytic tissues such as skeletal muscle, MCT4 has a lower affinity for lactate than MCT1 and mediumtes lactate efflux (Dimmer et al., 2000; Halestrap and Meredith, 2004). In accord with its expression in glycolytic tissues MCT4 is a known target of HIF-1 which mediumtes its up regulation in response to hypoxia (Ullah et al., 2006). MCT1 expression has been shown to be reduced by the tumour suppressor p53 under hypoxia (Boidot et al., 2012). Loss of p53, was shown to result in increased MCT1 protein levels in human colon cancer cells under hypoxic conditions, likely due to increased mRNA stability (Boidot et al., 2012). MCT1 is also upregulated in response to extracellular lactate in L6 rat skeletal muscle cells via a ROS dependent mechanism (Hashimoto et al., 2007). This may be of relevance in the tumour micro-environment which is considerably acidic (pH 6.5-6.9) compared to normal tissues (pH 7.2-7.4) due in part to increased lactate production (Estrella et al., 2013).

Recent studies suggest that lactate may be much more than a waste product, in fact, it is hypothesised to form the basis of a metabolic symbiosis between different populations of cells within a tumour. As illustrated in *Figure 7*, this symbiosis involves glucose metabolism in hypoxic, tumour cells producing lactate which is effluxed by MCT4. Lactate is taken up via MCT1 in oxidative tumour cells and metabolized within mitochondria, thereby allowing conservation of glucose for use in hypoxic cells dependent on glycolysis

(Sonveaux et al., 2008b). This theory is based upon studies by Sonveaux et al who found that lactate could be used as a fuel by oxidative tumour cells (Sonveaux et al., 2008b). They demonstrated that MCT1 was exclusively expressed in the oxygenated regions of xenograft tumours. Additionaly MCT1 inhibition by α-cyano-4-hydroxycinnamate (CHC) in human cervial cancer cells, a mouse model of lung cancer and xenotransplanted human colon cancer cells, resulted in switching to glycolysis from lactate fueled energy production and *in vivo* caused reduced tumour growth and hypoxic cell death (Sonveaux et al., 2008b).

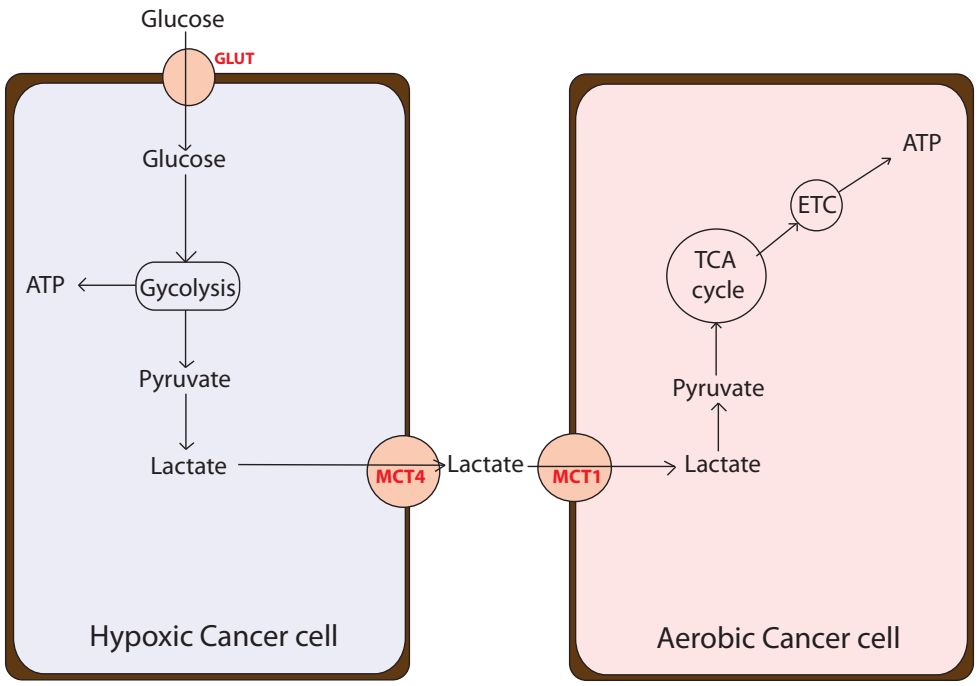



***Figure 7. The Lactate Symbiosis*** *Theory. Schematic illustrating the lactate symbiosis theory, lactate produced from glycolysis in hypoxic cancer cells is exported by the monocarboxylate transporter 4 (MCT4, red) only to be taken up by aerobic cancer cells using MCT1 (Red) for metabolism via the TCA cycle.*

## 1.2 Cell Signalling and metabolic adaptations in cancer

Recent research has revealed that the metabolic reprogramming observed in cancer cells is directly controlled by signalling pathways involving known oncogenes and tumour suppressor genes (reviewed in (DeBerardinis et al., 2008; Vander Heiden et al., 2009)). These include the oncogenes Akt (PI3K/Akt/mTOR pathway), cMyc and HIF1α in addition to the tumour suppressor genes p53 and AMPK.

### 1.2.1 Dysregulation of the Akt pathway

Akt (or Protein kinase B) is a highly conserved serine/threonine kinase in the phosphoinositide 3 kinase (PI3K) signalling pathway, that functions to promote cell growth, proliferation, metabolism, and cell survival (Liang and Slingerland, 2003; Manning and Cantley, 2007). Dysregulated activation of Akt is frequently observed in cancers (Altomare et al., 2002; Balsara et al., 2004; Yuan et al., 2000) and involves several mechanisms. For example, Akt is constitutively activated in cancer through inactivation of the tumour suppressor PTEN (Cantley and Neel, 1999) or activation of the upstream kinase PI3K (Samuels et al., 2004).

The metabolic consequence of Akt activation is to promote aerobic glycolysis in cancer cells (Elstrom et al., 2004). Human glioblastoma cell lines have been used to show that activated Akt produced high rates of glucose consumption and lactate production compared to cells lacking Akt activity (Elstrom et al., 2004). This stimulation of aerobic glycolysis was achieved by Akt acting at several points in glucose metabolism. For example, activated Akt induces the expression of GLUT1 (Barthel et al., 1999) and translocation of GLUT4 to the cell membrane

(Kohn et al, 1996). Akt stimulates basal hexokinase activity (Rathmell et al., 2003) as well as promoting its association with the mitochondrial outer membrane (Majewski et al., 2004). Additionally, Akt phosphorylates and activates phosphofructokinase 2 (PFK2), thereby indirectly enhancing PFK1 activity (Deprez et al., 1997).

Akt also promotes the flux of carbon into biosynthetic pathways such as lipid synthesis by phosphorylating and activating the enzyme ATP-citrate lyase (ACL) (Berwick et al., 2002). ACL converts cytosolic citrate to acetyl-CoA, a substrate for lipid synthesis, which is essential for the synthesis of membranes and therefore cell growth (Bauer et al., 2005). Citrate is also a negative allosteric regulator of PFK1 and its conversion to acetyl-CoA could also indirectly promote PFK1 and therefore glycolytic activity.

Dysregulated activation of Akt or the PI3K signalling pathway therefore promotes the glycolytic phenotype often observed in cancer cells as predicted by the Warburg hypothesis.

### 1.2.2 p53 and cancer metabolism

The tumour suppressor p53 was identified in 1979, and is one of the most commonly mutated genes in human cancer (Vogelstein et al., 2000). p53 is normally activated in response to cellular stress, which arrests the cell cycle and allows cells to repair any damage. Under severe stress it activates apoptosis, thereby preventing the perpetuation of many oncogenic mutations (reviewed in

(Vogelstein et al., 2000)). Recent studies have linked p53 to cellular metabolism since its normal its function opposes many of the metabolic adaptations normally observed in cancer cells (Maddocks and Vousden, 2011).

p53 operates to limit glycolytic flux via several different mechanisms. Firstly p53 limits glucose uptake by down-regulating the expression of glucose transporters, GLUT 1 and GLUT4 at the level of transcription (Schwartzenberg-Bar-Yoseph et al., 2004). p53 also indirectly reduces GLUT3 expression by restricting the activation of the transcription factor NF-κB (Kawauchi et al., 2008). The activity of PFK1 is also down regulated indirectly by p53 through the activity of TIGAR (TP53-induced-glycolysis-and apoptosis regulator). TIGAR functions as a bisphosphatase, reducing the levels of the PFK1 activator F2,6BP in the cell (Bensaad et al., 2006). Kondoh et al demonstrated that p53 caused a reduction in phophoglycerate mutase (PGM) protein levels in mouse embryo fibroblasts, however changes in mRNA levels were not observed suggesting p53 results in reduced translation or stability of PGM (Kondoh et al., 2005). Conversely investigations have found p53 response elements in the hexokinase II promoter region, that can be activated by mutant p53 (Mathupala et al., 1997). Consequently, the mutations in p53 commonly observed in cancer inactivate its function and eliminate the dampening regulation upon glycolytic flux.

In addition to inhibition of glycolysis, p53 promotes oxidative phosphorylation, thereby opposing the Warburg effect. Matoba et al identified SCO2 (Synthesis of Cytochrome c Oxidase 2) as a transcriptional target of p53 (Matoba et al., 2006).

SOC2 is essential for the assembling the cytochrome c oxidase II subunit into the cytochrome c oxidase complex of the electron transport chain (Matoba et al., 2006). Cytochrome c oxidase is the component of the electron transport chain where oxygen is consumed via its reduction forming water, therefore p53 directly regulates oxidative phosphorylation. This regulation is further evidenced by the significant reductions in oxygen consumption measured when p53 is disrupted in mice and in human colon cancer cells (Matoba et al., 2006). Furthermore, Glutaminase 2 (GLS2) also been identified as a p53 induced target gene (Hu et al., 2010; Suzuki et al., 2010). GLS2 is part of the glutaminolysis pathway producing the TCA cycle intermediate α-ketoglutarate. Increased GLS2 expression was shown to result in elevated oxygen consumption and ATP levels in several human cancer cell lines (Hu et al., 2010), indicating that GLS2 promotes oxidative phosphorylation, probably by increasing α-ketoglutarate levels. Additionally GLS2 expression has been linked to lower levels of intracellular reactive oxygen species (ROS) and increased reduced glutathione levels, indicating it plays a role in p53 mediumted antioxidant defence (Hu et al., 2010; Suzuki et al., 2010).

Finally, p53 also functions to regulate entry to the pentose phosphate pathway. Jiang et al recently demonstrated p53 mediumted inhibition of glucose-6-phosphate dehydrogenase the first enzyme in the oxidative pentose phosphate pathway (Jiang et al., 2011). They found that although the presence of p53 reduced glucose-6-phosphate dehydrogenase activity, it did not affect the levels of glucose-6-phosphate dehydrogenase mRNA or protein (Jiang et al., 2011). Co-

immunoprecipitation was used to demonstrate that p53 bound directly to glucose-6-phosphate dehydrogenase and further analysis indicated that p53 binding prevented formation of the active glucose-6-phosphate dehydrogenase dimer (Jiang et al., 2011). Entry into the pentose phosphate pathway is therefore inhibited by p53 and by inference, its inactivation in cancer cells may promote pentose phosphate pathway flux.

p53 promotes the use of glucose for maximal energy production and thus opposes the metabolic changes observed in cancer that promote biosynthesis of components required for proliferation. Investigations by Matoba et al illustrated the effect of p53 mutation upon metabolism in human colon cancer cells. Demonstrating that although total ATP concentrations were unchanged in human colon cancer cells with mutated p53 (relative to wild type cells), oxygen consumption was decreased whilst lactate production was significantly increased (Matoba et al., 2006). Inactivation of p53, considered to occur in the majority of human cancers (Brosh and Rotter, 2009), therefore serves to promote the Warburg effect in cancer cells.

### 1.2.3 cMyc

The cMyc oncogene is a transcription factor with a helix-loop-helix leucine zipper structure whose dysregulation is observed in many commonly occurring human cancers (Dang et al., 2009). In normal cells Myc is activated in response to growth factor signalling to promote proliferation, by activating genes involved in the cell cycle, metabolism, cell growth, adhesion and cytoskeletal organisation (Coller et al., 2000; Dean et al., 1986; Menssen and Hermeking, 2002). The

expression and activity of cMyc is usually tightly regulated and the protein has an extremely short half life of 30 minutes (Hann and Eisenman, 1984). The short half-life indicates that in the absence of growth factors, cMyc levels in the cell are low. The majority of human cancers over express cMyc either due to mutations in the gene itself or, indirectly, through genes involved in cMyc regulation (Meyer and Penn, 2008). The cMyc transcription factor regulates metabolism in cancer cells in a number of different ways.

One of the first observations of cMyc regulation of glycolytic metabolism was by Valera et al who used transgenic mice over expressing cMyc (Valera et al., 1995). Their investigations revealed that over expression of cMyc resulted in an increase in hepatic glycolysis, as measured by elevated lactate production, an increase in mRNA levels and activity of several glycolytic enzymes. Studies have since identified cMyc mediumted induction of LDHA, GLUT1, HK2, PFK, enolase1 and PDK1 (Kim et al., 2007b; Osthus et al., 2000; Shim et al., 1997). Recent work has also indicated that cMyc plays a role in the preferential splicing of the PKM2 isoform of PK by up-regulating the expression of the heterogeneous nuclear ribonucleoproteins (hnRNP) responsible for the regulation of PKM splicing (section 1.1.1.4) (David et al., 2010). Elevated cMyc activity is therefore thought to contribute to the increase in oxidative glycolysis often observed in tumours.

cMyc also has a role in glutamine metabolism, as demonstrated by Wise and colleagues using the SF188 cell line with amplified cMyc expression and shRNA control cells with repressed cMyc (Wise et al., 2008). They established that both

glutamine uptake and the expression of the glutamine importers ASCT2 and SN1 were significantly up-regulated by cMyc (Wise et al., 2008). They also used chromatin immuno-precipitation analysis to show cMyc bound the promoter regions of both transporter genes (Wise et al., 2008). cMyc also enhances glutaminase expression indirectly, by approximately 10 fold, through the repression of the microRNA's miR-23a and miR23b (Gao et al., 2009). It has also been suggested that cMyc confers a dependence on glutaminolysis. This is illustrated in studies in cell lines with inducible cMyc, where glutamine withdrawal triggered a significant increase in apoptosis in cell expressing active cMyc (Yuneva et al., 2007).

#### 1.2.4 HIF-1

Hypoxia inducible factor-1 (HIF-1) is the major transcription factor mediating cellular adaptation and survival under hypoxic conditions, regulating the expression of genes involved in angiogenesis, proliferation, metabolism, pH, migration and metastasis (Semenza, 2010). HIF-1 is a heterodimer composed of a constitutively expressed HIF-1β subunit and an oxygen dependent HIF-1α subunit. The latter is rapidly hydroxylated and targeted for degradation in oxygenated cells (Huang et al., 1998; Jaakkola et al., 2001; Wang and Semenza, 1995). The emergence of an hypoxic environment therefore stabilises HIF-1α and the entire HIF-1 complex. In addition HIF-1α can also be stabilised by oncogenic mutations such as those in the von Hippel-Lindau (VHL) protein (Mack et al., 2003) or by high levels of the monocarboxylates lactate and pyruvate (Lu et al., 2005).

Immunohistochemistry studies have revealed that HIF1α is over expressed in many different types of cancer (Talks et al., 2000; Zhong et al., 1999). Additionally in most types of cancer HIF1α over-expression has been demonstrated to correlate with poor clinical outcome such as mortality, metastasis and a poor response to therapy (Baba et al., 2010; Hoffmann et al., 2008; Vaupel and Mayer, 2007).

HIF-1 activity contributes to the glycolytic switch observed in the majority of cancers promoting glycolysis via up-regulation of many glycolytic enzymes and by suppression of oxidative phosphorylation. This includes up-regulation of: glucose transporters GLUT1 and GLUT3 (Chen et al., 2001; O'Rourke et al., 1996), hexokinase isoforms HKI and HKII (Iyer et al., 1998; Riddle et al., 2000), phosphoglucose isomerase, phosphofructokinase isoform PFKL, phosphofructokinase 2 isoform PFKFB3, aldolase A, triose phosphate isomerase, glyceraldehyde-3-phosphate dehydrogenase, phosphoglycerate kinase 1, phosphoglycerate mutase B, enolase 1 and pyruvate kinase M (Funasaka et al., 2005; Gess et al., 2004; Marin-Hernandez et al., 2009; Obach et al., 2004; Semenza et al., 1994; Takahashi et al., 1998). Under hypoxic conditions, HIF1$\alpha^{-/-}$ embryonic stem cells have reductions in the levels of mRNAs encoding glucose transporters and glycolytic enzymes mentioned above relative to HIF1$\alpha^{+/+}$ control cells (Iyer et al., 1998). Additionally, HIF-1 induces the expression of lactate dehydrogenase A whose regeneration of $NAD^+$ enables continued glycolytic flux. HIF-1 induction of the monocarboxylate transporter MCT4, catalysing the export of lactate from the cell also prevents build up of lactate and

intracellular acidosis (Firth et al., 1995; Ullah et al., 2006). Finally, HIF-1 up-regulates expression of pyruvate dehydrogenase kinase 1 (PDK1) which phosphorylates and inhibits the pyruvate dehydrogenase (PDH) complex. The PDH complex converts pyruvate to acetyl-CoA for entry into the TCA cycle and thereby HIF-1 suppresses entry of pyruvate to the cycle (Kim et al., 2006). These HIF-1 induced changes in metabolism serve to reduce oxygen consumption and optimise metabolism for hypoxic conditions.

Interactions between the HIF-1 and other transcription factors such as cMyc have also been reported. HIF-1 counters the normal function of Myc by several different mechanisms. For example, the induction of growth arrest under hypoxic conditions by displacing Myc from the promoter of $p21^{cip1}$ a cyclin dependent kinase inhibitor (Koshiji et al., 2004). However, investigations with human P439-6B cells, that conditionally over express cMyc, have found that dysregulated cMyc cooperates with HIF-1 to promote expression of HKII and PDK1; thereby promoting glucose metabolism (Kim et al., 2007b). Finally, recent studies have also revealed that the pyruvate kinase isoform PKM2 interacts with HIF-1 by functioning as a transcriptional coactivator in HeLa cells. This enhances HIF-1 binding to hypoxia response elements in DNA, thereby forming a positive feedback loop promoting glucose metabolism (Luo et al., 2011).

*Figure 8* summarises the sites at which these oncogenic signalling proteins regulate cellular metabolism. Therefore indicating the importance of the activity of these proteins in determining the metabolic phenotype of cancer cells.

## 1.3 The tumour micro-environment and metabolic adaptations in cancer

Tumours are not simply a homogeneous population of cells, since they display significant cellular and environmental organisation. They contain non-cancerous cells such as fibroblasts in addition to cancerous cells all embedded in an extracellular matrix (Fukumura and Jain, 2007). The physiological micro-environment of tumours differs drastically from that of normal tissue. The tumour micro-environment is characterized by regions of hypoxia, nutrient deprivation, acidosis and high interstitial fluid pressure (Vaupel, 2004). The disorganised vasculature, the lack of lymphatics within tumours, the alterations in energy metabolism, all serve to contribute to the hostile micro-environment (Leu et al., 2000; Vaupel et al., 1989). The micro-environment features are not uniform and develop concentration gradients within tumours, which in turn affect the proliferative capacity and viability of cells. This leads to the development of distinct zones of proliferating, quiescent and necrotic regions within the tumour (Sutherland, 1986), as illustrated in *Figure 1*. Many of these features of the tumour micro-environment are known to contribute to the failure of many current cancer therapies (Gray et al., 1953; Jackson, 1989; Mellor et al., 2005b; Teicher, 1994).

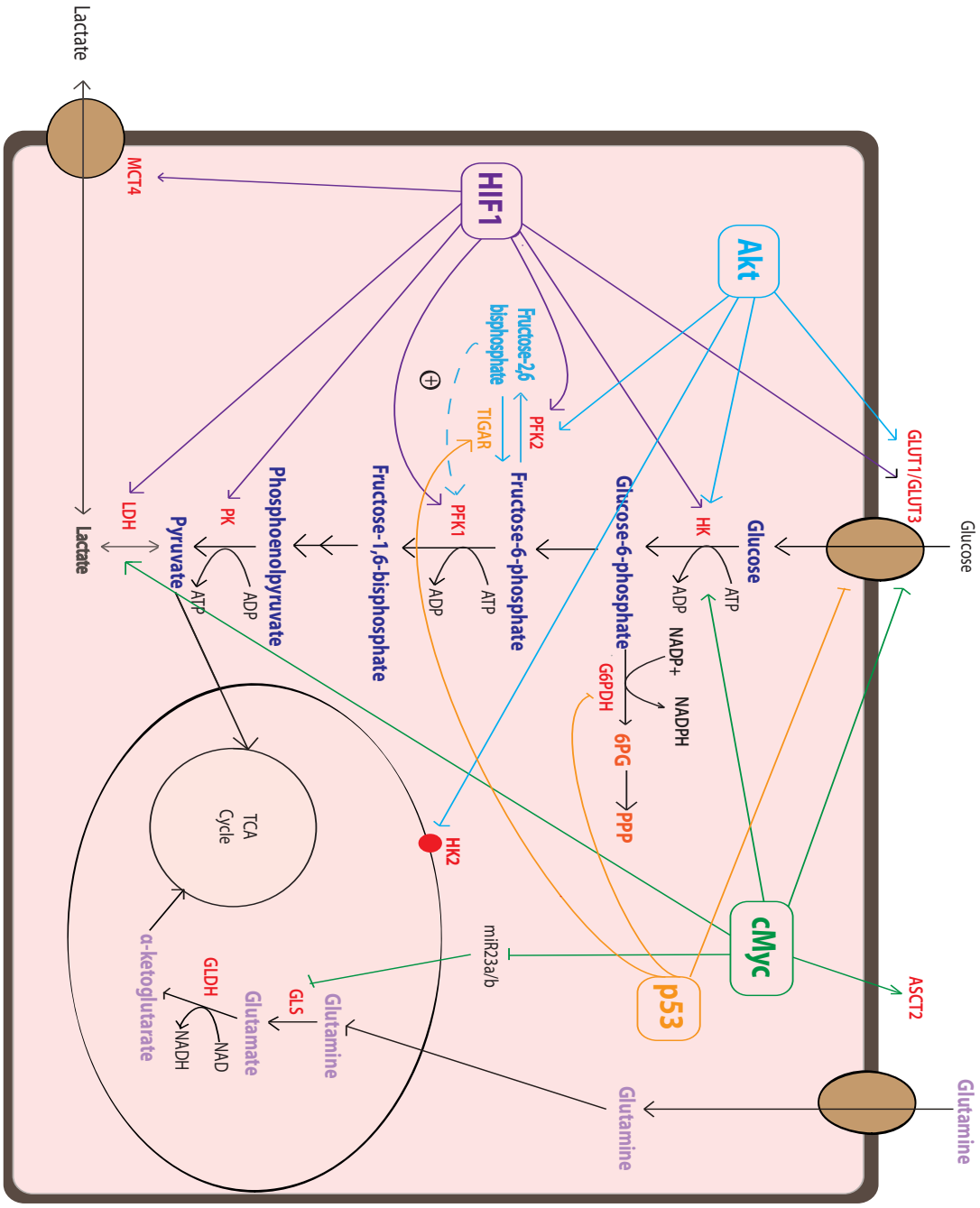



***Figure 8. Metabolic regulation.*** *Schematic indicating the sites at which cellular metabolism is regulated by HIF1 (purple), Akt (blue), cMyc (green) and p53 (orange). A tapered arrow (➔) indicates positive regulation where as a bar (-|) indicates inhibition. The glycolytic pathway is represented in blue, the pentose phosphate pathway in orange and the glutaminolysis in purple.*

It is possible that the tumour micro-environment may contribute to the altered metabolic strategies observed in cancer cells, which enable cancer cells to survive the hostile conditions. Studies profiling nutrient metabolism in micro-regions of human breast cancer tumours showed higher maximal activities of glycolytic enzymes in samples from the centre of the tumour than the periphery. Furthermore, glucose consumption and lactate production were significantly higher in tissue samples from the centre of the tumour relative to those from the periphery (dos Santos et al., 2004). This work supports the hypothesis of differing metabolic strategies in different micro-regions of a tumour. This section will detail the tumour micro-environment and any metabolic adaptations resulting from it.

### 1.3.1 Tumour hypoxia

Normal mammalian tissues have an $O_2$ tension of 2-9% (40mm Hg) and hypoxia is usually defined as ≤2% oxygen or less than 2.5mmHg (Bertout et al., 2008; Vaupel and Mayer, 2007). Investigations have shown that hypoxia is a common feature of many different types of solid cancers including, cervical, breast, prostate and brain (Hockel et al., 1991; Parker et al., 2004; Rampling et al., 1994; Vaupel et al., 1991). Tumour hypoxia has also been associated with malignant progression, metastases, and resistance to treatment and is correlated with poor patient prognosis (Brizel et al., 1996; Brown, 2002; Hockel et al., 1993; Hockel et al., 1996; Nordsmark et al., 2005).

Tumour hypoxia is a consequence of several different factors, including the inadequate tumour vasculature. Tumour blood vessels have severe structural and functional abnormalities, which result in irregular blood flow and oxygen delivery (Brown and Giaccia, 1998; Vaupel et al., 1989). Hypoxia is exacerbated by the diffusion limit of oxygen in solid tissues since cells that are situated beyond this limit develop chronic hypoxia (Brown and Giaccia, 1998). The oxygen diffusion limit is dependent on a number of factors, including intracapillary oxygen tension and oxygen consumption rate. However studies in mouse tumours showed that oxygen levels decreased exponentially with distance from the blood vessel, reaching hypoxic values (3 mmHg) at approximately 200 μm away (Torres Filho et al., 1994). Consistent with this, Grimes and colleagues recently determined an oxygen diffusion limit to be 233 ± 22 μm from measurements performed in tumour spheroids (Grimes et al., 2014).

Hypoxia has a broad range of consequences for the tumour. It is known to inhibit proliferation through the regulation of the cyclin dependent kinase inhibitors p27 and p21 (Gardner et al., 2001; Koshiji et al., 2004). In addition, cells have been shown to down-regulate global protein synthesis under hypoxic conditions to conserve ATP supplies (Koumenis et al., 2002). Finally, prolonged or severe hypoxia can result in cell death via apoptosis (reviewed in(Greijer and van der Wall, 2004)), or necrosis where energy levels are critically low (Eguchi et al., 1997).

Cancer cells can adapt to moderate hypoxia and undertake growth using HIF-1. As detailed in section 1.2.4, HIF-1 is a heterodimeric transcription factor, which

is stabilised under hypoxic conditions (Huang et al., 1998; Wang and Semenza, 1995). Active HIF-1 has been shown to target several hundred genes (Xia et al., 2009) including those involved in energy metabolism (section 1.2.4). Active HIF-1 also targets genes involved in improving oxygen delivery such as the angiogenic vascular endothelial growth factor (VEGF), which stimulates neovascularization (Forsythe et al., 1996) and the erythrocyte growth factor erythropoietin (EPO), which increases erythrocyte production (Semenza and Wang, 1992). Additionally, several HIF-1 target genes are involved in tumour metastasis. These include the transcription factor TWIST, which promotes the epithelial-mesenchymal transition (EMT) (Yang et al., 2008) and the urokinase plasminogen activator receptor (uPAR), which plays a critical role in cellular invasion contributing to extracellular matrix degradation (Sullivan and Graham, 2007).

Various investigations have implicated tumour hypoxia in the resistance of tumours to therapy. It is long known that the sensitivity of cells to x-ray radiation (radiotherapy) were three times greater under well oxygenated compared to anoxic conditions (Gray et al., 1953). As illustrated in *Figure 9*, radiosensitivity decreases substantially when the oxygen partial pressure falls below 25-30 mmHg (Vaupel et al., 2001). Oxygen is widely thought to bind to free radicals on DNA produced by radiation thereby "fixing" the DNA damage (Wachsberger et al., 2003). This theory has been validated by studies using radiosensitizers such as metronidazole, an electron accepting agent that replaces oxygen in this reaction, sensitising hypoxic tumours to radiation (Brown, 1975).

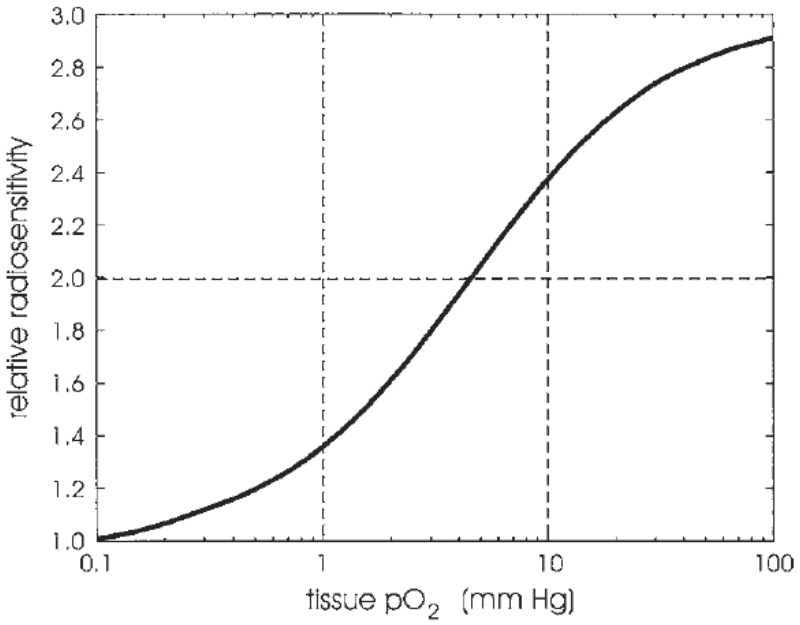



***Figure 9. The dependence of tumour cell relative radiosensitivity to tissue oxygenation.*** *Figure with permission from (Vaupel et al., 2001), illustrating the dependence of radiotherapy on oxygen concentration,*

Hypoxia has also been linked to resistance to chemotherapy by both direct and indirect mechanisms. For example, some chemotherapy drugs require oxygen for their mechanism of action. This is illustrated by bleomycin, which functions to fragment DNA using reactive free radicals of oxygen (Teicher, 1994; Teicher et al., 1981). Similarly HIF-1 has been shown to induce the expression of the multidrug efflux pump P-glycoprotein, which confers resistance to numerous anti cancer drugs (Comerford et al., 2002).

Hypoxic exposure has numerous effects on cancer cells. Extreme hypoxia causes cells to either cease proliferation or undergo apoptosis (Gardner et al., 2001; Greijer and van der Wall, 2004), whereas moderate hypoxia is associated with adaptation and malignant progression via HIF-1 (Hockel and Vaupel, 2001; Rademakers et al., 2008). Activated HIF-1 promotes aerobic glycolysis up

regulating the expression of the majority of the glycolytic enzymes (section 1.2.4). Consequently hypoxia can be expected to have a major effect upon cellular metabolism. However many of the glycolytic enzymes are tightly regulated at the post transcriptional level (section 1.1) and so detailed profiling of the metabolic adaptations under hypoxia is required to determine whether flux control is altered.

### 1.3.2 Acidosis

Acidosis is a common feature of many tumours due to the production of lactate from aerobic glycolysis (Warburg et al., 1927). Carbon dioxide from the TCA cycle and pentose phosphate pathways also contributes via production of carbonic acid (Helmlinger et al., 2002; Warburg et al., 1927). Extracellular pH ($pH_{ex}$) values in the range of 6.5-7.0 have been recorded for most tumours relative to the $pH_{ex}$ of 7.2-7.4 observed in normal tissues (Gerweck and Seetharaman, 1996; Gillies et al., 2002; Helmlinger et al., 1997; Martin and Jain, 1994; Sedlakova et al., 2014). The intracellular pH ($pH_{in}$) of tumour cells (7.2-7.5) is similar, or slightly more alkaline, than normal cells (Chiche et al., 2010). Since intracellular acidosis affects cell function and can trigger apoptosis (Lagadic-Gossmann et al., 2004), the $pH_{in}$ is tightly regulated, seemingly at the expense of the extracellular environment.

There are two major strategies employed to regulate the internal $pH_{in}$; the extrusion of lactate and protons from the cell and the import of alkalizing bicarbonate ions (Sedlakova et al.). The expression and/or activity of several of the proteins responsible for proton and lactate export such as the vaculolar

proton pump (V-ATPase), the sodium/proton exchanger (NHE1) and monocarboxylate transporters MCT1 and MCT4 are increased in many cancers (Martinez-Zaguilan et al., 1993; McLean et al., 2000; Pinheiro et al., 2008b; Sennoune et al., 2004; Webb et al., 2011). Intracellular alkalization is achieved by the import of bicarbonate through the $Na^+$ coupled $HCO_3^-$ cotransporter NBCn1 (SLC4A7). NBCn1 is up regulated in breast cancer relative to normal breast tissue and plays a significant role in the regulation of $pH_{in}$ (Boedtkjer et al., 2013). Bicarbonate transporters work in conjunction with bicarbonate generating proteins such as the carbonic anhydrases (CAs), in particular the HIF-1 inducible CAIX (Sedlakova et al., 2014; Wykoff et al., 2000). Together, these mechanisms result in maintenance of a neutral to alkaline $pH_{in}$ together with the generation of an acidic $pH_{ex}$.

pH is acknowledged to affect the activity of metabolic enzymes. For example, PFK-1 is inhibited by lactate that favours the dissociation of the active PFK-1 tetramer to dimers (Costa Leite et al., 2007). Early studies by Trivedi and Danforth, using mouse muscle PFK-1 identified a dramatic increase in PFK activity between pH7.0-7.3, as illustrated in *Figure 10* (Trivedi and Danforth, 1966). It is therefore possible that the slightly alkaline pH observed in tumour cells compared to normal cells could promote glycolysis. However, recent studies have called this hypothesis into question demonstrating decreased aerobic glycolysis in MCF7 cells exposed to acidosis (pH6.7) relative to control conditions (pH7.4) (Lamonte et al., 2013). This is evidenced by metabolic profiling studies showing that exposure to acidosis (pH6.7) resulted in a decrease in lactate production from isotope labelled glucose (Lamonte et al.,

2013). They also revealed increased utilization of the TCA cycle, pentose phosphate pathway and glutaminolysis through induction of G6PDH and GLS2 expression suggesting that acidosis has a significant effect on metabolic strategy (Lamonte et al., 2013).

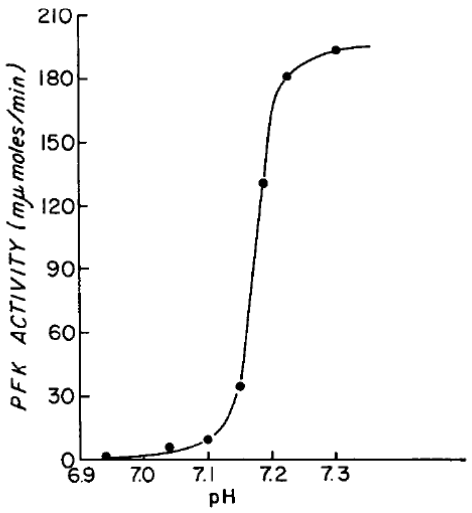



***Figure 10. The effect of pH on the activity of mouse muscle PFK.*** *Diagram with permission from (Trivedi and Danforth, 1966) showing the effect of pH on mouse muscle PFK activity at 0.22mM fructose-6-phosphate.*

Acidosis had also been linked to tumour invasion and metastasis, suppression of immune responses, inflammation, angiogenesis and resistance to chemo and radiotherapy (Kato et al., 2013; Shi et al., 2001; Webb et al., 2011). Hence, acidosis of the tumour micro-environment has a significant effect on the phenotype and metabolic strategies of the cells within a tumour.

### 1.3.3 Quiescence

Tumours contain a significant population of quiescent cells, evidenced by the low mean tumour proliferative fraction (19 ± 15 % n=126) determined in immunohistochemistry studies of the proliferation marker Ki-67 in solid tumours (Sahin et al., 1991). Quiescence is defined as a viable but non-dividing

state. The presence of quiescent cells is considered to have a major effect on tumour response to chemotherapy in addition to other aspects of cell physiology including metabolism.

Early work characterised quiescence in monolayer cultures, where cells were grown to high densities to induce quiescence via contact inhibition and was referred to as plateau phase. These investigations determined that relative to cells in the proliferative phase, quiescent cells displayed, G1 DNA content (>97%), reduced RNA content (≥50%), approximately 50% reduction in cell volume, unaffected viability and were more sensitive to single doses of X-rays (Wallen et al., 1984; Wallen et al., 1985). Recent experiments by Coller and colleagues have begun to characterise quiescence at the gene expression level (Coller et al., 2006). They used DNA microarrays to study monolayers of cells induced into quiescence by several different mechanisms including, mitogen withdrawal, contact inhibition and loss of adhesion relative to proliferating cells. It was shown that a specific set of genes were induced regardless of the mechanism of quiescence induction. These genes promoted the non-dividing state and ensured its reversibility, specifically this includes genes such as Max interacting protein 1 (*MXI1)*, that controls cell proliferation in mouse models (Coller et al., 2006).

The mechanism by which the quiescent population of cells develops is not completely clear, but the tumour micro-environment is thought to play an important role. For example, hypoxia has been demonstrated to inhibit proliferation through regulation of p27 and p21 cyclin dependent kinase

inhibitors (Gardner et al., 2001; Koshiji et al., 2004). Hypoxic regions of KHT tumours contain a smaller percentage of cells actively proliferating (Siemann and Keng, 1988). It has been established that glucose deprivation and acidosis can also reduce the growth rate (Casciari et al., 1992).

The energetic demands of quiescent cells and the metabolic strategies they employ are expected to differ extensively from those of proliferating cells, which are required to completely replicate their contents for division. This may suggest that quiescent cells have a dramatically reduced metabolic rate relative to proliferating cells. This is supported by studies using non-tumorigenic cytokine dependent FL5.12 murine cells. In these cells, stimulation of cell growth by interleukin-3 resulted in increased glycolytic flux, reduced oxygen consumption, increased glucose consumption and increased lactate production (Bauer et al., 2004).

More recent investigations however have challenged this hypothesis suggesting that quiescent cells are highly metabolically active. Lemons et al used metabolomics techniques to study metabolic flux in human fibroblasts monolayer cultures and induced into quiescence via contact inhibition (Lemons et al., 2010). The rate of flux through glycolysis, the pentose phosphate pathway (PPP) and the TCA cycle were similar to that of proliferating fibroblasts. However, analysis of the PPP showed that proliferating cells utilised ribose-5-phosphate for nucleotide synthesis whereas quiescent cells recycled it back to glycolytic intermediumtes. In addition levels of NADPH generating enzymes such as G6PDH and 6-phosphogluconate dehydrogenase were elevated in quiescent

cells. This data lead to the hypothesis that quiescent cells utilize the PPP for the generation of NADPH, which can be used either for detoxification of free radicals or for biosynthetic purposes (Lemons et al., 2010). Consistent with increased generation of NADPH to protect against free radicals, the ratio of reduced to oxidised glutathione was significantly increased in quiescent fibroblasts relative to proliferating fibroblasts (section 1.1.2)(Lemons et al., 2010). Finally, the importance of PPP activity in quiescence cells was illustrated by the significant increase in cell death via apoptosis in quiescent relative to proliferating fibroblasts resulting from inhibition of the pathway (Lemons et al., 2010).

Recent studies have also recently detected changes in glycogen metabolism in contact inhibited quiescent ovarian adenocarcinoma cells (Witney et al., 2014). They used positron emission tomography (PET) of the radiotracers $^{18}$FDG, to measure glucose uptake, and $^{18}$F-*N*-(methyl-(2-fluoroethyl)-1H-[1,2,3]triazole-4-yl)glucosamine ($^{18}$FNFTG), to detect *de novo* glycogenesis. Although there was no change in glucose uptake between quiescent and proliferating cells, the former increased glycogen storage potentially as energy source to be utilized upon re-entry to the cell cycle (Witney et al., 2014). The metabolic adaptations of quiescent cells in tumours therefore seems to differ from those in proliferating tumour cells but have not been completely elucidated.

The presence of quiescent cells has long been known to contribute to the failure of various chemotherapeutic agents as most drugs target aspects of the replication process (Jackson, 1989; Mellor et al., 2005a). Quiescent cells are additionally thought to contribute to the problem of tumour recurrence

following therapy, re-entering the cell cycle once they have better access to nutrients due the removal of the outer oxygenated proliferating tumour cells by chemo- or radio-therapy (Desoize and Jardillier, 2000; Durand, 1997). Studies assessing the proliferative capacity of advanced serious ovarian cancer have shown a high proportion of Ki-67 negative (quiescent) cells in the primary tumour was associated with a less favourable outcome for patients in remission (Kondoh et al., 2010).

Therefore the presence of a quiescent population of cells has a significant effect on the tumour and its response to therapy, but the metabolic strategies employed by the cells in these populations has not been fully clarified.

## 1.4 Summary and project aims.

Alterations in the metabolic strategies of cancer cells, first observed by Otto Warburg, are now recognised as a emerging hallmark of cancer (Hanahan and Weinberg, 2011; Warburg, 1956b). Numerous studies have found that cancer cells reorganise their metabolism increasing their consumption of the nutrients glucose and glutamine (Bode et al., 1995; Gillies et al., 2008). A significant fraction of the glucose consumed by cancer cells is oxidised to lactate, a process called aerobic glycolysis (Warburg, 1956). In addition, glucose derived carbon is utilized in the pentose phosphate pathway for synthesis of the reducing agent NADPH and nucleotide precursors (Boros et al., 1997; Yang et al., 2007). Glutamine is metabolised by the glutaminolysis pathway and has been shown to be a key anaplerotic precursor in cancer cells, replenishing the TCA cycle

intermediumtes in addition to being oxidised for energy production (Daye and Wellen, 2012; DeBerardinis et al., 2007). Reprogramming of metabolism allows cancer cells to respond to both biosynthetic demands for proliferation and to adapt to the hostile micro-environment that is often encountered in the tumour. The prevalence of these metabolic alterations renders metabolism a potential therapeutic target for the treatment of cancer (reviewed in (Ganapathy-Kanniappan and Geschwind, 2013)). In addition, dietary energy restriction, leading to lower circulating glucose levels significantly reduces the growth and progression of many differing tumour types, including mammary, colon and prostate (Mukherjee et al., 1999; Thompson et al., 2004; Wheatley et al., 2008).

The mechanism by which these alterations in metabolism occur are not yet completely revealed and can probably be attributed to several factors. These include activation of oncogenes such as HIF-1 and cMyc, which regulate glycolytic gene expression (Cairns et al., 2011). DNA Mutations affecting metabolic enzymes or regulators such as p53 (reviewed in (Chen et al., 2007b)), or the development of a hostile tumour micro-environment also aid in reprogramming cellular metabolism (Cairns et al., 2011). Furthermore, micro-environmental stresses contribute to the failure of many current cancer therapies, including chemo and radio-therapy (Gray et al., 1953; Jackson, 1989; Mellor et al., 2005a; Teicher, 1994). Initial investigations suggest that different metabolic strategies are used to adapt to these micro-environmental stresses (Lamonte et al., 2013; Lemons et al., 2010), however these strategies have to date not been fully characterised.

Although the tumour micro-environment is thought to play a key role in the mechanism of metabolic reprogramming, the majority of studies investigating metabolic regulation in cancer have been performed in tumour cell lines maintained as two dimensional (2D) monolayer cultures (examples include (Behrooz and Ismail-Beigi, 1997; Christofk et al., 2008a; Kim et al., 2007a; Osthus et al., 2000; Schwartzenberg-Bar-Yoseph et al., 2004; Yi et al., 2012)). The monolayer culture systems, fail to take into account many of the aspects of the three-dimensional tumour microenvironment. For example they cannot replicate the gradients of nutrients, oxygen, or waste that are observed *in vivo*. In addition, experiments in 2D monolayer cultures frequently fail to reproduce phenomena observed in vivo, for example differing gene expression profiles and response to chemotherapy (Camphausen et al., 2005; Desoize and Jardillier, 2000).

**The aim of this study is to characterise metabolic adaptations of tumour cells to micro-environmental stresses including hypoxia and quiescence relative to the metabolism of oxygenated proliferating tumour cells in a three-dimensional model system.**

Early metabolic profiling studies attempted to identify rate limiting steps which regulated the flux through biochemical pathways (Krebs, 1970). More recently this has been replaced by metabolic control analysis which recognises the potential for the control of flux to be distributed among enzymes in a pathway (Kacser and Burns, 1973). Metabolic control analysis examined the degree to which each enzyme controls flux through a pathway, defined as the flux control coefficient, which is defined as the decrease in pathway flux caused by a 1%

decrease in enzyme activity (Moreno-Sanchez et al., 2010). As mentioned in section 1.1.1 there are a number of different mechanisms by which metabolic flux can be regulated. These include long-term mechanisms such as up or down regulation of enzyme expression. For example, Altenburg and Greulich have shown that most glycolytic enzymes are over-expressed in 70% of human cancers (Altenberg and Greulich, 2004). In addition, flux may be altered by the expression of alternate isoenzyme such as the hexokinase II (HKII) isoform which is over-expressed in cancer cells (Mathupala et al., 2009; Ros and Schulze, 2013; Wilson, 2003). Shorter-term mechanisms include enzyme activation or inhibition by allosteric effectors or by covalent modification. For example, covalent modification of LDH-A by tyrosine phosphorylation enhances its activity by promoting formation of the active tetramer and the binding of NADH (Fan et al., 2011). Finally, flux can be regulated by the accessibility of substrates either via compartmentalization or by the use of metabolites in branching pathways. For example, pyruvate dehydrogenase is inhibited by phosphorylation in many cancers due to the activity of pyruvate dehydrogenase kinase 1, thereby reducing flux of pyruvate into the TCA cycle and increasing lactate production (McFate et al., 2008).

In this study metabolic adaptations will be analysed systematically, to include examination of nutrient utilization under different micro-environment conditions. This will involve measuring the expression of nutrient transporters, nutrient usage from the medium and measurement of the rate of glycolytic flux indicating the *in vivo* usage of the pathway. Each of these measurements will be done under different micro-environmental conditions. Furthermore, analysis of

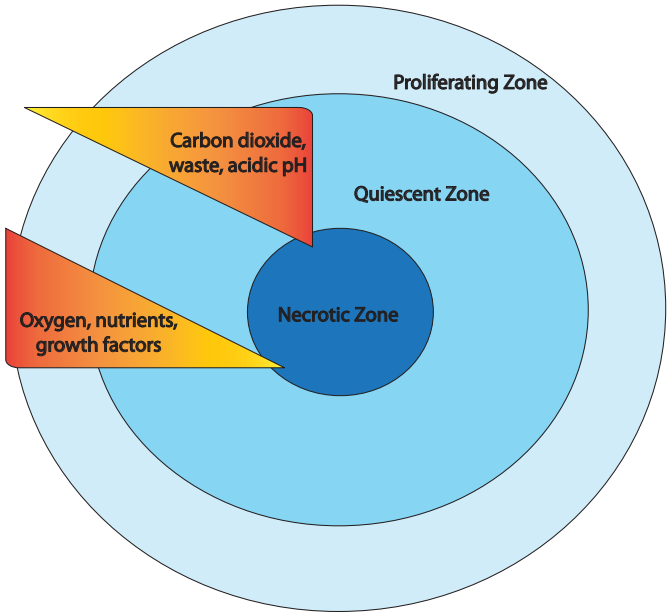
intracellular adaptations at the enzymatic level will assess any changes in the Michaelis-Menten characteristics of key enzymes. Differences in protein expression levels will be measured and may indicate changes in gene transcription or translation. Disparity between expression and activity levels could indicate changes in enzyme regulation at the post-translational level.

The three-dimensional (3D) multicellular tumour spheroid (MCTS) tissue culture model will be employed in this study to more accurately simulate the micro-environment observed within solid tumours. MCTS are three-dimensional aggregates of cells that have been used widely in research since they retain many of the features of the avascular regions of solid tumours (Sutherland, 1988). MCTS have a well-defined geometry, which is illustrated in *Figure 11*. As MCTS reach 200-500μm in diameter, inward gradients of oxygen/nutrients are established resulting in distinct populations of cells arranged concentrically with outer proliferating and an inner quiescent population. At diameters above approximately 500μm a necrotic core develops due to the hostile micro-environment (Hirschhaeuser et al., 2010; Lin and Chang, 2008; Sutherland, 1988). In addition to reproducing the chemical gradients observed in tumours *in vivo*, MCTS have a number of other advantages making them an attractive cell culture model. The gene expression profile and morphology of cells growth in 3D culture has been shown to more closely represent tumours *in vivo* (Hirschhaeuser et al.; Lee et al., 2013). Cells cultured in 3D have also been found to more accurately reproduce the drug sensitivity of tumour cells *in vivo* (Desoize and Jardillier, 2000). For example, breast cancer cells (MDA-231) have a significantly higher $IC_{50}$ for cisplatin when cultured as MCTS ($IC_{50}$ =100 μM)

compared to monolayer culture ($IC_{50}$ = <10 μM) (Ohmori et al., 1998). They also mimic the tumour micro-environment more closely in terms of cell-cell interactions and the presence of an extracellular matrix (Nederman et al., 1984). Finally, early studies revealed that several metabolic features such as rate of lactate production also differs between cells grown as 2D monolayers and MCTS (Rodriguez-Enriquez et al., 2008). MCTS therefore represent an important experimental model being intermediate in complexity between 2D monolayer culture and solid tumours samples.

As mentioned previously the prevalence of metabolic alterations in cancer has lead to its identification as a therapeutic target. This systematic analysis will give an indication of *in vivo* enzyme activities and differences in flux between the conditions would indicate the differences in the metabolic strategies employed. This could enable the identification of the main sites of control of flux through the pathway. Since metabolic pathways such as glycolysis are utilized in all cell types of the body for metabolism it is essential to identify the sites of metabolic control with the largest differences from normal cells, which will be the most suitable potential therapeutic targets.

A.




B.

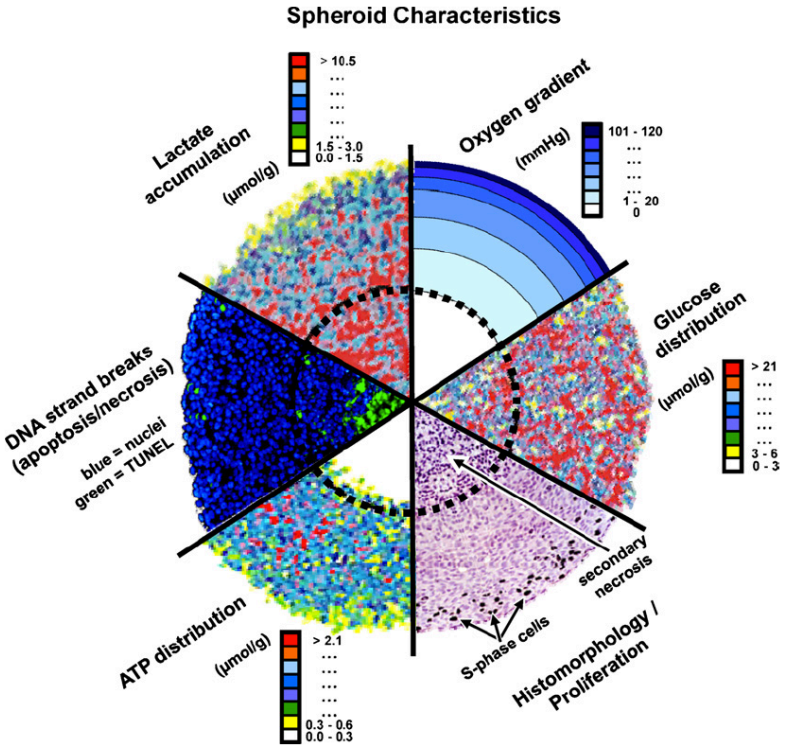



***Figure 11. The micro-environment within multicellular tumour spheroids.*** *(A) A schematic illustrating the spherical geometry of tumour spheroids, populations of cells are organised concentrically with an outer population of proliferating cells, an inner quiescent population and a necrotic core, the formation of these layers is attributed to the gradients initiated of decreasing oxygen, nutrients and growth factors and opposing increases in carbon dioxide, waste and acidic pH. (B) Various analyses of tumour spheroid sections taken from (Hirschhaeuser et al., 2010), via autoradiography, the tunnel assay, bioluminescence imaging and oxygen microelectrodes, illustrating the gradients present within the spheroid.*

# 2. Materials and Methods

## 2.1 Materials

The RPMI-1640 medium, foetal bovine serum and trypsin with EDTA were purchased from Invitrogen (Paisley, UK). The penicillin and streptomycin was from Lonza (Wokingham, UK). AnaeroGen sachets and Anaerobic indicator were from Fisher Scientific (UK). Protease inhibitors and glutamate pyruvate transaminase were from Roche (Mannheim, Germany). The DC detergent compatible protein assay and Kaleidoscope Precision Plus protein standards were from Bio Rad Laboratories (Hercules, USA). The reduced and oxidised forms of β-Nicotinamide-adenine dinucleotide (NADPH) and β-Nicotinamide-Adenine Dinucleotide Phosphate (NADP), Glucose-6-phosphate Dehydrogenase, Hexokinase, and NAD Lithium Salt were from Calbiochem – Merck Ltd (Nottingham, UK). EZ-Chemiluminescence Detection kit for HRP was from Geneflow Ltd. Primary antibodies to GLUT1, GLUT3, MCT1, MCT4, p27 and c-Myc antibody HRP (all raised in rabbit) as well as c-Myc overexpression 293T lysate were purchased from Santa Cruz biotechnology Inc (USA). Primary antibodies to Glucose 6 phosphate dehydrogenase, glutamate dehydrogenase, pyruvate kinase (HRP) and lactate dehydrogenase (HRP) as well as secondary anti rabbit and anti-goat antibodies conjugated to HRP were from Abcam UK. The primary antibody to HIF-1α was from Becton Dickinson UK Ltd. Primary antibodies to PFKP, hexokinase II and ASCT2 were from New England Biolabs (Herts, UK). Primary antibodies to PFKL and PFKM were from Sigma-Aldrich. (Dorset, UK). The primary antibody to Ki-67 and the polyclonal goat anti mouse HRP secondary antibody was from Dako UK (Ely, UK). The primary antibody to

pimonidazole was included in a kit from Chemicon International Inc (USA). Normal horse serum and universal anti-mouse anti-rabbit secondary antibody for IHC was from Vector Laboratories Inc (California, USA). Novocastra Novolink polymer was from Leica biosystems. The [5-$^{3}$H] glucose was from PerkinElmer. The [U-$^{13}$C] glucose was from Cambridge Isotope Laboratories Inc (Andover, USA). All other reagents were from Sigma-Aldrich (Dorset, UK)

## 2.2 Methods

### 2.2.1 Generation and analysis of the tumour spheroid model

#### *2.2.1.1 Cell culture and tumour spheroid (TS) production*

DLD1 human colon adenocarcinoma cells were obtained from Dr Roger Phillips (University of Bradford, UK) and were primarily grown as monolayers in RPMI-1640 medium with L-Glutamine and 25 mM HEPES, supplemented with 10% (v/v) fetal calf serum and penicillin (100 IU ml$^{-1}$)/streptomycin (100 mg ml$^{-1}$). To generate TS, exponentially growing DLD1 cells were transferred to a flask containing a base coat of 0.75% (w/v) agarose prepared in serum free medium, at a density of 2.5 x $10^{5}$ cell ml$^{-1}$ in 20 ml. The flask was left stationary for 16 hours (37°C, 5% $CO_2$). Large cell aggregates were removed by gravity sedimentation and small cell aggregates were transferred to a spinner culture flask with a final volume of 150 ml serum containing medium. Spinner flasks were stirred at 55 rpm (Techne MCS-104S) (37°C, 5% $CO_2$), allowing spheroids to form. Medium was refreshed every 48 hours.

#### *2.2.1.2 TS Growth*

TS diameter was used as a measure of growth. The TS diameters of at least 20 TS in a 1 ml fraction were measured per time point using a graduated calibrated microscope eyepiece graticule (100 points per 10 mm), conversion to micrometers allowed calculation of volume.

#### *2.2.1.3 Generation of Hypoxic TS ($TS^H$)*

DLD1 TS with a 200-400 μm diameter, typically at day 2 of TS growth where TS had an average diameter of 232 ± 7 μm (n = 200 TS), were transferred to a 96 well plate, containing a base coat of 0.75 % (w/v) agrose in serum-free medium, in 100 μl medium. The plate was placed in a 3.5 litre anaerobic chamber for 16-18 hours at 37°C, with an Anaero*Gen* sachet, containing ascorbic acid and activated carbon that absorb the oxygen in the chamber and produce carbon dioxide. Previous studies in this laboratory have shown that using the Anaero*Gen* system oxygen concentration drop rapidly in the chamber from 20.6% to 0.1% in 45 minutes. The oxygen concentration then remained stable at 0.1% for the remainder of the 24 hour period measured (Mellor et al., 2005b). Hypoxic conditions were confirmed in this study using an anaerobic indicator strip, a cotton strip containing the redox indicator resazurin that undergoes a colour change from white to red on exposure to oxygen.

#### *2.2.1.4 Generation of Quiescent TS ($TS^Q$)*

Proliferating TS with a 200-400 μm diameter were exchanged into medium containing 0.1% (w/v) fatty acid free BSA instead of 10% (v/v) fetal calf serum. Serum or growth factor withdrawal is a well established technique that has

previously been used to generate quiescent DLD 1 TS in this laboratory (Mellor et al., 2005a). This serum-free medium was refreshed, by replacing 80% of the medium following gravity sedimentation of the TS, every 48 hours for seven days at which point the spheroids were harvested. At this point the spheroids measured 257 ± 11 μm (mean ± S.E.M)(n =200 TS).

#### *2.2.1.5 Viability/Outgrowth assay hypoxic tumour spheroids*

The viability of $TS^H$ compared to $TS^N$ was assayed by measuring the amount of cellular outgrowth from the spheroid following hypoxic exposure. After hypoxic incubation tumour spheroids were transferred to an uncoated 96-well tissue culture plate and 200 μl of fresh medium. The tumour spheroids attached to the plates and were incubated for 72 h to allow cellular outgrowth from the tissue. Following outgrowth, the medium was aspirated and replaced with 150 ml 5 g/l methylene blue in 50% (v/v) methanol to fix and stain cells. The wells were washed three times in PBS and the radial outgrowth measured using a graduated microscope eye-piece graticule. The radius of the tumour spheroids was subtracted from the measurements and the degree of outgrowth was expressed as a fraction of spheroid size.

#### *2.2.1.6 Immunohistochemistry*

TS were harvested and fixed overnight in 10% neutral buffered formalin (pH7). Neutral buffered formalin was then removed and the TS embedded in 2% (w/v) agarose in 4% (v/v) formalin which was allowed to set on ice before being removed and placed in a tissue cassette. This was routinely processed (Histopathology Department, John Radcliffe Hospital, Oxford, UK). The

processed, agarose-embedded, TS were embedded in paraffin wax and 5 μm sections were cut using a microtome.

2.2.1.6.1 Immunohistochemistry analysis of the proliferation status of cells within $TS^N$ and $TS^Q$ using the proliferation marker Ki-67 and the quiescence marker $p27^{kip1}$.

TS sections were de-paraffinized and re-hydrated using graded alcohols to water. Formalin fixation forms protein cross links that mask the antigenic sites in the TS sections, therefore antigen retrieval was performed as previously optimised for these antibodies (Mellor et al., 2005a), by incubating slides in 50 mM Tris/200 mM EDTA buffer, pH 9.0 in a Decloaking chamber (Biocare Medical) (25 p.s.i for 2 minutes). The Tris EDTA solution is designed to break the formalin cross links and therefore unmask the antigens. Slides were blocked with normal horse serum at 2.5% (Vector Laboratories Inc, California, USA) prior to incubation with the primary monoclonal antibody (mouse anti-human), Ki-67 (1:100) or $p27^{Kip1}$ (1:150), for 1 hour at room temperature. Bound Ki-67 antibody was detected using an anti-mouse secondary whilst $p27^{Kip1}$ bound antibody was detected using a Novolink polymer kit (Leica biosystems). Detection was achieved using DAB substrate chromogen and hematoxylin counterstain.

### 2.2.1.6.2 Analysis of the oxygenation status of $TS^N$ and $TS^H$.

To determine the oxygenation status, TS were cultured with 100μM pimonidazole (Sigma) present in the medium for the final 16 hours of TS growth. TS were harvested, fixed and processed as above. TS sections were cut and were de-paraffinized and re-hydrated using graded alcohols to water. Antigen revival was performed as previously optimised for the Chemicon hydroxy-probe

pimonidazole monoclonal antibody by incubating slides in 50 mM Tris/200 mM EDTA buffer, pH 8.0 in a Decloaking chamber (Biocare Medical) (15 p.s.i for 2 minutes). Slides were blocked with normal horse serum (Vector Laboratories Inc, California, USA) prior to incubation with the primary monoclonal antibody (mouse anti-human), hydroxy probe (1:100) for 1 hour at room temperature. Bound antibody was detected using a universal anti-mouse anti -rabbit secondary (Vector IMMpress). Detection was achieved using DAB substrate chromogen and counterstained with hematoxylin.

### 2.2.2 TS metabolic adaptations

#### *2.2.2.1 Metabolic capacity*

TS between 200-400 μm in diameter were used for metabolic analysis. TS homogenates were prepared from each flask of TS. Following gravity sedimentation the growth medium was discarded and the TS were re-suspended in homogenisation buffer (0.05M Tris-HCl (pH 8.0) with protease inhibitors) TS were then homogenized extensively using a glass homogenizer. Aliquots (50 μl) stored at -80°C. Protein concentration of TS homogenates was determined using the DC Brad (BioRad) protein assay according to the manufacture's protocol.

##### 2.2.2.1.1 Measurement of specific enzyme activities.

The activities of enzymes catalysing the key reactions in energy generating pathways were measured in the TS homogenates using photometric assays (Hitachi Model U-2010 spectrometer). These assays were developed by Board et al (Board et al., 1990) and optimised in this laboratory by Bloch et al (Bloch et al., 2014). Reactions were monitored by continuous recording of the change in absorbance at 340 nm due to NAD(P)H oxidation/NAD(P) reduction either

within the reaction or a coupled one. Enzyme specific activity was then calculated from the initial rate of change of absorbance using the Beer Lambert law. The conditions for measurement of the specific activity of selected enzymes are shown in Table 1

2.2.2.1.2 Western blot determination of enzyme expression levels

TS homogenates were mixed with reducing Lameli sample buffer (0.03 M Tris HCl, 1% (w/v) SDS, 6% (v/v), 7.6 mg/ml DDT, 3.5% (v/v) β-mercaptoethanol) and heated at 95°C for 10 minutes. 10 μg of total protein was separated by SDS PAGE electrophoresis using a 6-10% SDS gel depending on the size of the protein of interest. Protein was then transferred to a nitrocellulose membrane, which was blocked overnight at 4°C or at room temperature for 1-2 hours with 5% milk or BSA (w/v) in PBS-T. The enzymes of interest were detected according to the antibody conditions shown in Table 2. Blots were washed twice for 10 mins in phosphate buffered saline with Tween-20 0.01% (v/v) (PBS-T) and immuno-reactivity assessed via ECL using the EZ-Chemiluminescence Detection kit for HRP from Geneflow Ltd

### *2.2.2.2 Glycolytic flux*

Glycolytic flux in TS 200-400 μm in diameter was determined by measuring the rate of [5-$^{3}$H] glucose detritiation. The $^{3}$H radiolabel in this metabolite is removed from glucose in water during the triose phosphate isomerisation and enolase steps of the glycolytic pathway, the amount of labelled water released in a given time is then assessed to determine the in vivo rate of the pathway.

TS were washed twice and re-suspended in 5ml sterile PBS, the solution was mixed well before transferring 0.5ml to each of 6 wells in an uncoated 24 well plate. Each well was supplemented with 0.5ml growth medium supplemented with 10mM glucose, FCS and PS. After a 30-minute incubation, 0.5 ml of medium supplemented with 0.04miCi/mM [5-$^{3}$H] glucose was added, following this the TS were incubated for 16 hours (37°C, 5% $CO_2$). Following the incubation medium was removed from the test wells and immediately frozen at -20°C. The $^{3}H_2O$ produced was separated from labelled [5-$^{3}$H] glucose in the samples by column chromatography using a DOWEX-borate column. Borate forms complexes carbohydrates in the sample binding them to the stationary phase of the column whilst the $^{3}H_2O$ produced in the sample is eluted with 2ml of water. The radioactivity in the water elutate was measured by scintillation counting. All values were normalized to protein content measured from control wells.

### 2.2.3 Metabolite concentrations

Media samples were taken at defined time points during TS growth and stored immediately at -20°C. The level of metabolites in the medium at each time point was measured using photometric assays (Hitachi Model U-2010 spectrometer). These NAD(P) reduction linked reactions, listed in table 3, were monitored by recording the final absorbance at 340 nm. The final absorbance values were then related to a standard curve produced from known metabolite concentrations to determine the metabolite concentration in the medium. The conditions for the measurement of the selected metabolites are recorded in Table 3.

### 2.2.3 Intracellular metabolite analysis

To analyse glucose utilization, TS were exchanged into DNEM medium (1g/l glucose) supplemented with 2g/l [U-$^{13}$C glucose] for 30 or 120 minutes prior to metabolite extraction. Metabolic activity was quenched by rapidly cooling the culture flasks in an ethanol dry ice bath, excess medium was removed and TS transferred to a pre cooled 2ml eppendorf tube. TS were then pelleted by centrifugation at 10,000g, 0°C, 30 secs and were washed 3 times in cold PBS. Metabolites were extracted from the TS pellet with 50µl chloroform and 1.3nmoles adonitol internal standard added, the tube was vortexed and incubated on ice for 15 minutes with occasional vortexing and sonication, prior to centrifugation 16,100g, 0°C for 5mins. The supernatant was then added to a fresh tube with 100µl double distilled $H_2O$, vortexed and centrifuged again at 16,100g, 0°C for 5mins the aqueous and organic phases were separated and stored at -80°C before being transferred to metabolomics Australia for analysis by GC- Mass spectrometry.

### 2.2.4 Data Analysis

Data analysis of TS growth and enzyme activity was performed using GraphPad Prism. TS diameter growth data was fitted with a one phase exponential association curve with the equation $Y=Ymax(1-e^{-K-X})$ where Y represents spheroid diameter (µm), X signifies TS age (days) and K is a rate constant. TS volume was fitted with an exponential growth curve, $Y=Ae^{KX}$, where Y represents spheroid volume ($mm^3$) and X signifies TS age (days). Y begins at A and increases exponentially with a rate constant K.

Enzyme assays were analysed using linear regression analysis of the raw spectrophotometric data to give reaction rates. Enzyme activity was then calculated according to the Beer Lambert law, and corrected for total protein concentration. Conditions were compared using one-way ANOVA and Bonferroni's multiple comparison test.

Western blots were analysed using Image J, raw data was normalised to give expression levels relative to the mean densitometry observed in $TS^N$ on each western blot. Slight variations between in the position of the band at the correct molecular weight between conditions were contributed to different isoforms or protein modifications, the major band was analysed in each case. Conditions were compared using one-way ANOVA and Bonferroni's multiple comparison test. Initial investigations showed that β actin levels were not consistent between the three micro-environmental conditions utilized in this study. This is consistent with studies by Farmer et al who determined that changes in cell growth conditions may alter actin synthesis (Farmer et al., 1983). Therefore in this study sample loading was controlled by protein concentration.

| Target Enzyme | Buffer System | Enzymes Added | Biochemical Added | Reaction Monitored | Start of reaction |
|---|---|---|---|---|---|
| Hexokinase | 0.05M Tris HCl (pH 8.0), 13mM $MgSO_4$ | 2.4U/ml glucose 6 phosphate dehydrogenase | 0.55mM ATP, 0.22mM NADP, | NADP reduction | TS homogenate of 0.1mg total protein content |
| Glucose 6 phosphate Dehydrogenase | 0.055M Tris HCl (pH7.8), 3.3mM $MgSO_4$ | | 0.2mM NADP, 2mM glucose 6 phosphate | NADP reduction | TS homogenate of 0.05mg total protein content |
| Phospho-fructokinase | 50mM Tris HCl (pH 7.6), 5mM $MgSO_4$, 5mM $NH_4SO_4$ | 2.5U Triose phosphate isomerase, 1.5U aldolase, 3.6U α glycerophosphate dehydrogenase | 0. 5mM fructose-6-phosphate, 1mM ATP, 0.25mM NADH | NADH oxidation | TS homogenate of 0.1mg total protein content |
| Glutamate dehydrogenase | 100mM Triethanolamine (pH7.3), | | 50mM ammonium acetate, 0.1mM NADH, 0.25mM EDTA, 33.8mM alpha ketoglutarate | NADH oxidation | TS homogenate of 0.1mg total protein content |
| Lactate dehydrogenase | 0.2M Tris HCl (pH7.3) | | 0.22mM NADH, 4mM sodium pyruvate | NADH oxidation | TS homogenate of 0.05mg total protein content |
| Pyruvate Kinase | 0.05M Imidazole HCl (pH7.6), 0.12M KCl, 62mM $MgSO_4$ | 0.2mg/ml Lactate dehydrogenase | 1.48mM ATP, 0.22mM NADH, 3mM phosphoenolpyruvate | NADH oxidation | TS homogenate of 0.05mg total protein content |

**Table 1 Conditions for measurement of enzyme activity and monitored reactions**

| Enzyme | TS homogenate | Primary Antibody conditions | Secondary antibody conditions |
|---|---|---|---|
| Hexokinase | 50 µg | Hexokinase II Rabbit mAb 1:1000 (v/v) in 5% milk in PBS-T20 | Anti Rabbit (HRP) 1:2000 (v/v) in PBS-T20 |
| Glucose-6-Phosphate Dehydrogenase | 10 µg | Glucose 6 Phosphate Dehydrogenase antibody (Rabbit) 1:1000 (v/v) in 5% milk in PBS-T20 | Anti Rabbit (HRP) 1:2000 (v/v) in PBS-T20 |
| Phosphofructokinase P | 10 µg | Phosphofructokianse P Rabbit mAb 1:1000 (v/v) in 5%milk PBS-T20 | Anti Rabbit (HRP) 1:2000 (v/v) in PBS-T20 |
| Phosphofructokinase M | 10 µg | Phosphofructokianse M mouse mAb 1:1000 (v/v) in 5%milk PBS-T20 | Anti mouse (HRP) 1:2000 (v/v) in 5% milk PBS-T20 |
| Phosphofructokinase L | 30 µg | Phosphofructokianse L mouse mAb 1:500 (v/v) in 5%milk PBS-T20 | Anti mouse (HRP) 1:2000 (v/v) in 5% milk PBS-T20 |
| PFKFB3 | 10 µg | PFKFB3 polyclonal antibody rabbit 1:1000 (v/v) in 5% BSA PBS-T20 | Anti Rabbit (HRP) 1:2000 (v/v) in 5% BSA PBS-T20 |
| Glutamate Dehydrogenase | 10 µg | Glutamate Dehydrogenase antibody (goat) 1:10000 (v/v) in 5% milk in PBS-T20 | Anti Goat (HRP)1:2000 (v/v) in 5% milk in PBS-T20 |
| Pyruvate Kinase | 10 µg | Pyruvate Kinase antibody (HRP) 1:10000 (v/v) in in 5% milk in PBS-T20 | N/A |
| Lactate Dehydrogenase | 10 µg | Lactate Dehydrogenase antibody (HRP) 1:10000 (v/v) in 5% milk in PBS-T20 | N/A |
| GLUT 1 | 10µg no heat | Glut1 rabbit polyclonal antibody 1:2000 (v/v) in 5% milk PBS-T20 | Anti Rabbit (HRP) 1:2000 (v/v) in 5% BSA PBS-T20 |
| GLUT 3 | 10µg no heat | Glut3 (v/v)1:1000 in 5%milk PBS-T20 | Anti Rabbit (HRP) 1:2000 (v/v) in 5% BSA PBS-T20 |
| ASCT2 | 10µg no heat | ASCT2 (G11) rabbit polycolonal antibody 1:1000 (v/v) in 5% BSA in PBS T20 | Anti Rabbit (HRP) 1:2000 (v/v) in 5% BSA PBS-T20 |
| MCT1 | 10µg no heat | MCT1 (H-70) Rabbit polyclonal antibody 1:1000 (v/v) in 5% milk in PBS-T20 | Anti Rabbit (HRP) 1:2000 (v/v) in 5% BSA PBS-T20 |
| MCT4 | 10µg no heat | MCT4 (H-90) Rabbit polyclonal antibody 1:1000 (v/v)in 5% milk in PBS-T20 | Anti Rabbit (HRP) 1:2000 (v/v) in 5% BSA PBS-T20 |
| HIF 1 | 10µg | HIF-1α Monoclonal mouse purified IgG1 clone 54 1:1000 (v/v)in 5% milk in PBS-T20 | Anti mouse (HRP) 1:2000 (v/v) in 5% milk PBS-T20 |
| c-Myc | 10µg | cMyc mouse mAb (HRP) 1:1000 (v/v)in 5% milk in PBS-T20 | N/A |

**Table 2 Western Blot Conditions**

| Metabolite | Conditions | Reaction |
|---|---|---|
| Glucose | 50mM Tris HCl pH8.0, 13mM $MgSO_4$, 4mM ATP , 1mM NADP, 0.005mg/ml Glucose 6 phosphate dehydrogenase, 0.0106 mg/ml hexokinase, Glucose 50µM - 500µM (sample) | 1. Glucose + ATP ➔ glucose 6 phosphate + ADP (HK)<br>2. Glucose 6 phosphate + NADP ➔6 phosphogluconate +NADPH |
| Lactate | 0.05 M Tris HCl, pH8.0, 3.3 mM MgSO4, 10 mM Glutamate, 2 mM NAD+, 0.02mg/ml glutamate pyruvate transaminase, 0.01mg/ml lactate Dehydrogenase, lactate 2-30µg (sample) | 1. L-lactate +$NAD^+$ ➔ Pyruvate + NADH (LDH reaction)<br>2. Pyruvate + L-glutamate ➔ 2-oxoglutarate + L-alanine (GPT reaction) |
| Glutamine | **Reaction 1** 0.1M acetate buffer pH5, 1U/ml glutaminase, glutamine x mM **Reaction 2** 0.05M Tris-EDTA 0.001M pH 9, 330 mM hydrazine, $NAD^+$ 1.5mM , ADP 0.5mM, 15U/ml glutamate dehydrogenase, glutamate x | 1. Glutamine + $H_2O$ ➔ glutamate + $NH_4^+$ (glutaminase reaction 1 hour 37°c)<br>2. Glutamate + $NAD^+$ +$H_2O$ ➔ α ketoglutarate + $NH_4^+$ + NADH (glutamate dehydrogenase reaction) |

**Table 3 Conditions for measurement of metabolite levels in the growth medium**

## 3.1 Establishing Micro-environmental Stress in Tumour Spheroids

Solid tumours *in vivo* comprise heterogeneous populations of cells that include proliferating, hypoxic, quiescent and necrotic cells, as illustrated in figure 1. As stated in section 1.3, these populations of cells arise due to concentration gradients of oxygen, nutrients, pH, growth factors etc in the solid tumour, that affect the proliferative capacity and viability of cells within the tumour (Vaupel, 2004). As a consequence of the three dimensional architecture and cellular variation *in vivo* the selection of a suitable experimental model is crucial for investigating cancer biology.

The majority of investigations on the regulation of metabolism in cancer have employed two dimensional monolayer cell culture models (examples include (Christofk et al., 2008b). Monolayer cultures have the advantage of simplicity and reproducibility, but they lack many of the complex features of tumours *in vivo* including the 3D microenvironment and structural features such as the extracellular matrix (reviewed in (Li et al., 2005)). Alternative three dimensional models include tumour biopsy samples which give an accurate representation of *in vivo* features, but are harder to obtain, difficult to manipulate and the extra complexity renders analysis difficult. Further options include mouse xenograft tumours, which are derived from human tumour cells that are transplanted into immunocompromised mice (Richmond and Su, 2008). Tumour xenografts have the advantage of comprising human tumour tissue, being reproducible and effectively reproducing the *in vivo* microenvironment of the tumour however they are costly, technically challenging

and time consuming to produce (Richmond and Su, 2008; Teicher, 2006). Tumour spheroids (TS) are three-dimensional aggregates of cells that represent a mid point in complexity between the classically used monolayer cultures and tumour biopsy material which have been used widely in research (Mueller-Klieser, 1997). TS are readily manipulated, contain the same nutrient and metabolite gradients as *in vivo* tumours and are highly reproducible, thus making them a suitable model system for this study.

To determine the effect of the microenvironment on tumour cell metabolism, this study utilized tumour spheroids that were exposed to distinct micro-environmental stresses. In this section the tumour spheroid model is characterised under normoxia and high proliferation status and compared to hypoxic ($TS^{H}$) and quiescent tumour spheroids ($TS^{Q}$).

### 3.1.1 Tumour spheroid growth

Tumour spheroids (TS) comprised of DLD1 human colon carcinoma cells were generated using the liquid overlay technique followed by growth in spinner culture. DLD1 dukes type C colorectal adenocarcinoma cells are a well characterised, fast growing cell line as evidenced by a doubling time of 20-24h (Ahmed et al., 2013; Trainer et al., 1988) that have been used to successfully generate tumour spheroids in a number of studies (Grimes et al., 2014; Mellor et al., 2005a). Examination of TS diameter suggested that TS growth begins to plateau after 20 days (*Figure 12*a). This

is consistent with previous studies demonstrating spheroids grown beyond 21-24 days (1000 μm diameter) collapse and fragment, due to central necrosis leading to structural instability (Hall et al., 2004). However, assessment of TS volume indicated continued growth for the entire 20-day period measured, the volume increased exponentially with a rate constant of 0.14 $days^{-1}$, indicating that TS doubled in volume every 5.1 days (*Figure 12*b).

TS were grown in RPMI 1640 medium pH 7.44 containing 11.1 mM glucose and 2.1mM glutamine, the glucose concentration of this media is 2 fold higher than the 5.5 mM mean blood glucose concentration observed *in vivo.* The concentration of glucose in the medium has a significant effect upon metabolism (Iyer et al., 2010; Marin-Hernandez et al., 2014), with Marin-Hernandez and colleagues finding differences in the distribution of glycolytic flux control between hyperglycaemia (25mM) and hypoglycaemia (2.5mM). However, RPMI 1640 medium containing 11.1 mM glucose has been used in numerous previous studies upon DLD1 TS (Bloch et al., 2014; Hall et al., 2004; Mellor and Callaghan; Mellor et al., 2005a) including those profiling metabolism during TS growth (Bloch et al., 2014). This concentration of glucose prevents hypoglycemia occurring in cancer cell lines that often have high glycolytic rates.

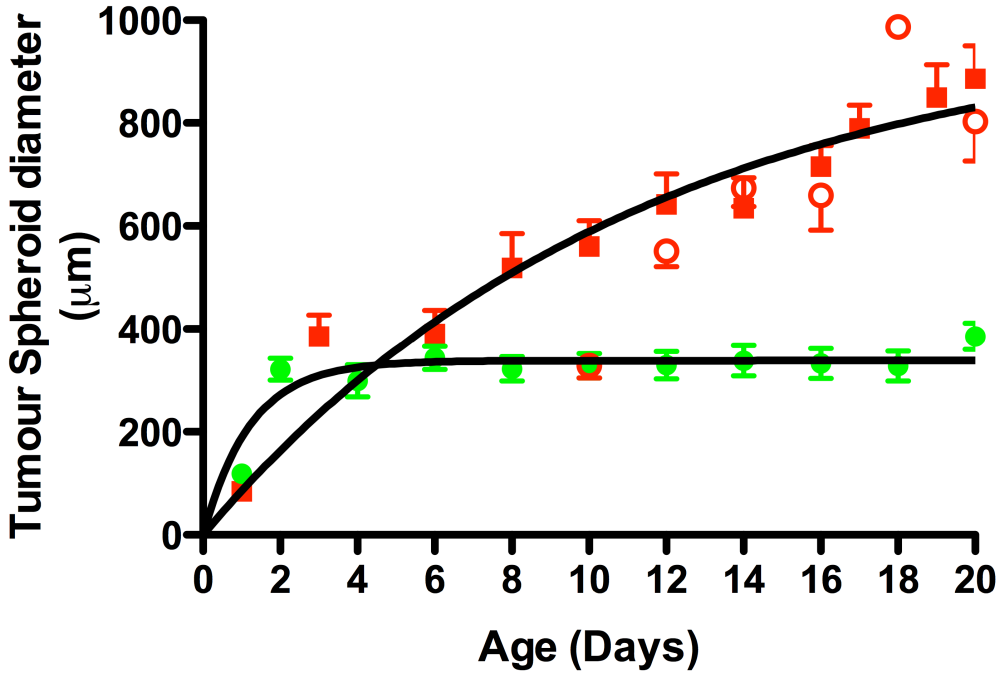
Analysis of glucose depletion and lactate accumulation in the medium, section 3.2, established that TS depleted 292 ± 42 μmoles $(mg\ total\ protein)^{-1}$ of glucose (*Figure 19*) and released a net of 131 ± 32 μmoles $(mg\ total\ protein)^{-1}$ of lactate (*Figure 25*)

over 24 H. An average of 0.8mg total protein was produced per batch of TS. Medium was therefore replaced every 48 hours to prevent nutrient depletion and accumulation of waste products such as lactate.

### 3.1.2 Generation of quiescent TS

Quiescent tumour spheroids ($TS^Q$) were generated by serum withdrawal, a technique previously optimised in this laboratory (Mellor et al., 2005a). Briefly TS in the correct size range were exchanged into medium containing 0.1% fatty acid BSA in place of foetal bovine serum, and cultured for 7 days with the medium refreshed every 48h. Quiescence is defined as a reversible non-dividing state; therefore the diameter of the TS was monitored to ensure that growth halted and quiescence was achieved. $TS^Q$ once exchanged into serum-less medium displayed minimal growth during the measured period, both the diameter (*Figure 12*a) and volume (*Figure 12*b) was observed to level off dramatically. Evaluation of $TS^Q$ volume established a growth constant (K) of 0.03 $days^{-1}$ indicating TS doubled in volume every 21.3 days. This is significantly lower ($p<0.0001$) than the growth constant (K) of 0.14 $days^{-1}$ observed in proliferating TS ($TS^N$) and is consistent with quiescence (*Figure 12*b). To confirm the induced growth arrest was reversible, $TS^Q$ were exchanged into medium containing serum at day 10, and their capacity to proliferate assessed. As shown in *Figure 12*a and 1b, these spheroids return to exponential growth comparable to that of $TS^N$ with a growth constant of 0.16 $days^{-1}$ indicating a doubling time of 4.77 days, which is a 4.5 fold increase in growth.

A.




B.

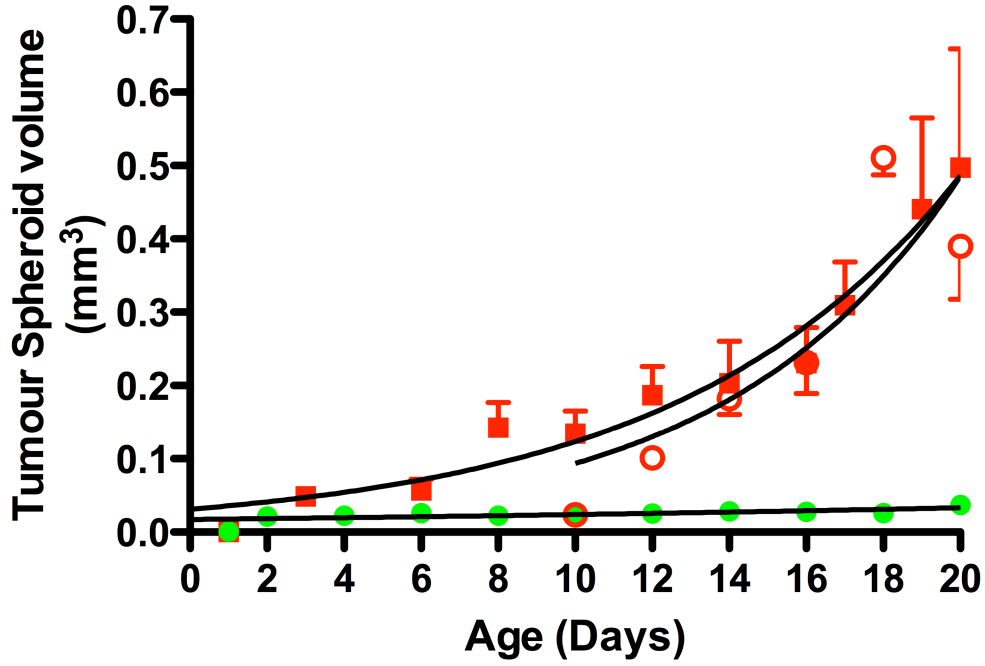



***Figure 12. Growth curves for tumour spheroid diameter (A) and volume (B).*** *(A) The diameter of tumour spheroids (n=20) was measured every 48 hours and used to calculate volume (mm³). Data represents the mean ± S.E.M. A one phase exponential association curve with the equation* $Y=Ymax(1-e^{-K \cdot X})$ *was fitted to the tumour spheroid diameter data. (B) An exponential growth curve with the equation* $Y=Ae^{KX}$ *was fitted to the tumour spheroid volume data. Quiescent tumour spheroids (●), were generated by exchanging proliferating tumour spheroids (■) into medium containing 0.1% fatty acid free BSA instead of 10% FCS. To confirm reversibility of quiescence, quiescent tumour spheroids were exchanged back into medium containing serum on day 10 (○).*

The proliferation status of the TS was also assessed by immunohistochemical detection of the proliferation marker Ki-67, a nuclear protein expressed during all active phases of the cell cycle but absent in quiescent cells (Scholzen and Gerdes, 2000). In addition concomitant immunohistochemical detection of the quiescence marker $p27^{Kip1}$, a cyclin dependent kinase (CDK) inhibitor, was used to define the quiescent state. The majority of the cells in the $TS^N$ were Ki-67 positive (70%) (*Figure 13*A), which indicates a high proportion of cells in active proliferation as expected at this stage of the growth curve (*Figure 12*b). In concurrence, the $TS^N$ displayed a limited number of cells positive for the quiescence marker $p27^{Kip1}$, which were located in the centre of the spheroid (*Figure 13*D). In $TS^Q$, the staining patterns were reversed relative to $TS^N$, the proportion of cells staining positive for Ki-67 was dramatically decreased to 40%(*Figure 13*B), supporting the minimal growth displayed by these spheroids in *Figure 12*. In contrast, the majority of the cells in the $TS^Q$ were positive for the quiescence marker $p27^{Kip1}$ (80%) (*Figure 13*E). These results confirm the difference in proliferative capacity of $TS^N$ compared to $TS^Q$ and indicate the validity of this TS based model for quiescence

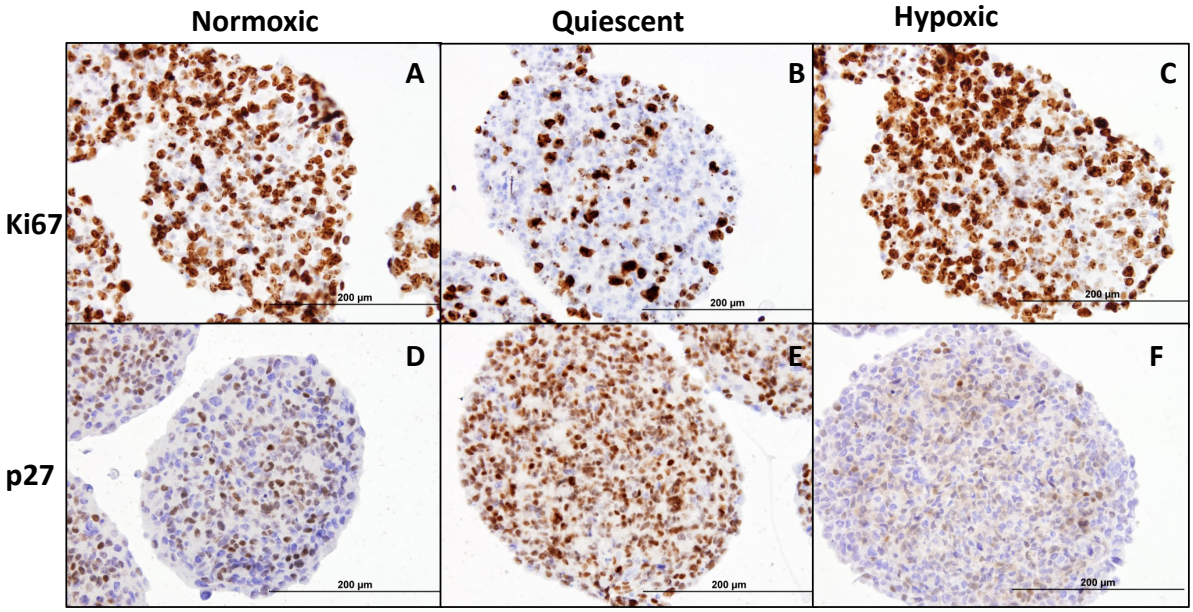



***Figure 13*** *Immunohistochemical staining of proliferation marker Ki-67 and the quiescence marker p27$^{Kip1}$ expression in TS. TS were fixed in formalin and embedded in paraffin wax. Immunohistochemistry was performed on sections (5µm) to detect the proliferation marker Ki67 and the quiescence marker p27$^{Kip1}$. Sections were counterstained with haematoxylin and mounted with aquamount. The scale bar corresponds to 200 µm.*

### 3.1.3 Generation of hypoxic TS

The 3D structure of tumours exposes cells to various naturally occurring micro-environmental stresses (Brown and Giaccia, 1998). One of them, hypoxia, is a feature of many tumours due to the limit of oxygen diffusion at approximately 200 µm (Torres Filho et al., 1994; Wilson and Hay, 2011). Assessment of TS oxygenation was reported by detection of cell staining with pimonidazole. Pimonidazole (2-nitroimadazole) is a reductively activated hypoxia marker that forms a hydroxylamine which covalently binds to thiol containing proteins specifically in hypoxic cells (Varia et al., 1998). Immunohistochemical analysis determined that TS between 200 µm and 400 µm in diameter (0.03 mm$^3$), grown at 21% $O_2$ (TS$^N$), were

fully oxygenated (*Figure 14*A). Hypoxic TS, ($TS^H$), were generated using the AnaeroGen system, a method that was previously optimised in this laboratory (Mellor et al., 2005b). Briefly TS were transferred to a hypoxic chamber at 0.1% $O_2$, for 16 hours prior to harvesting $TS^H$. Following the 16 hr incubation, $TS^H$ displayed a marked increase in positive immunohistochemical staining of pimonidazole when compared to $TS^N$ (*Figure 14*b). $TS^H$ also displayed comparable immunohistochemical staining of the proliferation marker Ki67 and quiescence marker $p27^{Kip1}$ to $TS^N$ (*Figure 13*F) with a high proportion of the cells in the spheroid staining positive for Ki67 (*Figure 13*C). This indicated that $TS^H$ contained a high proportion of actively proliferating cells, despite the hypoxic stress.

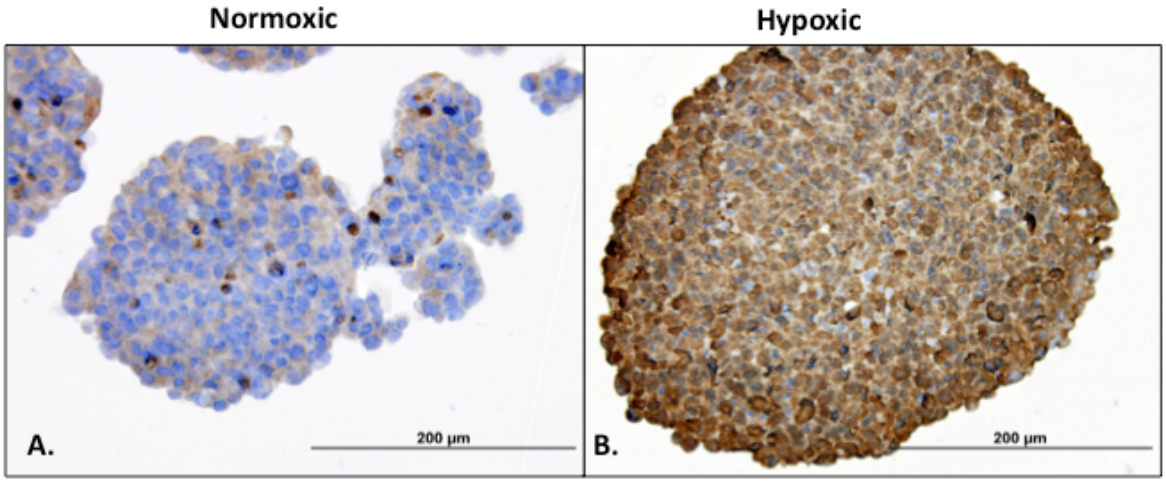



***Figure 14. Immunohistochemical staining of the hypoxia marker pimonidazole in $TS^N$ (A.) and $TS^H$ (B.).*** *TS were cultured with 100µM pimonidazole present in the medium prior to being fixed in formalin and embedded in paraffin wax. Immunohistochemistry was performed on sections (5µm) to detect pimonidazole. Sections were counterstained with haematoxylin and mounted with aquamount. The scale bar corresponds to 200 µm.*

The viability of the $TS^H$ following incubation was confirmed using an outgrowth assay, which assessed the proliferative capacity of the cells. The latter was detected by measuring outgrowth of cells from the attached spheroid after 72 hr. There was no statistically significant difference in the radial outgrowth observed between $TS^H$

and $TS^N$ (*Figure 15*). It was therefore concluded that the cells in the $TS^H$ were viable, as they retained the ability to proliferate at a rate identical to normoxic tissue.

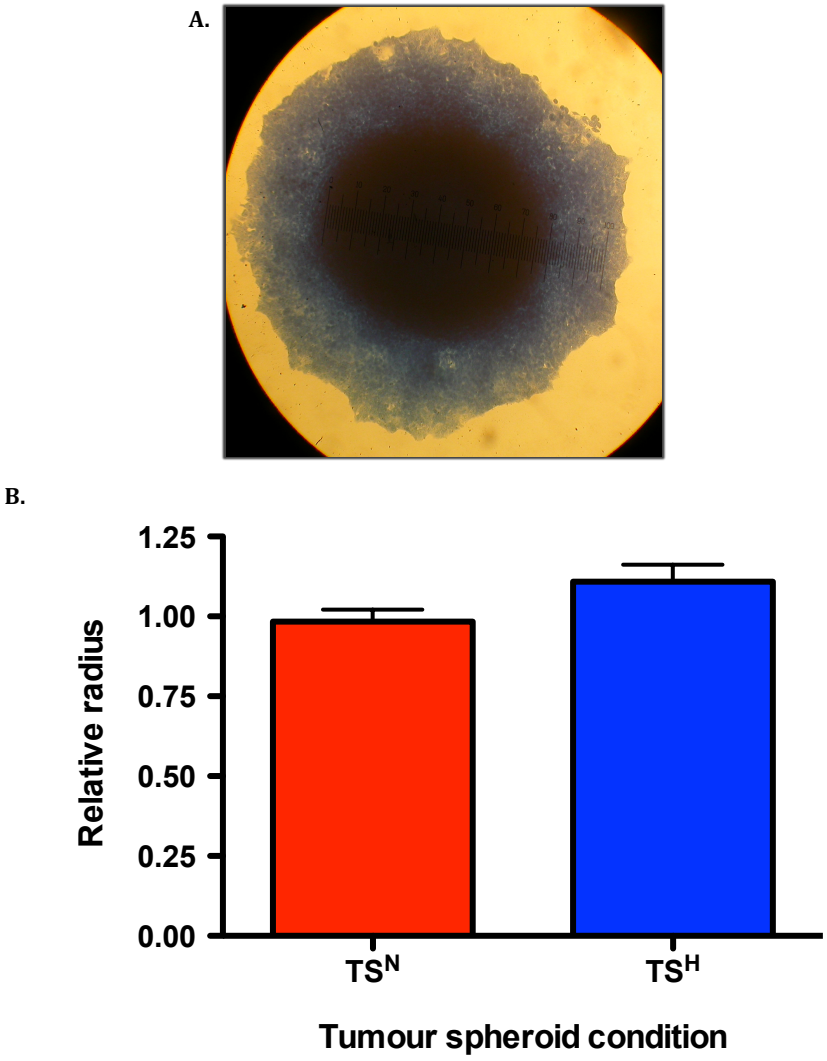
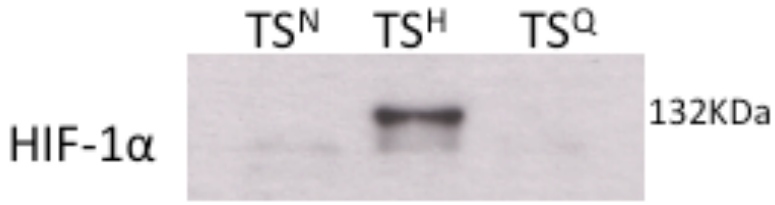



***Figure 15. The viability of tumour spheroids following hypoxic incubation.*** *Viability of the $TS^H$ (blue) relative to $TS^N$ (Red) was determined using an outgrowth assay. TS were transferred to an uncoated 96 well plate with 200µl of fresh medium and incubated for 72 hours.. (A) A photograph of representative tumour spheroid with outgrowth is shown. (B) The resulting radial outgrowth was measured using a graduated microscope eyepiece graticule and the ratio to spheroid radius recorded as relative radius. a histogram of the mean ± S.E.M of the relative radius is shown. A T test of the data gives a p value of 0.125 (n=3).*

### 3.1.4 Metabolic regulators

The cellular response to alterations in the micro-environment will involve the actions of several signalling pathways and transcription factors. The major transcription factor mediating cellular adaptation and survival under hypoxia is the hypoxia inducible factor 1 (HIF-1). It is known to target a broad range of genes involved in angiogenesis, cell survival, metabolism, pH regulation, adhesion, extracellular matrix remodelling, migration and metastasis (Semenza, 2010). HIF-1 is a heterodimer composed of a constitutively expressed HIF-1β subunit and an oxygen dependent HIF-1α subunit that is hydroxylated and targeted for degradation under aerobic conditions (Jaakkola et al., 2001). Previous studies relating HIF-1α expression to oxygen levels have shown that in HeLa cells, HIF-1α protein levels increased exponentially as $O_2$ concentrations dipped below 2%, peaking at 0.5% (Jiang et al., 1996). In concurrence with this study, a significant increase in the intensity of HIF-1α protein was detected in western immunoblots of $TS^H$ (0.1% $O_2$) (3.3 fold) relative to $TS^N$ (21% $O_2$)(*Figure 16*). Certain oncogenic mutations, such as those in the von Hippel-Lindau (VHL) protein (Mack et al., 2003), can however result in oxygen independent HIF-1α expression, which may explain the basal levels present in $TS^N$ and $TS^Q$ (*Figure 16*).

A.




B.

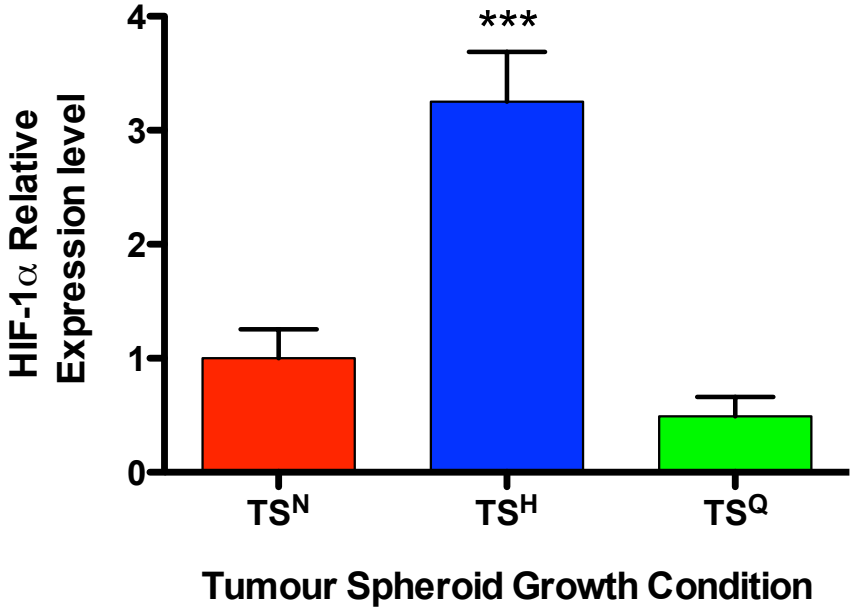



***Figure 16 The relative levels of HIF-1α in tumour spheroids grown under different micro-environmental stresses.*** *Western blots used 10μg of total protein homogenate using at least four independent samples from $TS^N$ (red), $TS^H$ (blue) and $TS^Q$ (Green). Positive controls were cell lysates from DLD1 cells incubated with cobalt chloride. Blots were probed with a mouse monoclonal primary antibody. An example blot is shown (A). Densitometry was performed using image J, the mean values ± S.E.M are expressed relative to the mean intensity for the $TS^N$ for each blot (B). Significant differences as analysed by ANOVA are indicated *** P<0.001.*

The deregulation of the transcription factor cMyc is also observed in many commonly occurring human cancers (Dang et al., 2009; Miller et al., 2012). cMyc is best characterised as a driver of proliferation and has been shown to up regulate expression from a range of genes including those involved in the cell cycle and nutrient metabolism (Coller et al., 2000). These metabolic genes include nutrient transporters such as GLUT1 and ASCT2 as well as glycolytic enzymes, hexokinase 2,

phosphofructokinase M, enolase 1 and lactate dehydrogenase A (Gao et al., 2009; Osthus et al.; Shim et al., 1997). cMyc also indirectly up regulates the expression of the glutaminolytic enzyme glutaminase (Gao et al., 2009; Osthus et al., 2000; Shim et al., 1997). Finally, studies have indicated a relationship between cMyc and HIF-1, with cMyc over-expression enhancing the stability of the HIF-1$\alpha$ subunit under both normoxic and hypoxic conditions (Doe et al., 2012). Figure 6A demonstrates that low levels of cMyc were observed in $TS^N$ homogenates as detected by western blot. cMyc protein levels were amplified 2 fold in response to hypoxia in $TS^H$ ($p<0.05$) but in contrast, growth of TS in quiescent conditions led to a 0.3 fold reduction in cMyc levels, although this change was not statistically significant relative to cMyc levels in $TS^N$ (Figure 17).

### 3.1.5 Summary and conclusions

These preliminary experiments demonstrate the feasibility producing of tumour spheroids grown under a variety of conditions representing different aspects of the tumour microenvironment. Analysis of the growth of tumour spheroids resulted in the selection of spheroids that were 200-400 μm in diameter. This was typically at day 2 of TS growth where TS had an average diameter of 232 ± 7 μm. At this stage immunohistochemical examination of the proliferation marker ki67 and the quiescence marker $p27^{Kip1}$ (*Figure 13*) indicated that the spheroids were predominantly composed of actively proliferating cells. In addition, analysis of the hypoxia marker pimonidazole (*Figure 14*) demonstrated that the spheroids were

fully oxygenated. Analysis at this stage of tumour spheroid growth enables the comparative examination of distinct micro-environmental conditions. Spheroids grown above the maximum 400 μm diameter used in this study develop areas of hypoxia and quiescence (*Figure 11*)(Sutherland, 1988), this however renders analysis of the distinct stresses difficult.

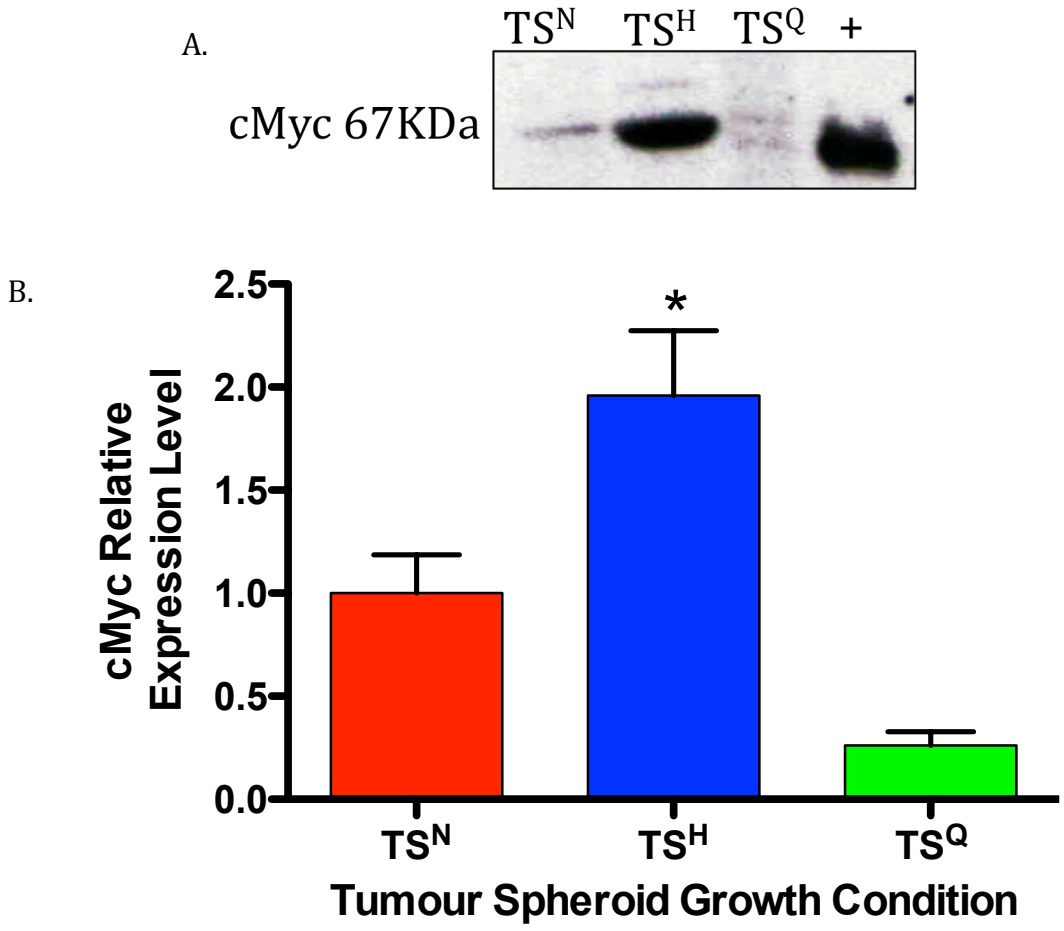



**Figure 17** ***The relative levels of the metabolic regulator c-Myc in tumour spheroids grown under different micro-environmental stresses.*** *Western blots used 10μg of total protein homogenate with at least four independent samples from $TS^N$ (red), $TS^H$ (blue) and $TS^Q$ (Green). Positive controls were run of 293T cell lysates transfected with c-Myc. Blots were probed with a primary monoclonal mouse antibody to cMyc. An example blot is shown (A). Densitometry was performed using image J, values are expressed relative to the mean intensity for the $TS^N$ ± S.E.M for each blot (B). Significant differences as analysed by ANOVA are indicated * P<0.05.*

The induction of the micro-environmental stress states of hypoxia and quiescence upon the spheroids was performed by previously optimised methods (Mellor et al., 2005a; Mellor et al., 2005b). The production of quiescent spheroids was confirmed by the significant reduction in immunohistochemical staining of the proliferation marker Ki67 and simultaneous increase in staining of the quiescence marker $p27^{Kip1}$ relative to proliferating spheroids (*Figure 13*). The viability of these quiescent spheroids was established by measurement of spheroid growth upon return to proliferating conditions (*Figure 12*). Production of hypoxic spheroids was confirmed using immunohistochemistry to analyse staining of the hypoxia marker pimonidazole (*Figure 14*) and the viability of hypoxic spheroids validated via analysis of spheroid outgrowth (*Figure 15*). This Further characterisation of the spheroids involved analysis of the levels of key metabolic regulators within the spheroids, including HIF-1$\alpha$ (*Figure 16*) and cMyc (Figure 17), both of which were significantly increased in hypoxic spheroids. These studies demonstrated successful induction of micro-environmental stress on viable tumour spheroids. These spheroids were concluded to be a suitable model system to use in subsequent investigations studying the effect of micro environmental conditions on the metabolic adaptations found within the different populations of cells present within a tumour.

## 3.2 Nutrient utilization

Cancer is characterized by uncontrolled proliferation. In order to fuel this high growth rate, cancer cells require an increased supply of nutrients to generate ATP and biomass. Numerous studies have demonstrated that tumour cells increase their consumption of glucose and glutamine (Bode et al., 1995; Gillies et al., 2008). As stated earlier (section 1.), glucose is utilized by cancer cells both for energy via aerobic glycolysis leading to lactate production (Warburg, 1956b), and as a biosynthetic precursor. Furthermore glutamine is utilized by cancer cells as both an anaplerotic precursor and as a substrate for energy production (DeBerardinis et al., 2007). The objective of the investigations in this section is to use the tumour spheroids developed in section 3.1 to determine how micro-environmental stress effects the utilization of nutrients.

To achieve this objective the subsequent experiments measured: the relative levels of glucose, glutamine and lactate transporters, the depletion of glucose and glutamine from the growth medium, the accumulation of lactate in the growth medium, the glycolytic flux and the metabolic fate of glucose in the tumour spheroids.

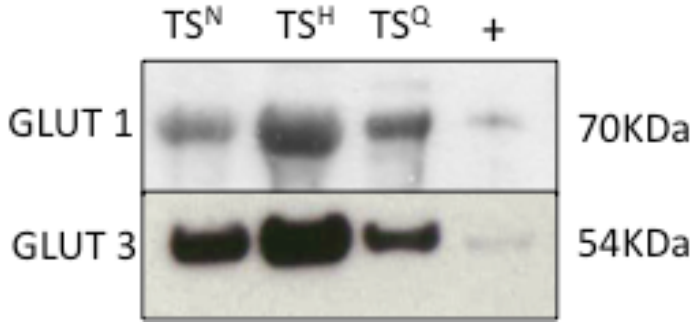
### 3.2.1 Glucose

Numerous studies have shown that cancer cells have increased rates of glucose uptake in comparison to non-transformed cells (Hatanaka, 1974)(section 1.1.1).

Concomitantly, the over-expression of glucose transporters including GLUT1 and GLUT3 in cancer cells has been frequently observed (Ayala et al., 2010; Baer et al., 1997; Brown and Wahl, 1993; Haber et al., 1998; Jozwiak et al., 2012; Shen et al., 2011; Younes et al., 1997a). Both GLUT1 and GLUT3 have high affinity for glucose (GLUT 1 $K_{m\ glucose}$ 1.6 mM, GLUT3 $K_{m\ 2\text{-}deoxyglucose}$ 1.4 mM) (Gould and Holman, 1993; Simpson et al., 2008). The high affinities of these transporters result in both being saturated at normal blood glucose concentrations of 5.5mM, and therefore glucose uptake is thought to be proportional to the level of transporter expression at the cell surface membrane. Both GLUT 1 and GLUT3 contain hypoxia response elements in their promoters that bind HIF-1 up regulating their transcription, which may explain the high levels of these transporters observed in many cancers.

The relative levels of these transporters in the TS exposed to the different micro-environmental conditions were measured by densitometric analysis of western immunoblots produced from TS homogenates (*Figure 18*). In hypoxia, GLUT1 protein levels in the TS rose by 1.5 fold relative to that in normoxia, but this increase was not statistically significant. Similarly although GLUT1 levels were observed to decrease by 2 fold in $TS^{Q}$ relative to $TS^{N}$, the change was not statistically significant. In contrast, levels of GLUT3 were amplified significantly in $TS^{H}$ relative to $TS^{N}$, with a 2-fold difference in levels observed. Again although slightly lower levels of GLUT3 were measured in $TS^{Q}$ than $TS^{N}$ the difference did not reach statistical significance.

A.




B.

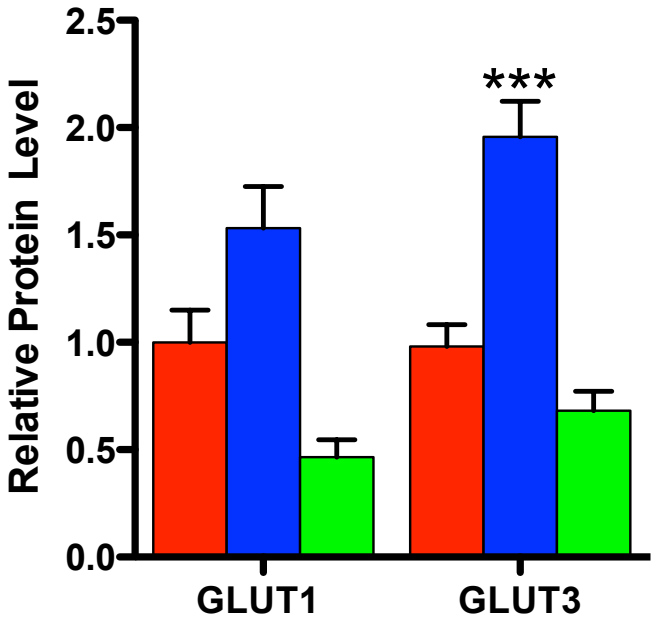



***Figure 18. Relative expression levels of glucose transporters in TS.*** *(A) Western blots were preformed using 10μg of total protein homogenate of at least four independent samples from TS$^N$ (red), TS$^H$ (blue) and TS$^Q$ (Green). Positive controls were run from DLD1 cell lysates. Blots were probed with rabbit polyclonal primary antibodies to GLUT1 and GLUT3 respectively. Representative western blots are shown. (B) Densitometry was performed using image J values (mean ± S.E.M) were expressed relative to the mean intensity for the TS$^N$. Significant differences as analysed by ANOVA are indicated; *** P<0.001.*

Glucose concentration in the medium was measured during the last 24 hours of tumour spheroid growth using a spectrophotometric assay, and the amount of glucose depleted during growth related to the final TS protein concentration. TS$^N$ were able to deplete 292 ± 42 μ moles mg protein$^{-1}$ of glucose from the growth

medium over the 24 hour period. Quiescent spheroids depleted 547 ± 98 μ moles $mg^{-1}$ of glucose from the medium over 24H which was a statistically significant increase ($p<0.05$) of 1.9 fold relative to $TS^N$. However, there were no significant differences between the glucose depletion in $TS^N$ and $TS^Q$ observed at earlier time points in the assay (*Figure 19*). This significant increase in glucose depletion observed in $TS^Q$ was unexpected as quiescent cells were traditionally thought to be less metabolically active than their proliferating counterparts (see section 1.3.3).

To prevent spheroid re-oxygenation, glucose concentration in the medium could only be measured at the start and end of the 16-hour hypoxic incubation for $TS^H$. The initial concentration of glucose in the medium was a mean of 10.4 ± 0.5 mM this was depleted by 14.1 ± 8 μ moles mg $protein^{-1}$ during the hypoxic incubation leaving a mean glucose concentration of 9.8 ± 0.5 mM. Glycolysis is thought to be the major energy production pathway under hypoxic conditions therefore it would be expected that glycolysis contributes extensively to this depletion.

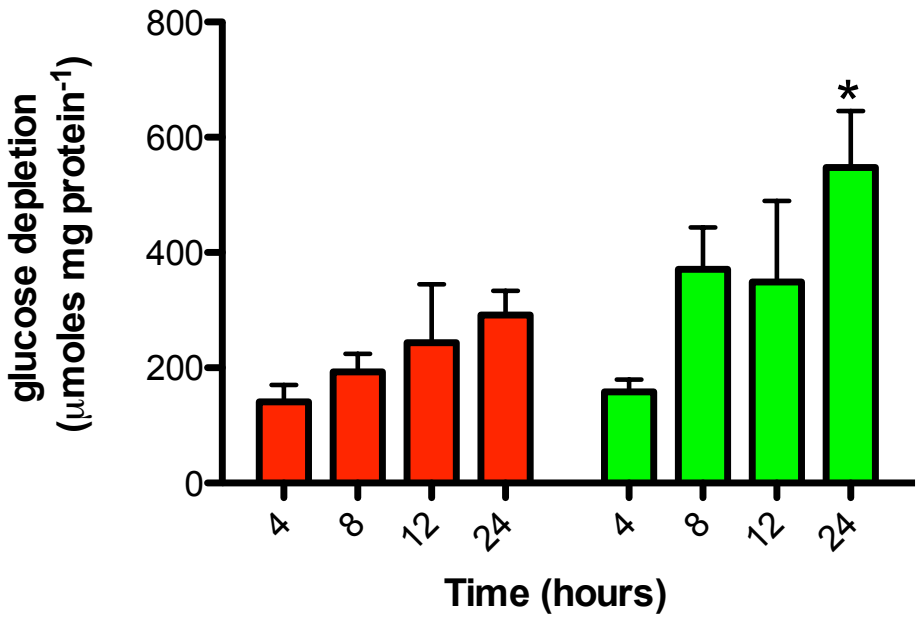
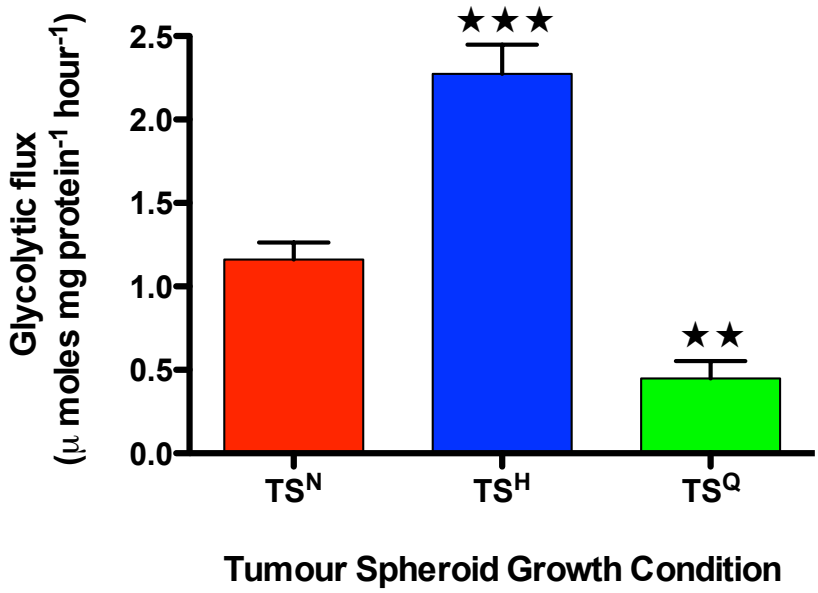



***Figure 19. Glucose depletion from the growth medium.*** *Glucose levels in the medium were determined at various time points via spectrophotometric assays. The amount of glucose depleted from the growth medium was related to total protein concentration, the values expressed represent the mean ± S.E.M of at least four independent experiments. Each time point represents the cumulative depletion from the beginning of the experiment at 0 hours. Glucose depletion in $TS^N$ is represented in red and in $TS^Q$ in green. Significant differences as analysed by ANOVA are indicated ★ $p<0.05$.*

The next step to directly assess the rate of glucose metabolism included measuring the rate of flux through the glycolytic pathway. This was achieved using radio-labelled-[5-$^3$H] glucose. The $^3$H radiolabel in this metabolite is removed from glucose in water during the triose phosphate isomerisation and enolase steps of the glycolytic pathway. The $^3H_2O$ released is then separated from the radio-labelled glucose in the medium using a DOWEX column and quantified by scintillation counting. Measurement of the rate of $^3H_2O$ production provides a measurement of metabolite flux through the glycolytic pathway. The glycolytic flux in control spheroids $TS^N$ was 1.16 ± 0.1 μmoles mg protein$^{-1}$ hour$^{-1}$, this rose by 2 fold in spheroids grown under hypoxic conditions to 2.27 ± 0.2 μmoles mg protein$^{-1}$ hour$^{-1}$. This statistically

significant ($p<0.001$) increase in glycolytic rate concurs with the hypothesis that hypoxic cells are reliant on glycolysis for their ATP production. Conversely the flux through glycolysis was significantly reduced ($p<0.01$) in $TS^Q$ to 0.45 ± 0.1 µmoles mg protein$^{-1}$ hour$^{-1}$, which was 2.6 fold lower than the glycolytic flux observed in $TS^N$. This decrease in glycolytic flux correlates with the hypothesis that quiescent cells have a dramatically decreased metabolic rate due to their reduced biosynthetic requirements (Section 1.3.3). However this lower glycolytic flux does raise the question of the metabolic fate of the excess glucose accumulation observed in the $TS^Q$ (*Figure 19*).




| | $TS^N$ | $TS^H$ | $TS^Q$ |
|---|---|---|---|
| Glycolytic Flux<br>µmol hour$^{-1}$ (mg protein)$^{-1}$ | 1.16 ± 0.1<br>(n = 4) | 2.27 ± 0.2<br>(n = 4) | 0.45 ± 0.1<br>(n = 5) |

***Figure 20 Glycolytic flux in tumour spheroids****. Glycolytic flux was determined by measuring the rate or detritiation of [5-$^3$H] glucose, and standardised to the total protein concentration. Values shown are the mean rate ± SEM from at least four independent experiments, rates are expressed as µmol glucose detritiated per hour per mg of total protein. Significant differences analysed by ANOVA are indicated *** P<0.001 **P<0.01.*

In order to further investigate glucose utilization in quiescent TS, metabolomics studies were performed on $TS^N$ and $TS^Q$. Metabolomics studies were not performed with hypoxic TS, as prevention of re-oxygenation during the experiment was not feasible using the AnaeroGen system. These experiments traced the metabolic fate of $^{13}C$ from universally labelled $^{13}C$ glucose ([U-$^{13}C$] glucose). TS were exposed to [U-$^{13}C$] glucose for 30 or 120 minutes prior to metabolite extraction and the $^{13}C$ labelling of metabolites was analysed by GC-MS.

The $^{13}C$ enrichment data was normalised for the percentage of labelled $^{13}C$ glucose available in the medium and is shown in (*Figure 21*). The enrichment of glucose-derived carbon in a wide range of metabolic intermediumtes from glycolysis, the pentose phosphate pathway, the TCA cycle and amino acid metabolism were analysed. Although there appears to be few differences between the TS growth conditions and time points used. These data reveal that in both $TS^N$ and $TS^Q$ there are high levels of glucose-derived carbon in metabolites of the glycolytic and pentose phosphate pathways such as glucose-6-phosphate, 6-phosphogluconic acid and 3-phosphoglycerate. This together with the low enrichment of glucose-derived carbon in intermediumtes of the TCA cycle illustrates the glycolytic nature of these TS. This is consistent with Otto Warburg's theory that cancer cells employ aerobic glycolysis as a metabolic strategy (Warburg, 1956b).

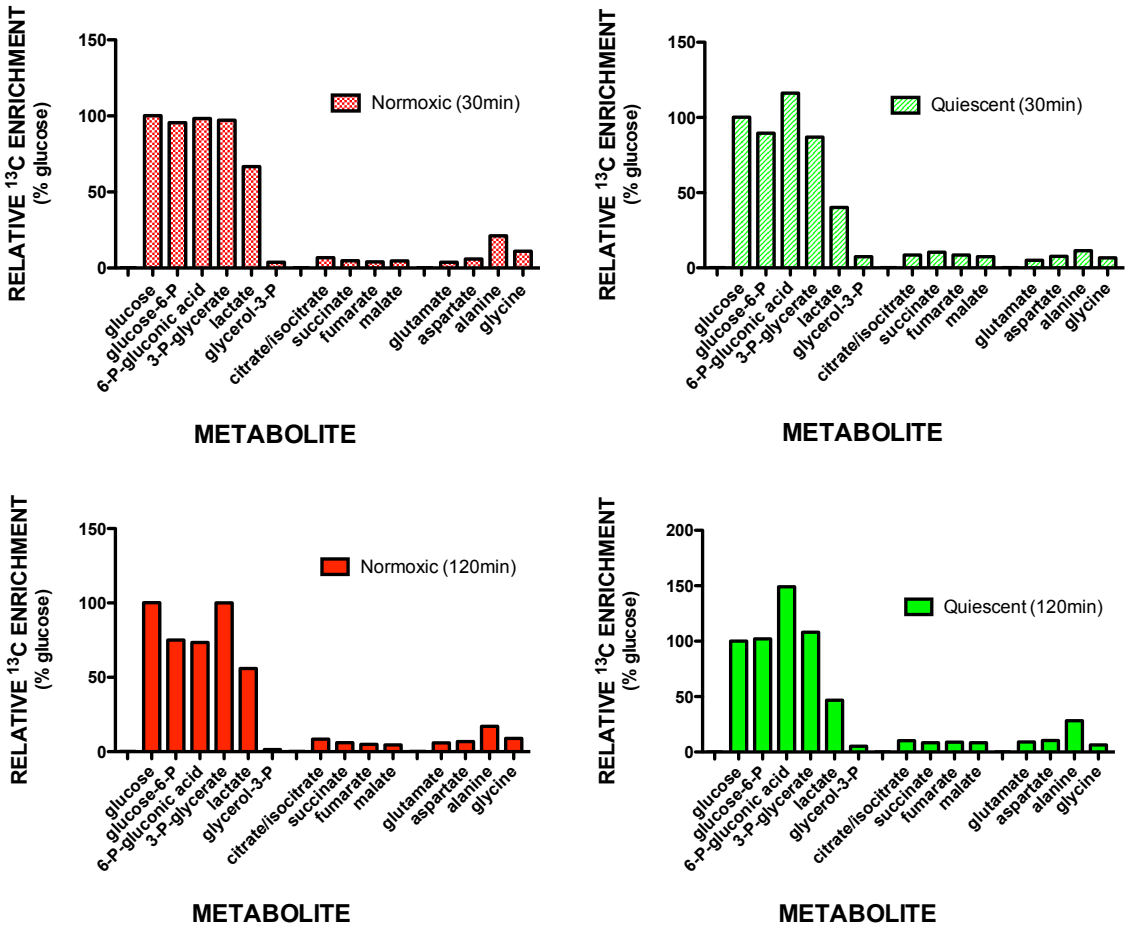



***Figure 21 Relative glucose derived $^{13}C$ enrichment of intracellular metabolites.*** *GC-MS Metabolic fate analysis of [U-$^{13}C$] glucose in tumour spheroids. TS were incubated with medium containing [U-$^{13}C$] glucose for 30 minutes ($TS^N$ red hashed, $TS^Q$ green hashed) and 120 minutes ($TS^N$ red, $TS^Q$ green), prior to metabolite extraction and analysis via GC-MS. Relative $^{13}C$ enrichment (y axis) refers to the percentage of the metabolite pool labelled normalised for the fraction of labelled glucose used in the study.*

### 3.2.2 Glutamine

Glutamine is the most abundant amino acid in the plasma (Bode, 2001) and plays a pivotal role in cancer cell metabolism (Eagle, 1955; Kovacevic and McGivan, 1983). It is utilized both as a nitrogen donor for biosynthesis and its carbon

skeleton can be catabolised for energy production (section 1.1.3). ASCT2 is an amino acid exchanger and is the transporter responsible for the majority of glutamine uptake in cancer cells (Fuchs and Bode, 2005). It has high-affinity ($K_m$ 20 μM) for glutamine and other small neutral amino acids, including asparagine (Fuchs and Bode, 2005) (Utsunomiya-Tate et al., 1996).

The relative ASCT2 expression levels found under the different micro environmental conditions were measured by western immunoblot analysis of TS homogenates. ASCT2 protein was detected under all the micro-environmental conditions employed in this study (*Figure 22*A). However densitometric analysis of these western immunoblots revealed that the amount of ASCT2 protein detected did not vary significantly between the TS homogenates prepared from normoxic, hypoxic or quiescent tumour spheroids (*Figure 22*B).

Glutamine concentrations in the medium were measured twice, at twelve-hour intervals, during the final 24 hours of TS growth (*Figure 23*). These measurements revealed a dramatic difference in the profile of glutamine depletion between control $TS^N$ and $TS^Q$. Glutamine depletion was significantly increased ($p<0.01$) after twelve hours in $TS^Q$ to 45.6 ± 9.6 μmoles (mg protein)$^{-1}$, a dramatic 5.5 fold rise from the 8.3 ± 3.2 μmoles (mg protein) $^{-1}$ depleted in $TS^N$. However, after twenty-four hours the difference between the glutamine depletion was no longer statistically significant, with $TS^N$ depleting 39.7 ± 7.6 μ moles (mg protein)$^{-1}$ of glutamine and $TS^Q$ 58.9 ± 7.4 μ moles (mg protein)$^{-1}$.

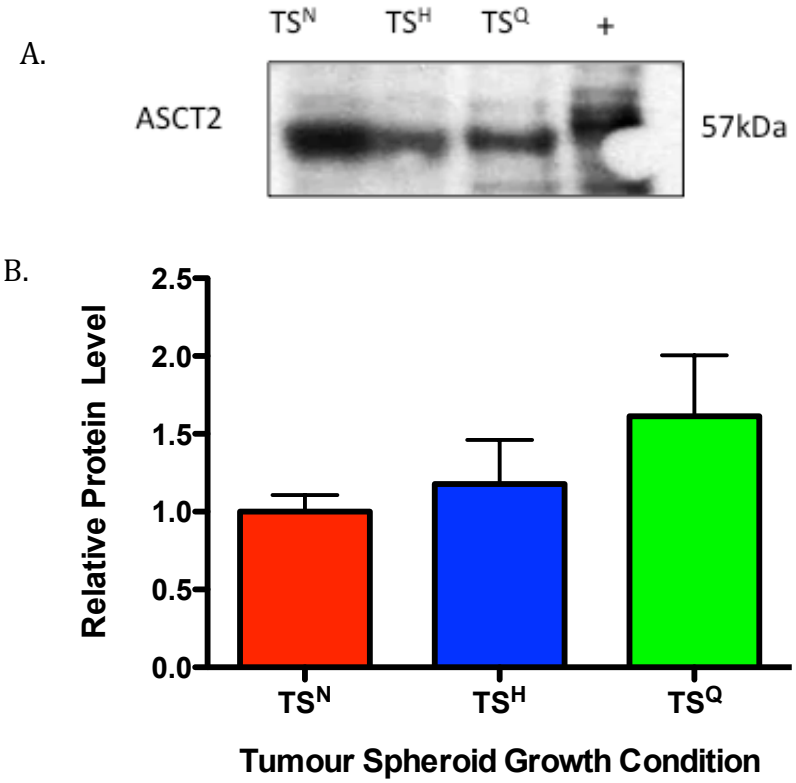



***Figure 22 Relative levels of the glutamine transporter ASCT2.*** *Western blots were preformed using 10µg of total protein homogenate of at least four independent samples from $TS^N$ (red), $TS^H$ (blue) and $TS^Q$ (Green) . Positive controls (+) were cell lysates from HeLa cells. Blots were probed with rabbit polyclonal primary antibodies to ASCT2. An representative blot is shown in panel (A). Densitometry was performed using image J, values are expressed relative to the mean (± S.E.M) intensity for the $TS^N$ for each blot in panel (B).*

To prevent re-oxygenation of $TS^H$ glutamine concentration in the medium could only be measured at the start and end of the hypoxic incubation. Measurements at these time points determined glutamine was present in the medium at 1.3 ± 0.1 µmoles (mg protein)$^{-1}$ at the beginning of the hypoxic incubation. This was depleted by 8.0 ± 2.6 µmoles glutamine (mg protein)$^{-1}$ during the 16 hour hypoxic incubation to a final concentration of 1.2 ± 0.1 mM.

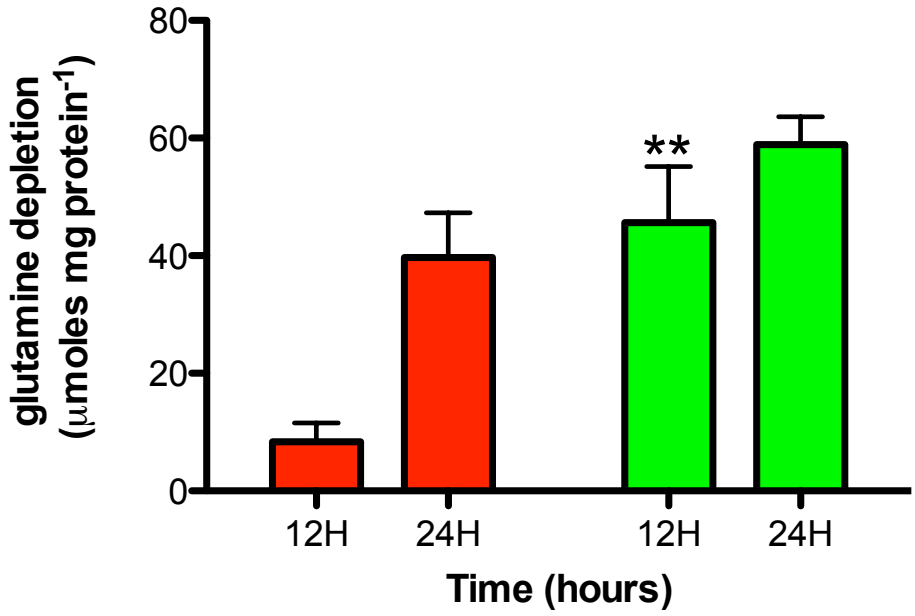



***Figure 23. Glutamine depletion from the growth medium.*** *Glutamine levels in the medium were determined at 12-hour intervals via spectrophotometric assays, and expressed as glutamine depletion from the medium. The values expressed represent the mean ± S.E.M of at least four independent experiments, each time point represents the cumulative depletion from the beginning of the experiment at 0 hours.* $TS^N$ are represented in red and $TS^Q$ are in green. *Significant differences, as determined by ANOVA, are indicated ** P<0.01.*

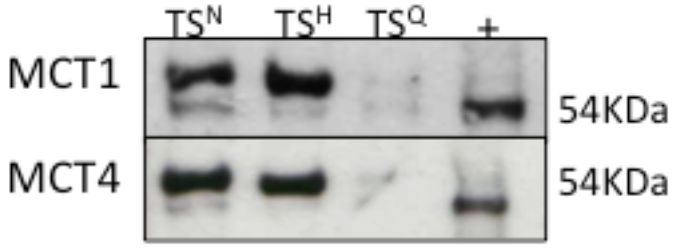
### 3.2.3 Lactate

Increased lactate production is a hallmark of cancer (Warburg, 1956b). Lactate can be produced both from oxidation of glucose and glutamine, and has been considered to be a waste product of tumour metabolism contributing to extracellular acidosis. However, recent studies suggest a symbiosis between hypoxic tumour cells that have a predominantly glycolytic metabolism and the cells in the oxygenated regions of tumours that can utilize lactate as a substrate to fuel oxidative metabolism (Sonveaux et al., 2008b).

Lactate transport across the cell membrane is facilitated by members of the monocarboxylate transporter (MCT) family (Ganapathy et al., 2009). MCT1 has a high affinity for lactate ($K_{m\ Lactate}$ 3.5mM), and is thought to import lactate into oxygenated tumour cells (Bonen, 2001; Sonveaux et al., 2008b). Western immunobloting of MCT1 levels in homogenates produced from the TS detected strong signals for MCT1 in $TS^N$ and $TS^H$ (*Figure 24*A). Densitometric analysis revealed that the mean MCT1 protein level amplified ($p<0.01$) 1.5 fold in hypoxic $TS^H$ relative to $TS^N$ (*Figure 24*B). The levels of MCT1 protein detected by immunoblot were decreased in $TS^Q$ homogenates (*Figure 24*A), densitometry measurements confirmed this 3.3 fold reduction was statistically significantly ($p<0.001$) in $TS^Q$ in comparison to $TS^N$ (*Figure 24*B).

MCT4 has a low affinity for lactate ($K_{m\ Lactate}$ 17-34 mM) and functions as an exporter of lactate in glycolytic tissues to regulate internal pH (Bonen, 2001). Immunoblot analysis of MCT4 levels in TS homogenates revealed a similar pattern to that observed for MCT1 (*Figure 24*A). MCT4 was significantly ($p<0.001$) up-regulated by 1.5 fold in $TS^H$ compared to $TS^N$ (*Figure 24*B). This concurs with previous studies showing that MCT4 expression is up-regulated by HIF 1 (Ullah et al., 2006). In contrast, there was no statistically significant difference in MCT4 levels in $TS^Q$ relative to $TS^N$.

A.




B.

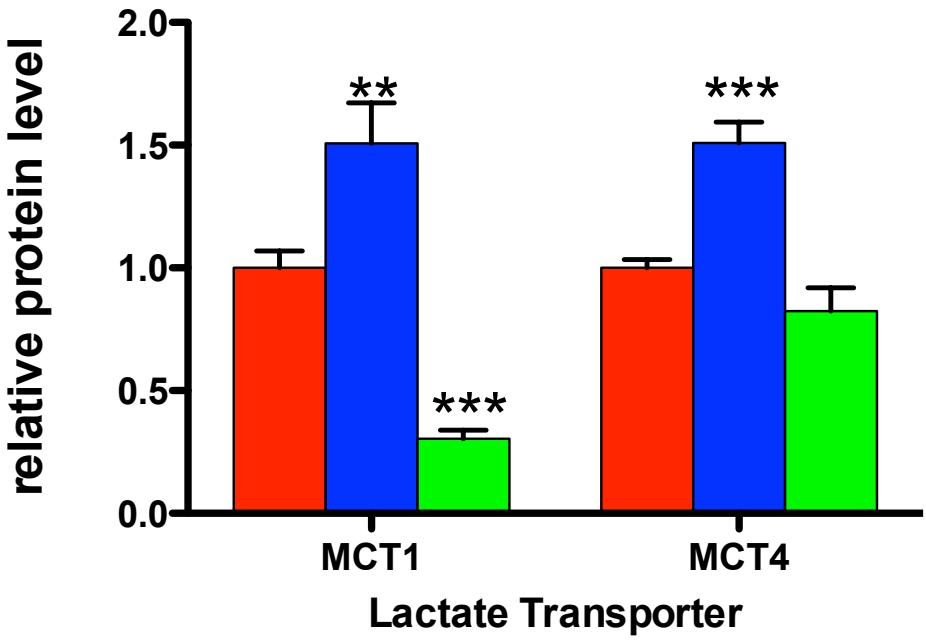



***Figure 24 Relative levels of the lactate transporters MCT1 and MCT4. (****A.) Western blots were preformed using 10µg of total protein homogenate of at least four independent samples from $TS^N$ (red), $TS^H$ (blue) and $TS^Q$ (Green). Positive controls were lystates of HeLa cell. Blots were probed with rabbit polyclonal primary antibodies to MCT1 and MCT4 respectively. Representative blots are shown in panel (A). Densitometry was performed on the major band using image J, values are expressed relative to the mean intensity (± S.E.M ) for the $TS^N$ for each blot (B). Significant differences are indicated *** P<0.001 **P>0.01 * P<0.05*

Lactate concentrations in the medium during tumour spheroid growth were also measured using a spectrophotometric assay (*Figure 25*). This technique measures net lactate production from the tumour spheroids, however it does not give an indication of whether lactate is also being taken up and utilized as a substrate for oxidative phosphorylation by cells within the tumour spheroids (Sonveaux et al., 2008b). Net lactate production was amplified significantly ($p<0.05$) over twenty-four hours in $TS^Q$ to 232 ± 30 µmoles (mg protein)$^{-1}$,

relative to the 131 ± 32 μ moles mg protein$^{-1}$ measured in the medium of $TS^N$. No statistically significant differences between $TS^N$ and $TS^Q$ net lactate production in the medium were recorded at earlier time points in the assay (*Figure 25*).

To prevent $TS^H$ re-oxygenation lactate concentration in the medium could only be measured at the start and end of a 16-hour hypoxic incubation in the Anaerogen chamber. During the 16 hour hypoxic incubation, $TS^H$ produced a net 16.3 ± 3.8 μmoles (mg protein)$^{-1}$ of lactate in the medium. If glucose is exclusively being metabolised by glycolysis to produce lactate, two moles of lactate are produced per mole of glucose consumed. As mentioned previously (section 3.2.1) 14.1 μ moles mg$^{-1}$ of glucose was depleted from the medium during the hypoxic incubation. This suggests that glucose is not being exclusively metabolised by glycolysis to produce lactate in $TS^H$.

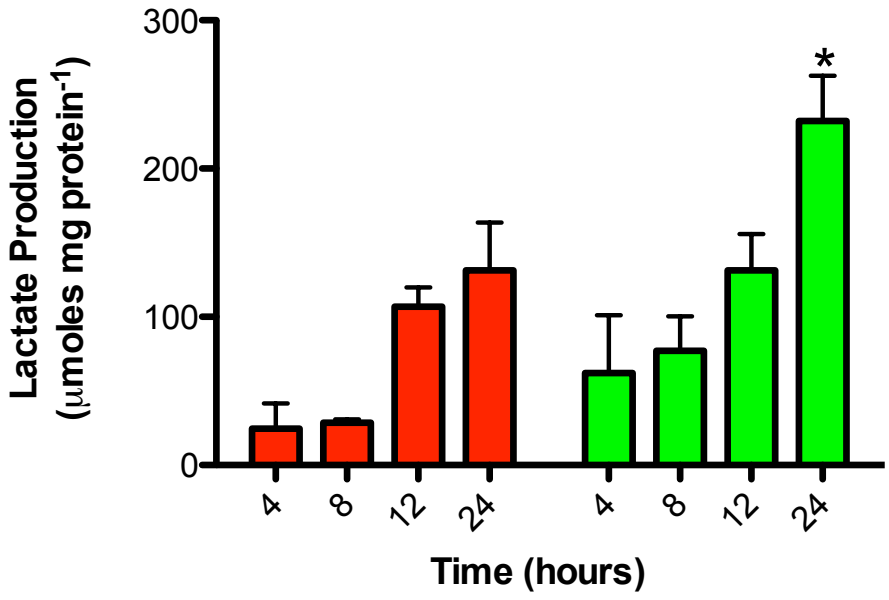



***Figure 25. Rate of Lactate accumulation in the medium.*** *Lactate levels in the medium were determined at various time points via spectrophotometric assays, lactate production was related to total protein concentration. The values expressed represent the mean ± S.E.M of at least four independent experiments. Each time point represents the cumulative production from the beginning of the experiment at 0 hours.* $TS^N$ are represented in red and $TS^Q$ are in green. *Significant differences as determined by ANOVA are indicated * P<0.05.*

### 3.2.4 Summary and conclusions

The objective of the experiments presented in this section was to determine whether micro-environmental stress affects nutrient utilization in tumour spheroids. The results indicate that tumour spheroids grown under different micro-environmental stresses differ considerably in how they utilize nutrients, implying differences in their metabolic strategies.

Under hypoxic conditions significant increases in the levels of the HIF-1 responsive glucose transporter GLUT3 (*Figure 18*), the rate of glycolytic flux (*Figure 20*) and expression of the lactate transporter MCT4 (*Figure 24*) were observed. It was also shown that glucose was depleted and lactate produced in the medium during the hypoxic incubation. Consistent with the hypothesis that hypoxic cells are reliant on glycolysis for their ATP production.

A number of changes were observed in TSQ relative to TSN. Firstly, although there was no significant change in the levels of the glucose transporters assayed (*Figure 18*), a significant increase in glucose depletion from the medium was observed over twenty-four hours (*Figure 19*). This increase in glucose depletion from the medium may be due to changes in the levels or activity of other glucose transporters. Conversely, the flux through the glycolytic pathway was significantly reduced (*Figure 20*) in TSQ relative to TSN. The extra glucose depletion from the medium in TSQ may be attributed to an increase in flux through the pentose phosphate pathway or into glycogen synthesis. Consistent

with the high enrichment of the pentose phosphate pathway intermediate 6-phosphogluconic acid observed in the metabolomic experiments (*Figure 21*)

Glutamine depletion from the medium was also significantly increased in $TS^Q$ over twelve hours (*Figure 23*), which is in agreement with the low glycolytic flux in $TS^Q$ suggesting that glutamine is the favoured nutrient for ATP production $TS^Q$. There was however no significant difference between $TS^Q$ and $TS^N$ in glutamine depletion from the medium over twenty-four hours (*Figure 23*). It is conceivable that glutamine uptake increases as glucose concentration in the medium decreases in $TS^N$ to ensure a constant supply of nutrients.

Finally, despite the statistically significant decrease in glycolytic flux there was a 1.8 fold increase in lactate accumulation in the medium over twenty-four hours in $TS^Q$ relative to $TS^N$. This may be a result of glutamine metabolism (DeBerardinis et al., 2007)(*Figure 6*) or due to reduced lactate re-uptake and utilization as a substrate for oxidative phosphorylation (Sonveaux et al., 2008b).

These experiments demonstrate that tumour spheroids grown under different micro-environmental stresses differ extensively in nutrient utilization therefore suggesting that they employ different metabolic strategies to meet their energy requirements.

## 3.3 Intracellular metabolic adaptations

In the previous section it was established that nutrient utilization differed between the different micro-environmental conditions employed in this study. The objective of this set of experiments was to investigate the molecular basis of these changes in nutrient utilization.

Detailing the changes in metabolite utilization was achieved by measuring changes in relative enzyme expression levels by western immunoblot. Additionally, enzyme activities were measured under optimised conditions, giving the maximal activity, or capacity, and indicating the total amount of active enzyme. Differences between the effects of the microenvironment on enzyme expression and specific activity indicate alterations in enzyme regulation at the post-translational level. The enzymes selected for this analysis are indicated in *Figure 26*, and represent points at which the pathways are highly regulated and have previously been shown to be affected by oncogenes (section 1.1).

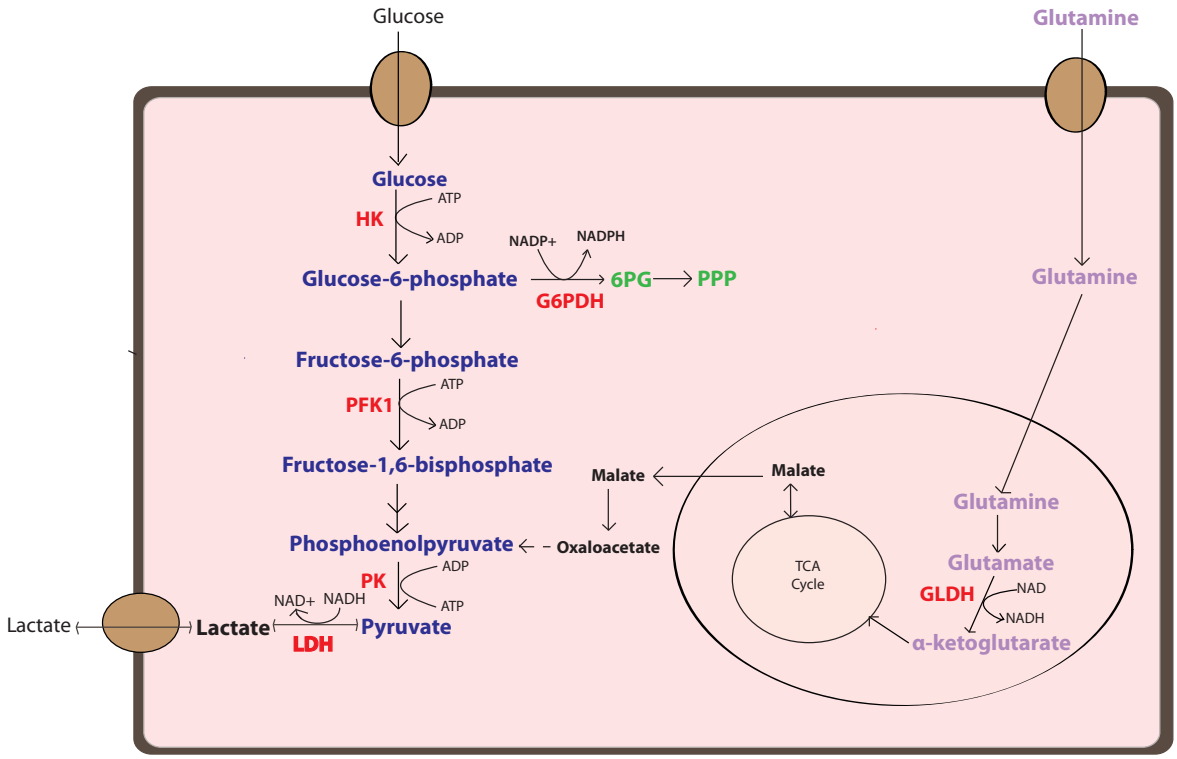



***Figure 26. Schematic illustrating the enzymes selected for this study****. Enzymes selected for this study from glycolysis (blue), the pentose phosphate pathway (green) and the glutaminolysis pathway (purple) are highlighted in red, whilst transport proteins are represented by ovals.*

### 3.3.1 Glycolytic pathway enzymes

The glycolytic enzymes Hexokinase (HK), Phosphofructokinase 1 (PFK1) and Pyruvate Kinase (PK) were selected for this study. These enzymes are points at which the glycolytic pathway is subject to substantial regulation, hence would be expected to have high flux control coefficients. The specific enzyme activity of HK, PFK1 and PK, were determined photometrically via $NAD(P)^+$/NAD(P)H linked reactions. These assays were developed by Board et al (Board et al., 1990) and optimised in this laboratory by Bloch et al (Bloch et al., 2014).

HK catalyses the phosphorylation of glucose forming glucose-6-phosphate with ATP hydrolysis. This traps glucose in the cell and maintains the concentration gradient for glucose uptake. Regulation of HK is achieved through product inhibition by glucose-6-phosphate. The specific activity of HK under normoxic conditions was 6.3 ± 1 nmol $min^{-1}$ (mg protein)$^{-1}$. Spheroids grown under hypoxia exhibited a 4.8 fold decrease in activity to 1.3 ± 0.3 nmol $min^{-1}$ (mg protein)$^{-1}$, although this did not reach statistical significance (*Figure 27*). This mirrored a significant ($p<0.01$) 5 fold reduction in HK protein level in $TS^H$ homogenates, measured by densitometric analysis of HK immunoblots (*Figure 28*). Conversely, the activity of HK in $TS^Q$ was increased by 1.9 fold to 12.1 ± 2.3 nmol $min^{-1}$ mg protein $^{-1}$ which was statistically significant ($p<0.05$) (*Figure 27*). However this was not accompanied by a statistically significant change in HK protein levels in $TS^Q$ homogenates (*Figure 28*).

PFK1 catalyses the phosphorylation of fructose-6-phosphate to form fructose-1,6-bisphosphate using ATP hydrolysis. PFK1 is subject to complex regulation being inhibited by ATP, low pH and citrate, and activated by AMP and by the allosteric activator fructose-2,6-bisphosphate. The product of the PFK1 reaction, fructose-1, 6-bisphosphate, also acts to allosterically activate PK. The activity of PFK1 measured in $TS^N$ homogenates was 29.7 ± 9.9 nmol $min^{-1}$ (mg protein)$^{-1}$. Although the value was increased by 2.3 fold to 69.3 ± 17.8 nmol $min^{-1}$ (mg protein)$^{-1}$ in $TS^Q$, the difference was not statistically significant. Similarly there was no change in PFK1 activity under hypoxic conditions, with a activity of 31.9 ± 6.9 nmol $min^{-1}$ (mg protein)$^{-1}$ recorded in $TS^H$ (*Figure 27*).

There are three isoforms of the PFK1 subunit; PFKM, PFKP and PFKL. Previous studies in breast cancer cell lines demonstrated that expression of the PFKL isoform of PFK1 correlated strongly with glycolytic efficiency and an aggressive phenotype (Zancan et al., 2010). Wang and colleges also showed a significant positive correlation between PFK-1 activity and PFK-P expression in breast cancer tissue (Wang et al., 2013). Therefore, monoclonal antibodies were utilized to ascertain the relative levels of each isoform under the different micro-environmental conditions (*Figure 28*). No statistically significant differences were observed in PFKP levels between the different conditions. However, the levels of both PFKM and PFKL were significantly reduced in $TS^H$ relative to $TS^N$, by 5.6 ($p<0.05$) and 6.3 ($p<0.01$) fold respectively. In both cases there was no statistical difference in enzyme expression in response to quiescence.

PK catalyses the final step of glycolysis, the transfer of a phosphate group from phosphoenolpyruvate to ADP forming ATP and pyruvate. PK is also subject to allosteric inhibition by ATP and alanine. In addition, altered isoenzyme expression of PK has been shown to occur with the PKM2 isoform being up-regulated in the majority of cancers (Hacker et al., 1998; Rempel et al., 1994; Wolf et al., 2011; Zancan et al., 2010). The activity of PK was significantly decreased ($P<0.05$) in homogenates produced from $TS^H$ to 0.55 ± 0.31 μmol $min^{-1}$ $(mg\ protein)^{-1}$ relative to the 2.2 ± 0.3 μmol $min^{-1}$ $(mg\ protein)^{-1}$measured in $TS^N$ homogenates (*Figure 27*). This 4 fold reduction in activity correlates with the 4 fold reduction ($p<0.01$) in PK expression level in $TS^H$ measured by densitometry analysis of immunoblots (*Figure 28*). In contrast, the specific activity of PK was increased dramatically in $TS^Q$ homogenates to 4.5 ± 0.3 μmol

$min^{-1}$ (mg protein)$^{-1}$ ($p<0.001$)(*Figure 27*). Although the PK protein expression level in these $TS^{Q}$ homogenates was increased 1.5 fold relative to that in $TS^{N}$ this increase did not reach statistical significance (*Figure 28*). The 2 fold increase in PK activity in quiescent TS homogenates may therefore be due to alterations in regulation at the post-translational level. For example studies have demonstrated that the PK isoform PKM2 is inhibited by tyrosine phosphorylation (Hitosugi et al., 2009).

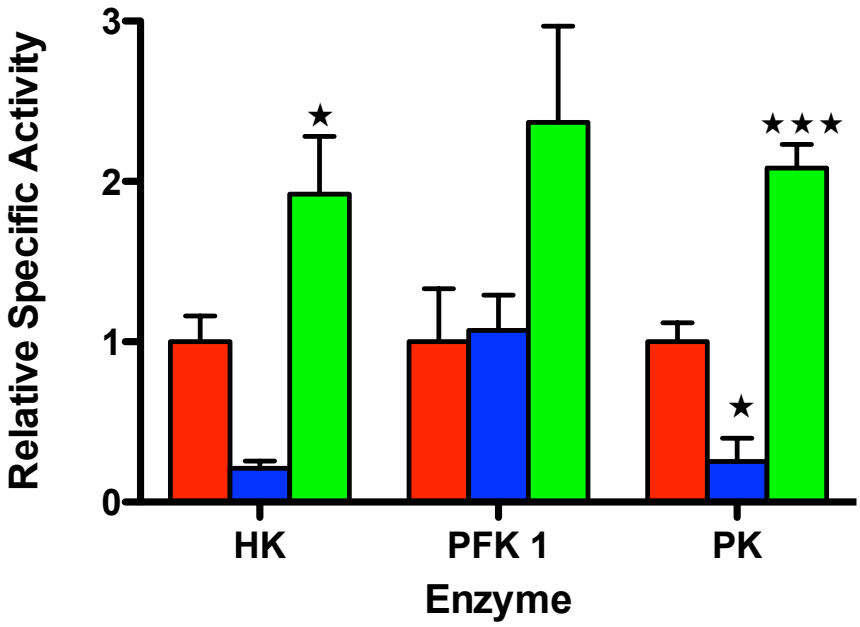
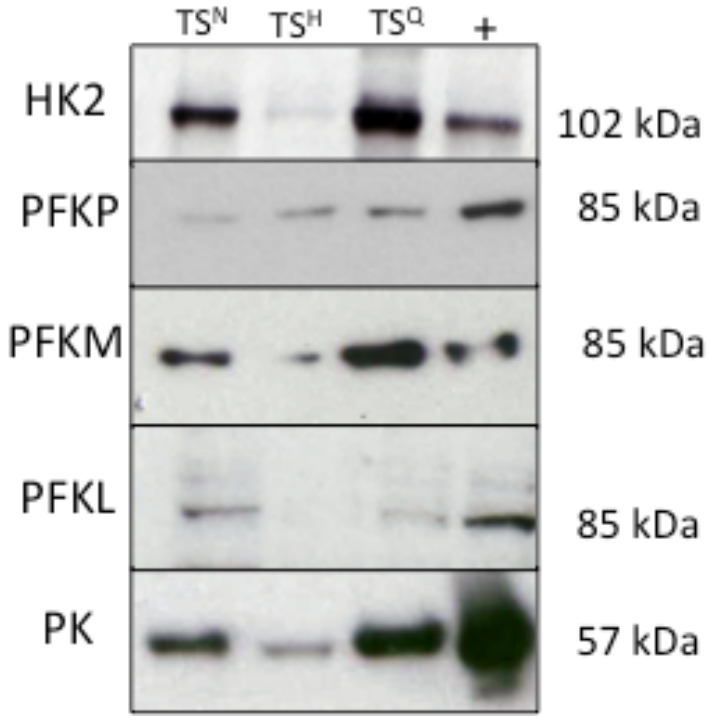



***Figure 27. Relative activities of key glycolytic enzymes.*** *Enzyme activity was measured via spectrophotometric analysis monitoring $NAD(P)^{+}$ reduction/NAD(P)H oxidation at 340nm in linked reactions. The maximal activities are displayed relative to the maximal activity observed in normoxia ± S.E.M, $TS^{N}$ (red), $TS^{H}$ (blue) and $TS^{Q}$ (Green), with significant differences indicated. Significant differences as analysed by ANOVA are indicated *** P<0.001 **P<0.01 * P<0.05.*

A.




B.

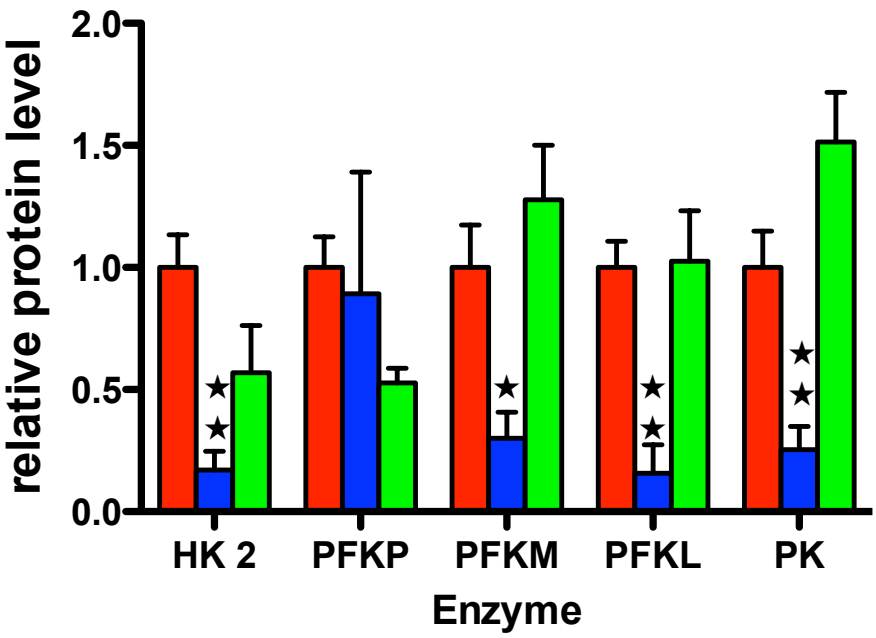



***Figure 28. Western blot analysis of the relative levels of glycolytic enzymes.*** (A) *The relative levels of each enzyme under the different conditions were determined by densitometric analysis of western blots. Blots were preformed on at least four independent total protein homogenates for each condition TSN (red), TS$^{H}$ (blue) and TS$^{Q}$ (Green). Positive controls comprised DLD1 cell lysates for HK2 and PFKP, HeLa cell lysates for PFKM and PFKL and pure protein for PK. Representative blots are shown. (B) Densitometry was performed using image J, values are expressed relative to the mean intensity ±S.E.M of TS$^{N}$ for each blot. Significant differences as analysed by ANOVA are indicated *** P<0.001 **P<0.01 * P<0.05.*

### 3.3.2 Glutaminolytic pathway enzymes

The mitochondrial glutamate dehydrogenase (GLDH) enzyme catalyses the reversible $NAD(P)^+$ linked oxidative deamination of glutamate to $\alpha$-ketoglutarate and ammonia. It is a highly regulated enzyme in the glutaminolytic pathway, being subject to control by a number of metabolites including inhibition by ATP and NADH, and activation by ADP and leucine (its regulation is reviewed in (Smith and Stanley, 2008).

The activity of GLDH in TS homogenates was significantly decreased by 5.2 fold in TS grown in hypoxic conditions to 4.4 ± 3 nmol $min^{-1}$ (mg protein)$^{-1}$relative to the 22.9 ± 2 nmol $min^{-1}$ (mg protein)$^{-1}$ measured in $TS^N$ (*Figure 29*). Conversely the expression levels of GLDH were increased 1.6 fold in $TS^H$ however this did not reach statistical significance (*Figure 30*). This may indicate a change in regulation at the post-translational level, for example, studies have shown that GLDH is subject to cystine specific ADP-ribosylation by SIRT4, leading to inhibition of GLDH activity (Csibi et al., 2013; Herrero-Yraola et al., 2001). In $TS^Q$ homogenates both the activity of 22.9 ± 4 nmol $min^{-1}$ (mg protein)$^{-1}$ (*Figure 29*) and the relative GLDH expression level (*Figure 30*) were not significantly different from those measured in $TS^N$ homogenates.

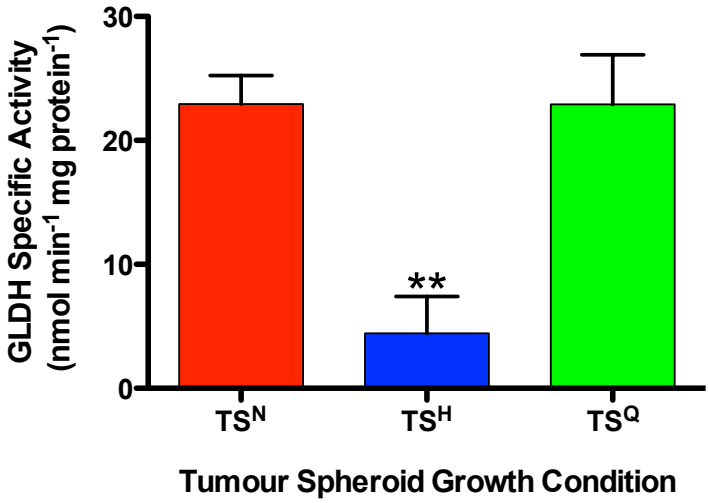



***Figure 29 Glutamate dehydrogenase activity.*** *Enzyme activity was measured via spectrophotometric analysis monitoring NADH oxidation at 340nm. The maximal activities (mean ± S.E.M) are displayed in nmol min$^{-1}$ (mg protein)$^{-1}$, TS$^{N}$ (red), TS$^{H}$ (blue) and TS$^{Q}$ (Green), with significant differences indicated. Significant differences as analysed by ANOVA are indicated **P<0.01.*

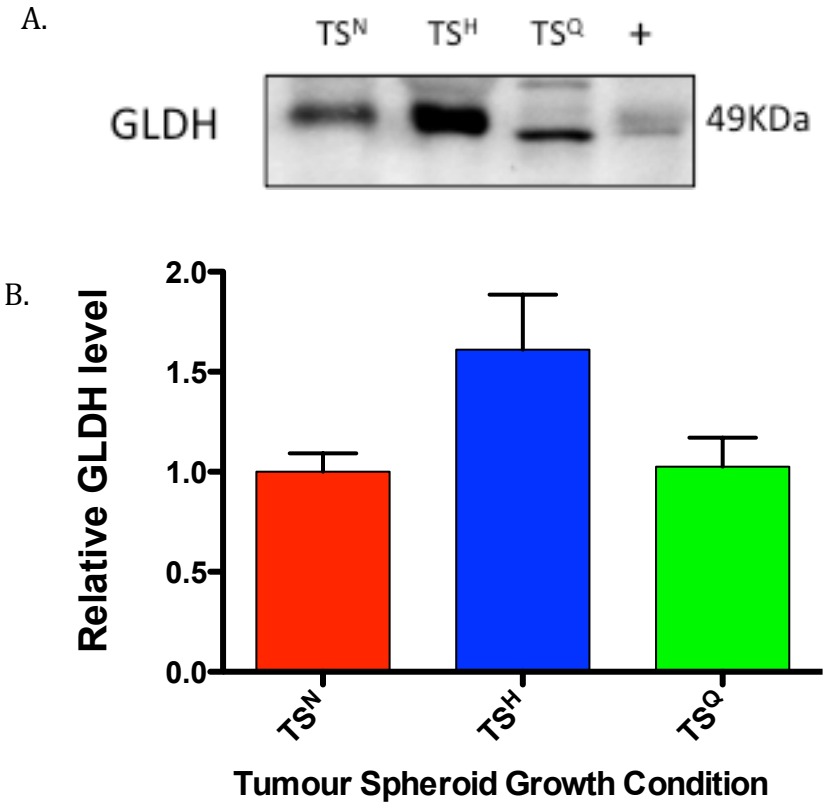



***Figure 30 Western blot analysis*** *of the relative expression levels of GLDH. The relative levels of GLDH under the different conditions were determined by densitometric analysis of western blots. Blots were preformed on at least four independent total protein homogenates for each condition; TS$^{N}$ (red), TS$^{H}$ (blue) and TS$^{Q}$ (Green). Positive controls comprised DLD1 cell lysates. An representative blot is shown. Densitometry was performed on the major band using image J, values are expressed relative to the mean (± S.E.M) intensity for the TS$^{N}$ for each blot. Data was analysed by ANOVA.*

### 3.3.3 Shunt Enzymes

Glucose 6 phosphate can either enter the glycolytic pathway, be converted to glycogen for storage or be siphoned into the pentose phosphate pathway to produce ribose-5-phosphate and NADPH. Ribose-5-phosphate is a biosynthetic precursor used in the synthesis of nucleotides, while NADPH is an important cellular reducing agent, and is used as a cofactor in the synthesis of many macromolecules. Glucose-6-phosphate dehydrogenase (G6PDH) catalyses the first reaction in the oxidative pentose phosphate pathway, the oxidation of glucose 6 phosphate to form 6-phosphogluconolactone with the simultaneous reduction of $NADP^+$ produce NADPH. Elevated expression and activity of G6PDH has previously been observed several different types of cancer including breast, colon, endometrial, cervical, prostatic and lung cancers (Furuta et al., 2010).

The activity of G6PDH in control $TS^N$ homogenates was 184 ± 17 nmol $min^{-1}$ (mg protein)$^{-1}$, growth under hypoxic conditions resulted in a statistically significant reduction ($p<0.05$) in maximal activity to 32.2 ± 12 nmol $min^{-1}$ (mg protein)$^{-1}$ (*Figure 31*). This mirrored the significant ($p<0.01$) 12.5 fold decrease in G6PDH expression levels observed in western blot analysis of $TS^H$ homogenates (*Figure 32*). Following TS production in quiescent conditions both the maximum activity at 251 ± 35 nmol $min^{-1}$ (mg protein)$^{-1}$ (*Figure 31*) and the relative protein expression level of G6PDH (*Figure 32*) did not differ significantly from that in $TS^N$.

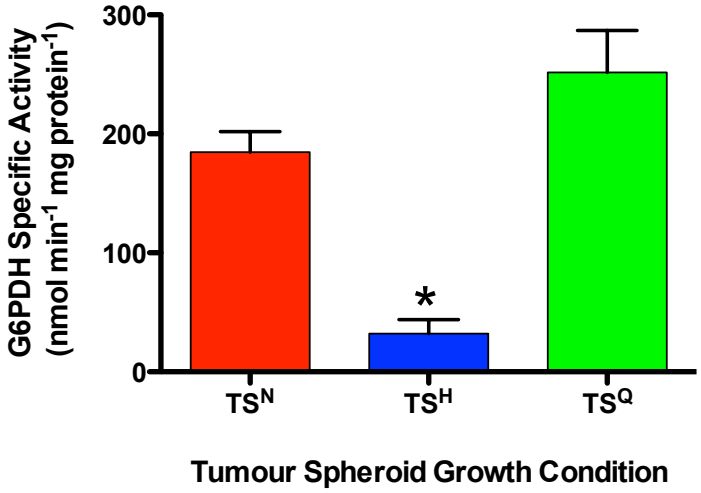



***Figure 31 Activity of G6PDH.*** *Enzyme activity was measured via spectrophotometric analysis monitoring NADP reduction at 340nm. The maximal activities (mean ± S.E.M) are displayed in nmol min$^{-1}$ (mg protein)$^{-1}$, TS$^{N}$ (red), TS$^{H}$ (blue) and TS$^{Q}$ (Green), with significant differences as analysed by ANOVA are indicated *P<0.05,**P<0.01.*

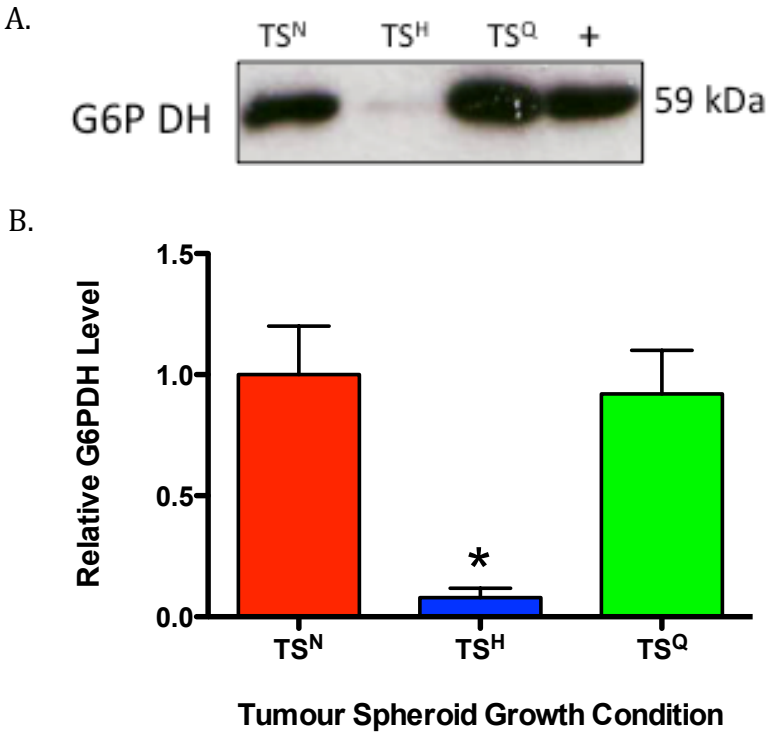



***Figure 32 Western blot analysis of the relative expression levels of G6PDH****. The relative levels of G6PDH under the different growth conditions were determined by densitometric analysis of western blots. Blots were preformed on at least four independent total protein homogenates for each condition TS$^{N}$ (red), TS$^{H}$ (blue) and TS$^{Q}$ (Green). Positive controls comprised DLD1 total cell lysates. A representative blot is shown (A). Densitometry was performed using image J, values (mean ± S.E.M) are expressed relative to the mean intensity for the TS$^{N}$ for each blot ±S.E.M (B). Data was analysed by ANOVA.*

Pyruvate is produced by glycolysis and has a number of potential metabolic fates, for example it can be converted into acetyl-CoA by the pyruvate dehydrogenase complex for use in the TCA cycle. Alternatively it can be reduced to lactate by Lactate dehydrogenase (LDH), regenerating $NAD^+$, which is essential for continued flux through glycolysis when uncoupled from the TCA cycle. The LDH reaction is reversible and can be used to regenerate pyruvate from lactate for use as a fuel for oxidative phosphorylation. The LDH A isoform has been shown to up regulated in numerous human cancers (Goldman et al., 1964). This isoform is a target of the oncogenic transcription factor c-Myc and Hypoxia inducible factor-1 (Firth et al., 1995; Goldman et al., 1964; Shim et al., 1997), the expression levels of both of which were found to be significantly increased in $TS^H$ relative to control $TS^N$ (*Figure 16* and Figure 17). Expression of the LDH A isoform has been shown to be correlated with poor prognosis in a several types of cancer (Kolev et al., 2008; Koukourakis et al., 2005; Koukourakis et al., 2003).

Analysis of maximum LDH activity and relative LDH expression levels revealed significant alterations from $TS^N$ under hypoxia and quiescence. The maximal activity of LDH in homogenates produced from control TS, $TS^N$, was 1.31 ± 0.2 μmol $min^{-1}$ (mg protein)$^{-1}$ (*Figure 33*). Unexpectedly, a dramatic 3.4 fold reduction ($p<0.05$) in activity to 0.38 ± 0.15 μmol $min^{-1}$ (mg protein)$^{-1}$ was measured in homogenates from TS grown under hypoxic conditions (*Figure 33*). this was mirrored by a significant ($p<0.01$) 3.3 fold decrease in the relative expression levels of LDH (*Figure 34*). In contrast, in $TS^Q$ both the maximum

activity of LDH at 2.32 ± 0.16 μmol $min^{-1}$ (mg protein)$^{-1}$ and the relative expression levels of LDH, were significantly increased relative to $TS^N$, by 1.8 fold ($p<0.01$) and 1.7 fold ($p<0.01$) respectively (*Figure 33*, *Figure 34*). The close correlation between the changes in activity and relative expression level under the different growth conditions indicate that LDH is principally regulated at the transcriptional level.

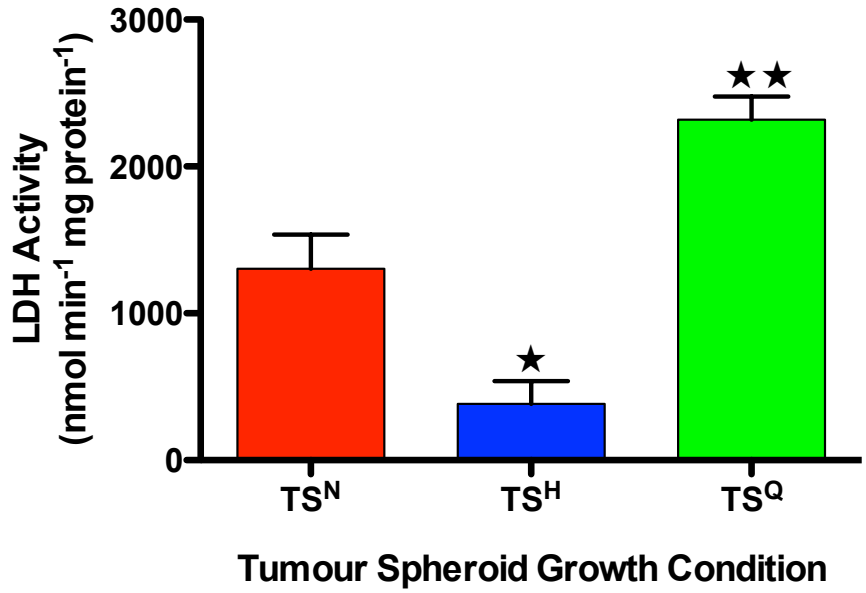
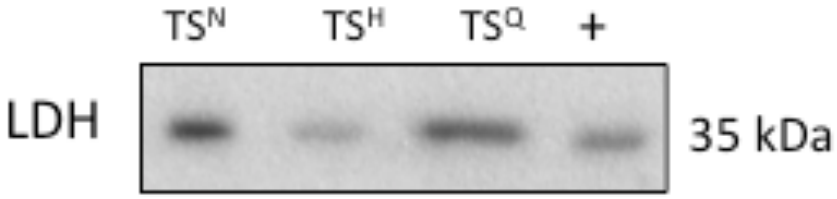



***Figure 33 Activity of LDH in tumour spheroids.*** *Maximal enzyme activity was measured via spectrophotometric analysis monitoring NADH oxidation at 340nm. The maximal activities are displayed in nmol $min^{-1}$ mg protein$^{-1}$ ± S.E.M, $TS^N$ (red), $TS^H$ (blue) and $TS^Q$ (Green), with significant differences indicated. Significant differences as analysed by ANOVA are indicated *P<0.05,**P<0.01.*

A.




B.

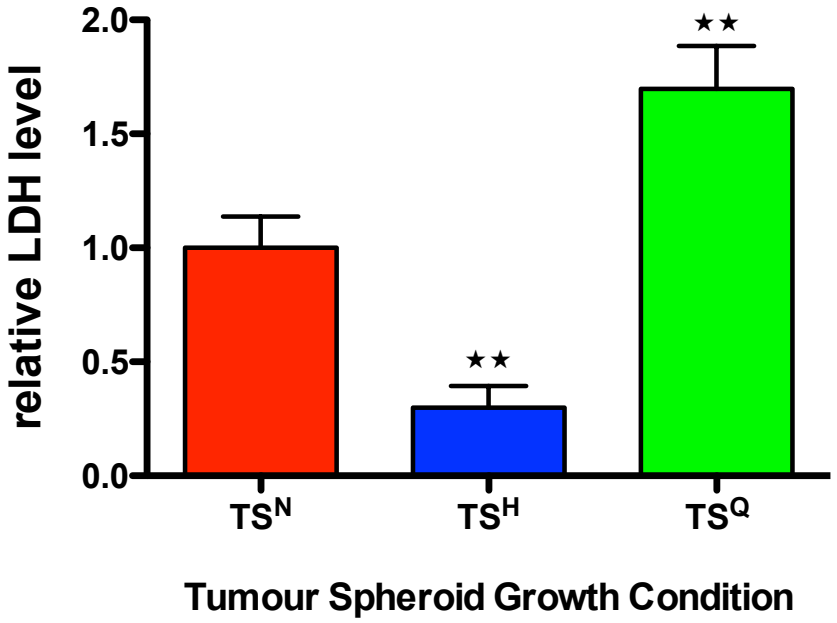



***Figure 34 Western blot analysis of the relative LDH expression levels in tumour spheroids.*** *The relative levels of LDH under the different conditions were determined by densitometric analysis of western blots. Blots were preformed on at least four independent total protein homogenates for each condition $TS^N$ (red), $TS^H$ (blue) and $TS^Q$ (Green). Positive controls (+) were run of DLD1 total cell lysates. (A.) A representative western blots is shown. (B) Densitometry was performed using image J, values are expressed relative to the mean intensity ±S.E.M for the $TS^N$ for each blot. Data was analysed by ANOVA**P<0.01.*

### 3.3.4 Summary of intracellular adaptations

The objective of the experiments presented here was to investigate the basis of differences in nutrient utilization observed under different micro-environmental conditions in tumour spheroids (detailed in section 3.2).

The activities of glycolytic enzymes in $TS^N$, were lower in enzymes at the beginning of the pathway, (HK), than those at the end of the pathway, (PK). This

correlates well with previous studies, such as those by Marín-Hernández et al, who measured maximal activities of glycolytic enzymes in, hepatocytes, AS-30D hepatoma cells and HeLa cells, showing that the enzymes with lower activity were those residing at the beginning of the pathway including HK and PFK. They also demonstrated that in AS-30D cells 71% of the glycolytic flux control resided in the first part of the pathway (i.e. GLUT and HK), using elasticity based analysis (Marin-Hernandez et al., 2006). It could therefore be predicted that the majority of the glycolytic flux control in the control $TS^N$ resides at the beginning of the pathway. Although this would require confirmation via further investigations, these enzymes therefore represent potential therapeutic targets for the inhibition of tumour glycolytic flux.

The activities and levels of the majority of the enzymes assayed were decreased in hypoxic $TS^H$ relative to $TS^N$ (*Figure 27 -Figure 34*). This reduction in protein levels correlates with previous investigations measuring inhibition of protein synthesis under severely hypoxic conditions (0.1-0.2% $O_2$) (Hernandez-Jimenez et al., 2012; Koumenis et al., 2002) similar to those employed in this study (0.1% $O_2$). However, studies have demonstrated that this inhibition of protein synthesis can be overcome in several breast cancer cell lines (Connolly et al., 2006).

In quiescent TS, statistically significant increases in specific activity were observed in the glycolytic enzymes HK and PK (*Figure 27*) as well as in LDH (*Figure 33*) where protein levels were also increased (*Figure 34*) relative to $TS^N$. The levels and activity of the other enzymes assayed, PFK1, GLDH and G6PDH did not differ significantly in $TS^Q$ relative to $TS^N$. This correlates well with the

observed increases in glucose and glutamine depletion and lactate accumulation observed in section 3.2 and contrasts with the hypothesis that quiescent tumour cells are less metabolically active than their proliferating counterparts.

The alterations in metabolic parameters measured hypoxic and quiescent tumour spheroids in this study relative to those in normoxic proliferating control tumour spheroids are summarised in *Table 4*.

| | HYPOXIA | QUIESCENCE |
|---|---|---|
| Hif1α | ↑↑ | ↔ |
| cMyc | ↑↑ | ↔ |
| | | |
| Glucose uptake | n/a | ↑↑ |
| Glycolytic flux | ↑↑ | ↓↓ |
| GLUT1 | ↑ | ↔ |
| GLUT3 | ↑↑ | ↔ |
| | | |
| Glutamine uptake | n/a | ↑ (12h) |
| ASCT2 | ↔ | ↔ |
| | | |
| Lactate production | n/a | ↑↑ |
| MCT1 (import) | ↑↑ | ↓↓ |
| MCT4 (export) | ↑↑ | ↔ |
| | | |
| HK2 | ↓<br>↓↓ | ↑↑<br>↔ |
| | | |
| PFK | ↔ | ↑ |
| PFK-P | ↔ | ↔ |
| PFK-M | ↓↓ | ↔ |
| PFK-L | ↓↓ | ↔ |
| | | |
| PK | ↓↓<br>↓↓ | ↑↑<br>↑/↔ |
| | | |
| GLDH | ↓↓<br>↑ | ↔<br>↔ |
| | | |
| G6PDH | ↓↓<br>↓↓ | ↔<br>↔ |
| | | |
| LDH | ↓↓<br>↓↓ | ↑↑<br>↑↑ |
| | | |

***Table 4. Summary of the effect of micro-environmental stress on metabolism.*** *The changes in metabolism observed in hypoxic and quiescent TS relative to control normoxic proliferating TS are summarised. Changes in expression are indicated in red and activity in blue, an upwards arrow indicates up-regulation and downward indicates down-regulation finally two arrows indicate a statistically significant change.*

# 4. Discussion

Alterations in metabolism are considered to be an emerging hallmark of cancer, with numerous studies demonstrating that cancer cells reorganise their metabolism resulting in increased consumption of glucose and glutamine (Bode et al., 1995; Gillies et al., 2008; Hanahan and Weinberg, 2011). This metabolic reprogramming allows cancer cells to respond to both biosynthetic demands for proliferation and to adapt to the hostile micro-environment that is often encountered within a tumour. The aetiology of these metabolic alterations are not currently fully understood but many components have been identified, including reprogramming resulting from oncogene activation and stress resulting from the developing hostile micro-environment within the tumour (Cairns et al., 2011). Due to the consistency of metabolic alterations, energy metabolism is considered a potential therapeutic target for cancer treatment (reviewed in (Ganapathy-Kanniappan and Geschwind, 2013)). The development of populations of hypoxic and quiescent cells within the tumour mass as a consequence of micro-environmental stress are known to contribute to the failure of many current cancer therapies, including chemo and radio-therapy (Gray et al., 1953; Jackson, 1989; Mellor et al., 2005a; Teicher, 1994). Initial investigations have suggested that tumour cells employ different metabolic strategies to adapt to theses stresses (Lamonte et al., 2013; Lemons et al., 2010), but these have not yet been fully characterised. Therefore the aim of this study was to characterise the metabolic adaptations of tumour cells to different micro-

environmental stresses including hypoxia and quiescence relative to the metabolism of oxygenated proliferating tumour cells.

Although the hostile tumour micro-environment has been identified as a potential contributor to metabolic reprogramming, the majority of studies investigating metabolic regulation in cancer have been performed in tumour cells grown in 2D monolayer cultures (see section 1.4). This type of culture does not take into account many aspects of the 3D tumour microenvironment, for example the monolayer culture fails to reproduce the gradients in nutrients, oxygen and waste products that are observed *in vivo (Figure 1*). Therefore, the multicellular tumour spheroid (TS) 3D cell culture model was adopted in this study. TS have several advantages including the simulation of the gradients of metabolites present within tumours *in vivo.* This leads to the development of distinct populations of cells as they grow in diameter, mimicking the micro-environment of a tumour (*Figure 11*) (Hirschhaeuser et al., 2010; Lin and Chang; Sutherland, 1988).

This study determined that the energy metabolism of tumour spheroids is significantly affected by exposure to micro-environmental stress. TS modelling the oxygenated proliferating regions of a tumour exhibited metabolic adaptations consistent with the Warburg effect (Warburg et al., 1927) with glucose being metabolised to produce lactate in the presence of oxygen (*Figure 19*, *Figure 21*, *Figure 25*). In addition, these spheroids were observed to metabolise glucose via the pentose phosphate pathway (*Figure 21*) and to extract glutamine from the growth medium (*Figure 23*). TS incubated in hypoxic

conditions, although being observed to down regulate many metabolic enzymes (section 3.3), exhibited adaptations consistent with the Pasteur effect; with increased glycolytic flux and the uptake of glucose from the medium and net production of lactate (section 3.2). Finally, although the induction of quiescence in TS resulted in a decrease in glycolytic flux (*Figure 20*), the increase in glucose and glutamine uptake along with lactate production (section 3.2) indicates that these spheroids are metabolically active.

## 4.1 Proliferating tumour spheroids ($TS^N$)

During this study, the human colon carcinoma cell line DLD1 was utilized to generate tumour spheroids (Bloch et al., 2014; Grimes et al., 2014; Mellor et al., 2005a). Following analysis of TS growth (*Figure 12*) spheroids between 200-400μm in diameter at day 2 of growth were selected for this study. Previous studies have determined that TS below 400μm in diameter do not contain necrotic cells (Kim and Forbes, 2007). This correlates with the immunohistochemistry data in this study showing that the majority of the cells in TS of this size range stained positive for the proliferation marker Ki-67. This indicates that they are actively proliferating, which is supported by the minimal staining of the quiescence marker p27 (*Figure 13*). In addition, recent work evaluating oxygen levels in DLD1 tumour spheroids determined TS of this size range are oxygenated (*Figure 35*), with an experimentally derived oxygen diffusion distance of 233 ± 22 μm (Grimes et al., 2014). In addition, the oxygenation of TS was confirmed in this study by immunohistochemistry of the

hypoxia marker pimonidazole showing that the TS between 200-400μm in diameter were oxygenated (*Figure 14*), Furthermore spheroids at this size, 200-400 μm in diameter, would be predicted to have developed chemical gradients (Hirschhaeuser et al., 2010) such as those in oxygen as shown in Figure 35 (Grimes et al., 2014)

These tumour spheroids represent a simplified experimental model of proliferating layers of solid tumours. The extent to which they model the *in vivo* tumour however is limited. Tumours contain heterogeneous populations of cancerous and stromal cells such as fibroblasts (Fukumura and Jain, 2007), not present in these TS. The different populations of cells within tumour are thought to interact metabolically via the lactate symbiosis for example (section 1.1.4)(Sonveaux et al., 2008a). TS grown above the maximum 400 μm in diameter used in this study do develop heterogeneous populations of cancer cells including hypoxic and quiescent cells (Sutherland, 1988), which may interact, however this would renders analysis of distinct stresses difficult. These TS additionally have many advantages over 2D monolayer cell culture in addition to the development of nutrient gradients (Hirschhaeuser et al., 2010). These include having a more closely representative gene expression profile of tumours *in vivo* than cells in 2D culture (Hirschhaeuser et al., 2010; Lee et al., 2013). Alterations in protein expression are demonstrated in this study, for example different levels of HK2, PFKP, GLDH and LDH (*Figure 28*, *Figure 30*, *Figure 34*A) were detected by western blot in homogenates from DLD1 oxygenated proliferating TS and cell lysates from DLD1 cells grown in 2D culture.

Therefore TS at this stage of growth were composed of proliferating oxygenated cells and consequently these TS provide an experimental model of proliferating layers of solid tumours.. Analysis and induction of distinct micro-environmental stresses upon TS at this stage of growth enabled the comparative examination of metabolic adaptation to different micro-environmental conditions.

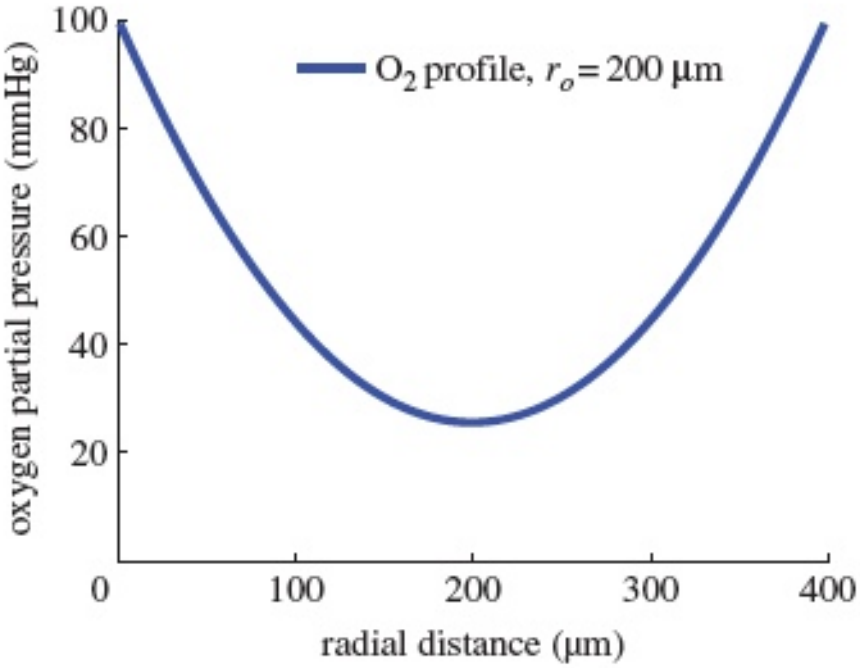



***Figure 35.*** *The simulated $O_2$ profile of DLD1 TS 400μm in diameter with an oxygen diffusion distance of 233μm, from Grimes and colleagues (Grimes et al., 2014)*

The Warburg effect is defined as the metabolism of glucose to produce lactic acid, despite the presence of adequate oxygen (Warburg et al., 1927). This phenomenon is widely observed in proliferating cells both cancerous, such as the ascites cells of Warburg's initial experiments (Warburg, 1956b) and non cancerous such as proliferating lymphocytes (Wang et al., 1976). The proliferating TS in this study depleted glucose from the medium at a rate of 292 ± 42 μ moles (mg protein)$^{-1}$ of glucose over 24 hours which is equivalent to 0.014 mg ($10^5$ cells)$^{-1}$ day$^{-1}$ (*Figure 19*). This rate is comparable with measurements by

Tannock and Kopelayn on a human bladder cancer cell line grown as spheroids, where a glucose depletion rate of 0.02mg ($10^5$ cells)$^{-1}$ day$^{-1}$ was determined (Tannock and Kopelyan, 1986). These proliferating TS also exhibited a demonstrable glycolytic flux (*Figure 20*) and a net production of lactate (*Figure 25*) during their growth. This is consistent with features described by the Warburg effect. In addition, preliminary metabolomic analysis of the metabolic fate of glucose-derived carbon confirmed the dependence of these TS on glycolysis. High carbon enrichment was measured in components of the glycolytic pathway and very low levels in the components of the TCA cycle showing that minimal amounts of glucose derived carbon are metabolised by the TCA cycle in these normoxic proliferating TS (*Figure 21*). This is consistent with previous studies by DeBerardinis who used $^{13}$C NMR spectroscopy to show that glucose was predominantly metabolised by aerobic glycolysis with >90% of labelled $^{13}$C glucose being converted to lactate and alanine (DeBerardinis et al., 2007)

As mentioned previously (section 1.4), the distribution of flux control in a metabolic pathway can be affected by several different mechanisms. These include long-term measures, such as regulation of enzyme expression levels, or the proportion or presence of different isoforms. For example, the majority of glycolytic enzymes have been determined to be over expressed in 70% of human cancers (Altenberg and Greulich, 2004). Alternatively, short-term mechanisms include enzyme activation or inhibition by cellular intermediumtes or redox reactions. For example, glutamate dehydrogenase is allosterically regulated by cellular markers of bioenergetic status, being activated by ADP and inhibited by

ATP (Smith and Stanley, 2008). The consequences of these modifications in metabolic regulation could result in differences in the distribution of flux control in the glycolytic pathway of cancer cells relative to non-tumorigenic cells. The *in vitro* specific activity and relative levels of key metabolic enzymes (*Figure 26*) were therefore investigated in this study. Differences in such factors could indicate alterations in enzyme regulation.

Investigations by Marín-Hernández and colleagues analysed metabolic control in the glycolytic pathway of HeLa cervical carcinoma and AS-30D rodent hepatoma cells relative to that in hepatocytes (Marin-Hernandez et al., 2006). This was achieved by measurement of maximal enzyme activities ($V_{max}$), determining the active enzyme content and by evaluating how blocks of enzymes controlled flux through the pathway by elasticity analysis. Elasticity analysis involves determination of elasticity coefficients, defined as the degree to which variations in any of the ligands, i.e. substrates, of an enzyme or block or enzymes changes the rate of reaction (Moreno-Sanchez et al., 2008). From elasticity coefficients flux control coefficients can then be calculated (Moreno-Sanchez et al., 2008). In both HeLa and AS-30D cells, hexokinase (HK) and phosphofructokinase (PFK1) were among the enzymes with the lowest measured activities (Marin-Hernandez et al., 2006). Elasticity analysis of glycolytic flux in AS-30D hepatoma cells determined that the majority of control resided in the initial stages of the pathway with the block of enzymes producing glucose-6-phosphate (70%) i.e. the glucose transporter and HK. In addition, they indicated that PFK1 had low control over glycolytic flux control these cells, probably as a result of being fully

activated by fructose-2,6-bisphosphate and AMP at the concentrations found in tumour cells (Marin-Hernandez et al., 2006).

In this study, HK had the lowest measured capacity ($V_{max}$) in the glycolytic pathway of the control Normoxic TS at 6.3 ± 1 nmol $min^{-1}$ mg $protein^{-1}$, followed closely by PFK1 with a $V_{max}$ of 29.7± 9.9 nmol $min^{-1}$ mg $protein^{-1}$. The $V_{max}$ of these enzymes were several fold lower that that of the enzymes residing at the end of the glycolytic pathway, PK and LDH with maximal activities measured at 2.2 ± 0.3 μmol $min^{-1}$ mg protein and 1.31± 0.2 μmol $min^{-1}$ mg protein respectively (section 3.3). This suggests that in these proliferating DLD1 TS the control of glycolytic flux is likely to also lie at the beginning of the glycolytic pathway, therefore controlling flux by squeezing entry into the pathway. However further studies would be required to confirm this, such as elasticity analysis determining the effect of changes in metabolite concentrations upon flux or calculation of flux control coefficients by measuring the effects of specific inhibitors on flux (Moreno-Sanchez et al., 2008).

The pentose phosphate pathway, which is illustrated in *Figure 5*, plays a key role in biosynthetic pathways by providing ribose-5-phosphate, a precursor in the synthesis of nucleotides, and NADPH, a major cofactor and antioxidant (Wood, 1986)(section 1.1.2). This pathway is likely to be essential to maintain proliferation in TS. This is consistent with initial metabolomic analysis of the fate of $^{13}C$ glucose demonstrating high enrichment of $^{13}C$ in the pentose phosphate pathway intermediate 6-phophogluconic acid (*Figure 21*). In addition, enzymatic studies revealed high activity/capacity for glucose-6-phosphate dehydrogenase

(G6PDH), which catalyses the initial reaction in the oxidative pentose phosphate pathway (*Figure 31*). Together this evidence demonstrates that the pentose phosphate pathway is active in the cells of these normoxic TS.

Glutamine is a key nutrient for cancer cells. Its carbon skeleton is utilized both as an anaplerotic precursor and for energy production via oxidation, while its amino and amine nitrogen groups are used as nitrogen donors in the synthesis of nucleotides (section 1.1.3, (Daye and Wellen, 2012; DeBerardinis et al., 2007)). Consistent with studies demonstrating the importance of glutamine uptake for cell growth (Tannock and Kopelyan, 1986) these studies demonstrate the expression of the glutamine transporter ASCT2 (*Figure 22*), a key mediumtor of tumour glutamine uptake (Fuchs and Bode, 2005). In addition, a considerable depletion of glutamine from the medium of 39.7 ± 7.6 μmoles (mg protein)$^{-1}$ was measured over 24 hours during TS growth (*Figure 23*). Additionally, expression of the oncogenic transcription factor, cMyc, which targets many aspects of the glutaminase pathway (section 1.2.4), was detected in these TS (Figure 17).

Spheroids 200-400 μm in diameter represent the well oxygenated, proliferating population of cells present at the tumour periphery close to blood vessels (Sutherland, 1986). Proliferating oxygenated tumour cells have been well studied in the literature mainly in 2D monolayer culture systems (examples include (DeBerardinis et al., 2007; Osthus et al., 2000; Schwartzenberg-Bar-Yoseph et al., 2004; Yi et al., 2012)), as well as 3D systems (Kim and Forbes, 2007; Mandujano-Tinoco et al., 2013). In keeping with previous studies on proliferating cells (Wang et al., 1976; Warburg et al., 1927), these spheroids

were determined to metabolise glucose for energy production via aerobic glycolysis. This was evidenced by their avid uptake of glucose from the medium, net lactate production and glycolytic flux. Additionally, these studies indicate that the pentose phosphate pathway, which is essential for biosynthesis and therefore proliferation, is active in these spheroids. Further experiments would be required to determine the flux through this pathway. Finally, consistent with studies identifying the importance of glutamine and glutaminolysis to cancer cell metabolism (DeBerardinis et al., 2007), glutamine uptake from the medium was observed during the growth of these TS. Therefore, these TS represent the control condition within this study, modelling the proliferating layers of a tumour and exhibiting metabolic adaptations consistent with the Warburg effect. All further micro-environment induced alternations in metabolism surveyed in this study were related to the observations in these oxygenated proliferating TS.

### 4.3 Hypoxic tumour spheroids ($TS^{H}$)

Hypoxia is a widespread feature of many different types of solid tumours including, cervical, breast, prostate and brain (Hockel et al., 1991; Parker et al., 2004; Rampling et al., 1994; Vaupel et al., 1991). Several investigations have shown that tumour hypoxia is associated with malignant progression, metastases, resistance to chemotherapy and poor patient prognosis (Brizel et al., 1996; Brown, 2002; Hockel et al., 1993; Hockel et al., 1996; Nordsmark et al., 2005). Due to its extensive presence in tumours and the severe consequences of

hypoxia in cancer, this project aimed to establish the effect of hypoxia on the energetic metabolism of TS.

Numerous studies profiling the oxygen partial pressure in tumours have identified regions where the oxygen partial pressure is below 2.5 mmHg (0.35% $O_2$) (Collingridge et al., 1999; Hockel et al., 1991; Rampling et al., 1994; Vaupel et al., 2002) which is defined as severe hypoxia. Hypoxic TS ($TS^H$) were generated for this study by incubating TS in a hypoxic chamber at 0.1% $O_2$ for 16 hours. Therefore this method generated spheroids that modelled regions of severe hypoxia. The viability (*Figure 15*) and proliferative status (*Figure 13*) of these spheroids was confirmed following the hypoxic incubation to ascertain the suitability of this method for TS generation.

Louis Pasteur initially observed the effects of oxygen levels on cellular metabolism in his studies on fermentation in yeast (Berg et al., 2007). He determined that a metabolic switch occurred at low oxygen concentrations where glycolysis is uncoupled from the oxidative phosphorylation pathway (Berg et al., 2007; Seagroves et al., 2001). This switch allows the sustained production of ATP in an oxygen independent manner. Consistent with these observations, a statistically significant 2 fold increase in glycolytic rate was measured in hypoxic TS relative to TS produced under normoxic conditions (*Figure 20*), suggesting an increased dependence on glycolysis for ATP production in hypoxic TS. In addition, the ratio of lactate accumulation in the medium to glucose depletion increased dramatically during the 16 hour hypoxic incubation to 1.2 relative to 0.45 during 24 hours of TS growth under normoxic

conditions. A maximum of 2 molecules of lactate can be produced per glucose metabolised, so this increase is consistent with a metabolic shift, suggesting a greater proportion of glucose is being converted to lactate in hypoxic TS than in normoxic TS.

Cellular adaptation and survival to hypoxic conditions is mediumted by transcription factors such as HIF-1 (Semenza, 2010). HIF-1 is a heterodimer composed of a constitutively expressed HIF-1β subunit and an oxygen dependent HIF-1α subunit that is degraded under normoxic conditions (Jaakkola et al., 2001). Western immunoblot analyses determined that HIF-1α protein levels were increased by 3.3 fold in $TS^H$ relative to $TS^N$ consistent with stabilisation of the protein in these spheroids (*Figure 16*). This correlates with previous studies in HeLa cell lines where HIF-1α protein levels were shown to increase exponentially at $O_2$ concentrations below 2% (Jiang et al., 1996). Activated HIF-1 has previously been shown to up regulate the expression level of many of the enzymes involved in glucose metabolism and the glycolytic pathway. These include the glucose transporters GLUT1 and GLUT3, hexokinase isoforms I and II, phosphofructokinase L, pyruvate kinase M, lactate dehydrogenase A and the lactate transporter MCT4 (see section 1. 2.4)(Chen et al., 2001; Firth et al., 1995; Iyer et al., 1998; Luo et al., 2011; O'Rourke et al., 1996; Riddle et al., 2000; Semenza et al., 1994; Ullah et al., 2006).

A two-fold amplification in the level of the oncogenic transcription factor cMyc was also detected in hypoxic TS relative to normoxic TS (Figure 17). Like HIF-1, cMyc has been shown to up-regulate the expression of a number of genes

involved in the glycolytic pathway. These include the glucose transporter GLUT1, HKII, PFK and LDHA (Osthus et al., 2000; Shim et al., 1997).

In comparison to $TS^N$, increased expression levels of the glucose transporters GLUT1 and GLUT3 (*Figure 18*) and the lactate transporter MCT4 (*Figure 24*) were measured in hypoxic TS. This is consistent with studies detailing these transporters as transcriptional targets of active HIF-1 and cMyc (Baumann et al., 2007; Osthus et al., 2000; Ullah et al., 2006). As mentioned previously, Marín–Hernández and colleagues determined that glycolytic flux in AS-30D hepatoma cells was mainly controlled by glucose transport and hexokinase (70%), (Marin-Hernandez et al., 2006). Further studies analysing hexokinase and glucose transport kinetics in HeLa and AS-30D hepatoma cells led the group to suggest that glucose transport exerted higher control of glycolytic flux than hexokinase in cancer cells, due to the lower $V_{max}$ and catalytic efficiency measured (Rodriguez-Enriquez et al., 2009). Both GLUT 1 and GLUT 3 have a high affinity for glucose (GLUT 1 $K_{m\ glucose}$ 1.6 mM, GLUT3 $K_{m\ 2\text{-}deoxyglucose}$ 1.4 mM) (Gould and Holman, 1993; Simpson et al., 2008), which results in their saturation at normal blood glucose concentrations of 5.5 mM. Therefore, glucose uptake is thought to be proportional to the level of expression of these transporters at the cell membrane. Hence, the increased expression of glucose transporters in hypoxic TS suggests an increased capacity for glucose uptake and may be a major factor contributing to the 100% increase in glycolytic flux measured in hypoxic TS (*Figure 20*).

The maximal capacity ($V_{max}$) and protein levels of the majority of the enzymes comprising the glycolytic pathway were reduced in hypoxic TS compared to normoxic TS, which contrasts, with many previous studies (section 3.3.1). These investigations measured an 5 fold decrease in the levels of HKII protein in hypoxic TS relative to that in normoxic TS mirroring a 4.8 fold decrease in the measured activity of HK in these TS (*Figure 27*, *Figure 28*). The close correlation between the decrease in HK activity and reduction in HKII protein measured in hypoxic TS suggests that changes in protein levels rather than post-translational regulation is responsible for the reduced HK activity. These results differ from previous studies such as those by Kim and colleagues who measured enhanced HKII mRNA, protein, and activity levels in response to the presence of active HIF-1, induced by incubation at 0.1% oxygen for 29 hours and cMyc expression in human lymphoma P439-6 cells grown as monolayers (Kim et al., 2007b). However, these contrasting results could be due to the different experimental systems employed. Due to their three dimensional structure, the oxygen tensions in spheroids could be expected to be significantly lower than those in monolayer cultures. In addition, Kim and colleagues measured HKII expression after 22-48 hours of hypoxia and HK activity after 29 hours (Kim et al., 2007b). This is significantly longer than the 16 hour hypoxic incubation employed in this study. The longer hypoxic incubation perhaps allows development of hypoxia tolerance and preferential protein synthesis of enzymes such as HK in the glycolytic pathway required for adaptation and survival (Hochachka et al., 1996).

No statistically significant alterations in the maximal activity of PFK were observed in this study. Interestingly, the PFK maximum activity recorded in $TS^{H}$

1.9 μmol hour$^{-1}$ (mg protein)-1 (*Figure 27*) correlates closely with the flux through glycolysis under this condition measured in section 3.2.1 at 2.27 ± 0.2 μmol hour$^{-1}$ (mg protein)$^{-1}$ (*Figure 20*). This could suggest that under hypoxic conditions PFK1 has a higher glycolytic flux control coefficient. Although Marín-Hernández showed a 4 fold increase in the glycolytic flux control coefficient of PFK-1 in hypoxic (0.1-0.2% $O_2$ for 24 hours) HeLa cells relative to normoxic cells, the majority of flux control was attributed to glycogen degradation, glucose transport and hexokinase activity(Marin-Hernandez et al., 2010). Therefore, contrasting with the hypothesis that the majority of glycolytic flux control resides with PFK-1 in hypoxic TS. Additionally, contrasting with this hypothesis the maximal activity of HK measured in hypoxic conditions is significantly lower than that of the glycolytic flux and of PFK-1. However, this could be attributed to the inability of the assay to fully measure the activity of all HK isoforms. For example, Board et al identified an additional glucose phosphorylating activity in tumour cells, which had properties similar to hepatic glucokinase (Board et al., 1995) Further metabolic control experiments would therefore be required to establish the contribution of PFK1 to control of glycolytic flux under hypoxic conditions.

The protein levels of the PFK isoforms PFKM and PFKL were both significantly reduced in hypoxic TS by 5.6 and 6.3 fold relative to the levels in normoxic TS. This is inconsistent with studies by Semenza and colleagues showing that PFKL is a transcriptional target of active HIF-1 (Semenza et al., 1994). However, Semenza and colleagues did not measure PFKL protein levels in response to HIF-1 activation.

Both the maximal capacity ($V_{max}$) and protein level of PK were decreased by 4 fold in hypoxic TS relative to normoxic TS in this study, again suggesting that PK activity was regulated by changes in protein level rather than post-translational modification. These changes in PK expression contrast with a number of previous studies including those by Semenza et al, showing induction of PKM mRNA under hypoxic conditions of 1% $O_2$ in HeLa cells (Semenza et al., 1994). In addition to more recent studies utilizing real time RT-PCR to show that the mRNA levels of both PKM1 and PKM2 were significantly increased in response to 24 hours of hypoxia (1% $O_2$) in mouse embryonic fibroblasts (Luo et al., 2011). Furthermore, immunoblot analysis of protein levels in HeLa cells grown in monolayer culture, showed a 1.6 and 1.7 fold increase of PKM2 levels in nuclear and cytosolic extracts exposed to hypoxia (1% $O_2$) for 24 hours (Luo et al., 2011). The hypoxic conditions in these studies were significantly higher oxygen concentrations of 1% $O_2$ (Luo et al., 2011) compared to the 0.1% $O_2$ employed in hypoxic incubations in this study, which may affect the severity of hypoxic response observed. In addition, cells were exposed to hypoxia for 24 hours relative to the 16 hour incubation in this study, perhaps allowing development of hypoxia tolerance (Hochachka et al., 1996).

A 3 fold reduction in both LDH expression and maximal activity was observed in hypoxic TS relative to normoxic TS (*Figure 33*, *Figure 34*). This once more suggests changes in protein level rather than post-translational regulation are responsible for the diminished maximal activities observed in hypoxic TS. These results contrast with previous studies showing an approximately 100% HIF-1

dependent induction of LDHA protein in HeLa cells grown in monolayer culture under hypoxic (0.3% $O_2$) conditions for 48 hours (Maher et al., 2007). In addition, cMyc expression in lymphoid cells was shown to correlate with LDHA mRNA levels measured by northern blot and LDH activity (Shim et al., 1997). These contrasting observations could be due to differences in, the models used, the oxygen concentrations employed during the hypoxic incubation and the time frame of the hypoxic incubation.

The wide spread reduction in enzyme levels in hypoxic TS in this study may be due to inhibition of protein synthesis as a result of the severity of our hypoxic conditions (0.1% $O_2$). Previous studies analysing the incorporation of $^{3}H$ methionine into protein have determined that exposure of PC12 cells, a rat pheochromocytoma cell line, to 0.1% $O_2$ for 4 or 24 hour resulted in a significant decrease in protein synthesis compared to normoxic controls (Hernandez-Jimenez et al., 2012). In agreement, studies by Koumenis and colleagues determined a significant reduction in protein synthesis, measured by the rate of $^{35}S$ methionine incorporation, was also observed in lung carcinoma A549 cells exposed to severe hypoxia (0.02%) for 1 or 2 hours (Koumenis et al., 2002). Furthermore, they noted that this hypoxia-induced reduction in protein synthesis was not a result of a decrease in the rate of mRNA synthesis, as the incorporation of [$^{3}H$] uridine into poly(A)$^{+}$ RNA did not decrease in hypoxic cells (Koumenis et al., 2002). This is consistent with preliminary gene expression profiling studies from our investigation in hypoxic TS that determined levels of HK1, HK2, PFKP, PFKL, PKM2 and LDHA mRNA relative to normoxic TS (Table 5). Further work profiling mRNA levels of these genes using RT-PCR would be

needed to confirm these changes in gene expression. Inhibition of protein synthesis under the severely hypoxic conditions employed in this study may therefore be the cause of the reduced levels of glycolytic enzymes observed in hypoxic TS.

The increased glycolytic flux in hypoxic spheroids (*Figure 20*) despite the decreased enzyme levels measured (*Figure 27Figure 28*) demonstrates that the glycolytic capacity, determined by the amount of active enzymes, is sufficient to support the increased *in vivo* activity of the pathway. Illustrating the difference between *in vitro* enzyme actives measured under optimal conditions, which can be affected by factors such as changes in gene transcription and post-translational modification. and the *in vivo* enzyme activity which is often lower. These lower *in vivo* activities can be due to activity of the reverse reaction, limited substrate levels, product inhibition or allosteric regulation for example (Stitt and Gibon, 2014).

Glucose-6-phophate dehydrogenase is the initial enzyme in the oxidative branch of the pentose phosphate pathway. Studies in PC12 cells have shown that the levels of glucose-6-phosphate dehydrogenase mRNA and enzymatic activity are increased significantly in response to longer-term (48 hours) incubation under moderately hypoxic (3% $O_2$) conditions (Gao et al., 2004). However, in this study both the maximal activity and protein level of glucose-6-phosphate dehydrogenase were significantly reduced (*Figure 31*,*Figure 32*). This could be a consequence of the severely hypoxic conditions (0.1% $O_2$). As mentioned previously, studies have revealed inhibition of protein synthesis under these

conditions (Hernandez-Jimenez et al., 2012). Alternatively, this could be due to a hypoxia induced reduction in proliferative rate and a reduced demand for the products of this pathway. For example, exposure of Rat1a fibroblasts to hypoxia (0.1-0.5% $O_2$) resulted in a significant $G_1$ arrest as a result of induction of the cyclin dependent kinase inhibitor, p27 (Gardner et al., 2001).

Recent studies have identified an important role for glutamine in hypoxic cancer cells as a carbon source for the synthesis of citrate; a major biosynthetic precursor in the synthesis of fatty acids essential for cellular growth and proliferation (Sun and Denko, 2014; Wise et al., 2011). Wise and colleagues employed isotopic tracers in SF188 glioblastoma cells to show that under hypoxic (0.5% $O_2$) conditions sufficient for HIF-1α stabilization, glutamine became the major source of citrate, via a reverse order of TCA cycle reactions where α ketoglutarate from glutaminolysis was reductively carboxylated (Wise et al., 2011). In addition, HIF-1 activation (0.5% $O_2$) was shown to reduce the activity of the α ketoglutarate dehydrogenase complex, via promotion of the ubiquitination and proteolysis of the E1 subunit of the complex, hence inhibiting glutamine oxidation via the TCA cycle (Sun and Denko, 2014). During this study, a mean glutamine depletion from the medium of 8.0 ± 2.6 μmoles (mg protein)$^{-1}$ was measured during the 16 hour hypoxic (0.1%) incubation, consistent with an important role for glutamine in cell growth under hypoxic conditions. However, the maximal capacity of glutamate dehydrogenase (GLDH) was significantly reduced by 5.2 fold (*Figure 29*) in hypoxic TS compared to TS produced under normoxic conditions, despite a 1.6 fold increase in GLDH protein levels in these TS (*Figure 30*). This contrasting change in capacity and expression could indicate

altered post-translational modification of GLDH. For example, cystine specific ADP-ribosylation of GLDH by SIRT4 has been shown to inhibit its activity (Herrero-Yraola et al., 2001), and investigations have shown that SIRT4 expression in DLD1 cells resulted in a significant decrease in glutamine uptake and proliferation (Csibi et al., 2013). Further work would be required to assess post-translational modifications of GLDH, for example, previous studies have assessed ADP ribosylation of GLDH by monitoring the transfer of radiolabel from [$^{32}$P]NAD to GLDH (Haigis et al., 2006; Kim et al., 2012).

These TS represent the hypoxic regions of a tumour. As would be predicted by the Pasteur effect, these spheroids reprogram their metabolism to generate ATP via the glycolytic pathway coupled to lactate production to regenerate $NAD^+$. This reprogramming is supported by the 2 fold increase in glycolytic flux observed in hypoxic TS relative to those produced under normoxic conditions, suggesting an increased dependence upon glycolysis for ATP production. The conditions employed in the production of these TS (0.1% $O_2$ 16 hours) were sufficient for stabilisation of the major hypoxia regulator HIF-1$\alpha$. However the levels and activities of many glycolytic enzymes were decreased in these TS, probably due to the severely hypoxic conditions utilized, which are known to inhibit protein synthesis. Further studies measuring the rate of incorporation of radio labelled amino acids into protein could be used to confirm this. The increase in glycolytic flux despite reduced enzyme in these hypoxic TS demonstrated that the glycolytic capacity of these TS is in excess of the *in vivo* utilization of the pathway. It could be hypothesised that under these severely hypoxic conditions the cells in these TS prioritise survival rather than adaptation

or growth, which could be clarified by further experiments at differing oxygen concentrations.

## 4.4 Quiescent tumour spheroids ($TS^{Q}$)

Tumours are known contain a considerable population of cells that are in a quiescent state (Sahin et al., 1991), which contribute to the failure of various chemotheraputic agents targeting aspects of the cell replication process (Jackson, 1989; Mellor et al., 2005a). This quiescent population of cells is also thought to contribute to the problem of tumour recurrence following therapy (Desoize and Jardillier, 2000; Durand, 1997). The energetic demands and metabolic strategies of these quiescent cells are thought to differ extensively from those of the proliferating cells present within a tumour (Bauer et al., 2004; Lemons et al., 2010)(Section 1.3.3). Due to the prevalence of quiescent cells within tumours and their significant therapeutic consequences, the effects of quiescence upon energetic metabolism were characterised in TS in this study.

There are a number of different model systems that have been utilized to study quiescence in previous investigations. These include two-dimensional monolayer culture models where cells are induced into quiescence by either serum withdrawal resulting in growth factor deprivation, contact inhibition by growth to high cell densities or loss of adhesion through disruption of cell-substratum adhesisons (Coller et al., 2006; Lemons et al., 2010). These models however, have the same limitations as other monolayer cultures mentioned

earlier (section 1.4), namely failing to reproduce the many aspects of the tumour microenvironment. Tumour spheroids have also been used to model the quiescent regions in tumours. As mentioned previously (Section 1.4) TS have a well-defined geometry developing distinct populations of cells such as an outer proliferating population and a deeper quiescent population. At diameters above 500 μm a central necrotic core also develops (*Figure 11*)(Hirschhaeuser et al., 2010; Lin and Chang, 2008; Sutherland, 1988). In order to investigate the quiescent population in TS, a number of different approaches have been utilized, including comparison of spheroids of different sizes, which display varying proportions of the three layers. Kim and Forbes, compared small 275 μm diameter TS, predominantly composed of proliferating cells and large 800 μm diameter TS, which would have equal populations of proliferating and quiescent cells, as well as a "non metabolically active" necrotic core (*Figure 36*) (Kim and Forbes). The manuscript stated "*the difference in metabolism between these types of spheroid gives an indication of how metabolism changes in cells as they become quiescent*" (Kim and Forbes, 2007). However, the presence of multiple cell types in a single TS greatly complicates analyses. In addition, this fails to take account of the effects of the necrotic core upon metabolism. Zhang and colleagues showed high levels of lactate in the necrotic core of DLD1 TS using FT-IR (Zhang et al., 2012), suggesting an highly acidic environment, which may affect the metabolism of adjacent cell populations (section 1.3.2). An alternative approach to study quiescent regions in TS is the selective dissociation of cells from the spheroid to isolate different populations of cell. This approach was utilised by Mandujano-Tinoco and colleagues in MCF-7 TS, where they used trypsin to dissociate the outer proliferating cells of large TS from the internal quiescent

cells to study the metabolism of the different populations (Mandujano-Tinoco et al., 2013). This dissociation is a technically challenging procedure and additionally fails to take into account the effects of the inner necrotic core upon metabolism. In addition in these large TS there will be areas of hypoxia, due to the diffusion limit of $O_2$ in tissue, further complicating analysis.

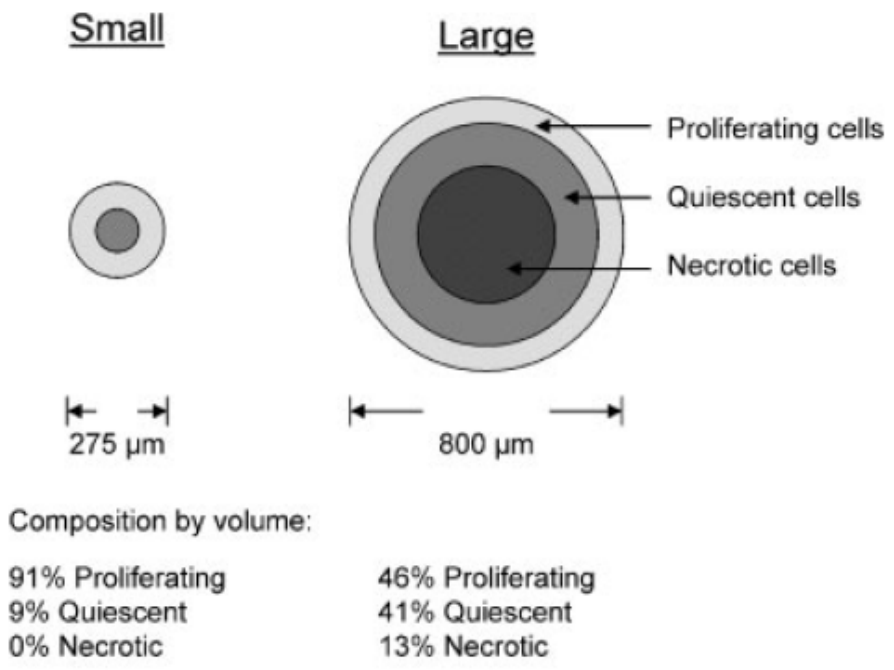



***Figure 36. The relative proportions of proliferating and quiescent cells in tumour spheroids of different sizes.*** *Diagram with permission from Kim and Forbes 2010 illustrating the different proportions of proliferating, quiescent and necrotic cells present in small and large tumour spheroids (Kim and Forbes, 2007).*

In this study, quiescent TS were generated by serum withdrawal, a technique that has previously been successfully utilized in this laboratory (Mellor et al., 2005a). Following serum withdrawal, TS showed minimal growth during the 20 day period (*Figure 12*). Although consistent with the definition of quiescence they retained the capacity to proliferate as shown by the return to exponential growth when returned to serum-containing medium (*Figure 12*). These TS also

displayed a dramatic increase in levels of the quiescence marker $p27^{Kip1}$ (*Figure 13* E) consistent with a quiescent phenotype. This method is technically simple and due to the defined spheroid size range (200-400μm diameter) it enables analysis of quiescent cell populations whilst maintaining metabolite gradients.

The energetic demands, and therefore the metabolic strategies employed by quiescent cells, are expected to differ considerably from those of proliferating cells that are required to replicate their entire contents for division. Quiescent cells are therefore thought to have a severely decreased metabolic rate relative to proliferating cells. This is supported by a 2.6 fold decrease in glycolytic rate measured by the rate of $^3H_2O$ production from [5-$^3$H] glucose in $TS^Q$ relative to proliferating $TS^N$ (*Figure 20*). This also correlates with work by Kim and Forbes who measured significantly lower glycolytic fluxes in large TS containing quiescent cells than small TS containing predominantly proliferating cells via NMR (Kim and Forbes, 2007). In contrast, Mandujano-Tinoco and colleagues determined similar rates of glycolysis in the quiescent and proliferative fractions of dissociated MCF-7 spheroids via measurement of the rate of lactate production (Mandujano-Tinoco et al., 2013). However, this approach fails to take into account the contribution of glutamine metabolism to lactate production.

In contrast to the reduced glycolytic flux, a 1.9 fold increase in glucose depletion from the medium was measured in $TS^Q$ over 24 hours relative to proliferating $TS^N$ despite no statistically significant alterations in the levels of glucose transporters (*Figure 18*, *Figure 19*). This disparity between glucose depletion and glycolytic flux raises the question as to the metabolic fate of the excess glucose

consumed by quiescent TS. Recent studies by Witney and colleagues measured increased glycogen storage in HEY Rab25 cells induced into quiescence by contact inhibition (Witney et al., 2014). Glycogen could therefore potentially be stored as an energy source for utilization upon re-entry to the cell cycle. Previous studies have shown increased glycogen accumulation in a number of cancer cell lines following exposure to hypoxic micro-environmental stress (Iida et al., 2012; Pelletier et al., 2012; Pescador et al., 2010). These studies could therefore suggest that cancer cells up regulate glycogen storage in response to micro-environmental stress in order to survive the harsh micro-environmental conditions that develop within a tumour. Hence analysis of the glycogen content of these quiescent TS may identify the fate of the excess glucose. This could be achieved by several methods including, Periodic Acid Schiff staining, an immunohistochemistry stain for glycogen, or by biochemical titration using glucoamylase to break down stored glycogen to glucose for analysis (Pelletier et al., 2012).

Preliminary metabolomic analysis confirmed that despite the low glycolytic flux measured, glucose derived carbon was predominantly metabolised by the glycolytic and pentose phosphate pathways in quiescent TS. High levels of glucose-derived carbon were measured in glycolytic metabolites including glucose-6-phosphate, 3-phosphoglycerate and lactate as well as 6-phosphogluconic acid, a component of the pentose phosphate pathway (*Figure 21*). In addition, there were very low levels of glucose derived carbon in the components of the TCA cycle showing minimal glucose metabolism by the TCA cycle in these TS (*Figure 21*).

Analysis of the maximal specific activities and levels of enzymes in the glycolytic pathway revealed that although there were no statistically significant changes in the enzyme levels, the capacity of HK, PFK1 and PK were all increased in $TS^{Q}$ relative to $TS^{N}$ (*Figure 27*, *Figure 28*). This suggests higher proportion of each enzyme is in the active state in these quiescent TS. For example, the pyruvate kinase isozyme PKM2 is inhibited in proliferating cells in response to growth factor signalling. This is achieved through phosphorylation at tyrosine residue 105 by the activated fibroblast growth factor receptor type 1 (Hitosugi et al., 2009). Confirmation of this however, would require further analysis. For example there are specific antibodies towards PKM2 phosphorylated at $Y^{105}$, which could be used to assess the relative content of the phospho-PKM2 by immunoblotting. The maximal capacity of HK at 12.1 ± 2.3 nmol $min^{-1}$ (mg $protein)^{-1}$ is still the lowest in the glycolytic pathway in quiescent TS, closely followed by PFK1 at 69.3 ± 17.8 nmol $min^{-1}$ (mg $protein)^{-1}$. The activity of PK is several fold higher at 4.5 ± 0.3 μmol $min^{-1}$ (mg $protein)^{-1}$. This correlates with studies mentioned earlier (section 4.1) by Marin-Hernandez et al, showing that HK and PFK-1 were among the glycolytic enzymes with lowest maximal activities in rat AS-30 hepatoma and HeLa human cervical carcinmona cells (Marin-Hernandez et al., 2006). Elasticity analysis determined that the majority of flux control was located at the beginning of the glycolytic pathway in AS-30D cells (Marin-Hernandez et al., 2006). Similar to observations in proliferating TS (section 4.1), the significantly lower activities of HK and PFK1 may suggest that flux control in these quiescent TS also lies at the beginning of the glycolytic pathway. However, further work would be required to confirm this hypothesis

such as determining the effect of inhibition of these enzymes upon flux through the pathway (Moreno-Sanchez et al., 2008).

An alternate "sink" for the excess glucose in quiescent TS is the pentose phosphate pathway (PPP). This pathway branches from glycolysis and functions to produce ribose-5-phosphate and NADPH both of which are important biosynthetic precursors (Wood, 1986)(section 1.1.2). Hence it could be hypothesised that flux through this pathway would be significantly reduced in quiescent cells. In contrast, initial metabolomic investigations measured high levels of glucose derived carbon in the pentose phosphate pathway intermediate 6-phosphogluconic acid in quiescent TS (*Figure 21*). Also the levels and activity of glucose-6-phosphate dehydrogenase, the initial enzyme in oxidative pathway, are not significantly altered from those recorded in proliferating TS (*Figure 31*, *Figure 32*). Furthermore, in recent metabolomics studies by Lemons and colleagues, the flux through the oxidative branch of the PPP was not significantly altered in fibroblasts induced into quiescence by contact inhibition or serum starvation (Lemons et al., 2010). They showed that contact inhibited quiescent fibroblasts had increased flux through the non-oxidative pentose phosphate pathway, thereby recycling intermediates back to the glycolytic pathway (Lemons et al., 2010). Differing from the results in this study, Lemons et al showed increased levels of glucose-6-phosphate dehydrogenase in fibroblasts induced into quiescence via contact inhibition and serum starvation relative to the levels in proliferating fibroblasts (Lemons et al., 2010). This disparity could be due to the different cell types employed in these studies, the primary human

dermal fibroblasts utilized by Lemons et al are a non cancerous cell line contrasting with the DLD1 colon carcinoma cells used here (Lemons et al., 2010).

The pentose phosphate pathway is utilized in quiescent cells to generate NADPH in order to regenerate the reduced forms of glutathione or thioredoxin to protect against oxidative stress. An increased ratio of reduced to oxidised glutathione in quiescent fibroblasts and inhibition of the pentose phosphate pathway by dehydropiandrosterone (DHEA) significantly increased cell death in contact inhibited quiescent fibroblasts relative to proliferating fibroblasts (Lemons et al., 2010). There are a number of methods that can be used to analyse pentose phosphate pathway flux. For example, Tosuko and colleagues assessed flux through the pathway by measuring the amount of $^{14}C$ from universally radiolabelled glucose incorporated in newly synthesised RNA relative to the total RNA pool (Tsouko et al., 2014). More traditionally the rate of flux through the oxidative PPP is measured by comparing the rate of $^{14}CO_2$ release from [1-$^{14}C$] glucose, which occurs at the 6-phosphogluconate reaction in the pentose phosphate pathway and in reactions of the TCA to the rate of $^{14}CO_2$ release from [6-$^{14}C$] glucose. The positional labelling of $^{14}C$ is indistinguishable between [1-$^{14}C$] glucose and [6-$^{14}C$] glucose after the triose phosphate isomerase reaction; hence the difference in $CO_2$ release allows estimation of flux through the oxidative pentose phosphate pathway (Fan et al., 2014; Rodriguez-Rodriguez et al., 2013). Therefore, these methods could be used to further investigate the role of the pentose phosphate pathway in quiescent spheroids, since its potential as a therapeutic target is highlighted in these previous studies.

Furthermore, glucose derived carbon can be utilized for lipid synthesis with the glycolytic intermediate dihydroxyacetone-phosphate being reduced by glycerol 3-phosphate dehydrogenase to form glycerol-3-phosphate a precursor of phospholipids and triacylglycerols. Previous studies have shown that the activity of glycerol 3-phosphate dehydrogenase is significantly higher in human bladder cancer tissue samples than in non-neoplastic adjacent tissue samples (Turyn et al., 2003). Slightly higher levels of glucose derived carbon were observed in glycerol-3-phosphate in quiescent TS than normoxic TS *(Figure 21)*. However, carbon enrichment of glycerol-3-phosphate was very low in both types of TS indicating that minimal amounts of glucose derived carbon metabolised by this lipogenic pathway.

Glutamine is known to be a major nutrient in cancer cells (*Figure 6*), the metabolism of which is commonly altered in cancer cells. Early studies measuring the uptake of radiolabelled glutamine in human hepatoma tumour spheroids found that the rate of glutamine uptake per mg total protein measured over 1 minute was significantly higher in large TS, 0.85-1.5mm in diameter, than in small TS, 0.3-0.7mm in diameter (Pawlik et al., 2000). As stated by Kim and Forbes (*Figure 36*), large TS would be predicted to have a higher proportion of quiescent cells present than the small TS (Kim and Forbes, 2007). This suggests that glutamine uptake in TS is increased by the presence of quiescent cells, however the increased surface area of the large TS may also have an effect on glutamine uptake. In contrast, Lemons et al analysed glutamine levels in the medium to show that fibroblasts grown in monolayer culture and induced into quiescence by contact inhibition or serum starvation consumed approximately

half as much glutamine per mg protein as proliferating fibroblasts (Lemons et al., 2010). These differences could be due to cell type, for instance, Pawlik et al used a hepatoma cancer cell line whereas Lemons et al utilized non-cancerous primary human dermal fibroblasts. Alternatively it may be down to the culture system with the studies utilizing tumour spheroids and monolayer cultures respectively. In this study, although no alterations in the levels of the major glutamine transporter ASCT2 were detected between quiescent and proliferating TS (*Figure 22*), there were dramatic changes in glutamine depletion from the medium. Quiescent TS depleted 5.5 fold more glutamine over 12 hours than proliferating $TS^N$ (*Figure 23*). This along with the significantly decreased glycolytic flux might suggest that glutamine is the favoured nutrient for ATP production in quiescent TS. However, after 24 hours this difference dropped to 1.5 fold and was no longer statistically significant (*Figure 23*). It is conceivable that glutamine uptake in $TS^N$ increases as glucose concentration in the medium decreases to ensure a constant supply of nutrients. This could therefore result in the later increase in glutamine uptake observed in $TS^N$.

Analysis of the metabolic fate of U-$^{13}$C glutamine by Lemons et al, resulted in similar rapid labelling of glutamate, α ketoglutarate, succinate, malate and citrate in both proliferating and contact inhibited quiescent fibroblasts, indicating the use of glutamine as an anaplerotic precursor (Lemons et al., 2010). Consistent with this there were no significant alterations in quiescent TS in the level or activity of glutamate dehydrogenase compared to proliferating TS (*Figure 29*, *Figure 30*). Further analysis of the metabolic fate of glutamine in quiescent fibroblasts determined an increased "reverse TCA cycle" flux to generating

citrate through the reductive carboxylation of α ketoglutarate (Lemons et al., 2010). This citrate could then be used in fatty acid synthesis consistent with the increased incorporation of $^{14}C$ into fatty acid in quiescent fibroblasts fed [U-$^{14}C$] glucose (Lemons et al., 2010). Glutamine is therefore a key metabolite in quiescent cells and future analysis of the rate of flux through the glutaminolysis pathway and metabolic fate of glutamine in quiescent tumour spheroids via metabolomic studies would greatly clarify the metabolic adaptations in these spheroids.

Lemons et al did not show the production of lactate from glutamine via the malic enzyme. However, glutamine could be a major source of the increased lactate accumulation measured in the medium of quiescent tumour spheroids over 24 hours in this study (*Figure 25*). Metabolomics studies show similar levels of glucose-derived carbon in lactate from quiescent and proliferating DLD1 TS (*Figure 21*), which suggests that glucose is not the source of the 1.8 fold increase lactate accumulation in the medium of quiescent TS. Alternatively, this increase in lactate accumulation in the medium of quiescent TS could be due to reduced lactate reuptake and oxidation in quiescent TS. This hypothesis is consistent with the drastically reduced levels of the lactate transporter MCT1 in quiescent spheroids (*Figure 24*). The MCT1 lactate symporter was shown to be essential for lactate uptake in a human cervical cancer cell line (Sonveaux et al., 2008b). Hence the reduction in MCT1 levels in these TS may indicate a reduced rate of lactate uptake from the medium.

Both the maximal activity and level of the LDH enzyme are amplified by 1.8 and 1.7 fold respectively in quiescent TS (*Figure 33*, *Figure 34*). This close correlation suggests that LDH is principally regulated at the transcriptional level in quiescent DLD1 TS. However, LDH catalyses a bidirectional reaction and the relative expression of LDH-A, which favours the production of lactate and LDH-B favouring the reverse reaction (Adeva et al., 2013) were not determined, analysis of which could further characterise lactate metabolism in these spheroids.

Although the presence of quiescent cells within tumours that contribute to the failure of many therapeutic strategies has long been recognized (Jackson, 1989; Mellor et al., 2005a), relative little is currently known about the metabolic strategies employed within these cells. This study, like that of Lemons et al (Lemons et al., 2010), suggests that these quiescent cells are metabolically active as evidenced by their increased uptake of glucose and glutamine. In addition, this is the first study to systematically characterise metabolism in these quiescent tumour spheroids. It raises a number of questions for further investigation including the metabolic fate of glutamine and the activity of the pentose phosphate pathway in quiescent TS. Finally, the work here predominantly focuses upon the activity of glycolysis. Mandujano-Tinoco and colleagues showed that in MCF-7 tumour spheroids glycolysis contributed less than 10% to total ATP supply in both proliferating and quiescent cell layers (Mandujano-Tinoco et al., 2013). This highlights the need to assess the activity of the TCA cycle in these quiescent TS and the contribution of oxidative phosphorylation to ATP supply and finally raises the question about why they are so metabolically active. Quiescent cells are thought to contribute to the problem of tumour recurrence

following therapy, re-entering the cell cycle once they have better access to nutrients due to the removal of the outer oxygenated proliferating tumour cells by chemo- or radio- therapy (Desoize and Jardillier, 2000; Durand, 1997). It would therefore make sense that they ensure viability by generating NADPH in order to regenerate the reduced forms of glutathione or thioredoxin to protect against oxidative stress, in addition to degrading and re-synthesising any damaged macromolecules, as suggested by Lemons et al (Lemons et al., 2010).

## 4.5 Conclusions

Numerous studies have established that cancer cells reprogram their metabolism (Bode et al., 1995; Gillies et al., 2008; Hanahan and Weinberg, 2011), leading to metabolism being considered a potential therapeutic target for cancer treatment (reviewed in (Ganapathy-Kanniappan and Geschwind, 2013)). Although the aetiology of these metabolic alterations is not currently understood, the hostile micro-environment within the tumour is thought to contribute (Cairns et al., 2011). This leads to the development of hypoxic and quiescent cell populations that are inherently difficult to treat with chemo and radio therapy (Gray et al., 1953; Jackson, 1989; Mellor et al., 2005a; Teicher, 1994). The aim of this study was to characterise the metabolic adaptations undertaken by tumour cells to different micro-environmental stresses including hypoxia and quiescence relative to oxygenated, proliferating cells.

This study is the first to characterise the metabolic adaptations to micro-environmental stress using tumour spheroids of a defined size range, between

200-400μm. These spheroids have the advantage of more closely modelling the environment and gene expression profile in a tumour than their two dimensional monolayer cell culture counterparts (Hirschhaeuser et al., 2010). At the target size range, the spheroids contain predominantly proliferating cells (*Figure 13*) and are fully oxygenated. However chemical gradients of nutrients and catabolites will have developed in TS of this size (Hirschhaeuser et al., 2010). Analysis at this stage of growth therefore enables the comparative examination of the effect of distinct micro-environmental conditions on the metabolism of the tumour spheroids.

Consistent with numerous studies illustrating the presence of the Warburg effect in rapidly proliferating cells (Wang et al., 1976; Warburg et al., 1927), oxygenated proliferating spheroids exhibited a Warburg like metabolism with glucose being oxidised to produce lactate in the presence of oxygen. In addition, metabolomics investigations determined that glucose was also extensively metabolised by the pentose phosphate pathway, a vital pathway in proliferating cells for biosynthesis. Finally, concurrent with studies illustrating the importance of glutamine for cancer cell growth (DeBerardinis et al., 2007; Eagle, 1955; Tannock and Kopelyan, 1986) these spheroids demonstrated avid extraction of glutamine from the growth medium.

Hypoxic tumour spheroids exhibited metabolic adaptations consistent with the Pasteur effect of increased glycolytic flux, glucose uptake and lactate production (Seagroves et al., 2001). However, although the levels of the major transcription factor mediating the response to hypoxia, HIF-1$\alpha$ were increased (Semenza,

2010), the protein levels of many of its known target genes were significantly decreased. This was perhaps a result of inhibition of protein synthesis at the low oxygen concentrations present in these spheroids (Hernandez-Jimenez et al., 2012). This reinforces the complex array of biological effects seen in solid tumours *in vivo,* which are likely to show a gradation of hypoxia.

Finally, the previously poorly characterised quiescent spheroids exhibited a number of interesting adaptations in their metabolism. Firstly although exhibiting a decrease in glycolytic flux, glucose depletion from the medium was significantly increased over 24 hours, perhaps suggesting increased glycogen storage or pentose phosphate pathway utilization. Secondly, glutamine uptake was avid even in the presence of available glucose in the medium. Glutamine has numerous important bio-energetic and biosynthetic roles in the cell, hence further studies profiling the metabolic fate of glutamine would be advantageous in fully characterising the metabolism of quiescent cells. Finally, lactate accumulation in the medium over 24 hours was also significantly increased in quiescent spheroids. There are several possible causes of this including; increased glutamine metabolism forming lactate or reduced lactate uptake via MCT1 further illustrating the importance of further research to fully characterise the metabolic adaptations of these quiescent cells. These metabolic adaptations to the different micro-environmental conditions are summarised in *Figure 37*.

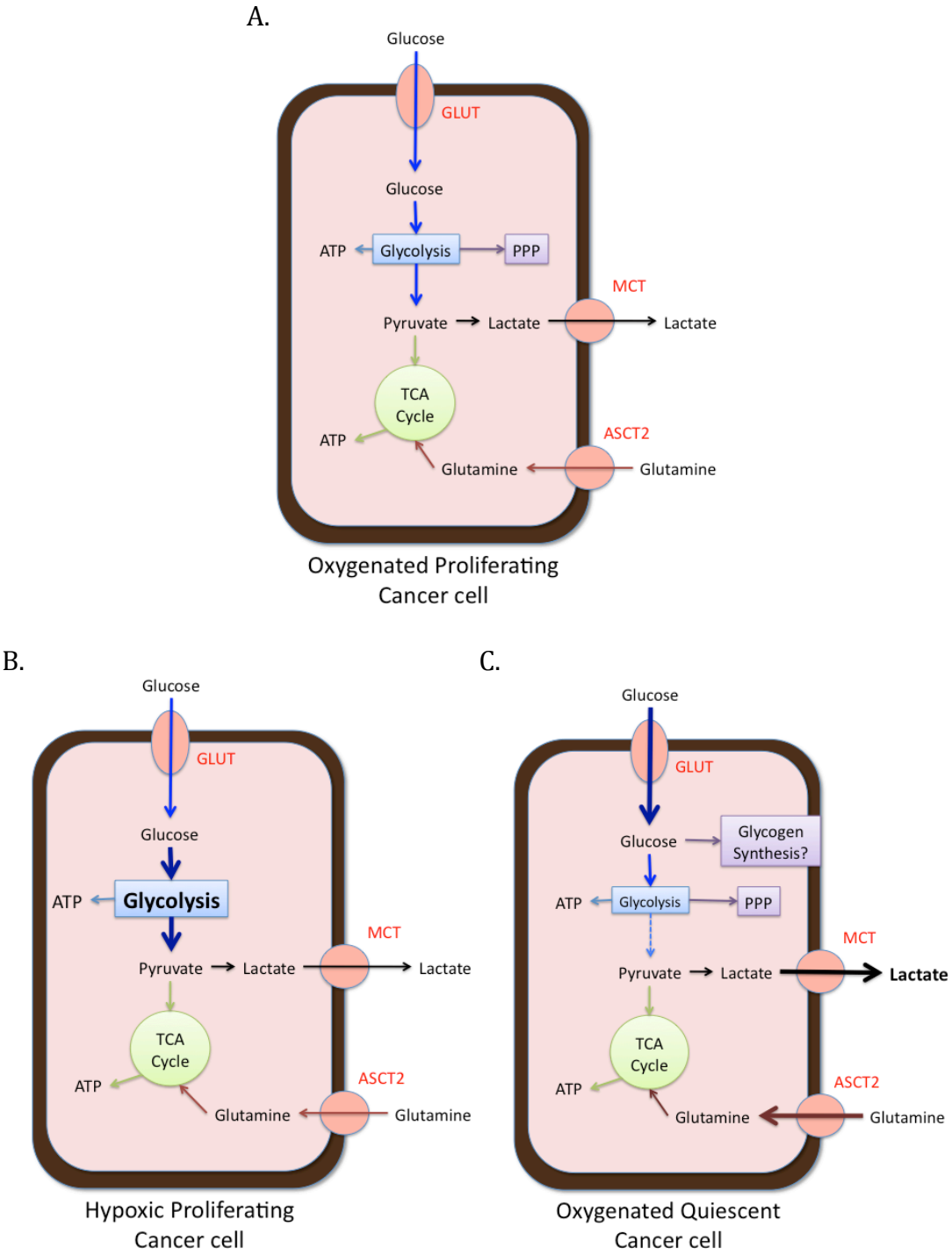



***Figure 37. Summary of the alterations in metabolism induced by micro-environmental stress observed in tumour spheroids.*** *The alterations in metabolic parameters observed in tumour spheroids exposed to hypoxia or induced into quiescence relative to oxygenated proliferating TS are summarised. (A) Oxygenated proliferating TS exhibited metabolic adaptations consistent with the Warburg effect, metabolising glucose via glycolysis to produce lactate in the presence of oxygen, in addition these TS metabolised glucose via the pentose phosphate pathway (PPP) and took glutamine up from the medium. (B) Hypoxic TS, exhibited increased glycolytic flux. (C) Quiescent TS, exhibited increased glucose and glutamine uptake, decreased glycolytic flux leading to the suggestion of increased glycogen synthesis, utilization of the PPP and increased lactate accumulation in the medium.*

*In vivo* these different populations of cells present within a tumour are not distinct instead they interact with one another. Sonveaux and colleagues demonstrated this interaction when they determined that lactate taken up by MCT1 could be utilized as a fuel for oxidative metabolism in oxygenated tumour cells (Sonveaux et al., 2008b). This led to the development of the lactate symbiosis hypothesis that is illustrated in *Figure 7*, in which glucose is metabolised in hypoxic, glycolytic tumour cells to produces lactate that is then taken up by oxidative tumour cells via MCT1 and used a substrate for oxidative phosphorylation (Sonveaux et al., 2008b). This symbiosis allows the conservation of glucose for use in hypoxic cells dependent upon glycolysis (Sonveaux et al., 2008b). Furthermore, these micro-environment conditions are not mutually exclusive. For example hypoxia may contribute to the aetiology of quiescence through its inhibition of proliferation through the regulation of p27 and p21 cyclin dependent kinase inhibitors (Gardner et al., 2001; Koshiji et al., 2004). Hence, there may be populations of cells present within a tumour that are both hypoxic and quiescent. The interaction of these different micro-environmental stresses merit further investigation.

This study demonstrates that the metabolic strategies employed by tumour spheroids differ upon exposure to distinct micro-environmental stresses. This tumour spheroid model of micro-environmental stress is unique, allowing comparative examination of the results of micro-environmental stress upon metabolism. A number of techniques were utilized to profile the effects of micro environmental stress upon metabolism in these spheroids providing a detailed account of the metabolic strategies encountered. These studies show that micro-

environmental stress must be taken into account in the development of anti-cancer therapies targeting metabolism.

These studies lay the foundations for future studies indentifying metabolic target sites for anti-cancer therapies. As mentioned previously studies have shown the majority of glycolytic flux control is located at the beginning of the pathway specifically at the glucose transport and hexokinase reactions (Marin-Hernandez et al., 2006). Consistent with this suggestion, hexokinase was the glycolytic enzyme with lowest maximal capacity ($V_{max}$) measured under all micro-environmental stress conditions analysed in this study (section 3.3.1), thus highlighting its potential as a therapeutic target. However, early studies investigating metabolic control of glycolysis in normal cells such as; erythrocytes, rat cardiac muscle, rat hepatocytes and rabbit skeletal muscle, identified the major sites of glycolytic control to be glucose transport, hexokinase and phosphofructokinase (Kashiwaya et al., 1994; Rapoport et al., 1976; Torres et al., 1986; Torres et al., 1989). The non-specific inhibition of hexokinase activity by compounds such as 2-deoxy-D-glucose may therefore have a significant toxic affect upon normal cells in the body resulting in adverse side effects (Dwarakanath and Jain, 2009). Therefore specific targeting of the HKII isoform, which is over expressed in cancer cells, may be more effective (Patra et al., 2013). Alternatively glucose transport may be targeted, studies have shown the GLUT1 inhibitor WZB117 has anticancer effects in both cancer cell lines and in nude mouse models (Liu et al., 2012). However as GLUT transporters are also present in normal tissues (Uldry and Thorens, 2004), targeting GLUT transporters could also lead to specificity problems. These problems could

potentially be overcome using vector-conjugated liposomes, for example, as carriers to actively target the therapeutic compound to the tumour tissue (reviewed in (Huwyler et al., 2008)). Many tumour cells over express the folate receptor, consequently folate-conjugated liposomes have been shown to result in increased tumour drug delivery (Huwyler et al., 2008). For example, a 17 fold increase in doxorubicin levels were measured in mouse lymphoma cells using folate targeted liposomes relative to non targeted controls (Shmeeda et al., 2006). The maximal capacities measured for pyruvate kinase and lactate dehydrogenase at the end of the glycolytic pathway are at many fold higher than the measured glycolytic flux. Metabolomics analysis indicated that the pentose phosphate pathway is active under both normoxic and quiescent conditions in tumour spheroids (figure 10 results). This pathway is important for cellular survival producing NADPH, which regenerates the reduced forms of glutathione or thioredoxin to protect against oxidative stress (Gorrini et al., 2013). The pentose phosphate pathway could therefore be a potential target for the development of therapeutic strategies targeting the quiescent population of cancer cells that has traditionally been know to contribute to the failure of many chemotherapeutic agents (Jackson, 1989; Mellor et al., 2005a). Finally the significant alterations in glutamine uptake in quiescent tumour spheroids measured in this study merit further investigation and may lead to an alternate strategy targeting the quiescent populations of cancer cell within a tumour.

# 5. Appendix

## 5.1 Isoprotomer Distribution

The distribution of mass isoprotomers of the selected metabolites was also analysed. This is shown in (*Figure 38*) labelled isoprotomers are expressed in increasing molecular masses with M1 being the lightest and hence having the lowest number of labelled $^{13}C$ present, the distribution of isoprotomers expressed as a fraction of the total distribution. Although as with the enrichment data there does not appear to be any significant differences in the distribution of isoprotomers between $TS^{Q}$ and $TS^{N}$, this was a preliminary experiment and so further repeats would be required to confirm this statistically. However some interesting observations can be made from this data. For example the presence of several isoprotomers of 3 phosphoglycerate (3PGA) in addition to the fully labelled M3 isoprotomer could suggest a proportion of glucose-derived carbon deviated from the glycolytic pathway and re-entered a later stage, maybe cycling through the pentose phosphate pathway. This is consistent with recent studies observing cycling of glucose-derived carbon through the PPP in both proliferating and quiescent cells (Lemons et al., 2010).

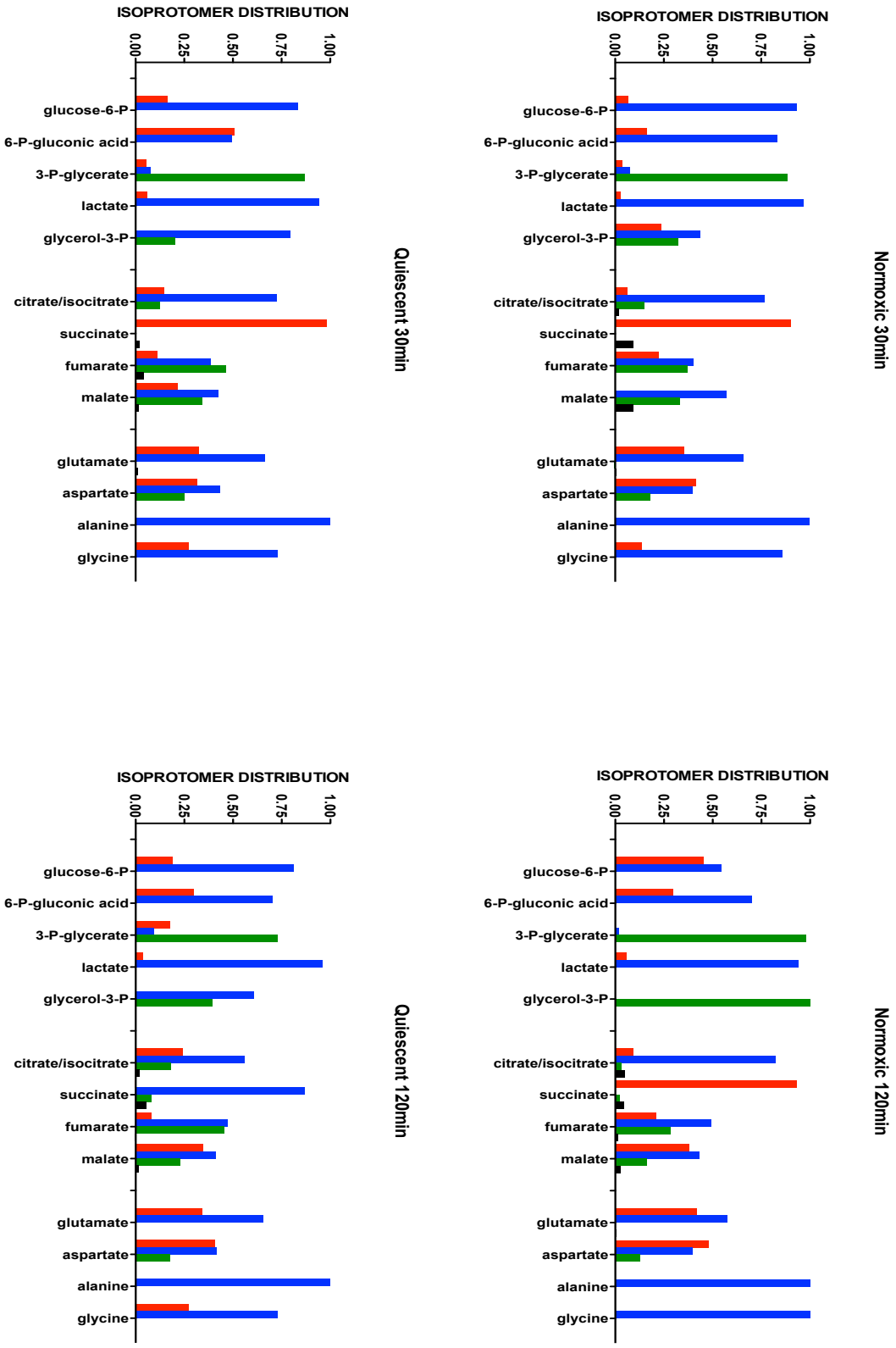



***Figure 38. Isoprotomer Distribution.*** *Isotomoper distribution is expressed as the fraction of the total distribution of labelled isopopomers. Isotopomers are expressed in increasing mass molecular mass with M1 (red), M2 (blue) M3(green) and M4 (black).*

## 5.2 Gene expression profiling

### 5.2.1 Gene expression profiling methods

RNA was extracted from tumour spheroids using TRIZOL. For each sample, 100ng of total RNA was amplified and labelled with the 3' IVT Express Kit (Affymetrix, Santa Clara, CA) following the manufacturer's recommendations. Biotin-labelled fragmented cRNA (10 µg) was hybridized to GeneChip Human Genome U133 Plus 2.0 arrays (Affymetrix), covering more than 47000 transcripts representing 39000 human genes. Hybridization occurred at 45°C for 16 hours in a Hybridization Oven 640 (Affymetrix). Chips were then washed and stained in a Fluidics Station 450 (Affymetrix) and scanned with a GeneChip Scanner 3000 (Affymetrix). Data was then analysed using GeneSpring 7.3.1 software (Agilent).

### 5.2.2 Gene Expression profiling of key metabolic enzymes

| Gene | Hypoxia | Quiescence |
|---|---|---|
| GLUT 1 | 2.73 | 0.60 |
| GLUT 3 | 8.24 | 0.83 |
| HK1 | 2.06 | 1.31- |
| HK2 | 2.37 | 0.83- |
| G6P DH | 1.03 | 1.08 |
| PFK L | 1.42 | 1.08 |
| PFK M | 0.80 | 0.95 |
| PKM2 | 1.53 | 0.85 |
| GLS | 0.82 | 0.93 |
| GLS2 | 0.95 | 0.89 |
| MCT1 | 0.66 | 0.92 |
| MCT4 | 1.09 | 2.07 |

**Table 5. Preliminary gene expression profiling studies, values are expressed relative to normoxia control condition**

# 6. References


Adeva, M., Gonzalez-Lucan, M., Seco, M., and Donapetry, C. (2013). Enzymes involved in l-lactate metabolism in humans. Mitochondrion *13*, 615-629.

Ahmad, A., Ahmad, S., Schneider, B.K., Allen, C.B., Chang, L.Y., and White, C.W. (2002). Elevated expression of hexokinase II protects human lung epithelial-like A549 cells against oxidative injury. Am J Physiol Lung Cell Mol Physiol *283*, L573-584.

Ahmed, D., Eide, P.W., Eilertsen, I.A., Danielsen, S.A., Eknaes, M., Hektoen, M., Lind, G.E., and Lothe, R.A. (2013). Epigenetic and genetic features of 24 colon cancer cell lines. Oncogenesis *2*, e71.

Airley, R.E., and Mobasheri, A. (2007). Hypoxic regulation of glucose transport, anaerobic metabolism and angiogenesis in cancer: novel pathways and targets for anticancer therapeutics. Chemotherapy *53*, 233-256.

Altenberg, B., and Greulich, K.O. (2004). Genes of glycolysis are ubiquitously overexpressed in 24 cancer classes. Genomics *84*, 1014-1020.

Altomare, D.A., Tanno, S., De Rienzo, A., Klein-Szanto, A.J., Skele, K.L., Hoffman, J.P., and Testa, J.R. (2002). Frequent activation of AKT2 kinase in human pancreatic carcinomas. J Cell Biochem *87*, 470-476.

Amann, T., and Hellerbrand, C. (2009). GLUT1 as a therapeutic target in hepatocellular carcinoma. Expert Opin Ther Targets *13*, 1411-1427.

Anastasiou, D., Poulogiannis, G., Asara, J.M., Boxer, M.B., Jiang, J.K., Shen, M., Bellinger, G., Sasaki, A.T., Locasale, J.W., Auld, D.S.*, et al.* (2011). Inhibition of pyruvate kinase M2 by reactive oxygen species contributes to cellular antioxidant responses. Science *334*, 1278-1283.

Arora, K.K., and Pedersen, P.L. (1988). Functional significance of mitochondrial bound hexokinase in tumor cell metabolism. Evidence for preferential phosphorylation of glucose by intramitochondrially generated ATP. J Biol Chem *263*, 17422-17428.

Ashizawa, K., Willingham, M.C., Liang, C.M., and Cheng, S.Y. (1991). In vivo regulation of monomer-tetramer conversion of pyruvate kinase subtype M2 by glucose is mediated via fructose 1,6-bisphosphate. J Biol Chem *266*, 16842-16846.

Atsumi, T., Chesney, J., Metz, C., Leng, L., Donnelly, S., Makita, Z., Mitchell, R., and Bucala, R. (2002). High expression of inducible 6-phosphofructo-2-kinase/fructose-2,6-bisphosphatase (iPFK-2; PFKFB3) in human cancers. Cancer research *62*, 5881-5887.

Au, S.W., Gover, S., Lam, V.M., and Adams, M.J. (2000). Human glucose-6-phosphate dehydrogenase: the crystal structure reveals a structural NADP(+) molecule and provides insights into enzyme deficiency. Structure *8*, 293-303.

Augustin, R. (2010). The protein family of glucose transport facilitators: It's not only about glucose after all. IUBMB Life *62*, 315-333.

Ayala, F.R., Rocha, R.M., Carvalho, K.C., Carvalho, A.L., da Cunha, I.W., Lourenco, S.V., and Soares, F.A. (2010). GLUT1 and GLUT3 as potential prognostic markers for Oral Squamous Cell Carcinoma. Molecules *15*, 2374-2387.

Baba, Y., Nosho, K., Shima, K., Irahara, N., Chan, A.T., Meyerhardt, J.A., Chung, D.C., Giovannucci, E.L., Fuchs, C.S., and Ogino, S. (2010). HIF1A overexpression is associated with poor prognosis in a cohort of 731 colorectal cancers. Am J Pathol *176*, 2292-2301.

Baer, S.C., Casaubon, L., and Younes, M. (1997). Expression of the human erythrocyte glucose transporter Glut1 in cutaneous neoplasia. Journal of the American Academy of Dermatology *37*, 575-577.

Balsara, B.R., Pei, J., Mitsuuchi, Y., Page, R., Klein-Szanto, A., Wang, H., Unger, M., and Testa, J.R. (2004). Frequent activation of AKT in non-small cell lung carcinomas and preneoplastic bronchial lesions. Carcinogenesis *25*, 2053-2059.

Bao, B.Y., Ting, H.J., Hsu, J.W., and Lee, Y.F. (2008). Protective role of 1 alpha, 25-dihydroxyvitamin D3 against oxidative stress in nonmalignant human prostate epithelial cells. Int J Cancer *122*, 2699-2706.

Barthel, A., Okino, S.T., Liao, J., Nakatani, K., Li, J., Whitlock, J.P., Jr., and Roth, R.A. (1999). Regulation of GLUT1 gene transcription by the serine/threonine kinase Akt1. J Biol Chem *274*, 20281-20286.

Bauer, D.E., Harris, M.H., Plas, D.R., Lum, J.J., Hammerman, P.S., Rathmell, J.C., Riley, J.L., and Thompson, C.B. (2004). Cytokine stimulation of aerobic glycolysis in hematopoietic cells exceeds proliferative demand. FASEB J *18*, 1303-1305.

Bauer, D.E., Hatzivassiliou, G., Zhao, F., Andreadis, C., and Thompson, C.B. (2005). ATP citrate lyase is an important component of cell growth and transformation. Oncogene *24*, 6314-6322.

Baumann, M.U., Zamudio, S., and Illsley, N.P. (2007). Hypoxic upregulation of glucose transporters in BeWo choriocarcinoma cells is mediated by hypoxia-inducible factor-1. Am J Physiol Cell Physiol *293*, C477-485.

Behrooz, A., and Ismail-Beigi, F. (1997). Dual control of glut1 glucose transporter gene expression by hypoxia and by inhibition of oxidative phosphorylation. J Biol Chem *272*, 5555-5562.

Bensaad, K., Tsuruta, A., Selak, M.A., Vidal, M.N., Nakano, K., Bartrons, R., Gottlieb, E., and Vousden, K.H. (2006). TIGAR, a p53-inducible regulator of glycolysis and apoptosis. Cell *126*, 107-120.

Berg, Tymoczko J, and Stryer L (2007). The Integration of Metabolism. In Biochemistry, Zimmerman, ed. (Freeman and Company ), p. 761.

Bergstrom, J., Furst, P., Noree, L.O., and Vinnars, E. (1974). Intracellular free amino acid concentration in human muscle tissue. J Appl Physiol *36*, 693-697.

Bertout, J.A., Patel, S.A., and Simon, M.C. (2008). The impact of O2 availability on human cancer. Nat Rev Cancer *8*, 967-975.

Berwick, D.C., Hers, I., Heesom, K.J., Moule, S.K., and Tavare, J.M. (2002). The identification of ATP-citrate lyase as a protein kinase B (Akt) substrate in primary adipocytes. J Biol Chem *277*, 33895-33900.

Bloch, K., Smith, H., van Hamel Parsons, V., Gavaghan, D., Kelly, C., Fletcher, A., Maini, P., and Callaghan, R. (2014). Metabolic Alterations During the Growth of Tumour Spheroids. Cell Biochem Biophys *68*, 615-628.

Bluemlein, K., Gruning, N.M., Feichtinger, R.G., Lehrach, H., Kofler, B., and Ralser, M. (2011). No evidence for a shift in pyruvate kinase PKM1 to PKM2 expression during tumorigenesis. Oncotarget *2*, 393-400.

Boada, J., Roig, T., Perez, X., Gamez, A., Bartrons, R., Cascante, M., and Bermudez, J. (2000). Cells overexpressing fructose-2,6-bisphosphatase showed enhanced pentose phosphate pathway flux and resistance to oxidative stress. FEBS Lett *480*, 261-264.

Boado, R.J., Black, K.L., and Pardridge, W.M. (1994). Gene expression of GLUT3 and GLUT1 glucose transporters in human brain tumors. Brain Res Mol Brain Res *27*, 51-57.

Board, M., Colquhoun, A., and Newsholme, E.A. (1995). High Km glucose-phosphorylating (glucokinase) activities in a range of tumor cell lines and inhibition of rates of tumor growth by the specific enzyme inhibitor mannoheptulose. Cancer research *55*, 3278-3285.

Board, M., Humm, S., and Newsholme, E.A. (1990). Maximum activities of key enzymes of glycolysis, glutaminolysis, pentose phosphate pathway and tricarboxylic acid cycle in normal, neoplastic and suppressed cells. Biochem J *265*, 503-509.

Bode, B.P. (2001). Recent molecular advances in mammalian glutamine transport. J Nutr *131*, 2475S-2485S; discussion 2486S-2477S.

Bode, B.P., Kaminski, D.L., Souba, W.W., and Li, A.P. (1995). Glutamine transport in isolated human hepatocytes and transformed liver cells. Hepatology *21*, 511-520.

Boedtkjer, E., Moreira, J.M., Mele, M., Vahl, P., Wielenga, V.T., Christiansen, P.M., Jensen, V.E., Pedersen, S.F., and Aalkjaer, C. (2013). Contribution of Na+,HCO3(-)-cotransport to cellular pH control in human breast cancer: a role for the breast cancer susceptibility locus NBCn1 (SLC4A7). Int J Cancer *132*, 1288-1299.

Boidot, R., Vegran, F., Meulle, A., Le Breton, A., Dessy, C., Sonveaux, P., Lizard-Nacol, S., and Feron, O. (2012). Regulation of monocarboxylate transporter MCT1 expression by p53 mediates inward and outward lactate fluxes in tumors. Cancer research *72*, 939-948.

Bonen, A. (2001). The expression of lactate transporters (MCT1 and MCT4) in heart and muscle. Eur J Appl Physiol *86*, 6-11.

Boros, L.G., Puigjaner, J., Cascante, M., Lee, W.N., Brandes, J.L., Bassilian, S., Yusuf, F.I., Williams, R.D., Muscarella, P., Melvin, W.S.*, et al.* (1997). Oxythiamine and dehydroepiandrosterone inhibit the nonoxidative synthesis of ribose and tumor cell proliferation. Cancer research *57*, 4242-4248.

Brizel, D.M., Scully, S.P., Harrelson, J.M., Layfield, L.J., Bean, J.M., Prosnitz, L.R., and Dewhirst, M.W. (1996). Tumor oxygenation predicts for the likelihood of distant metastases in human soft tissue sarcoma. Cancer research *56*, 941-943.

Brosh, R., and Rotter, V. (2009). When mutants gain new powers: news from the mutant p53 field. Nat Rev Cancer *9*, 701-713.

Brown, J.M. (1975). Selective radiosensitization of the hypoxic cells of mouse tumors with the nitroimidazoles metronidazole and Ro 7-0582. Radiation research *64*, 633-647.

Brown, J.M. (2002). Tumor microenvironment and the response to anticancer therapy. Cancer Biol Ther *1*, 453-458.

Brown, J.M., and Giaccia, A.J. (1998). The unique physiology of solid tumors: opportunities (and problems) for cancer therapy. Cancer research *58*, 1408-1416.

Brown, N.J., Higham, S.E., Perunovic, B., Arafa, M., Balasubramanian, S., and Rehman, I. (2013). Lactate dehydrogenase-B is silenced by promoter methylation in a high frequency of human breast cancers. PLoS One *8*, e57697.

Brown, R.S., and Wahl, R.L. (1993). Overexpression of Glut-1 glucose transporter in human breast cancer. An immunohistochemical study. Cancer *72*, 2979-2985.

Bungard, C.I., and McGivan, J.D. (2004). Glutamine availability up-regulates expression of the amino acid transporter protein ASCT2 in HepG2 cells and stimulates the ASCT2 promoter. Biochem J *382*, 27-32.

Bustamante, E., and Pedersen, P.L. (1977). High aerobic glycolysis of rat hepatoma cells in culture: role of mitochondrial hexokinase. Proc Natl Acad Sci U S A *74*, 3735-3739.

Bustamante, E., and Pedersen, P.L. (1980). Mitochondrial hexokinase of rat hepatoma cells in culture: solubilization and kinetic properties. Biochemistry *19*, 4972-4977.

Cairns, R.A., Harris, I.S., and Mak, T.W. (2011). Regulation of cancer cell metabolism. Nat Rev Cancer *11*, 85-95.

Calvo, M.B., Figueroa, A., Pulido, E.G., Campelo, R.G., and Aparicio, L.A. (2010). Potential role of sugar transporters in cancer and their relationship with anticancer therapy. Int J Endocrinol *2010*.

Camphausen, K., Purow, B., Sproull, M., Scott, T., Ozawa, T., Deen, D.F., and Tofilon, P.J. (2005). Influence of in vivo growth on human glioma cell line gene expression: convergent profiles under orthotopic conditions. Proc Natl Acad Sci U S A *102*, 8287-8292.

Cancer Research UK (2014). Cancer Stats: Cancer Statistics for the UK (http://www.cancerresearchuk.org/cancer-info/cancerstats/).

Cantley, L.C., and Neel, B.G. (1999). New insights into tumor suppression: PTEN suppresses tumor formation by restraining the phosphoinositide 3-kinase/AKT pathway. Proc Natl Acad Sci U S A *96*, 4240-4245.

Cantuaria, G., Fagotti, A., Ferrandina, G., Magalhaes, A., Nadji, M., Angioli, R., Penalver, M., Mancuso, S., and Scambia, G. (2001). GLUT-1 expression in ovarian carcinoma: association with survival and response to chemotherapy. Cancer *92*, 1144-1150.

Casciari, J.J., Sotirchos, S.V., and Sutherland, R.M. (1992). Variations in tumor cell growth rates and metabolism with oxygen concentration, glucose concentration, and extracellular pH. Journal of cellular physiology *151*, 386-394.

Casneuf, V.F., Fonteyne, P., Van Damme, N., Demetter, P., Pauwels, P., de Hemptinne, B., De Vos, M., Van de Wiele, C., and Peeters, M. (2008). Expression of SGLT1, Bcl-2 and p53 in primary pancreatic cancer related to survival. Cancer investigation *26*, 852-859.

Chaneton, B., Hillmann, P., Zheng, L., Martin, A.C., Maddocks, O.D., Chokkathukalam, A., Coyle, J.E., Jankevics, A., Holding, F.P., Vousden, K.H.*, et al.* (2012). Serine is a natural ligand and allosteric activator of pyruvate kinase M2. Nature *491*, 458-462.

Chang, S., Lee, S., Lee, C., Kim, J.I., and Kim, Y. (2000). Expression of the human erythrocyte glucose transporter in transitional cell carcinoma of the bladder. Urology *55*, 448-452.

Chen, C., Pore, N., Behrooz, A., Ismail-Beigi, F., and Maity, A. (2001). Regulation of glut1 mRNA by hypoxia-inducible factor-1. Interaction between H-ras and hypoxia. J Biol Chem *276*, 9519-9525.

Chen, E.I., Hewel, J., Krueger, J.S., Tiraby, C., Weber, M.R., Kralli, A., Becker, K., Yates, J.R., 3rd, and Felding-Habermann, B. (2007a). Adaptation of energy metabolism in breast cancer brain metastases. Cancer research *67*, 1472-1486.

Chen, Z., Lu, W., Garcia-Prieto, C., and Huang, P. (2007b). The Warburg effect and its cancer therapeutic implications. J Bioenerg Biomembr *39*, 267-274.

Chesney, J. (2006). 6-phosphofructo-2-kinase/fructose-2,6-bisphosphatase and tumor cell glycolysis. Curr Opin Clin Nutr Metab Care *9*, 535-539.

Chiche, J., Brahimi-Horn, M.C., and Pouyssegur, J. (2010). Tumour hypoxia induces a metabolic shift causing acidosis: a common feature in cancer. J Cell Mol Med *14*, 771-794.

Christofk, H.R., Vander Heiden, M.G., Harris, M.H., Ramanathan, A., Gerszten, R.E., Wei, R., Fleming, M.D., Schreiber, S.L., and Cantley, L.C. (2008a). The M2 splice isoform of pyruvate kinase is important for cancer metabolism and tumour growth. Nature *452*, 230-233.

Christofk, H.R., Vander Heiden, M.G., Wu, N., Asara, J.M., and Cantley, L.C. (2008b). Pyruvate kinase M2 is a phosphotyrosine-binding protein. Nature *452*, 181-186.

Coller, H.A., Grandori, C., Tamayo, P., Colbert, T., Lander, E.S., Eisenman, R.N., and Golub, T.R. (2000). Expression analysis with oligonucleotide microarrays reveals that MYC regulates genes involved in growth, cell cycle, signaling, and adhesion. Proc Natl Acad Sci U S A *97*, 3260-3265.

Coller, H.A., Sang, L., and Roberts, J.M. (2006). A new description of cellular quiescence. PLoS Biol *4*, e83.

Collingridge, D.R., Piepmeier, J.M., Rockwell, S., and Knisely, J.P. (1999). Polarographic measurements of oxygen tension in human glioma and surrounding peritumoural brain tissue. Radiother Oncol *53*, 127-131.

Comerford, K.M., Wallace, T.J., Karhausen, J., Louis, N.A., Montalto, M.C., and Colgan, S.P. (2002). Hypoxia-inducible factor-1-dependent regulation of the multidrug resistance (MDR1) gene. Cancer research *62*, 3387-3394.

Connolly, E., Braunstein, S., Formenti, S., and Schneider, R.J. (2006). Hypoxia inhibits protein synthesis through a 4E-BP1 and elongation factor 2 kinase pathway controlled by mTOR and uncoupled in breast cancer cells. Molecular and cellular biology *26*, 3955-3965.

Cooper, R., Sarioglu, S., Sokmen, S., Fuzun, M., Kupelioglu, A., Valentine, H., Gorken, I.B., Airley, R., and West, C. (2003). Glucose transporter-1 (GLUT-1): a

potential marker of prognosis in rectal carcinoma? British journal of cancer *89*, 870-876.

Costa Leite, T., Da Silva, D., Guimaraes Coelho, R., Zancan, P., and Sola-Penna, M. (2007). Lactate favours the dissociation of skeletal muscle 6-phosphofructo-1-kinase tetramers down-regulating the enzyme and muscle glycolysis. Biochem J *408*, 123-130.

Csibi, A., Fendt, S.M., Li, C., Poulogiannis, G., Choo, A.Y., Chapski, D.J., Jeong, S.M., Dempsey, J.M., Parkhitko, A., Morrison, T.*, et al.* (2013). The mTORC1 pathway stimulates glutamine metabolism and cell proliferation by repressing SIRT4. Cell *153*, 840-854.

Dang, C.V., Le, A., and Gao, P. (2009). MYC-induced cancer cell energy metabolism and therapeutic opportunities. Clinical cancer research : an official journal of the American Association for Cancer Research *15*, 6479-6483.

David, C.J., Chen, M., Assanah, M., Canoll, P., and Manley, J.L. (2010). HnRNP proteins controlled by c-Myc deregulate pyruvate kinase mRNA splicing in cancer. Nature *463*, 364-368.

Daye, D., and Wellen, K.E. (2012). Metabolic reprogramming in cancer: unraveling the role of glutamine in tumorigenesis. Semin Cell Dev Biol *23*, 362-369.

Dean, M., Levine, R.A., Ran, W., Kindy, M.S., Sonenshein, G.E., and Campisi, J. (1986). Regulation of c-myc transcription and mRNA abundance by serum growth factors and cell contact. J Biol Chem *261*, 9161-9166.

DeBerardinis, R.J., Lum, J.J., Hatzivassiliou, G., and Thompson, C.B. (2008). The biology of cancer: metabolic reprogramming fuels cell growth and proliferation. Cell Metab *7*, 11-20.

DeBerardinis, R.J., Mancuso, A., Daikhin, E., Nissim, I., Yudkoff, M., Wehrli, S., and Thompson, C.B. (2007). Beyond aerobic glycolysis: transformed cells can engage in glutamine metabolism that exceeds the requirement for protein and nucleotide synthesis. Proc Natl Acad Sci U S A *104*, 19345-19350.

Deprez, J., Vertommen, D., Alessi, D.R., Hue, L., and Rider, M.H. (1997). Phosphorylation and activation of heart 6-phosphofructo-2-kinase by protein kinase B and other protein kinases of the insulin signaling cascades. J Biol Chem *272*, 17269-17275.

Desoize, B., and Jardillier, J. (2000). Multicellular resistance: a paradigm for clinical resistance? Crit Rev Oncol Hematol *36*, 193-207.

Dewhirst, M.W. (2009). Relationships between cycling hypoxia, HIF-1, angiogenesis and oxidative stress. Radiation research *172*, 653-665.

Dimmer, K.S., Friedrich, B., Lang, F., Deitmer, J.W., and Broer, S. (2000). The low-affinity monocarboxylate transporter MCT4 is adapted to the export of lactate in highly glycolytic cells. Biochem J *350 Pt 1*, 219-227.

Doe, M.R., Ascano, J.M., Kaur, M., and Cole, M.D. (2012). Myc posttranscriptionally induces HIF1 protein and target gene expression in normal and cancer cells. Cancer research *72*, 949-957.

dos Santos, M.A., Borges, J.B., de Almeida, D.C., and Curi, R. (2004). Metabolism of the microregions of human breast cancer. Cancer letters *216*, 243-248.

Durand, R.E. (1997). Tumor repopulation during radiotheraphy: quantitation in two xenografted human tumors. Int J Radiat Oncol Biol Phys *39*, 803-808.

Duvel, K., Yecies, J.L., Menon, S., Raman, P., Lipovsky, A.I., Souza, A.L., Triantafellow, E., Ma, Q., Gorski, R., Cleaver, S.*, et al.* (2010). Activation of a metabolic gene regulatory network downstream of mTOR complex 1. Mol Cell *39*, 171-183.

Dwarakanath, B., and Jain, V. (2009). Targeting glucose metabolism with 2-deoxy-D-glucose for improving cancer therapy. Future oncology *5*, 581-585.

Eagle, H. (1955). Nutrition needs of mammalian cells in tissue culture. Science *122*, 501-514.

Eagle, H., Oyama, V.I., Levy, M., Horton, C.L., and Fleischman, R. (1956). The growth response of mammalian cells in tissue culture to L-glutamine and L-glutamic acid. J Biol Chem *218*, 607-616.

Eguchi, Y., Shimizu, S., and Tsujimoto, Y. (1997). Intracellular ATP levels determine cell death fate by apoptosis or necrosis. Cancer research *57*, 1835-1840.

Elstrom, R.L., Bauer, D.E., Buzzai, M., Karnauskas, R., Harris, M.H., Plas, D.R., Zhuang, H., Cinalli, R.M., Alavi, A., Rudin, C.M.*, et al.* (2004). Akt stimulates aerobic glycolysis in cancer cells. Cancer research *64*, 3892-3899.

Estrella, V., Chen, T., Lloyd, M., Wojtkowiak, J., Cornnell, H.H., Ibrahim-Hashim, A., Bailey, K., Balagurunathan, Y., Rothberg, J.M., Sloane, B.F.*, et al.* (2013). Acidity generated by the tumor microenvironment drives local invasion. Cancer research *73*, 1524-1535.

Fan, J., Hitosugi, T., Chung, T.W., Xie, J., Ge, Q., Gu, T.L., Polakiewicz, R.D., Chen, G.Z., Boggon, T.J., Lonial, S.*, et al.* (2011). Tyrosine phosphorylation of lactate dehydrogenase A is important for NADH/NAD(+) redox homeostasis in cancer cells. Molecular and cellular biology *31*, 4938-4950.

Fan, J., Ye, J., Kamphorst, J.J., Shlomi, T., Thompson, C.B., and Rabinowitz, J.D. (2014). Quantitative flux analysis reveals folate-dependent NADPH production. Nature *510*, 298-302.

Fanciulli, M., Bruno, T., Giovannelli, A., Gentile, F.P., Di Padova, M., Rubiu, O., and Floridi, A. (2000). Energy metabolism of human LoVo colon carcinoma cells: correlation to drug resistance and influence of lonidamine. Clinical cancer research : an official journal of the American Association for Cancer Research *6*, 1590-1597.

Fang, R., Xiao, T., Fang, Z., Sun, Y., Li, F., Gao, Y., Feng, Y., Li, L., Wang, Y., Liu, X.*, et al.* (2012). MicroRNA-143 (miR-143) regulates cancer glycolysis via targeting hexokinase 2 gene. J Biol Chem *287*, 23227-23235.

Fantin, V.R., St-Pierre, J., and Leder, P. (2006). Attenuation of LDH-A expression uncovers a link between glycolysis, mitochondrial physiology, and tumor maintenance. Cancer Cell *9*, 425-434.

Farmer, S.R., Wan, K.M., Ben-Ze'ev, A., and Penman, S. (1983). Regulation of actin mRNA levels and translation responds to changes in cell configuration. Molecular and cellular biology *3*, 182-189.

Firth, J.D., Ebert, B.L., and Ratcliffe, P.J. (1995). Hypoxic regulation of lactate dehydrogenase A. Interaction between hypoxia-inducible factor 1 and cAMP response elements. J Biol Chem *270*, 21021-21027.

Fischer, K., Hoffmann, P., Voelkl, S., Meidenbauer, N., Ammer, J., Edinger, M., Gottfried, E., Schwarz, S., Rothe, G., Hoves, S.*, et al.* (2007). Inhibitory effect of tumor cell-derived lactic acid on human T cells. Blood *109*, 3812-3819.

Flavahan, W.A., Wu, Q., Hitomi, M., Rahim, N., Kim, Y., Sloan, A.E., Weil, R.J., Nakano, I., Sarkaria, J.N., Stringer, B.W.*, et al.* (2013). Brain tumor initiating cells adapt to restricted nutrition through preferential glucose uptake. Nature neuroscience *16*, 1373-1382.

Forsythe, J.A., Jiang, B.H., Iyer, N.V., Agani, F., Leung, S.W., Koos, R.D., and Semenza, G.L. (1996). Activation of vascular endothelial growth factor gene transcription by hypoxia-inducible factor 1. Molecular and cellular biology *16*, 4604-4613.

Fuchs, B.C., and Bode, B.P. (2005). Amino acid transporters ASCT2 and LAT1 in cancer: partners in crime? Seminars in cancer biology *15*, 254-266.

Fuchs, B.C., Perez, J.C., Suetterlin, J.E., Chaudhry, S.B., and Bode, B.P. (2004). Inducible antisense RNA targeting amino acid transporter ATB0/ASCT2 elicits apoptosis in human hepatoma cells. Am J Physiol Gastrointest Liver Physiol *286*, G467-478.

Fukumura, D., and Jain, R.K. (2007). Tumor microenvironment abnormalities: causes, consequences, and strategies to normalize. J Cell Biochem *101*, 937-949.

Funasaka, T., Yanagawa, T., Hogan, V., and Raz, A. (2005). Regulation of phosphoglucose isomerase/autocrine motility factor expression by hypoxia. FASEB J *19*, 1422-1430.

Furuta, E., Okuda, H., Kobayashi, A., and Watabe, K. (2010). Metabolic genes in cancer: their roles in tumor progression and clinical implications. Biochimica et biophysica acta *1805*, 141-152.

Ganapathy, V., Thangaraju, M., and Prasad, P.D. (2009). Nutrient transporters in cancer: relevance to Warburg hypothesis and beyond. Pharmacol Ther *121*, 29-40.

Ganapathy-Kanniappan, S., and Geschwind, J.F. (2013). Tumor glycolysis as a target for cancer therapy: progress and prospects. Mol Cancer *12*, 152.

Gao, L., Mejias, R., Echevarria, M., and Lopez-Barneo, J. (2004). Induction of the glucose-6-phosphate dehydrogenase gene expression by chronic hypoxia in PC12 cells. FEBS Lett *569*, 256-260.

Gao, P., Tchernyshyov, I., Chang, T.C., Lee, Y.S., Kita, K., Ochi, T., Zeller, K.I., De Marzo, A.M., Van Eyk, J.E., Mendell, J.T.*, et al.* (2009). c-Myc suppression of miR-

23a/b enhances mitochondrial glutaminase expression and glutamine metabolism. Nature *458*, 762-765.

Gao, X., Wang, H., Yang, J.J., Liu, X., and Liu, Z.R. (2012). Pyruvate kinase M2 regulates gene transcription by acting as a protein kinase. Mol Cell *45*, 598-609.

Gardner, L.B., Li, Q., Park, M.S., Flanagan, W.M., Semenza, G.L., and Dang, C.V. (2001). Hypoxia inhibits G1/S transition through regulation of p27 expression. J Biol Chem *276*, 7919-7926.

Gatenby, R.A., and Gillies, R.J. (2004). Why do cancers have high aerobic glycolysis? Nat Rev Cancer *4*, 891-899.

Gerweck, L.E., and Seetharaman, K. (1996). Cellular pH gradient in tumor versus normal tissue: potential exploitation for the treatment of cancer. Cancer research *56*, 1194-1198.

Gess, B., Hofbauer, K.H., Deutzmann, R., and Kurtz, A. (2004). Hypoxia up-regulates triosephosphate isomerase expression via a HIF-dependent pathway. Pflugers Arch *448*, 175-180.

Gillies, R.J., Raghunand, N., Karczmar, G.S., and Bhujwalla, Z.M. (2002). MRI of the tumor microenvironment. J Magn Reson Imaging *16*, 430-450.

Gillies, R.J., Robey, I., and Gatenby, R.A. (2008). Causes and consequences of increased glucose metabolism of cancers. J Nucl Med *49 Suppl 2*, 24S-42S.

Goldman, R.D., Kaplan, N.O., and Hall, T.C. (1964). Lactic Dehydrogenase in Human Neoplastic Tissues. Cancer research *24*, 389-399.

Gorrini, C., Harris, I.S., and Mak, T.W. (2013). Modulation of oxidative stress as an anticancer strategy. Nature reviews Drug discovery *12*, 931-947.

Gould, G.W., and Holman, G.D. (1993). The glucose transporter family: structure, function and tissue-specific expression. Biochem J *295 ( Pt 2)*, 329-341.

Gray, L.H., Conger, A.D., Ebert, M., Hornsey, S., and Scott, O.C. (1953). The concentration of oxygen dissolved in tissues at the time of irradiation as a factor in radiotherapy. Br J Radiol *26*, 638-648.

Greijer, A.E., and van der Wall, E. (2004). The role of hypoxia inducible factor 1 (HIF-1) in hypoxia induced apoptosis. J Clin Pathol *57*, 1009-1014.

Grimes, D.R., Kelly, C., Bloch, K., and Partridge, M. (2014). A method for estimating the oxygen consumption rate in multicellular tumour spheroids. Journal of the Royal Society, Interface / the Royal Society *11*, 20131124.

Guo, G.F., Cai, Y.C., Zhang, B., Xu, R.H., Qiu, H.J., Xia, L.P., Jiang, W.Q., Hu, P.L., Chen, X.X., Zhou, F.F.*, et al.* (2011). Overexpression of SGLT1 and EGFR in colorectal cancer showing a correlation with the prognosis. Med Oncol *28 Suppl 1*, S197-203.

Haber, R.S., Rathan, A., Weiser, K.R., Pritsker, A., Itzkowitz, S.H., Bodian, C., Slater, G., Weiss, A., and Burstein, D.E. (1998). GLUT1 glucose transporter expression in colorectal carcinoma: a marker for poor prognosis. Cancer *83*, 34-40.

Haber, R.S., Weinstein, S.P., O'Boyle, E., and Morgello, S. (1993). Tissue distribution of the human GLUT3 glucose transporter. Endocrinology *132*, 2538-2543.

Hacker, H.J., Steinberg, P., and Bannasch, P. (1998). Pyruvate kinase isoenzyme shift from L-type to M2-type is a late event in hepatocarcinogenesis induced in rats by a choline-deficient/DL-ethionine-supplemented diet. Carcinogenesis *19*, 99-107.

Haigis, M.C., Mostoslavsky, R., Haigis, K.M., Fahie, K., Christodoulou, D.C., Murphy, A.J., Valenzuela, D.M., Yancopoulos, G.D., Karow, M., Blander, G.*, et al.* (2006). SIRT4 inhibits glutamate dehydrogenase and opposes the effects of calorie restriction in pancreatic beta cells. Cell *126*, 941-954.

Halestrap, A.P., and Meredith, D. (2004). The SLC16 gene family-from monocarboxylate transporters (MCTs) to aromatic amino acid transporters and beyond. Pflugers Arch *447*, 619-628.

Halestrap, A.P., and Price, N.T. (1999). The proton-linked monocarboxylate transporter (MCT) family: structure, function and regulation. Biochem J *343 Pt 2*, 281-299.

Halestrap, A.P., and Wilson, M.C. (2012). The monocarboxylate transporter family--role and regulation. IUBMB Life *64*, 109-119.

Hall, M.D., Martin, C., Ferguson, D.J., Phillips, R.M., Hambley, T.W., and Callaghan, R. (2004). Comparative efficacy of novel platinum(IV) compounds with established chemotherapeutic drugs in solid tumour models. Biochemical pharmacology *67*, 17-30.

Hanahan, D., and Weinberg, R.A. (2000). The hallmarks of cancer. Cell *100*, 57-70.

Hanahan, D., and Weinberg, R.A. (2011). Hallmarks of cancer: the next generation. Cell *144*, 646-674.

Hann, S.R., and Eisenman, R.N. (1984). Proteins encoded by the human c-myc oncogene: differential expression in neoplastic cells. Molecular and cellular biology *4*, 2486-2497.

Hashimoto, T., Hussien, R., Oommen, S., Gohil, K., and Brooks, G.A. (2007). Lactate sensitive transcription factor network in L6 cells: activation of MCT1 and mitochondrial biogenesis. FASEB J *21*, 2602-2612.

Hatanaka, M. (1974). Transport of sugars in tumor cell membranes. Biochimica et biophysica acta *355*, 77-104.

Helmlinger, G., Sckell, A., Dellian, M., Forbes, N.S., and Jain, R.K. (2002). Acid production in glycolysis-impaired tumors provides new insights into tumor metabolism. Clinical cancer research : an official journal of the American Association for Cancer Research *8*, 1284-1291.

Helmlinger, G., Yuan, F., Dellian, M., and Jain, R.K. (1997). Interstitial pH and pO2 gradients in solid tumors in vivo: high-resolution measurements reveal a lack of correlation. Nat Med *3*, 177-182.

Hensley, C.T., Wasti, A.T., and DeBerardinis, R.J. (2013). Glutamine and cancer: cell biology, physiology, and clinical opportunities. J Clin Invest *123*, 3678-3684.

Hernandez-Jimenez, M., Ayuso, M.I., Perez-Morgado, M.I., Garcia-Recio, E.M., Alcazar, A., Martin, M.E., and Gonzalez, V.M. (2012). eIF4F complex disruption causes protein synthesis inhibition during hypoxia in nerve growth factor (NGF)-differentiated PC12 cells. Biochimica et biophysica acta *1823*, 430-438.

Herrero-Yraola, A., Bakhit, S.M., Franke, P., Weise, C., Schweiger, M., Jorcke, D., and Ziegler, M. (2001). Regulation of glutamate dehydrogenase by reversible ADP-ribosylation in mitochondria. EMBO J *20*, 2404-2412.

Hirschhaeuser, F., Menne, H., Dittfeld, C., West, J., Mueller-Klieser, W., and Kunz-Schughart, L.A. (2010). Multicellular tumor spheroids: an underestimated tool is catching up again. Journal of biotechnology *148*, 3-15.

Hitosugi, T., Kang, S., Vander Heiden, M.G., Chung, T.W., Elf, S., Lythgoe, K., Dong, S., Lonial, S., Wang, X., Chen, G.Z.*, et al.* (2009). Tyrosine phosphorylation inhibits PKM2 to promote the Warburg effect and tumor growth. Sci Signal *2*, ra73.

Hochachka, P.W., Buck, L.T., Doll, C.J., and Land, S.C. (1996). Unifying theory of hypoxia tolerance: molecular/metabolic defense and rescue mechanisms for surviving oxygen lack. Proc Natl Acad Sci U S A *93*, 9493-9498.

Hockel, M., Knoop, C., Schlenger, K., Vorndran, B., Baussmann, E., Mitze, M., Knapstein, P.G., and Vaupel, P. (1993). Intratumoral pO2 predicts survival in advanced cancer of the uterine cervix. Radiother Oncol *26*, 45-50.

Hockel, M., Schlenger, K., Aral, B., Mitze, M., Schaffer, U., and Vaupel, P. (1996). Association between tumor hypoxia and malignant progression in advanced cancer of the uterine cervix. Cancer research *56*, 4509-4515.

Hockel, M., Schlenger, K., Knoop, C., and Vaupel, P. (1991). Oxygenation of carcinomas of the uterine cervix: evaluation by computerized O2 tension measurements. Cancer research *51*, 6098-6102.

Hockel, M., and Vaupel, P. (2001). Tumor hypoxia: definitions and current clinical, biologic, and molecular aspects. J Natl Cancer Inst *93*, 266-276.

Hoffmann, A.C., Mori, R., Vallbohmer, D., Brabender, J., Klein, E., Drebber, U., Baldus, S.E., Cooc, J., Azuma, M., Metzger, R.*, et al.* (2008). High expression of HIF1a is a predictor of clinical outcome in patients with pancreatic ductal adenocarcinomas and correlated to PDGFA, VEGF, and bFGF. Neoplasia *10*, 674-679.

Holten, D., Procsal, D., and Chang, H.L. (1976). Regulation of pentose phosphate pathway dehydrogenases by NADP+/NADPH ratios. Biochemical and biophysical research communications *68*, 436-441.

Hoshino, A., Hirst, J.A., and Fujii, H. (2007). Regulation of cell proliferation by interleukin-3-induced nuclear translocation of pyruvate kinase. J Biol Chem *282*, 17706-17711.

Hu, W., Zhang, C., Wu, R., Sun, Y., Levine, A., and Feng, Z. (2010). Glutaminase 2, a novel p53 target gene regulating energy metabolism and antioxidant function. Proc Natl Acad Sci U S A *107*, 7455-7460.

Huang, L.E., Gu, J., Schau, M., and Bunn, H.F. (1998). Regulation of hypoxia-inducible factor 1alpha is mediated by an O2-dependent degradation domain via the ubiquitin-proteasome pathway. Proc Natl Acad Sci U S A *95*, 7987-7992.

Hue, L., and Rousseau, G.G. (1993). Fructose 2,6-bisphosphate and the control of glycolysis by growth factors, tumor promoters and oncogenes. Advances in enzyme regulation *33*, 97-110.

Huwyler, J., Drewe, J., and Krahenbuhl, S. (2008). Tumor targeting using liposomal antineoplastic drugs. International journal of nanomedicine *3*, 21-29.

Iida, Y., Aoki, K., Asakura, T., Ueda, K., Yanaihara, N., Takakura, S., Yamada, K., Okamoto, A., Tanaka, T., and Ohkawa, K. (2012). Hypoxia promotes glycogen synthesis and accumulation in human ovarian clear cell carcinoma. Int J Oncol *40*, 2122-2130.

Israelsen, W.J., Dayton, T.L., Davidson, S.M., Fiske, B.P., Hosios, A.M., Bellinger, G., Li, J., Yu, Y., Sasaki, M., Horner, J.W.*, et al.* (2013). PKM2 isoform-specific deletion reveals a differential requirement for pyruvate kinase in tumor cells. Cell *155*, 397-409.

Iyer, N.V., Kotch, L.E., Agani, F., Leung, S.W., Laughner, E., Wenger, R.H., Gassmann, M., Gearhart, J.D., Lawler, A.M., Yu, A.Y.*, et al.* (1998). Cellular and developmental control of O2 homeostasis by hypoxia-inducible factor 1 alpha. Genes Dev *12*, 149-162.

Iyer, V.V., Yang, H., Ierapetritou, M.G., and Roth, C.M. (2010). Effects of glucose and insulin on HepG2-C3A cell metabolism. Biotechnology and bioengineering *107*, 347-356.

Jaakkola, P., Mole, D.R., Tian, Y.M., Wilson, M.I., Gielbert, J., Gaskell, S.J., von Kriegsheim, A., Hebestreit, H.F., Mukherji, M., Schofield, C.J.*, et al.* (2001). Targeting of HIF-alpha to the von Hippel-Lindau ubiquitylation complex by O2-regulated prolyl hydroxylation. Science *292*, 468-472.

Jackson, R.C. (1989). The problem of the quiescent cancer cell. Advances in enzyme regulation *29*, 27-46.

Jenkins, C.M., Yang, J., Sims, H.F., and Gross, R.W. (2011). Reversible high affinity inhibition of phosphofructokinase-1 by acyl-CoA: a mechanism integrating glycolytic flux with lipid metabolism. J Biol Chem *286*, 11937-11950.

Jeong, S.M., Xiao, C., Finley, L.W., Lahusen, T., Souza, A.L., Pierce, K., Li, Y.H., Wang, X., Laurent, G., German, N.J.*, et al.* (2013). SIRT4 has tumor-suppressive activity and regulates the cellular metabolic response to DNA damage by inhibiting mitochondrial glutamine metabolism. Cancer Cell *23*, 450-463.

Jiang, B.H., Semenza, G.L., Bauer, C., and Marti, H.H. (1996). Hypoxia-inducible factor 1 levels vary exponentially over a physiologically relevant range of O2 tension. Am J Physiol *271*, C1172-1180.

Jiang, P., Du, W., Wang, X., Mancuso, A., Gao, X., Wu, M., and Yang, X. (2011). p53 regulates biosynthesis through direct inactivation of glucose-6-phosphate dehydrogenase. Nat Cell Biol *13*, 310-316.

Jozwiak, P., Krzeslak, A., Pomorski, L., and Lipinska, A. (2012). Expression of hypoxia-related glucose transporters GLUT1 and GLUT3 in benign, malignant and non-neoplastic thyroid lesions. Mol Med Rep *6*, 601-606.

Jun, Y.J., Jang, S.M., Han, H.L., Lee, K.H., Jang, K.S., and Paik, S.S. (2011). Clinicopathologic significance of GLUT1 expression and its correlation with Apaf-1 in colorectal adenocarcinomas. World J Gastroenterol *17*, 1866-1873.

Kacser, H., and Burns, J.A. (1973). The control of flux. Symp Soc Exp Biol *27*, 65-104.

Kang, S.S., Chun, Y.K., Hur, M.H., Lee, H.K., Kim, Y.J., Hong, S.R., Lee, J.H., Lee, S.G., and Park, Y.K. (2002). Clinical significance of glucose transporter 1 (GLUT1) expression in human breast carcinoma. Jpn J Cancer Res *93*, 1123-1128.

Kashiwaya, Y., Sato, K., Tsuchiya, N., Thomas, S., Fell, D.A., Veech, R.L., and Passonneau, J.V. (1994). Control of glucose utilization in working perfused rat heart. J Biol Chem *269*, 25502-25514.

Kato, Y., Ozawa, S., Miyamoto, C., Maehata, Y., Suzuki, A., Maeda, T., and Baba, Y. (2013). Acidic extracellular microenvironment and cancer. Cancer Cell Int *13*, 89.

Kawauchi, K., Araki, K., Tobiume, K., and Tanaka, N. (2008). p53 regulates glucose metabolism through an IKK-NF-kappaB pathway and inhibits cell transformation. Nat Cell Biol *10*, 611-618.

Kim, B.J., and Forbes, N.S. (2007). Flux analysis shows that hypoxia-inducible-factor-1-alpha minimally affects intracellular metabolism in tumor spheroids. Biotechnology and bioengineering *96*, 1167-1182.

Kim, E.A., Yang, S.J., Choi, S.Y., Lee, W.J., and Cho, S.W. (2012). Inhibition of glutamate dehydrogenase and insulin secretion by KHG26377 does not involve ADP-ribosylation by SIRT4 or deacetylation by SIRT3. BMB reports *45*, 458-463.

Kim, J.W., Gao, P., and Dang, C.V. (2007a). Effects of hypoxia on tumor metabolism. Cancer Metastasis Rev *26*, 291-298.

Kim, J.W., Gao, P., Liu, Y.C., Semenza, G.L., and Dang, C.V. (2007b). Hypoxia-inducible factor 1 and dysregulated c-Myc cooperatively induce vascular endothelial growth factor and metabolic switches hexokinase 2 and pyruvate dehydrogenase kinase 1. Molecular and cellular biology *27*, 7381-7393.

Kim, J.W., Tchernyshyov, I., Semenza, G.L., and Dang, C.V. (2006). HIF-1-mediated expression of pyruvate dehydrogenase kinase: a metabolic switch required for cellular adaptation to hypoxia. Cell Metab *3*, 177-185.

Kohn, A.D., Summers, S.A., Birnbaum, M.J., and Roth, R.A. (1996). Expression of a constitutively active Akt Ser/Thr kinase in 3T3-L1 adipocytes stimulates glucose uptake and glucose transporter 4 translocation. J Biol Chem *271*, 31372-31378.

Kolev, Y., Uetake, H., Takagi, Y., and Sugihara, K. (2008). Lactate dehydrogenase-5 (LDH-5) expression in human gastric cancer: association with hypoxia-inducible factor (HIF-1alpha) pathway, angiogenic factors production and poor prognosis. Ann Surg Oncol *15*, 2336-2344.

Kondoh, E., Mori, S., Yamaguchi, K., Baba, T., Matsumura, N., Cory Barnett, J., Whitaker, R.S., Konishi, I., Fujii, S., Berchuck, A.*, et al.* (2010). Targeting slow-proliferating ovarian cancer cells. Int J Cancer *126*, 2448-2456.

Kondoh, H., Lleonart, M.E., Gil, J., Wang, J., Degan, P., Peters, G., Martinez, D., Carnero, A., and Beach, D. (2005). Glycolytic enzymes can modulate cellular life span. Cancer research *65*, 177-185.

Koshiji, M., Kageyama, Y., Pete, E.A., Horikawa, I., Barrett, J.C., and Huang, L.E. (2004). HIF-1alpha induces cell cycle arrest by functionally counteracting Myc. EMBO J *23*, 1949-1956.

Koukourakis, M.I., Giatromanolaki, A., Simopoulos, C., Polychronidis, A., and Sivridis, E. (2005). Lactate dehydrogenase 5 (LDH5) relates to up-regulated hypoxia inducible factor pathway and metastasis in colorectal cancer. Clin Exp Metastasis *22*, 25-30.

Koukourakis, M.I., Giatromanolaki, A., Sivridis, E., Bougioukas, G., Didilis, V., Gatter, K.C., and Harris, A.L. (2003). Lactate dehydrogenase-5 (LDH-5) overexpression in non-small-cell lung cancer tissues is linked to tumour hypoxia, angiogenic factor production and poor prognosis. British journal of cancer *89*, 877-885.

Koumenis, C., Naczki, C., Koritzinsky, M., Rastani, S., Diehl, A., Sonenberg, N., Koromilas, A., and Wouters, B.G. (2002). Regulation of protein synthesis by hypoxia via activation of the endoplasmic reticulum kinase PERK and phosphorylation of the translation initiation factor eIF2alpha. Molecular and cellular biology *22*, 7405-7416.

Kovacevic, Z., and McGivan, J.D. (1983). Mitochondrial metabolism of glutamine and glutamate and its physiological significance. Physiol Rev *63*, 547-605.

Krebs, H.A. (1970). Rate control of the tricarboxylic acid cycle. Adv Enzyme Regul *8*, 335-353.

Kroemer, G., and Pouyssegur, J. (2008). Tumor cell metabolism: cancer's Achilles' heel. Cancer Cell *13*, 472-482.

Krzeslak, A., Wojcik-Krowiranda, K., Forma, E., Jozwiak, P., Romanowicz, H., Bienkiewicz, A., and Brys, M. (2012). Expression of GLUT1 and GLUT3 glucose transporters in endometrial and breast cancers. Pathology oncology research : POR *18*, 721-728.

Kunkel, M., Reichert, T.E., Benz, P., Lehr, H.A., Jeong, J.H., Wieand, S., Bartenstein, P., Wagner, W., and Whiteside, T.L. (2003). Overexpression of Glut-1 and increased glucose metabolism in tumors are associated with a poor prognosis in patients with oral squamous cell carcinoma. Cancer *97*, 1015-1024.

Kuo, W., Lin, J., and Tang, T.K. (2000). Human glucose-6-phosphate dehydrogenase (G6PD) gene transforms NIH 3T3 cells and induces tumors in nude mice. Int J Cancer *85*, 857-864.

Lagadic-Gossmann, D., Huc, L., and Lecureur, V. (2004). Alterations of intracellular pH homeostasis in apoptosis: origins and roles. Cell Death Differ *11*, 953-961.

Lai, B., Xiao, Y., Pu, H., Cao, Q., Jing, H., and Liu, X. (2012). Overexpression of SGLT1 is correlated with tumor development and poor prognosis of ovarian carcinoma. Archives of gynecology and obstetrics *285*, 1455-1461.

Lamonte, G., Tang, X., Chen, J.L., Wu, J., Ding, C.K., Keenan, M.M., Sangokoya, C., Kung, H.N., Ilkayeva, O., Boros, L.G.*, et al.* (2013). Acidosis induces reprogramming of cellular metabolism to mitigate oxidative stress. Cancer Metab *1*, 23.

Lee, J.M., Mhawech-Fauceglia, P., Lee, N., Parsanian, L.C., Lin, Y.G., Gayther, S.A., and Lawrenson, K. (2013). A three-dimensional microenvironment alters protein expression and chemosensitivity of epithelial ovarian cancer cells in vitro. Lab Invest *93*, 528-542.

Leiblich, A., Cross, S.S., Catto, J.W., Phillips, J.T., Leung, H.Y., Hamdy, F.C., and Rehman, I. (2006). Lactate dehydrogenase-B is silenced by promoter hypermethylation in human prostate cancer. Oncogene *25*, 2953-2960.

Lemons, J.M., Feng, X.J., Bennett, B.D., Legesse-Miller, A., Johnson, E.L., Raitman, I., Pollina, E.A., Rabitz, H.A., Rabinowitz, J.D., and Coller, H.A. (2010). Quiescent fibroblasts exhibit high metabolic activity. PLoS Biol *8*, e1000514.

Leu, A.J., Berk, D.A., Lymboussaki, A., Alitalo, K., and Jain, R.K. (2000). Absence of functional lymphatics within a murine sarcoma: a molecular and functional evaluation. Cancer research *60*, 4324-4327.

Li, F., Wang, Y., Zeller, K.I., Potter, J.J., Wonsey, D.R., O'Donnell, K.A., Kim, J.W., Yustein, J.T., Lee, L.A., and Dang, C.V. (2005). Myc stimulates nuclearly encoded mitochondrial genes and mitochondrial biogenesis. Molecular and cellular biology *25*, 6225-6234.

Li, M., Li, C., Allen, A., Stanley, C.A., and Smith, T.J. (2010). The structure and allosteric regulation of glutamate dehydrogenase. Neurochem Int *59*, 445-455.

Liang, J., and Slingerland, J.M. (2003). Multiple roles of the PI3K/PKB (Akt) pathway in cell cycle progression. Cell Cycle *2*, 339-345.

Lin, R.Z., and Chang, H.Y. (2008). Recent advances in three-dimensional multicellular spheroid culture for biomedical research. Biotechnol J *3*, 1172-1184.

Liu, Y., Cao, Y., Zhang, W., Bergmeier, S., Qian, Y., Akbar, H., Colvin, R., Ding, J., Tong, L., Wu, S.*, et al.* (2012). A small-molecule inhibitor of glucose transporter 1 downregulates glycolysis, induces cell-cycle arrest, and inhibits cancer cell growth in vitro and in vivo. Mol Cancer Ther *11*, 1672-1682.

Lobo, C., Ruiz-Bellido, M.A., Aledo, J.C., Marquez, J., Nunez De Castro, I., and Alonso, F.J. (2000). Inhibition of glutaminase expression by antisense mRNA decreases growth and tumourigenicity of tumour cells. Biochem J *348 Pt 2*, 257-261.

Lu, H., Dalgard, C.L., Mohyeldin, A., McFate, T., Tait, A.S., and Verma, A. (2005). Reversible inactivation of HIF-1 prolyl hydroxylases allows cell metabolism to control basal HIF-1. J Biol Chem *280*, 41928-41939.

Lu, S.C. (2013). Glutathione synthesis. Biochimica et biophysica acta *1830*, 3143-3153.

Luo, W., Hu, H., Chang, R., Zhong, J., Knabel, M., O'Meally, R., Cole, R.N., Pandey, A., and Semenza, G.L. (2011). Pyruvate kinase M2 is a PHD3-stimulated coactivator for hypoxia-inducible factor 1. Cell *145*, 732-744.

Luzzatto, L. (1967). Regulation of the activity of glucose-6-phosphate dehydrogenase by NADP+ and NADPH. Biochimica et biophysica acta *146*, 18-25.

Macheda, M.L., Rogers, S., and Best, J.D. (2005). Molecular and cellular regulation of glucose transporter (GLUT) proteins in cancer. Journal of cellular physiology *202*, 654-662.

Mack, F.A., Rathmell, W.K., Arsham, A.M., Gnarra, J., Keith, B., and Simon, M.C. (2003). Loss of pVHL is sufficient to cause HIF dysregulation in primary cells but does not promote tumor growth. Cancer Cell *3*, 75-88.

Maddocks, O.D., and Vousden, K.H. (2011). Metabolic regulation by p53. J Mol Med (Berl) *89*, 237-245.

Maekawa, M., Taniguchi, T., Ishikawa, J., Sugimura, H., Sugano, K., and Kanno, T. (2003). Promoter hypermethylation in cancer silences LDHB, eliminating lactate dehydrogenase isoenzymes 1-4. Clin Chem *49*, 1518-1520.

Maher, J.C., Wangpaichitr, M., Savaraj, N., Kurtoglu, M., and Lampidis, T.J. (2007). Hypoxia-inducible factor-1 confers resistance to the glycolytic inhibitor 2-deoxy-D-glucose. Mol Cancer Ther *6*, 732-741.

Majewski, N., Nogueira, V., Bhaskar, P., Coy, P.E., Skeen, J.E., Gottlob, K., Chandel, N.S., Thompson, C.B., Robey, R.B., and Hay, N. (2004). Hexokinase-mitochondria interaction mediated by Akt is required to inhibit apoptosis in the presence or absence of Bax and Bak. Mol Cell *16*, 819-830.

Mandujano-Tinoco, E.A., Gallardo-Perez, J.C., Marin-Hernandez, A., Moreno-Sanchez, R., and Rodriguez-Enriquez, S. (2013). Anti-mitochondrial therapy in human breast cancer multi-cellular spheroids. Biochimica et biophysica acta *1833*, 541-551.

Mankoff, D.A., Eary, J.F., Link, J.M., Muzi, M., Rajendran, J.G., Spence, A.M., and Krohn, K.A. (2007). Tumor-specific positron emission tomography imaging in patients: [18F] fluorodeoxyglucose and beyond. Clinical cancer research : an official journal of the American Association for Cancer Research *13*, 3460-3469.

Manning, B.D., and Cantley, L.C. (2007). AKT/PKB signaling: navigating downstream. Cell *129*, 1261-1274.

Marin-Hernandez, A., Gallardo-Perez, J.C., Ralph, S.J., Rodriguez-Enriquez, S., and Moreno-Sanchez, R. (2009). HIF-1alpha modulates energy metabolism in cancer cells by inducing over-expression of specific glycolytic isoforms. Mini reviews in medicinal chemistry *9*, 1084-1101.

Marin-Hernandez, A., Gallardo-Perez, J.C., Rodriguez-Enriquez, S., Encalada, R., Moreno-Sanchez, R., and Saavedra, E. (2010). Modeling cancer glycolysis. Biochimica et biophysica acta *1807*, 755-767.

Marin-Hernandez, A., Lopez-Ramirez, S.Y., Del Mazo-Monsalvo, I., Gallardo-Perez, J.C., Rodriguez-Enriquez, S., Moreno-Sanchez, R., and Saavedra, E. (2014). Modeling cancer glycolysis under hypoglycemia, and the role played by the differential expression of glycolytic isoforms. The FEBS journal *281*, 3325-3345.

Marin-Hernandez, A., Rodriguez-Enriquez, S., Vital-Gonzalez, P.A., Flores-Rodriguez, F.L., Macias-Silva, M., Sosa-Garrocho, M., and Moreno-Sanchez, R. (2006). Determining and understanding the control of glycolysis in fast-growth tumor cells. Flux control by an over-expressed but strongly product-inhibited hexokinase. The FEBS journal *273*, 1975-1988.

Martin, G.R., and Jain, R.K. (1994). Noninvasive measurement of interstitial pH profiles in normal and neoplastic tissue using fluorescence ratio imaging microscopy. Cancer research *54*, 5670-5674.

Martinez-Zaguilan, R., Lynch, R.M., Martinez, G.M., and Gillies, R.J. (1993). Vacuolar-type H(+)-ATPases are functionally expressed in plasma membranes of human tumor cells. Am J Physiol *265*, C1015-1029.

Mathupala, S.P., Heese, C., and Pedersen, P.L. (1997). Glucose catabolism in cancer cells. The type II hexokinase promoter contains functionally active response elements for the tumor suppressor p53. J Biol Chem *272*, 22776-22780.

Mathupala, S.P., Ko, Y.H., and Pedersen, P.L. (2006). Hexokinase II: cancer's double-edged sword acting as both facilitator and gatekeeper of malignancy when bound to mitochondria. Oncogene *25*, 4777-4786.

Mathupala, S.P., Ko, Y.H., and Pedersen, P.L. (2009). Hexokinase-2 bound to mitochondria: cancer's stygian link to the "Warburg Effect" and a pivotal target for effective therapy. Seminars in cancer biology *19*, 17-24.

Mathupala, S.P., Rempel, A., and Pedersen, P.L. (2001). Glucose catabolism in cancer cells: identification and characterization of a marked activation response of the type II hexokinase gene to hypoxic conditions. J Biol Chem *276*, 43407-43412.

Matoba, S., Kang, J.G., Patino, W.D., Wragg, A., Boehm, M., Gavrilova, O., Hurley, P.J., Bunz, F., and Hwang, P.M. (2006). p53 regulates mitochondrial respiration. Science *312*, 1650-1653.

Mazurek, S. (2011). Pyruvate kinase type M2: a key regulator of the metabolic budget system in tumor cells. Int J Biochem Cell Biol *43*, 969-980.

Mazurek, S., Boschek, C.B., and Eigenbrodt, E. (1997). The role of phosphometabolites in cell proliferation, energy metabolism, and tumor therapy. J Bioenerg Biomembr *29*, 315-330.

Mazurek, S., Boschek, C.B., Hugo, F., and Eigenbrodt, E. (2005). Pyruvate kinase type M2 and its role in tumor growth and spreading. Seminars in cancer biology *15*, 300-308.

McBrayer, S.K., Cheng, J.C., Singhal, S., Krett, N.L., Rosen, S.T., and Shanmugam, M. (2012). Multiple myeloma exhibits novel dependence on GLUT4, GLUT8, and GLUT11: implications for glucose transporter-directed therapy. Blood *119*, 4686-4697.

McCleland, M.L., Adler, A.S., Deming, L., Cosino, E., Lee, L., Blackwood, E.M., Solon, M., Tao, J., Li, L., Shames, D.*, et al.* (2013). Lactate dehydrogenase B is required for the growth of KRAS-dependent lung adenocarcinomas. Clinical cancer research : an official journal of the American Association for Cancer Research *19*, 773-784.

McCleland, M.L., Adler, A.S., Shang, Y., Hunsaker, T., Truong, T., Peterson, D., Torres, E., Li, L., Haley, B., Stephan, J.P.*, et al.* (2012). An integrated genomic screen identifies LDHB as an essential gene for triple-negative breast cancer. Cancer research *72*, 5812-5823.

McFate, T., Mohyeldin, A., Lu, H., Thakar, J., Henriques, J., Halim, N.D., Wu, H., Schell, M.J., Tsang, T.M., Teahan, O.*, et al.* (2008). Pyruvate dehydrogenase complex activity controls metabolic and malignant phenotype in cancer cells. J Biol Chem *283*, 22700-22708.

McLean, L.A., Roscoe, J., Jorgensen, N.K., Gorin, F.A., and Cala, P.M. (2000). Malignant gliomas display altered pH regulation by NHE1 compared with nontransformed astrocytes. Am J Physiol Cell Physiol *278*, C676-688.

Medina, R.A., and Owen, G.I. (2002). Glucose transporters: expression, regulation and cancer. Biological research *35*, 9-26.

Mellor, H.R., and Callaghan, R. (2011). Accumulation and distribution of doxorubicin in tumour spheroids: the influence of acidity and expression of P-glycoprotein. Cancer chemotherapy and pharmacology *68*, 1179-1190.

Mellor, H.R., Ferguson, D.J., and Callaghan, R. (2005a). A model of quiescent tumour microregions for evaluating multicellular resistance to chemotherapeutic drugs. British journal of cancer *93*, 302-309.

Mellor, H.R., Snelling, S., Hall, M.D., Modok, S., Jaffar, M., Hambley, T.W., and Callaghan, R. (2005b). The influence of tumour microenvironmental factors on the efficacy of cisplatin and novel platinum(IV) complexes. Biochemical pharmacology *70*, 1137-1146.

Menssen, A., and Hermeking, H. (2002). Characterization of the c-MYC-regulated transcriptome by SAGE: identification and analysis of c-MYC target genes. Proc Natl Acad Sci U S A *99*, 6274-6279.

Meyer, N., and Penn, L.Z. (2008). Reflecting on 25 years with MYC. Nat Rev Cancer *8*, 976-990.

Miller, D.M., Thomas, S.D., Islam, A., Muench, D., and Sedoris, K. (2012). c-Myc and cancer metabolism. Clinical cancer research : an official journal of the American Association for Cancer Research *18*, 5546-5553.

Minchenko, A., Leshchinsky, I., Opentanova, I., Sang, N., Srinivas, V., Armstead, V., and Caro, J. (2002). Hypoxia-inducible factor-1-mediated expression of the 6-phosphofructo-2-kinase/fructose-2,6-bisphosphatase-3 (PFKFB3) gene. Its possible role in the Warburg effect. J Biol Chem *277*, 6183-6187.

Miranda-Goncalves, V., Honavar, M., Pinheiro, C., Martinho, O., Pires, M.M., Cordeiro, M., Bebiano, G., Costa, P., Palmeirim, I., Reis, R.M.*, et al.* (2013). Monocarboxylate transporters (MCTs) in gliomas: expression and exploitation as therapeutic targets. Neuro Oncol *15*, 172-188.

Mochiki, E., Kuwano, H., Katoh, H., Asao, T., Oriuchi, N., and Endo, K. (2004). Evaluation of 18F-2-deoxy-2-fluoro-D-glucose positron emission tomography for gastric cancer. World J Surg *28*, 247-253.

Mor, I., Cheung, E.C., and Vousden, K.H. Control of glycolysis through regulation of PFK1: old friends and recent additions. Cold Spring Harb Symp Quant Biol *76*, 211-216.

Mor, I., Cheung, E.C., and Vousden, K.H. (2011). Control of glycolysis through regulation of PFK1: old friends and recent additions. Cold Spring Harb Symp Quant Biol *76*, 211-216.

Moreno-Sanchez, R., Rodriguez-Enriquez, S., Marin-Hernandez, A., and Saavedra, E. (2007). Energy metabolism in tumor cells. The FEBS journal *274*, 1393-1418.

Moreno-Sanchez, R., Saavedra, E., Rodriguez-Enriquez, S., Gallardo-Perez, J.C., Quezada, H., and Westerhoff, H.V. (2010). Metabolic control analysis indicates a change of strategy in the treatment of cancer. Mitochondrion *10*, 626-639.

Moreno-Sanchez, R., Saavedra, E., Rodriguez-Enriquez, S., and Olin-Sandoval, V. (2008). Metabolic control analysis: a tool for designing strategies to manipulate metabolic pathways. Journal of biomedicine & biotechnology *2008*, 597913.

Mueller-Klieser, W. (1997). Three-dimensional cell cultures: from molecular mechanisms to clinical applications. Am J Physiol *273*, C1109-1123.

Mukherjee, J., Phillips, J.J., Zheng, S., Wiencke, J., Ronen, S.M., and Pieper, R.O. (2013). Pyruvate kinase M2 expression, but not pyruvate kinase activity, is up-regulated in a grade-specific manner in human glioma. PLoS One *8*, e57610.

Mukherjee, P., Sotnikov, A.V., Mangian, H.J., Zhou, J.R., Visek, W.J., and Clinton, S.K. (1999). Energy intake and prostate tumor growth, angiogenesis, and vascular endothelial growth factor expression. J Natl Cancer Inst *91*, 512-523.

Nagase, Y., Takata, K., Moriyama, N., Aso, Y., Murakami, T., and Hirano, H. (1995). Immunohistochemical localization of glucose transporters in human renal cell carcinoma. J Urol *153*, 798-801.

Nakashima, R.A., Mangan, P.S., Colombini, M., and Pedersen, P.L. (1986). Hexokinase receptor complex in hepatoma mitochondria: evidence from N,N'-dicyclohexylcarbodiimide-labeling studies for the involvement of the pore-forming protein VDAC. Biochemistry *25*, 1015-1021.

Nakashima, R.A., Paggi, M.G., and Pedersen, P.L. (1984). Contributions of glycolysis and oxidative phosphorylation to adenosine 5'-triphosphate production in AS-30D hepatoma cells. Cancer research *44*, 5702-5706.

Nakashima, R.A., Paggi, M.G., Scott, L.J., and Pedersen, P.L. (1988). Purification and characterization of a bindable form of mitochondrial bound hexokinase from the highly glycolytic AS-30D rat hepatoma cell line. Cancer research *48*, 913-919.

Nederman, T., Norling, B., Glimelius, B., Carlsson, J., and Brunk, U. (1984). Demonstration of an extracellular matrix in multicellular tumor spheroids. Cancer research *44*, 3090-3097.

Nishioka, T., Oda, Y., Seino, Y., Yamamoto, T., Inagaki, N., Yano, H., Imura, H., Shigemoto, R., and Kikuchi, H. (1992). Distribution of the glucose transporters in human brain tumors. Cancer research *52*, 3972-3979.

Noguchi, T., Inoue, H., and Tanaka, T. (1986). The M1- and M2-type isozymes of rat pyruvate kinase are produced from the same gene by alternative RNA splicing. J Biol Chem *261*, 13807-13812.

Nordsmark, M., Bentzen, S.M., Rudat, V., Brizel, D., Lartigau, E., Stadler, P., Becker, A., Adam, M., Molls, M., Dunst, J.*, et al.* (2005). Prognostic value of tumor oxygenation in 397 head and neck tumors after primary radiation therapy. An international multi-center study. Radiother Oncol *77*, 18-24.

O'Rourke, J.F., Pugh, C.W., Bartlett, S.M., and Ratcliffe, P.J. (1996). Identification of hypoxically inducible mRNAs in HeLa cells using differential-display PCR. Role of hypoxia-inducible factor-1. Eur J Biochem *241*, 403-410.

Obach, M., Navarro-Sabate, A., Caro, J., Kong, X., Duran, J., Gomez, M., Perales, J.C., Ventura, F., Rosa, J.L., and Bartrons, R. (2004). 6-Phosphofructo-2-kinase (pfkfb3) gene promoter contains hypoxia-inducible factor-1 binding sites necessary for transactivation in response to hypoxia. J Biol Chem *279*, 53562-53570.

Ohmori, T., Yang, J.L., Price, J.O., and Arteaga, C.L. (1998). Blockade of tumor cell transforming growth factor-betas enhances cell cycle progression and sensitizes human breast carcinoma cells to cytotoxic chemotherapy. Exp Cell Res *245*, 350-359.

Osthus, R.C., Shim, H., Kim, S., Li, Q., Reddy, R., Mukherjee, M., Xu, Y., Wonsey, D., Lee, L.A., and Dang, C.V. (2000). Deregulation of glucose transporter 1 and glycolytic gene expression by c-Myc. J Biol Chem *275*, 21797-21800.

Palmieri, D., Fitzgerald, D., Shreeve, S.M., Hua, E., Bronder, J.L., Weil, R.J., Davis, S., Stark, A.M., Merino, M.J., Kurek, R.*, et al.* (2009). Analyses of resected human brain metastases of breast cancer reveal the association between up-regulation of hexokinase 2 and poor prognosis. Mol Cancer Res *7*, 1438-1445.

Parker, C., Milosevic, M., Toi, A., Sweet, J., Panzarella, T., Bristow, R., Catton, C., Catton, P., Crook, J., Gospodarowicz, M.*, et al.* (2004). Polarographic electrode study of tumor oxygenation in clinically localized prostate cancer. Int J Radiat Oncol Biol Phys *58*, 750-757.

Patra, K.C., Wang, Q., Bhaskar, P.T., Miller, L., Wang, Z., Wheaton, W., Chandel, N., Laakso, M., Muller, W.J., Allen, E.L.*, et al.* (2013). Hexokinase 2 is required for tumor initiation and maintenance and its systemic deletion is therapeutic in mouse models of cancer. Cancer Cell *24*, 213-228.

Pawlik, T.M., Souba, W.W., Sweeney, T.J., and Bode, B.P. (2000). Amino acid uptake and regulation in multicellular hepatoma spheroids. The Journal of surgical research *91*, 15-25.

Pedersen, P.L. (2007). Warburg, me and Hexokinase 2: Multiple discoveries of key molecular events underlying one of cancers' most common phenotypes, the "Warburg Effect", i.e., elevated glycolysis in the presence of oxygen. J Bioenerg Biomembr *39*, 211-222.

Pedersen, P.L., Greenawalt, J.W., Chan, T.L., and Morris, H.P. (1970). A comparison of some ultrastructural and biochemical properties of mitochondria from Morris hepatomas 9618A, 7800, and 3924A. Cancer research *30*, 2620-2626.

Pelletier, J., Bellot, G., Gounon, P., Lacas-Gervais, S., Pouyssegur, J., and Mazure, N.M. (2012). Glycogen Synthesis is Induced in Hypoxia by the Hypoxia-Inducible Factor and Promotes Cancer Cell Survival. Frontiers in oncology *2*, 18.

Perez-Gomez, C., Campos-Sandoval, J.A., Alonso, F.J., Segura, J.A., Manzanares, E., Ruiz-Sanchez, P., Gonzalez, M.E., Marquez, J., and Mates, J.M. (2005). Co-expression of glutaminase K and L isoenzymes in human tumour cells. Biochem J *386*, 535-542.

Pertega-Gomes, N., Vizcaino, J.R., Miranda-Goncalves, V., Pinheiro, C., Silva, J., Pereira, H., Monteiro, P., Henrique, R.M., Reis, R.M., Lopes, C.*, et al.* (2011). Monocarboxylate transporter 4 (MCT4) and CD147 overexpression is associated with poor prognosis in prostate cancer. BMC Cancer *11*, 312.

Pescador, N., Villar, D., Cifuentes, D., Garcia-Rocha, M., Ortiz-Barahona, A., Vazquez, S., Ordonez, A., Cuevas, Y., Saez-Morales, D., Garcia-Bermejo, M.L.*, et al.* (2010). Hypoxia promotes glycogen accumulation through hypoxia inducible factor (HIF)-mediated induction of glycogen synthase 1. PLoS One *5*, e9644.

Peschiaroli, A., Giacobbe, A., Formosa, A., Markert, E.K., Bongiorno-Borbone, L., Levine, A.J., Candi, E., D'Alessandro, A., Zolla, L., Finazzi Agro, A.*, et al.* (2013). miR-143 regulates hexokinase 2 expression in cancer cells. Oncogene *32*, 797-802.

Pinheiro, C., Albergaria, A., Paredes, J., Sousa, B., Dufloth, R., Vieira, D., Schmitt, F., and Baltazar, F. (2010). Monocarboxylate transporter 1 is up-regulated in basal-like breast carcinoma. Histopathology *56*, 860-867.

Pinheiro, C., Longatto-Filho, A., Ferreira, L., Pereira, S.M., Etlinger, D., Moreira, M.A., Jube, L.F., Queiroz, G.S., Schmitt, F., and Baltazar, F. (2008a). Increasing expression of monocarboxylate transporters 1 and 4 along progression to invasive cervical carcinoma. Int J Gynecol Pathol *27*, 568-574.

Pinheiro, C., Longatto-Filho, A., Scapulatempo, C., Ferreira, L., Martins, S., Pellerin, L., Rodrigues, M., Alves, V.A., Schmitt, F., and Baltazar, F. (2008b). Increased expression of monocarboxylate transporters 1, 2, and 4 in colorectal carcinomas. Virchows Arch *452*, 139-146.

Plaitakis, A., and Zaganas, I. (2001). Regulation of human glutamate dehydrogenases: implications for glutamate, ammonia and energy metabolism in brain. J Neurosci Res *66*, 899-908.

Puskas, F., Gergely, P., Jr., Banki, K., and Perl, A. (2000). Stimulation of the pentose phosphate pathway and glutathione levels by dehydroascorbate, the oxidized form of vitamin C. FASEB J *14*, 1352-1361.

Rademakers, S.E., Span, P.N., Kaanders, J.H., Sweep, F.C., van der Kogel, A.J., and Bussink, J. (2008). Molecular aspects of tumour hypoxia. Molecular oncology *2*, 41-53.

Rampling, R., Cruickshank, G., Lewis, A.D., Fitzsimmons, S.A., and Workman, P. (1994). Direct measurement of pO2 distribution and bioreductive enzymes in human malignant brain tumors. Int J Radiat Oncol Biol Phys *29*, 427-431.

Rapoport, T.A., Heinrich, R., and Rapoport, S.M. (1976). The regulatory principles of glycolysis in erythrocytes in vivo and in vitro. A minimal comprehensive model describing steady states, quasi-steady states and time-dependent processes. Biochem J *154*, 449-469.

Rathmell, J.C., Fox, C.J., Plas, D.R., Hammerman, P.S., Cinalli, R.M., and Thompson, C.B. (2003). Akt-directed glucose metabolism can prevent Bax conformation change and promote growth factor-independent survival. Molecular and cellular biology *23*, 7315-7328.

Rempel, A., Bannasch, P., and Mayer, D. (1994). Differences in expression and intracellular distribution of hexokinase isoenzymes in rat liver cells of different transformation stages. Biochimica et biophysica acta *1219*, 660-668.

Rempel, A., Mathupala, S.P., and Perdersen, P.L. (1996). Glucose catabolism in cancer cells: regulation of the Type II hexokinase promoter by glucose and cyclic AMP. FEBS Lett *385*, 233-237.

Richmond, A., and Su, Y. (2008). Mouse xenograft models vs GEM models for human cancer therapeutics. Disease models & mechanisms *1*, 78-82.

Riddle, S.R., Ahmad, A., Ahmad, S., Deeb, S.S., Malkki, M., Schneider, B.K., Allen, C.B., and White, C.W. (2000). Hypoxia induces hexokinase II gene expression in human lung cell line A549. Am J Physiol Lung Cell Mol Physiol *278*, L407-416.

Riganti, C., Gazzano, E., Polimeni, M., Aldieri, E., and Ghigo, D. (2012). The pentose phosphate pathway: an antioxidant defense and a crossroad in tumor cell fate. Free Radic Biol Med *53*, 421-436.

Robey, R.B., and Hay, N. (2006). Mitochondrial hexokinases, novel mediators of the antiapoptotic effects of growth factors and Akt. Oncogene *25*, 4683-4696.

Rodriguez, S., Jafer, O., Goker, H., Summersgill, B.M., Zafarana, G., Gillis, A.J., van Gurp, R.J., Oosterhuis, J.W., Lu, Y.J., Huddart, R.*, et al.* (2003). Expression profile of genes from 12p in testicular germ cell tumors of adolescents and adults associated with i(12p) and amplification at 12p11.2-p12.1. Oncogene *22*, 1880-1891.

Rodriguez-Enriquez, S., Gallardo-Perez, J.C., Aviles-Salas, A., Marin-Hernandez, A., Carreno-Fuentes, L., Maldonado-Lagunas, V., and Moreno-Sanchez, R. (2008). Energy metabolism transition in multi-cellular human tumor spheroids. Journal of cellular physiology *216*, 189-197.

Rodriguez-Enriquez, S., Marin-Hernandez, A., Gallardo-Perez, J.C., and Moreno-Sanchez, R. (2009). Kinetics of transport and phosphorylation of glucose in cancer cells. Journal of cellular physiology *221*, 552-559.

Rodriguez-Rodriguez, P., Fernandez, E., and Bolanos, J.P. (2013). Underestimation of the pentose-phosphate pathway in intact primary neurons as revealed by metabolic flux analysis. Journal of cerebral blood flow and metabolism : official journal of the International Society of Cerebral Blood Flow and Metabolism *33*, 1843-1845.

Rofstad, E.K., Sundfor, K., Lyng, H., and Trope, C.G. (2000). Hypoxia-induced treatment failure in advanced squamous cell carcinoma of the uterine cervix is primarily due to hypoxia-induced radiation resistance rather than hypoxia-induced metastasis. British journal of cancer *83*, 354-359.

Ros, S., and Schulze, A. (2013). Glycolysis back in the limelight: systemic targeting of HK2 blocks tumor growth. Cancer Discov *3*, 1105-1107.

Rudlowski, C., Becker, A.J., Schroder, W., Rath, W., Buttner, R., and Moser, M. (2003). GLUT1 messenger RNA and protein induction relates to the malignant transformation of cervical cancer. Am J Clin Pathol *120*, 691-698.

Sahin, A.A., Ro, J.Y., el-Naggar, A.K., Wilson, P.L., Teague, K., Blick, M., and Ayala, A.G. (1991). Tumor proliferative fraction in solid malignant neoplasms. A

comparative study of Ki-67 immunostaining and flow cytometric determinations. Am J Clin Pathol *96*, 512-519.

Sakakibara, R., Kato, M., Okamura, N., Nakagawa, T., Komada, Y., Tominaga, N., Shimojo, M., and Fukasawa, M. (1997). Characterization of a human placental fructose-6-phosphate, 2-kinase/fructose-2,6-bisphosphatase. J Biochem *122*, 122-128.

Samuels, Y., Wang, Z., Bardelli, A., Silliman, N., Ptak, J., Szabo, S., Yan, H., Gazdar, A., Powell, S.M., Riggins, G.J., *et al.* (2004). High frequency of mutations of the PIK3CA gene in human cancers. Science *304*, 554.

Scholzen, T., and Gerdes, J. (2000). The Ki-67 protein: from the known and the unknown. Journal of cellular physiology *182*, 311-322.

Schwartzenberg-Bar-Yoseph, F., Armoni, M., and Karnieli, E. (2004). The tumor suppressor p53 down-regulates glucose transporters GLUT1 and GLUT4 gene expression. Cancer research *64*, 2627-2633.

Seagroves, T.N., Ryan, H.E., Lu, H., Wouters, B.G., Knapp, M., Thibault, P., Laderoute, K., and Johnson, R.S. (2001). Transcription factor HIF-1 is a necessary mediator of the pasteur effect in mammalian cells. Molecular and cellular biology *21*, 3436-3444.

Sedlakova, O., Svastova, E., Takacova, M., Kopacek, J., Pastorek, J., and Pastorekova, S. (2014). Carbonic anhydrase IX, a hypoxia-induced catalytic component of the pH regulating machinery in tumors. Front Physiol *4*, 400.

Semenza, G.L. (2010). Defining the role of hypoxia-inducible factor 1 in cancer biology and therapeutics. Oncogene *29*, 625-634.

Semenza, G.L., Roth, P.H., Fang, H.M., and Wang, G.L. (1994). Transcriptional regulation of genes encoding glycolytic enzymes by hypoxia-inducible factor 1. J Biol Chem *269*, 23757-23763.

Semenza, G.L., and Wang, G.L. (1992). A nuclear factor induced by hypoxia via de novo protein synthesis binds to the human erythropoietin gene enhancer at a site required for transcriptional activation. Molecular and cellular biology *12*, 5447-5454.

Sennoune, S.R., Bakunts, K., Martinez, G.M., Chua-Tuan, J.L., Kebir, Y., Attaya, M.N., and Martinez-Zaguilan, R. (2004). Vacuolar H+-ATPase in human breast cancer

cells with distinct metastatic potential: distribution and functional activity. Am J Physiol Cell Physiol *286*, C1443-1452.

Shen, Y.M., Arbman, G., Olsson, B., and Sun, X.F. (2011). Overexpression of GLUT1 in colorectal cancer is independently associated with poor prognosis. Int J Biol Markers *26*, 166-172.

Shi, Q., Le, X., Wang, B., Abbruzzese, J.L., Xiong, Q., He, Y., and Xie, K. (2001). Regulation of vascular endothelial growth factor expression by acidosis in human cancer cells. Oncogene *20*, 3751-3756.

Shim, H., Dolde, C., Lewis, B.C., Wu, C.S., Dang, G., Jungmann, R.A., Dalla-Favera, R., and Dang, C.V. (1997). c-Myc transactivation of LDH-A: implications for tumor metabolism and growth. Proc Natl Acad Sci U S A *94*, 6658-6663.

Shmeeda, H., Mak, L., Tzemach, D., Astrahan, P., Tarshish, M., and Gabizon, A. (2006). Intracellular uptake and intracavitary targeting of folate-conjugated liposomes in a mouse lymphoma model with up-regulated folate receptors. Mol Cancer Ther *5*, 818-824.

Siemann, D.W., and Keng, P.C. (1988). Characterization of radiation resistant hypoxic cell subpopulations in KHT sarcomas. (II). Cell sorting. British journal of cancer *58*, 296-300.

Simpson, I.A., Dwyer, D., Malide, D., Moley, K.H., Travis, A., and Vannucci, S.J. (2008). The facilitative glucose transporter GLUT3: 20 years of distinction. Am J Physiol Endocrinol Metab *295*, E242-253.

Smith, T.J., and Stanley, C.A. (2008). Untangling the glutamate dehydrogenase allosteric nightmare. Trends in biochemical sciences *33*, 557-564.

Sola-Penna, M., Da Silva, D., Coelho, W.S., Marinho-Carvalho, M.M., and Zancan, P. (2010). Regulation of mammalian muscle type 6-phosphofructo-1-kinase and its implication for the control of the metabolism. IUBMB Life *62*, 791-796.

Sonveaux, P., Vegran, F., Schroeder, T., Wergin, M., Verrax, J., Rabbani, Z., De Saedeleer, C., Kennedy, K., Diepart, C., Jordan, B.*, et al.* (2008a). Targeting lactate-fueled respiration selectively kills hypoxic tumor cells in mice. J Clin Invest *118*, 3930 - 3942.

Sonveaux, P., Vegran, F., Schroeder, T., Wergin, M.C., Verrax, J., Rabbani, Z.N., De Saedeleer, C.J., Kennedy, K.M., Diepart, C., Jordan, B.F.*, et al.* (2008b). Targeting

lactate-fueled respiration selectively kills hypoxic tumor cells in mice. J Clin Invest *118*, 3930-3942.

Stanton, R.C. (2012). Glucose-6-phosphate dehydrogenase, NADPH, and cell survival. IUBMB Life *64*, 362-369.

Stitt, M., and Gibon, Y. (2014). Why measure enzyme activities in the era of systems biology? Trends in plant science *19*, 256-265.

Sui, D., and Wilson, J.E. (1997). Structural determinants for the intracellular localization of the isozymes of mammalian hexokinase: intracellular localization of fusion constructs incorporating structural elements from the hexokinase isozymes and the green fluorescent protein. Arch Biochem Biophys *345*, 111-125.

Sullivan, R., and Graham, C.H. (2007). Hypoxia-driven selection of the metastatic phenotype. Cancer Metastasis Rev *26*, 319-331.

Sun, R.C., and Denko, N.C. (2014). Hypoxic regulation of glutamine metabolism through HIF1 and SIAH2 supports lipid synthesis that is necessary for tumor growth. Cell Metab *19*, 285-292.

Sutherland, R.M. (1986). Importance of critical metabolites and cellular interactions in the biology of microregions of tumors. Cancer *58*, 1668-1680.

Sutherland, R.M. (1988). Cell and environment interactions in tumor microregions: the multicell spheroid model. Science *240*, 177-184.

Suzuki, S., Tanaka, T., Poyurovsky, M.V., Nagano, H., Mayama, T., Ohkubo, S., Lokshin, M., Hosokawa, H., Nakayama, T., Suzuki, Y.*, et al.* (2010). Phosphate-activated glutaminase (GLS2), a p53-inducible regulator of glutamine metabolism and reactive oxygen species. Proc Natl Acad Sci U S A *107*, 7461-7466.

Swietach, P., Vaughan-Jones, R.D., and Harris, A.L. (2007). Regulation of tumor pH and the role of carbonic anhydrase 9. Cancer Metastasis Rev *26*, 299-310.

Takahashi, Y., Takahashi, S., Yoshimi, T., and Miura, T. (1998). Hypoxia-induced expression of phosphoglycerate mutase B in fibroblasts. Eur J Biochem *254*, 497-504.

Talks, K.L., Turley, H., Gatter, K.C., Maxwell, P.H., Pugh, C.W., Ratcliffe, P.J., and Harris, A.L. (2000). The expression and distribution of the hypoxia-inducible factors HIF-1alpha and HIF-2alpha in normal human tissues, cancers, and tumor-associated macrophages. Am J Pathol *157*, 411-421.

Tannock, I.F., and Kopelyan, I. (1986). Influence of glucose concentration on growth and formation of necrosis in spheroids derived from a human bladder cancer cell line. Cancer research *46*, 3105-3110.

Tannock, I.F., Steele, D., and Roberts, J. (1986). Influence of reduced concentration of L-glutamine on growth and viability of cells in monolayer, in spheroids, and in experimental tumours. British journal of cancer *54*, 733-741.

Teicher, B.A. (1994). Hypoxia and drug resistance. Cancer Metastasis Rev *13*, 139-168.

Teicher, B.A. (2006). Tumor models for efficacy determination. Mol Cancer Ther *5*, 2435-2443.

Teicher, B.A., Lazo, J.S., and Sartorelli, A.C. (1981). Classification of antineoplastic agents by their selective toxicities toward oxygenated and hypoxic tumor cells. Cancer research *41*, 73-81.

Thangaraju, M., Carswell, K.N., Prasad, P.D., and Ganapathy, V. (2009). Colon cancer cells maintain low levels of pyruvate to avoid cell death caused by inhibition of HDAC1/HDAC3. Biochem J *417*, 379-389.

Thompson, H.J., McGinley, J.N., Spoelstra, N.S., Jiang, W., Zhu, Z., and Wolfe, P. (2004). Effect of dietary energy restriction on vascular density during mammary carcinogenesis. Cancer Res *64*, 5643-5650.

Thun, M.J., DeLancey, J.O., Center, M.M., Jemal, A., and Ward, E.M. (2010). The global burden of cancer: priorities for prevention. Carcinogenesis *31*, 100-110.

Tian, W.N., Braunstein, L.D., Pang, J., Stuhlmeier, K.M., Xi, Q.C., Tian, X., and Stanton, R.C. (1998). Importance of glucose-6-phosphate dehydrogenase activity for cell growth. J Biol Chem *273*, 10609-10617.

Torres Filho, I.P., Leunig, M., Yuan, F., Intaglietta, M., and Jain, R.K. (1994). Noninvasive measurement of microvascular and interstitial oxygen profiles in a human tumor in SCID mice. Proc Natl Acad Sci U S A *91*, 2081-2085.

Torres, N.V., Mateo, F., Melendez-Hevia, E., and Kacser, H. (1986). Kinetics of metabolic pathways. A system in vitro to study the control of flux. Biochem J *234*, 169-174.

Torres, N.V., Souto, R., and Melendez-Hevia, E. (1989). Study of the flux and transition time control coefficient profiles in a metabolic system in vitro and the effect of an external stimulator. Biochem J *260*, 763-769.

Trainer, D.L., Kline, T., McCabe, F.L., Faucette, L.F., Feild, J., Chaikin, M., Anzano, M., Rieman, D., Hoffstein, S., Li, D.J.*, et al.* (1988). Biological characterization and oncogene expression in human colorectal carcinoma cell lines. Int J Cancer *41*, 287-296.

Trivedi, B., and Danforth, W.H. (1966). Effect of pH on the kinetics of frog muscle phosphofructokinase. J Biol Chem *241*, 4110-4112.

Tsai, H.J., and Wilson, J.E. (1996). Functional organization of mammalian hexokinases: both N- and C-terminal halves of the rat type II isozyme possess catalytic sites. Arch Biochem Biophys *329*, 17-23.

Tsouko, E., Khan, A.S., White, M.A., Han, J.J., Shi, Y., Merchant, F.A., Sharpe, M.A., Xin, L., and Frigo, D.E. (2014). Regulation of the pentose phosphate pathway by an androgen receptor-mTOR-mediated mechanism and its role in prostate cancer cell growth. Oncogenesis *3*, e103.

Tsutsumi, H., Tani, K., Fujii, H., and Miwa, S. (1988). Expression of L- and M-type pyruvate kinase in human tissues. Genomics *2*, 86-89.

Turyn, J., Schlichtholz, B., Dettlaff-Pokora, A., Presler, M., Goyke, E., Matuszewski, M., Kmiec, Z., Krajka, K., and Swierczynski, J. (2003). Increased activity of glycerol 3-phosphate dehydrogenase and other lipogenic enzymes in human bladder cancer. Hormone and metabolic research = Hormon- und Stoffwechselforschung = Hormones et metabolisme *35*, 565-569.

Uldry, M., and Thorens, B. (2004). The SLC2 family of facilitated hexose and polyol transporters. Pflugers Arch *447*, 480-489.

Ullah, M.S., Davies, A.J., and Halestrap, A.P. (2006). The plasma membrane lactate transporter MCT4, but not MCT1, is up-regulated by hypoxia through a HIF-1alpha-dependent mechanism. J Biol Chem *281*, 9030-9037.

Utsunomiya-Tate, N., Endou, H., and Kanai, Y. (1996). Cloning and functional characterization of a system ASC-like Na+-dependent neutral amino acid transporter. J Biol Chem *271*, 14883-14890.

Valera, A., Pujol, A., Gregori, X., Riu, E., Visa, J., and Bosch, F. (1995). Evidence from transgenic mice that myc regulates hepatic glycolysis. FASEB J *9*, 1067-1078.

Vander Heiden, M.G., Cantley, L.C., and Thompson, C.B. (2009). Understanding the Warburg effect: the metabolic requirements of cell proliferation. Science *324*, 1029-1033.

Varia, M.A., Calkins-Adams, D.P., Rinker, L.H., Kennedy, A.S., Novotny, D.B., Fowler, W.C., Jr., and Raleigh, J.A. (1998). Pimonidazole: a novel hypoxia marker for complementary study of tumor hypoxia and cell proliferation in cervical carcinoma. Gynecol Oncol *71*, 270-277.

Vaupel, P. (2004). Tumor microenvironmental physiology and its implications for radiation oncology. Semin Radiat Oncol *14*, 198-206.

Vaupel, P., Briest, S., and Hockel, M. (2002). Hypoxia in breast cancer: pathogenesis, characterization and biological/therapeutic implications. Wien Med Wochenschr *152*, 334-342.

Vaupel, P., Kallinowski, F., and Okunieff, P. (1989). Blood flow, oxygen and nutrient supply, and metabolic microenvironment of human tumors: a review. Cancer research *49*, 6449-6465.

Vaupel, P., and Mayer, A. (2007). Hypoxia in cancer: significance and impact on clinical outcome. Cancer Metastasis Rev *26*, 225-239.

Vaupel, P., Schlenger, K., Knoop, C., and Hockel, M. (1991). Oxygenation of human tumors: evaluation of tissue oxygen distribution in breast cancers by computerized O2 tension measurements. Cancer research *51*, 3316-3322.

Vaupel, P., Thews, O., and Hoeckel, M. (2001). Treatment resistance of solid tumors: role of hypoxia and anemia. Med Oncol *18*, 243-259.

Vogelstein, B., Lane, D., and Levine, A.J. (2000). Surfing the p53 network. Nature *408*, 307-310.

Wachsberger, P., Burd, R., and Dicker, A.P. (2003). Tumor response to ionizing radiation combined with antiangiogenesis or vascular targeting agents: exploring mechanisms of interaction. Clinical cancer research : an official journal of the American Association for Cancer Research *9*, 1957-1971.

Wagle, A., Jivraj, S., Garlock, G.L., and Stapleton, S.R. (1998). Insulin regulation of glucose-6-phosphate dehydrogenase gene expression is rapamycin-sensitive and requires phosphatidylinositol 3-kinase. J Biol Chem *273*, 14968-14974.

Walenta, S., Wetterling, M., Lehrke, M., Schwickert, G., Sundfor, K., Rofstad, E.K., and Mueller-Klieser, W. (2000). High lactate levels predict likelihood of metastases, tumor recurrence, and restricted patient survival in human cervical cancers. Cancer research *60*, 916-921.

Wallen, C.A., Higashikubo, R., and Dethlefsen, L.A. (1984). Murine mammary tumour cells in vitro. I. The development of a quiescent state. Cell Tissue Kinet *17*, 65-77.

Wallen, C.A., Ridinger, D.N., and Dethlefsen, L.A. (1985). Heterogeneity of X-ray cytotoxicity in proliferating and quiescent murine mammary carcinoma cells. Cancer research *45*, 3064-3069.

Wang, G., Xu, Z., Wang, C., Yao, F., Li, J., Chen, C., and Sun, S. (2013). Differential phosphofructokinase-1 isoenzyme patterns associated with glycolytic efficiency in human breast cancer and paracancer tissues. Oncol Lett *6*, 1701-1706.

Wang, G.L., and Semenza, G.L. (1995). Purification and characterization of hypoxia-inducible factor 1. J Biol Chem *270*, 1230-1237.

Wang, J., Yuan, W., Chen, Z., Wu, S., Chen, J., Ge, J., and Hou, F. (2012). Overexpression of G6PD is associated with poor clinical outcome in gastric cancer. Tumour Biol *33*, 95-101.

Wang, Q., Beaumont, K.A., Otte, N.J., Font, J., Bailey, C.G., van Geldermalsen, M., Sharp, D.M., Tiffen, J.C., Ryan, R.M., Jormakka, M.*, et al.* (2014). Targeting glutamine transport to suppress melanoma cell growth. Int J Cancer *135*, 1060-1071.

Wang, T., Marquardt, C., and Foker, J. (1976). Aerobic glycolysis during lymphocyte proliferation. Nature *261*, 702-705.

Warburg, O. (1956a). On respiratory impairment in cancer cells. Science *124*, 269-270.

Warburg, O. (1956b). On the origin of cancer cells. Science *123*, 309-314.

Warburg, O., Wind, F., and Negelein, E. (1927). The Metabolism of Tumors in the Body. J Gen Physiol *8*, 519-530.

Ward, P.S., and Thompson, C.B. (2012). Metabolic reprogramming: a cancer hallmark even warburg did not anticipate. Cancer Cell *21*, 297-308.

Webb, B.A., Chimenti, M., Jacobson, M.P., and Barber, D.L. (2011). Dysregulated pH: a perfect storm for cancer progression. Nat Rev Cancer *11*, 671-677.

Wheatley, K.E., Williams, E.A., Smith, N.C., Dillard, A., Park, E.Y., Nunez, N.P., Hursting, S.D., and Lane, M.A. (2008). Low-carbohydrate diet versus caloric restriction: effects on weight loss, hormones, and colon tumor growth in obese mice. Nutr Cancer *60*, 61-68.

Wilson, J.E. (2003). Isozymes of mammalian hexokinase: structure, subcellular localization and metabolic function. J Exp Biol *206*, 2049-2057.

Wilson, W.R., and Hay, M.P. (2011). Targeting hypoxia in cancer therapy. Nat Rev Cancer *11*, 393-410.

Wise, D.R., DeBerardinis, R.J., Mancuso, A., Sayed, N., Zhang, X.Y., Pfeiffer, H.K., Nissim, I., Daikhin, E., Yudkoff, M., McMahon, S.B.*, et al.* (2008). Myc regulates a transcriptional program that stimulates mitochondrial glutaminolysis and leads to glutamine addiction. Proc Natl Acad Sci U S A *105*, 18782-18787.

Wise, D.R., Ward, P.S., Shay, J.E., Cross, J.R., Gruber, J.J., Sachdeva, U.M., Platt, J.M., DeMatteo, R.G., Simon, M.C., and Thompson, C.B. (2011). Hypoxia promotes isocitrate dehydrogenase-dependent carboxylation of alpha-ketoglutarate to citrate to support cell growth and viability. Proc Natl Acad Sci U S A *108*, 19611-19616.

Witney, T.H., Carroll, L., Alam, I.S., Chandrashekran, A., Nguyen, Q.D., Sala, R., Harris, R., Deberardinis, R.J., Agarwal, R., and Aboagye, E.O. (2014). A novel radiotracer to image glycogen metabolism in tumors by positron emission tomography. Cancer research *74*, 1319-1328.

Wolf, A., Agnihotri, S., Micallef, J., Mukherjee, J., Sabha, N., Cairns, R., Hawkins, C., and Guha, A. (2011). Hexokinase 2 is a key mediator of aerobic glycolysis and promotes tumor growth in human glioblastoma multiforme. J Exp Med *208*, 313-326.

Wong, N., De Melo, J., and Tang, D. (2013). PKM2, a Central Point of Regulation in Cancer Metabolism. Int J Cell Biol *2013*, 11.

Wood, I.S., and Trayhurn, P. (2003). Glucose transporters (GLUT and SGLT): expanded families of sugar transport proteins. Br J Nutr *89*, 3-9.

Wood, T. (1986). Physiological functions of the pentose phosphate pathway. Cell Biochem Funct *4*, 241-247.

Wu, S., and Le, H. (2012). Dual roles of PKM2 in cancer metabolism. Acta Biochim Biophys Sin (Shanghai) *45*, 27-35.

Wykoff, C.C., Beasley, N.J., Watson, P.H., Turner, K.J., Pastorek, J., Sibtain, A., Wilson, G.D., Turley, H., Talks, K.L., Maxwell, P.H.*, et al.* (2000). Hypoxia-inducible expression of tumor-associated carbonic anhydrases. Cancer research *60*, 7075-7083.

Xia, X., Lemieux, M.E., Li, W., Carroll, J.S., Brown, M., Liu, X.S., and Kung, A.L. (2009). Integrative analysis of HIF binding and transactivation reveals its role in maintaining histone methylation homeostasis. Proc Natl Acad Sci U S A *106*, 4260-4265.

Yamamoto, T., Seino, Y., Fukumoto, H., Koh, G., Yano, H., Inagaki, N., Yamada, Y., Inoue, K., Manabe, T., and Imura, H. (1990). Over-expression of facilitative glucose transporter genes in human cancer. Biochemical and biophysical research communications *170*, 223-230.

Yang, C., Richardson, A.D., Smith, J.W., and Osterman, A. (2007). Comparative metabolomics of breast cancer. Pac Symp Biocomput, 181-192.

Yang, C., Sudderth, J., Dang, T., Bachoo, R.M., McDonald, J.G., and DeBerardinis, R.J. (2009). Glioblastoma cells require glutamate dehydrogenase to survive impairments of glucose metabolism or Akt signaling. Cancer research *69*, 7986-7993.

Yang, M.H., Wu, M.Z., Chiou, S.H., Chen, P.M., Chang, S.Y., Liu, C.J., Teng, S.C., and Wu, K.J. (2008). Direct regulation of TWIST by HIF-1alpha promotes metastasis. Nat Cell Biol *10*, 295-305.

Yang, W., Xia, Y., Ji, H., Zheng, Y., Liang, J., Huang, W., Gao, X., Aldape, K., and Lu, Z. (2011). Nuclear PKM2 regulates beta-catenin transactivation upon EGFR activation. Nature *480*, 118-122.

Yi, W., Clark, P.M., Mason, D.E., Keenan, M.C., Hill, C., Goddard, W.A., 3rd, Peters, E.C., Driggers, E.M., and Hsieh-Wilson, L.C. (2012). Phosphofructokinase 1 glycosylation regulates cell growth and metabolism. Science *337*, 975-980.

Younes, M., Brown, R.W., Stephenson, M., Gondo, M., and Cagle, P.T. (1997a). Overexpression of Glut1 and Glut3 in stage I nonsmall cell lung carcinoma is associated with poor survival. Cancer *80*, 1046-1051.

Younes, M., Lechago, L.V., Somoano, J.R., Mosharaf, M., and Lechago, J. (1997b). Immunohistochemical detection of Glut3 in human tumors and normal tissues. Anticancer Res *17*, 2747-2750.

Young, L.H., Renfu, Y., Russell, R., Hu, X., Caplan, M., Ren, J., Shulman, G.I., and Sinusas, A.J. (1997). Low-flow ischemia leads to translocation of canine heart GLUT-4 and GLUT-1 glucose transporters to the sarcolemma in vivo. Circulation *95*, 415-422.

Yuan, Z.Q., Sun, M., Feldman, R.I., Wang, G., Ma, X., Jiang, C., Coppola, D., Nicosia, S.V., and Cheng, J.Q. (2000). Frequent activation of AKT2 and induction of apoptosis by inhibition of phosphoinositide-3-OH kinase/Akt pathway in human ovarian cancer. Oncogene *19*, 2324-2330.

Yuneva, M., Zamboni, N., Oefner, P., Sachidanandam, R., and Lazebnik, Y. (2007). Deficiency in glutamine but not glucose induces MYC-dependent apoptosis in human cells. J Cell Biol *178*, 93-105.

Zancan, P., Sola-Penna, M., Furtado, C.M., and Da Silva, D. (2010). Differential expression of phosphofructokinase-1 isoforms correlates with the glycolytic efficiency of breast cancer cells. Mol Genet Metab *100*, 372-378.

Zhang, J.Z., Bryce, N.S., Siegele, R., Carter, E.A., Paterson, D., de Jonge, M.D., Howard, D.L., Ryan, C.G., and Hambley, T.W. (2012). The use of spectroscopic imaging and mapping techniques in the characterisation and study of DLD-1 cell spheroid tumour models. Integrative biology : quantitative biosciences from nano to macro *4*, 1072-1080.

Zhong, H., De Marzo, A.M., Laughner, E., Lim, M., Hilton, D.A., Zagzag, D., Buechler, P., Isaacs, W.B., Semenza, G.L., and Simons, J.W. (1999). Overexpression of hypoxia-inducible factor 1alpha in common human cancers and their metastases. Cancer research *59*, 5830-5835.

Zhou, Y., Tozzi, F., Chen, J., Fan, F., Xia, L., Wang, J., Gao, G., Zhang, A., Xia, X., Brasher, H.*, et al.* (2011). Intracellular ATP levels are a pivotal determinant of chemoresistance in colon cancer cells. Cancer research *72*, 304-314.

Zwerschke, W., Mazurek, S., Massimi, P., Banks, L., Eigenbrodt, E., and Jansen-Durr, P. (1999). Modulation of type M2 pyruvate kinase activity by the human papillomavirus type 16 E7 oncoprotein. Proc Natl Acad Sci U S A *96*, 1291-1296.